ВЕСТНИК ТРАНСПЛАНТОЛОГИИ И ИСКУССТВЕННЫХ ОРГАНОВ

VESTNIK TRANSPLANTOLOGII I ISKUSSTVENNYKH ORGANOV

RUSSIAN JOURNAL OF TRANSPLANTOLOGY AND ARTIFICIAL ORGANS

УЧРЕДИТЕЛИ: ОБЩЕРОССИЙСКАЯ ОБЩЕСТВЕННАЯ ОРГАНИЗАЦИЯ ТРАНСПЛАНТОЛОГОВ «РОССИЙСКОЕ ТРАНСПЛАНТОЛОГИЧЕСКОЕ ОБЩЕСТВО»

ФГБУ «НМИЦ ТИО ИМЕНИ АКАДЕМИКА В.И. ШУМАКОВА» МИНЗДРАВА РОССИИ

ФГАОУ ВО «ПЕРВЫЙ МГМУ ИМЕНИ И.М. СЕЧЕНОВА» МИНЗДРАВА РОССИИ (СЕЧЕНОВСКИЙ УНИВЕРСИТЕТ)

THE OFFICIAL JOURNAL OF ALL-RUSSIAN PUBLIC ORGANIZATION OF TRANSPLANTOLOGISTS "RUSSIAN TRANSPLANT SOCIETY"

SHUMAKOV NATIONAL MEDICAL RESEARCH CENTER OF TRANSPLANTOLOGY AND ARTIFICIAL ORGANS

I.M. SECHENOV FIRST MOSCOW STATE MEDICAL UNIVERSITY (SECHENOV UNIVERSITY)

2020. Том XXII. № 3

2020. Vol. XXII. № 3

Научно-практический журнал основан в 1999 г.
Регистр. № 018616

Scientific and Practical Journal was founded in 1999
Reg. № 018616

Журнал «Вестник трансплантологии и искусственных органов» включен ВАК РФ в перечень российских рецензируемых научных изданий, в которых должны быть опубликованы результаты диссертационных работ

"Russian Journal of Transplantology and Artificial Organs" is included in the list of leading peer-reviewed scientific publication editions, produced in the Russian Federation and is recommended for publication of primary results of dissertation research

Журнал «Вестник трансплантологии и искусственных органов» индексируется в Scopus и размещен на платформе Web of Science Core Collection: Emerging Science Citation Index

"Russian Journal of Transplantology and Artificial Organs" is indexed in Scopus and in the Emerging Science Citation Index of the Web of Science Core Collection

ISSN 1995-1191

Адрес для корреспонденции:

Россия, 123182, Москва, ул. Щукинская, 1
Тел./факс +7 (499) 193 87 62
E-mail: vestniktranspl@gmail.com
Интернет-сайт журнала: http://journal.transpl.ru
Научная электронная библиотека: http://elibrary.ru

Correspondence address:

1, Shchukinskaya st., Moscow 123182, Russia
Tel./Fax +7 (499) 193 87 62
E-mail: vestniktranspl@gmail.com
Journal's web site: http://journal.transpl.ru
Scientific eLibrary: http://elibrary.ru

Подписной индекс в каталоге «Газеты и журналы» – 80248

СОДЕРЖАНИЕ

CONTENTS

ТРАНСПЛАНТАЦИЯ СОЛИДНЫХ ОРГАНОВ В УСЛОВИЯХ ПАНДЕМИИ НОВОЙ КОРОНАВИРУСНОЙ ИНФЕКЦИИ COVID-19

SOLID ORGAN TRANSPLANTATION IN THE COVID-19 PANDEMIC

*В настоящем выпуске журнала опубликована статья, посвященная результатам национального многоцентрового исследования «**Р**аспространенность и **О**собенности **К**линического течения **КОР**онавирусной инфекции у РЕЦИПИЕНТов сердца, почки, печени» (**РОККОР-реципиент**), организованного под эгидой Российского трансплантологического общества.*

*Беспрецедентная по масштабам и последствиям пандемия, вызванная новым коронавирусом SARS-Cov-2, охватила почти все страны мира; не явилась исключением и Российская Федерация. Нынешний этап развития отечественной трансплантологии характеризуется наличием достаточно большого числа граждан – различного пола, возраста и социального статуса, – перенесших трансплантацию солидных органов. Реципиенты сердца, почки, печени, пожизненно получающие иммуносупрессивную терапию и имеющие ряд сопутствующих заболеваний, подвержены риску тяжелых осложнений COVID-19. С другой стороны, новая коронавирусная инфекция в условиях пандемии представляет опасность и для больных тяжелыми хроническими заболеваниями с терминальной стадией поражения жизненно важных органов – потенциальных реципиентов. В этих условиях необходимо оценить соотношение потенциальных пользы и риска трансплантации донорского органа. Для решения указанных выше вопросов, как и ряда других, касающихся особенностей клинического течения и лечения коронавирусной инфекции у реципиентов органов, было инициировано исследование **РОККОР-реципиент**, первые результаты которого представлены в журнале.*

Отрадно отметить, что в течение достаточно короткого времени удалось организовать

*This journal issue features a paper devoted to the results of a national multicenter observational study titled "Prevalence and Features of the Clinical Course of Coronavirus Infection in Heart, Kidney, and Liver Recipients" (**ROKKOR-recipient**), organized under the auspices of the Russian Transplant Society.*

*The new coronavirus disease 2019 (COVID-19) pandemic, unprecedented in scale and consequences, which is caused by the SARS-CoV-2 virus, has affected almost all countries in the world, including Russia. In the development of Russian transplantology currently, there is a fairly large number of solid organ recipients of different sex, age and social status. Heart, kidney, and liver recipients, who are permanently receiving immunosuppressive therapy and having a number of comorbidities, are at risk of severe complications from COVID-19. On the other hand, the new coronavirus infection in a pandemic is also dangerous for patients with severe chronic diseases with end-stage damage to vital organs – potential recipients. In these conditions, it is necessary to assess the relationship between the potential benefits and risks of donor organ transplantation. In order to address the above issues and a number of others related to the specifics of the clinical course and treatment of coronavirus infection in organ recipients, the **ROKKOR-recipient** study was initiated. The initial report is presented in the journal.*

It is pleasing to note that within a fairly short time, it was possible to organize and conduct a multicenter observational study involving 20 institutions from different regions of the Russian Federation. Here we report the results of the first stage of the study. The next stage is currently ongoing

и провести по-настоящему многоцентровое исследование с участием двадцати учреждений из различных регионов РФ. После завершения первого этапа, результаты которого опубликованы в настоящем выпуске, исследование продолжается. Результаты второго этапа мы планируем получить в конце 2020 года и опубликовать в первом номере «Вестника» в 2021 году.

С уважением,
академик РАН С.В. Готье

and the results are anticipated towards the end of 2020 and will be highlighted in the first issue of our journal in 2021.

Sincerely,
S.V. Gautier.
Member, Russian Academy of Sciences

По распоряжению Правительства РФ № 2206-р от 31 августа 2020 года НМИЦ ТИО им. ак. В.И. Шумакова вошел в список научных организаций, которые вправе самостоятельно присуждать ученые степени кандидата и доктора наук

ПРАВИТЕЛЬСТВО РОССИЙСКОЙ ФЕДЕРАЦИИ

РАСПОРЯЖЕНИЕ

от 31 августа 2020 г. № 2206-р

МОСКВА

Дополнить раздел I перечня научных организаций и образовательных организаций высшего образования, которым предоставляются права, предусмотренные абзацами вторым - четвертым пункта 3^1 статьи 4 Федерального закона "О науке и государственной научно-технической политике", утвержденного распоряжением Правительства Российской Федерации от 23 августа 2017 г. № 1792-р (Собрание законодательства Российской Федерации, 2017, № 35, ст. 5392; 2018, № 36, ст. 5677; 2019, № 36, ст. 5058), пунктом 4^1 следующего содержания:

"4^1. Федеральное государственное бюджетное учреждение "Национальный медицинский исследовательский центр трансплантологии и искусственных органов имени академика В.И.Шумакова" Министерства здравоохранения Российской Федерации".

Председатель Правительства Российской Федерации М.Мишустин

4654150

DOI: 10.15825/1995-1191-2020-3-8-17

COVID-19 IN SOLID ORGAN TRANSPLANT RECIPIENTS: INITIAL REPORT FROM NATIONAL MULTICENTER OBSERVATIONAL STUDY "ROKKOR-RECIPIENT"

S.V. Gautier[1, 2], A.O. Shevchenko[1, 3], O.M. Tsirulnikova[2, 1], S.M. Khomyakov[1], O.N. Kotenko[4], V.E. Vinogradov[4, 5], I.N. Abyzov[6], G.D. Avetisyan[7], A.Yu. Anisimov[8], L.Yu. Artyukhina[4], M.T. Bekov[1], V.A. Berdinsky[4], V.S. Bogdanov[4], A.Yu. Bykov[9], A.Yu. Vinokurov[10], A.Yu. Goncharova[1], D.P. Evdokimov[11], D.V. Ezersky[12], V.E. Zagainov[13], V.M. Zakharevich[1, 2], K.N. Zelenin[14], E.S. Ivanova[4], A.A. Kartashev[1], N.G. Kvadratova[1], I.G. Kim[4], N.N. Koloskova[1], V.L. Korobka[15], I.R. Kurbanuglov[1], M.A. Lysenko[4], I.A. Miloserdov[1, 2], Ya.G. Moisyuk[16], G.V. Nikolaev[17], I.V. Ostrovskaya[4], N.Yu. Petrova[18], A.V. Petryaev[19], A.V. Pinchuk[20], V.S. Platonov[21], V.N. Poptsov[1], Z.A. Porchkhidze[1], D.A. Saydulaev[1], A.D. Sapozhnikov[22], S.B. Semchenko[23], M.M. Skorobogatov[21], V.Yu. Tereshchenko[24], N.F. Frolova[4], D.V. Khalikova[1], T.A. Khalilulin[1, 2]

[1] Shumakov National Medical Research Center of Transplantology and Artificial Organs, Moscow, Russian Federation
[2] Sechenov University, Moscow, Russian Federation
[3] Pirogov Medical University, Moscow, Russian Federation
[4] Moscow City Scientific and Practical Center for Nephrology and Transplant Kidney Pathology, City Clinial Hospital No. 52, Moscow, Russian Federation
[5] Research Institute of Health Care Organization and Medical Management, Moscow, Russian Federation
[6] Republican Clinical Hospital, Cheboksary, Russian Federation
[7] Clinical Hospital No. 1, Smolensk, Russian Federation
[8] City Clinical Hospital No. 7, Kazan, Russian Federation
[9] State Novosibirsk Regional Clinical Hospital, Novosibirsk, Russian Federation
[10] Leningrad Regional Clinical Hospital, St. Petersburg, Russian Federation
[11] Regional Clinical Hospital, Krasnoyarsk, Russian Federation
[12] Sergeev Regional Clinical Hospital No. 1, Khabarovsk, Russian Federation
[13] Volga Regional Medical Center, Nizhny Novgorod, Russian Federation
[14] Ministry of Health of the Arkhangelsk Oblast, Arkhangelsk, Russian Federation
[15] Rostov Regional Clinical Hospital, Rostov-on-Don, Russian Federation
[16] Vladimirsky Moscow Regional Research Clinical Institute, Moscow, Russian Federation
[17] Almazov National Medical Research Centre, St. Petersburg, Russian Federation
[18] Saratov Regional Clinical Hospital, Saratov, Russian Federation
[19] Tula Regional Clinical Hospital, Tula, Russian Federation
[20] Sklifosovsky Research Institute of Emergency Care, Moscow, Russian Federation
[21] District Clinical Hospital, Khanty-Mansiysk, Russian Federation
[22] Shumakov National Medical Research Center of Transplantology and Artificial Organs in the city of Volzhsky, Volzhsky, Russian Federation
[23] Center for Organ and Tissue Transplantation, Regional Clinical Hospital No. 1, Tyumen, Russian Federation
[24] Kabanov City Clinical Hospital No. 1, Omsk, Russian Federation

We herein present our initial report from "ROKKOR-recipient", a national multicenter observational study. The prevalence, risk factors, clinical manifestations and outcomes of the novel coronavirus disease 2019 (COVID-19) in solid organ transplant recipients receiving immunosuppressive therapy were investigated. The study enrolled 251 COVID-19 patients (220 kidney recipients, 7 liver recipients, 1 liver-kidney recipient, and 23 heart recipients). The subjects came from 20 regions in Russia. The symptoms, clinical presentation, imaging and lab test results,

Corresponding author: Alexey Shevchenko. Address: 1, Shchukinskaya str., Moscow, 123182, Russian Federation. Phone: (495) 190-35-62. E-mail: alxxshevchenko@aol.com

therapy and outcomes of COVID-19 were described. It was established that solid organ transplant recipients with COVID-19 have a higher risk of developing adverse events. Predictors of adverse events include associated cardiovascular diseases, pulmonary diseases, diabetes, and kidney failure. Symptoms of the disease include dyspnea, rash and catarrhal signs, as well as initial low blood oxygen saturation (SpO_2 <92%), leukocytosis (white blood cell count >10×10^9/L), elevated creatinine levels (>130 μmol/L) and a marked decrease in glomerular filtration rate, requiring hemodialysis. Performing organ transplant surgery in COVID-19 does not increase the risk of adverse events but could save the lives of waitlisted terminally ill patients.

Keywords: organ transplantation, pandemic, COVID-19, SARS-CoV-2, risk factors, Russian Transplant Society.

INTRODUCTION

In the first half of 2020, the unprecedented magnitude and impact of the pandemic caused by the new SARS-CoV-2 coronavirus reached, with few exceptions, virtually every country in the world. By the end of July 2020, there have been more than 16 million cases and over 650,000 deaths. In Russia, between January 31 and July 17, 2020, 759,203 confirmed COVID-19 cases were detected, and 12,123 deaths were recorded [1]. The high rate of spread of the virus is caused by asymptomatic carrier state, high contagiosity, and long-term preservation in the environment. About 20% of patients need hospitalization, while mortality varies greatly from country to country and depends on a number of factors, ranging from 1 to 15.2% [2, 3].

The infection caused by the new SARS-CoV-2 coronavirus is a poorly studied disorder; despite the huge spread of coronavirus disease in the world, the number of observations in the recipients of transplanted organs is low. An important feature of this category of patients is the permanent risk of developing the transplant rejection which implies the need for immunosuppressive therapy. The patients of transplanted organs – heart, liver, kidneys – who are forced to receive immunosuppressive therapy for life and have a number of concomitant diseases are a group of potentially high risk of severe complications of COVID-19 [4, 5].

By early 2020, against the backdrop of the development of domestic transplantology, a large population of patients with transplanted organ had formed in the Russian Federation. Heart, liver and kidney transplantations allows to save life, to restore the ability of patients in critical, life-threatening conditions, to achieve physical and social rehabilitation. Recipients have a number of features due to physiology of transplanted organs and the need for life-long immunosuppressive therapy, which can have an unpredictable impact on the risk of SARS-CoV-2 virus infection and the clinical course of COVID-19 disease. In particular, immunosuppression increases the probability of infectious diseases [6] but reduces the risk of developing acute inflammatory response ("cytokine storm"); moreover, there is an assumption that calcineurin inhibitors which are the basis of complex immunosuppressive therapy, can inhibit intracellular replication of coronavirus [7].

The COVID-19 pandemic is dangerous not only for organ recipients, but also for severe patients with terminal heart, liver and kidney diseases included in the waiting list [8], and clinical data are needed to assess the risk-benefit ratio of surgery.

Under the auspices of the Russian Transplantology Society, the national multicenter study entitled "Prevalence and Features of the Clinical Course of Coronavirus Infection in Heart, Kidney, Liver Recipients" (ROK-KOR-Recipient) was organized to study the incidence, risk factors, clinical manifestations, and outcomes of the new coronavirus infection (COVID-19) in the recipients of the solid organs (heart, kidney, liver) receiving immunosuppressive therapy.

MATERIALS AND METHODS

Russian federal and regional centers providing medical assistance to recipients of transplanted organs in the conditions of the COVID-19 pandemic participated in the study. The inclusion criteria were the presence of a transplant organ, liver, kidney or heart, and the detected COVID-19 as well as the patient's informed consent to data processing.

The diagnosis of coronavirus infection caused by COVID-19 required either laboratory confirmation or the presence of characteristic clinical signs, including pneumonia [9], corresponding to the following ICD-10 codes: U07.1, U07.2, J12–J18. For laboratory diagnostics of SARS-CoV-2 virus infection, a viral RNA was isolated by polymerase chain reaction in samples taken from mucous membranes. The clinical criteria included signs of acute respiratory infection and respiratory failure as well as the oxygen saturation reduction at breathing atmospheric air (SpO_2 <92%) and characteristic changes detected by computer tomography of chest organs (ground glass attenuation), presence of reticular changes, consolidation sites and pulmonary tissue consolidations).

To determine the COVID-19 severity, the classification presented in the "Provisional Methodological Recommendations for Diagnosis, Prevention and Treatment of the New Coronavirus Infection of the Ministry if Health of the Russian Federation" [9] (Table 1) was used.

The study protocol included the collection and analysis of demographic and anthropometric data, as well as complaints, physical, laboratory and instrumental exa-

minations, transplant anamnesis, prescribed therapy and clinical outcomes of coronavirus infection. All recipients received immunosuppressive therapy with account for individual characteristics (individual tolerability, infection severity, risk of development of rejection etc.) as well as symptomatic and other pathogenetically based therapy determined by current clinical recommendations and treatment protocols considering clinical status.

The study results were statistically processed with the SPSS 18.0 software package (SPSS Inc., USA). Shapiro–Wilk W test was used to verify the normality of distribution. The significance of differences in the quantitative indicators meeting the normal distribution criteria was determined by Student's t-test, in other cases by Mann–Whitney U test. The groups were compared by non-parametric characteristics by Pearson chi-squared test (with observations in the group ≥10) and Fisher's exact test (with observations in the group <10). In all methods of statistical analysis, differences in $p < 0.05$ were considered to be significant.

Table 1

COVID-19 severity classification ("Temporary guidelines for the diagnosis, prevention and treatment of a new coronavirus infection of the Ministry of health of the Russian Federation" [9])

Severity	Criteria
Mild	t <38 °C, cough, weakness, throat pain Absence of criteria for medium and severe course
Medium	t >38 °C RR >22 Dyspnea at physical load Pneumonia at CT SpO_2 <95% CRP >10 mg/l
Severe	RR >30 SpO_2 ≤93% PaO_2/FiO_2 ≤300 mm Hg Progressing changes in lungs by radiology, CT (increase in lung changes by more than 50% in 24–48 h) Decreased level of consciousness, agitation Unstable hemodynamics (systolic blood pressure <90 mm Hg or diastolic blood pressure <60 mm Hg, urine output <20 ml/h) Arterial blood lactate >2 mmol/l qSOFA >2 points
Extremely severe	ARF, respiratory support needed (ALV) TSS MOSF

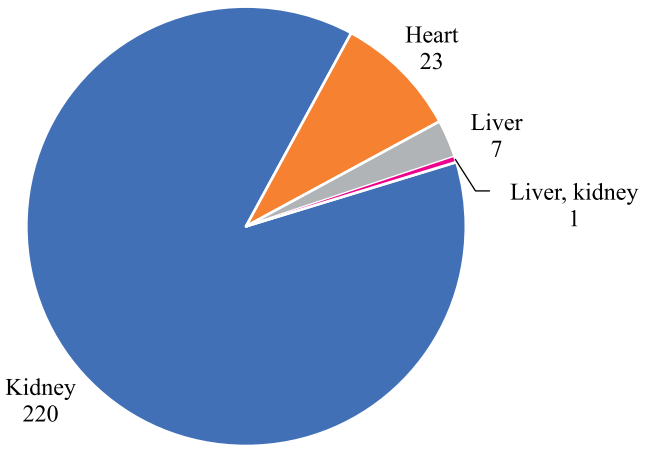

Fig. 1. Distribution of patients by transplanted organ

RESULTS

Between 01.04.2020 and 17.07.2020, 251 recipients with COVID-19 were identified and monitored in 20 regions of the Russian Federation, most of them in Moscow (66.9%)), Moscow region (5.6%), Leningrad region (4%) and Nizhny Novgorod region (4.0%) (Table 2).

The average age of patients was 48.3 ± 1.5 (13 to 77), 108 (43%) females, 143 (57%) males. The patients included 220 kidney recipients, 7 liver recipients, 1 liver and kidney recipient, 23 heart recipients (Fig. 1).

The average period from organ transplantation to the first clinical signs of COVID-19 was 363.6 ± 265.4 days (2 days to 11.5 years); 12 COVID-19 patients were diagnosed within the first 14 days after transplantation (6 after heart transplant, 6 after kidney transplant).

The most common symptoms of coronavirus infection were general discomfort and fatigue (84.4%), muscle pain (70.1%) and cough (68.9%), while anosmia and

Table 2

Distribution of organs recipients with COVID-19 by region

City, town, oblast (province)	Qty, n
Moscow	168
Moscow Oblast	14
Leningrad Oblast	10
Nizhny Novgorod Oblast	10
Novosibirsk Oblast	9
Omsk Oblast	5
Chuvash Republic	5
Republic of Tatarstan	4
St. Petersburg	4
Khanty-Mansiysk Autonomous District	4
Volgograd Oblast	3
Krasnoyarsk Kraj	3
Tula Oblast	3
Arkhangelsk Oblast	2
Rostov Oblast	2
Voronezh Oblast	1
Saratov Oblast	1
Smolensk Oblast	1
Tyumen Oblast	1
Khabarovsk Krai	1

rash were less frequent (13.5 and 4.4%, respectively), 12.4% of patients were asymptomatic (Table 3).

In most cases, the main clinical manifestation of COVID-19 was pneumonia (78.1%); the signs of extrapulmonary pathology – heart or kidney failure of various degrees of intensity – were observed in 38.3%, in 1.2% the paroxysm of atrial fibrillation developed. The average time from the first symptoms to visiting a doctor for medical treatment was 5.2 ± 3.1 days (1 to 12). At pre-assessment, the temperature above 38.5 °C was observed in 26%, 37–38.5 °C in 69.0%, in 10.8% the high temperature was not noted. In 19.3% of cases, with non-invasive determination SpO_2 <90%, in 41.2% – 90–95%, in 39.5% more than 95% was revealed.

At chest CT performed in 208 (82.9%) recipients, there were no changes (CT-0) in 12 (5.8%), ground-glass opacity which occupied less than 25% of the pulmonary parenchyma (CT-1) was found in 44 (21.2%), 25 to 50% of the pulmonary parenchyma (CT-2) in 52 (25.0%), 50 to 75% of the pulmonary parenchyma (CT-3) in 88 (42.3%), over 75% of the pulmonary parenchyma (CT-4) in 12 (5.8%).

Hospitalized were 233 patients (92.8%), the remaining 18 with a mild or asymptomatic course of coronavirus infection were observed outpatiently. In 39 patients hospitalized with COVID-19 clinical signs, the PCR primary test for virus DNA was negative, while retests were positive.

41 cases (16.3%) met the criteria for mild severity of COVID-19, 82 (32.8%), 60 (24.1%) for moderate, 67 (26.8%) for extreme severity (Fig. 2).

32 (12.8%) patients needed respiratory support (LV) with the average LV time of 9.3 ± 5.5 (3–17) days. 96 (38.3%) patients had non-invasive ventilation, while the remaining 123 had no need for ventilation. In connection with the development of expressed respiratory and heart failure in 4 patients with extremely severe COVID-19 course, the peripheral system of extracorporeal membrane oxygenation (ECMO) was implanted; two of them died on days 6 and 8 after the ECMO implantation, 2 achieved remission.

The average hospital stay was 16.1 ± 1.9 days (7 to 49). By 17.07.2020, 34 (13.5%) of the patient have died against COVID-19 infection, 186 (74.1%) were diagnosed with remission of the infectious disease, 31 (12.4%) continued treatment, 1 kidney recipient has been retransplanted.

Among liver recipients (n = 7) with COVID-19, no one was found to have either rejection or signs of transplant dysfunction; Five patients were discharged with remission, while two patients with the medium severity COVID-19 continue their treatment (hospital stay – 63 and 18 days). In 11 of 23 (47.8%) heart recipients, there were clinical signs of heart failure, and according to the endomyocardial biopsy, acute rejection of heart transplant was detected in only 7 patients – in 5 cases

Table 3

COVID-19 symptoms in organ recipients

Symptom	Rate, %
Tiredness	84.4
Muscle pain	70.1
Cough	68.9
Dyspnea	55.7
Chest discomfort	45.0
Catarrhal signs	30.0
Diarrhea	25.5
Chest pain	24.3
Anosmia	13.5
Rash	4.4
No symptoms	12.4

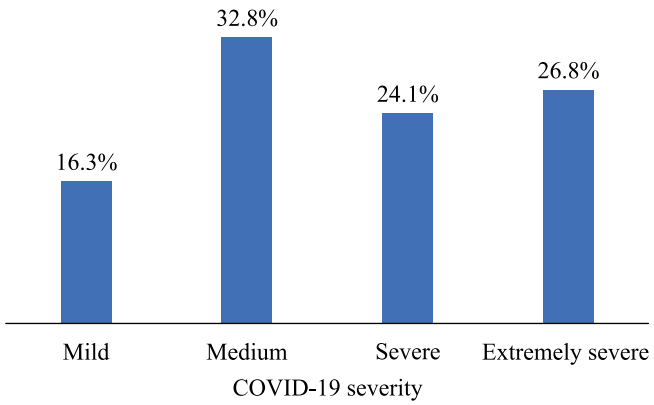

Fig. 2. The The distribution of recipients by COVID-19 severity

there were histologic signs of acute cell rejection, in two acute antibody-mediated rejection. One heart recipient with no sign of a heart transplant rejection died against the background of acute heart and respiratory failure, in all other cases remission was achieved. Of 220 kidney recipients, 78 (35.5%) had a decrease in the glomerular filtration speed of various degrees of expression. 17 cases had signs of acute cellular or antibody-mediated rejection, 2 cases – signs of acute tubular necrosis without signs of rejection. 37 (16.8%) kidney recipients needed substitution therapy. At the coronavirus infection remission, most patients had kidney function regeneration, 3 patients had a persistent loss of transplant function, and 1 had kidney retransplantation.

Table 4 shows average laboratory parameters determined before the pandemic (autumn-winter 2019), at the peak of the virus infection manifestation and a month after the remission.

At the coronavirus infection, lymphocytopenia was noted in 53.9% of patients, thrombocytopenia in 27.1%. The comparative analysis showed that in recipients with the coronavirus infection there was a significant decrease in the average white blood cell levels followed by their recovery (decrease from the initial 10.7 ± 3.3 × 10^9/l to

Table 4

Dynamics of laboratory parameters in kidney, liver, and heart recipients

Parameter	Initially	COVID-19 manifestation peak	Remission
RBC ($\times 10^{12}$/l)	3.5 ± 0.4	3.5 ± 0.2	3.6 ± 0.3
Hh (g/l)	97.9 ± 8.5	96.2 ± 7.0	108.9 ± 9.8
WBC ($\times 10^9$/l)	10.7 ± 3.3	**6.1 ± 0.7**[1]	9.2 ± 2.8
NEUT ($\times 10^9$/l)	37.6 ± 22.3	49.9 ± 11.6	34.9 ± 21.8
LYM ($\times 10^9$/l)	4.6 ± 3.3	5.1 ± 1.7	5.5 ± 1.1
MON ($\times 10^9$/l)	3.4 ± 1.7	5.9 ± 1.6	6.2 ± 3.2
PLT ($\times 10^9$/l)	233.6 ± 38.7	205.6 ± 22.4	213.3 ± 42.7
Fasting glucose, mmol/l	5.1 ± 1.1	5.6 ± 0.5	5.9 ± 1.5
Albumen, g/l	35.4 ± 2.9	35.6 ± 17.1	37.5 ± 1.8
Total bilirubin, mmol/l	7.6 ± 1.2	**11.6 ± 1.1**[1]	8.0 ± 0.9
AST, U/l	23.4 ± 9.6	**31.6 ± 5.8**[1]	**52.8 ± 13.4**[2]
ALT, U/l	15.3 ± 5.6	**31.9 ± 10.7**[1]	**65.2 ± 15.0**[2]
BUN, mmol/l	9.3 ± 7.3	**20.9 ± 4.4**[1]	15.3 ± 5.2
Creatinine, μmol/l	149.3 ± 18.7	**244.5 ± 32.3**[1]	150.1 ± 14.5
Ca, mmol/l	4.7 ± 0.3	**5.1 ± 1.7**[1]	3.9 ± 0.2
PT, s	14.5 ± 13.4	17.1 ± 12.8	18.1 ± 15.5
D-dimer, ng/ml	203.2 ± 104.2	**1304.3 ± 346.5**[1]	162.2 ± 107.1
APPT, s	30.6 ± 4.8	32.7 ± 3.4	35.9 ± 6.9

Note. The initial value of the indicators meant the values determined in the fall-winter of 2019. [1] – the value of the indicator at the peak of the manifestation of COVID-19 infection significantly differs from the baseline indicators and indicators against the background of remission; [2] – the value of the indicator against the background of remission significantly differs from the baseline values and values at the peak of the manifestation of COVID-19 infection.

$6.1 \pm 0.7 \times 10^9$/l at the coronavirus infection with subsequent recovery to $9.2 \pm 2.8 \times 10^9$/l after the remission onset). Mean levels of total bilirubin, urea, creatinine, potassium, and D-dimer increased at the acute infection and recovered 2–4 weeks after remission. At the same time, the increased mean levels of AST and ALT did not decrease after remission.

Although no effective etiotropic COVID-19 therapy has been available to date, the empirical treatment protocol included minimizing immunosuppressive therapy and prescribing medications with theoretically justified pathogenetic effects. Mycophenolic acid drugs were discontinued in all patients after clinical signs of viral infection were detected. With the viral infection manifested as immunosuppressive therapy, all heart recipients received tacrolimus preparations in monotherapy or in combination with methylprednisolone. Among 228 liver and kidney recipients, 2 (0.9%) received methylprednisolone in monotherapy, 8 (3.5%) received methylprednisolone in combination with everolymus, and 10 (4.4%) received everolymus in combination with cyclosporine or tacrolimus, 17 (7.5%) – cyclosporine in monotherapy or in combination with methylprednisolone, 191 (83.8%) – tacrolimus in monotherapy or in combination with methylprednisolone. Anticoagulant therapy (low molecular weight heparins) was provided to 74 hospitalized patients with D-dimer levels above 300 ng/ml. In addition to immunosuppressive therapy, hydroxychloroquine preparations were administered to 81 patients, preparations of IL-6 receptor antagonists: tocylizumab – 26, arilumab – 8, Janus kinase inhibitor (JAK) tofacitinib – 12, barycytinib – 9, IL-1beta inhibitor kanakinumab – 2, IL-17 inhibitor netakimab – 2, C-5 human complement component inhibitor eculizumab – 2 patients; 45 patients received immunoglobulin intravenously, 64 patients – fresh frozen plasma.

The analysis of adverse events showed that there were no liver recipients among 34 lethal cases, 33 underwent kidney transplantation (15% of all kidney recipients) and 1 – heart transplantation (4.3% of all heart recipients). It was revealed that the main fatal case predictor COVID-19 severity. Thus, according to the constructed prognostic model, in patients with a mild course of coronavirus infection, the expected fatal cases rate was 1.9% (95% CI: 0.1–4.3%), moderate – 9.7% (95% CI: 3.7–15.8%), severe – 11.8 (95% CI: 4.2–19.3%), extremely severe – 50% (95% CI: 32.4–67.6%).

Concomitant diseases were the factors reliably associated with COVID-19 severity and the risk of death of recipients, i. e. coronary heart disease, arterial hypertension, cerebrovascular disease and bronchospasm. As for the symptoms, these were the presence of shortness of breath, rash and catarrhal phenomena, and oxygen saturation at admission SpO_2 <92%, white blood cells $>10 \times 10^9$/l, an increase in creatinine levels of more than 130 μmol/l, and a significant decrease in the glomerular filtration rate requiring hemodialysis. At this, for other clinical and laboratory parameters, including age over

60, gender, the degree of increase in D-dimer levels, hydroxychloroquine preparations, etc., there was no significant relationship with the risk of adverse events against the background of COVID-19.

Between January 29 and July 1, 2020, which coincided with the period of the spread of coronavirus infection in Russia, organ transplantation was performed in 70 of the 251 patients included in the study, 56 kidney recipients, 12 heart recipients, 1 liver recipient, and 1 liver and kidney recipient. In 12 patients (4.8%) the infection was detected within the first 7 days after heart (n = 6) or kidney (n = 6) transplantation. Among the kidney recipients who died due to coronavirus infection, 5 (14.7%) died within 30 days after the kidney transplantation. One patient with COVID-19 diagnosed within a week after kidney transplantation, developed a transplant dysfunction, and on day 8 after the first operation was retransplanted. Comparative analysis did not reveal any reliable differences (p = 0.53) in the number of lethal cases between those who were operated during the COVID-19 pandemic (n = 11, 15.7%) and in 1995 to 2019 (n = 23, 12.7%).

DISCUSSION

The first results of the "ROKKOR-recipient" multicenter national study presented in the article which were obtained by analyzing the data of examination and observations of 251 liver, kidney and heart recipients with COVID-19 from 20 regions of Russia, indicate the importance of prevention and timely detection of coronavirus infection in recipients of transplanted organs. This is evidenced by the relatively high mortality (13.5%) at COVID-19. This is significantly higher than the mortality rates in the general populations of Russia (1.6%), the United States (3.4%) and China (5.4%) [3].

The lack of systematic data prevented a consensus on the impact of coronavirus infection on patients with transplanted organs. For example, one of the first reports by Chinese authors of 2 COVID-19 cases in patients with heart transplants suggested that immunosuppressive therapy may make the disease course easier for recipients and not progressing to the hyperinflammatory response stage [10]. Other Chinese authors in their analysis of the results of a small cohort study [11] concluded that there are no significant features of the course of coronavirus infection in the heart recipients. There exists an empirical hypothesis that calcineurin inhibitor, especially takrolimus, can specifically suppress coronavirus infection [12]. However, our study did not identify a link between various immunosuppressive drugs and the risk of severe course or complications of coronavirus infection. Among recipients with a severe course of coronavirus infection, the average blood concentration of the tacrolimus was lower, the percentage of patients who did not receive calcineurin inhibitor was higher, but this fact may be due to the immunosuppressive therapy reduced by attending physicians in a severe course of infection.

The study identified clinical and lab test predictors of severe COVID-19 and death of recipients. It is noteworthy that the association with the rate of adverse events was statistically significant for concomitant diseases (coronary heart disease, arterial hypertension, cerebrovascular disease, bronchospasm, diabetes mellitus, and renal failure) but not for age. In publications, age, along with concomitant cardiovascular and pulmonary diseases, obesity and diabetes mellitus, is presented as a risk factor for severe complications and death of COVID-19 patients [13, 14].

In this regard, the results of a major Russian study carried out on the basis of the I.M. Sechenov First Moscow State Medical University deserve attention. There 1,007 COVID-19 patients were included. The authors showed that acute respiratory distress syndrome caused by SARS-CoV-2 is more common in persons over 40 years of age with cardiovascular disease, type 2 diabetes mellitus and/or obesity [15].

According to the results obtained, the coronavirus infection in the recipients was most frequently expressed as pneumonia, though there was a high rate (38.3%) of extrapulmonary manifestations. The fact that the phenomena of blood insufficiency and kidney failure in most recipients were not related to the rejection of the transplanted organ against the backdrop of the immunosuppression reduction and occurred at COVID-19 remission may indicate a direct viral damage to the targeted organs.

Indeed, the membrane receptors of angiotensin transforming enzyme type 2 (ATE2) are found, besides lungs, on the surface of endothelium cells, smooth muscle cells, cardiomyocytes, etc. [16, 17]. The Russian authors have recently published a description of the clinical case of coronavirus myocardial lesions in an elderly patient with arterial hypertension [18].

Endothelium dysfunction resulted from the direct and indirect effect of coronavirus infection, platelet activation and system inflammatory response suggest a high risk of thrombotic complications [19]. Despite the fact that in the examined COVID-19 patients there was almost 6-times increase in the average levels of D-dimer, we did not identify the relationship between the levels of this marker and the risk of complications. This can be partially explained by the high frequency of empirical use of low-molecular heparin drugs in patients with high risk of developing thrombotic complications [9].

One of the most important issues discussed in various countries is the feasibility of performing organ transplantation in the context of the COVID-19 pandemic. The pandemic has been a major challenge for all national health systems. At the pandemic, the number of patients hospitalized with diseases requiring emergency care and surgical interventions [20, 21] including organ transplants [22] in the world is decreasing.

The risk of infection of organ recipients, especially in the early postoperative period, when maximum immunosuppression is required, is high due to the need for high doses of immunosuppressive medication and the risk of infection from unrecognized sources, donor, medical personnel, objects and food items. In our study, 6 heart recipients and 6 kidney recipients had SARS-CoV-2 virus detected within a week after transplantation, and the infection source remained unknown. This may be partially due to the limited capabilities of the laboratory diagnostics method itself and the probability of getting false negative results of the tests in the toolkit [23]. The donor's role as a source of infection is hardly considered; evidence of the possibility of SARS-CoV-2 virus infection through heart or kidney transplant is currently missing, although the amount of data is limited. At least a study of the biopsy results of four patients has not confirmed this possibility for SARS-CoV-1 virus [24]. It is important to note that our comparative analysis of the results of coronavirus infection in the recipients operated at the outbreak of the epidemic in Russia and in previous years, did not reveal any reliable differences.

Thus, the results of the "ROKKOR-transplant" study indicate that the presence of a transplanted organ increases the risk of adverse events at COVID-19. Risk factors for severe course and lethal cases in organ transplant recipients infected with the SARS-CoV-2 virus are concomitant cardiovascular and pulmonary diseases, diabetes mellitus and renal failure, the presence of dyspnea, rash and catarrhal signs as manifestation symptoms, as well as initially low oxygen saturation (SpO_2 <92%), white blood cells >10 × 10^9/l, an increase in creatinine levels of more than 130 μmol/l, and a significant decrease in the glomerular filtration rate requiring hemodialysis.

The analysis of the data obtained allowed us to draw an important conclusion that performing organ transplant surgery in COVID-19 does not increase the risk of adverse events but could save the lives of waitlisted terminally ill patients.

The authors declare no conflict of interest.

REFERENCES

1. WHO Coronavirus Disease (COVID-19) pandemic statistics [updated 2020 July 17]. Available from: https://covid19.who.int/region/euro/country/ru.
2. *Li Q, Guan X, Wu P et al.* Early transmission dynamics in Wuhan, China, of novel coronavirus-infected pneumonia. *N Engl J Med*. 2020; 382: 1199–1207.
3. The Johns Hopkins Coronavirus Resource Center (CRC) [Internet]. COVID-19 mortality in the most affected countries [updated 2020 July 29]. Available from: https://coronavirus.jhu.edu/data/mortality.
4. *Gori A, Dondossola D, Antonelli B, Mangioni D, Alagna L, Reggiani P et al.* Coronavirus disease 2019 and transplantation: A view from the inside. *Am J Transplant*. 2020; 1939–1940. doi: 10.1111/ajt.15853.
5. *Alberici F, Delbarba E, Manenti C et al.* A single center observational study of the clinical characteristics and short-term outcome of 20 kidney transplant patients admitted for SARS-CoV-2 pneumonia. *Kidney International*. 2020; 97 (6): 1083–1088. https://doi.org/10.1016/j.kint.2020.04.002.
6. *Russell CD, Millar JE, Baillie JK*. Clinical evidence does not support corticosteroid treatment for 2019-nCoV lung injury. *Lancet.* 2020; 395: 473–475.
7. *Siddiqi HK, Mehra MR.* COVID-19 illness in native and immunosuppressed states: A clinical-therapeutic staging proposal. *The Journal of Heart and Lung Transplantation.* 2020; 39 (5): 405–407. https://doi.org/10.1016/j.healun.2020.03.012.
8. *Junpeng Wang, Xin Li, Guanghui Cao, Xiaoqiang Wu, Zhiwei Wang, Tianzhong Yan.* COVID-19 in a Kidney Transplant Patient. *European Urology*. 2020; 77 (6): 769–770.
9. *Kamkin EG et al.* Temporary guidelines. Prevention, diagnosis and treatment of new coronavirus infection (COVID 2019), Version 6 (04/28/2020). Ministry of Health of the Russian Federation; 2020. [In Russ]. URL: http://www.rdkb.med.cap.ru/UserFiles/main/sitemap/doc/2290dc80-f2c5-4cfd-ac5c-e81d87523d97/28042020_mr_covid-19_v6.pdf.
10. *Li F, Cai J, Dong N.* First cases of COVID-19 in heart transplantation from China. *J Heart Lung Transplant*. 2020; 39: 418–419.
11. *Ren ZL, Hu R, Want ZW et al.* Epidemiological and clinical characteristics of heart transplant recipients during the 2019 coronavirus outbreak in Wuhan, China: a descriptive survey report. *J Heart Lung Transplant*. 2020; 39: 412–417.
12. *Carbajo-Lozoya J, Müller MA, Kallies S et al.* Replication of human coronaviruses SARS-CoV, HCoV-NL63 and HCoV-229E is inhibited by the drug FK506. *Virus Res.* 2020; 165 (1): 112–117. https://doi.org/10.1016/j.virusres.2012.02.002.
13. *Dzhioeva ON, Drapkina OM.* Osobennosti ul'trazvukovogo issledovaniya serdca u pacientov s novoi koronavirusnoi infekciei. *Arterial'naya gipertenziya*. 2020; 26 (3): 270–276. doi: 10.18705/1607-419X-2020-26-3-270-276.
14. *Clerkin KJ, Fried JA, Raikhelkar J, Sayer G, Griffin JM, Masoumi A et al.* Coronavirus disease 2019 (COVID-19) and cardiovascular disease. *Circulation*. 2020; 141 (20): 1648–1655. doi.org/10.1161/CIRCULATIONAHA.120.046941.
15. *Glybochko P, Fomin V, Avdeev S et al.* Clinical characteristics of 1007 intensive care unit patients with SARS-CoV-2 pneumonia. *Clin Pharmacol Ther*. 2020; 29 (2): 21–29. [In Russ]. doi 10.32756/0869-5490-2020-2-21-29.
16. *Hoffmann M, Kleine-Weber H, Schroeder S, Krüger N, Herrler T, Erichsen S et al.* SARS-CoV-2 Cell Entry Depends on ACE2 and TMPRSS2 and Is Blocked by a Clinically Proven Protease Inhibitor. *Cell*. 2020; https://doi.org/10.1016/j.cell.2020.02.052.
17. *Barbarash OL, Karetnikova VN, Kashtalap VV, Zvereva TN, Kochergina AM.* New coronavirus disease (CO-

VID-19) and cardiovascular disease. *Complex Issues of Cardiovascular Diseases*. 2020; 9 (2): 17–28. [In Russ]. doi: 10.17802/2306-1278-2020-9-2-17-28.
18. *Poteshkina NG, Lysenko MA, Kovalevskaya EA, Fomina DS, Samsonova IV, Parshin VV et al.* Cardiac damage in patients with COVID-19 coronavirus infection. *Arterial Hypertension.* 2020; 26 (3): 277–287. [In Russ]. doi: 10.18705/1607-419X-2020-26-3-277-287.
19. *Barinov VE, Boyarintsev VV.* Venous thrombotic complications as a satellite of the new coronavirus infection COVID-19. *Kremlevskaya medicina. Klinicheskii vestnik*. 2020; 2: 22–27. [In Russ]. doi: 10.26269/ayxs-2p77.
20. *De Filippo O, D'Ascenzo F, Angelini F et al.* Reduced rate of hospital admissions for ACS during COVID-19 outbreak in northern Italy. *N Engl J Med*. doi: 10.1056/NEJMc2009166.
21. *Garcia S, Albaghdadi MS, Meraj PM et al.* Reduction in ST-segment elevation cardiac catheterization laboratory activations in the United States during COVID-19 pandemic. *J Am Coll Cardiol.* 2020; 75 (22): 2871–2872. https://doi.org/10.1016/j.jacc.2020.04.011.
22. *Chui KK, Rao ARN, Chan HLY, Hui AY.* Impact of severe acute respiratory syndrome on liver transplantation service. *Transplantation Proceedings*. 2004; 36 (8): 2302–2303. https://doi.org/10.1016/j.transproceed.2004.08.018.
23. *Winichakoon P, Chaiwarith R, Liwsrisakun C et al.* Negative Nasopharyngeal and Oropharyngeal Swabs Do Not Rule Out COVID-19. *Journal of Clinical Microbiology.* 2020; 58 (5): e00297-20. doi: 10.1128/JCM.00297-20.
24. *Ding Y, He L, Zhang Q et al.* Organ distribution of severe acute respiratory syndrome (SARS) associated coronavirus (SARS-CoV) in SARS patients: implications for pathogenesis and virus transmission pathways. *J Pathol.* 2004; 203: 622–630.

The article was submitted to the journal on 20.08.2020

DOI: 10.15825/1995-1191-2020-3-18-25

TREATMENT OF BILIODIGESTIVE ANASTOMOTIC STRICTURES AFTER TRANSPLANTATION OF LEFT LATERAL SEGMENT OF THE LIVER

A.R. Monakhov[1, 2], B.L. Mironkov[1], M.A. Voskanov[1], S.V. Meshcheryakov[1], E.T. Azoev[1], K.O. Semash[1], T.A. Dzhanbekov[1], O.V. Silina[1], S.V. Gautier[1, 2]

[1] Shumakov National Medical Research Center of Transplantology and Artificial Organs, Moscow, Russian Federation

[2] Sechenov University, Moscow, Russian Federation

Many studies have shown that biliary complications after transplantation of the left lateral segment (LLS) of the liver reduce graft and recipient survival. Thus, timely correction of biliary complications, and strictures in particular, improves long-term outcomes in transplantation. **Objective:** to analyze our own experience in correcting biliary strictures in LLS graft transplantation. **Materials and methods.** From February 2014 to April 2020, 425 LLS grafts were transplanted in children. 19 (4.5%) patients were diagnosed with biliary strictures at different times after transplantation (from 0.2 to 97 months). **Results.** Biliary strictures were more often formed a year after transplantation (17.8 ± 23.9 months). In 14 out of the 19 patients, internal-external biliary drainage was successfully performed with phased replacement of the catheter with one that was larger in diameter (from 8.5 Fr to 14 Fr). The catheters were removed in 8 patients after completion of the treatment cycle. Restenosis was not observed during follow-up (13 ± 8.7 months) after the internal-external biliary drainage catheter had been removed. In 5 cases, antegrade passage of a guide wire through the stricture was unsuccessful. As a result, biliary reconstruction was performed in 4 (21.1%) patients and retransplantation was required in 1 (5.3%) patient. **Conclusion.** An antegrade minimally invasive approach can successfully eliminate biliary strictures in most children after liver LLS graft transplantation. The proposed technique is effective and safe.

Keywords: transplantation of the left lateral segment of the liver, long-term transplant outcomes, complications, biliary strictures, correction.

INTRODUCTION

Transplantation of liver fragments to children dates back to the late 1980s when R. Pichlmayer was the first in the world to use the method of split transplantation of the liver dividing it along the falciform ligament into the left lateral sector (LLS) and an enlarged right lobe that included liver segments I, IV–VIII [1]. However, in 1989, Strong performed the first successful LLS transplant from a live donor, thus pioneering, with Raia [2, 3], the relative transplants. The 90s marked a breakthrough in the field of surgical hepatology and transplantology. Since the mid-90s, liver fragments transplantation has been successfully performed in many countries, including Russia, with good outcomes and chances to save previously incurable patients. However, biliary complications have remained a serious issue, *tendo Achillis* of liver transplantation [4]. At the transplantation of liver fragments, a higher rate of such complications is common. The biliary complications rate at transplantation of liver fragments in children, according to various sources, ranges from 4% to 47.4% and is about 15% in most centers [5]. Biliary complications are commonly classified as biliary fistulas, or leaks, anastomotic strictures (AS), and non-anastomotic strictures (NAS) of biliary anastomosis [6].

The main risk factors of the development of biliary complications during transplantation of liver fragments are impaired arterial blood flow, the presence of an end biliary anastomosis, and such donor-dependent factors as coagulation injury of the ducts at withdrawal, the presence of several ducts, and their small diameter [7].

To date, there are a number of minimally invasive techniques aimed at correcting biliary strictures. Endoscopic retrograde stenting can be used in children; however, because the biliodigestive reconstruction option is main in pediatric practice, this technique cannot be widely used. Such technique as the double balloon enteroscopy is used in some clinics, though it also has limitations for use in children weighing 15 kilograms or less [6].

Percutaneous techniques are actively used in children with biliodigestive anastomosis strictures in two main options, balloon dilation and external drainage. If these

Corresponding author: Artem Monakhov. Address: 1, Shchukinskaya str., Moscow, 123182, Russian Federation. Phone: (906) 078-16-21. E-mail: a.r.monakhov@gmail.com

methods are ineffective, biliary reconstruction is indicated.

Of the Russian medical institutions, the Shumakov National Medical Research Center of Transplantology and Artificial Organs has the largest experience in the field of transplantation of liver fragments to children. Thus, the analysis of our own experience and a detailed presentation of the applied method of treatment of biliary strictures at the liver LLS transplantation may be both of scientific and practical interest.

MATERIALS AND METHODS

The present study is a retrospective analysis of a prospectively populated database as well as records in medical histories, laboratory results and instrumental studies. From February 2014 to April 2020, at the Shumakov Medical Research Center, 425 LLS liver transplants were performed in children: 399 cases from relative donors, 26 cases from cadaver donors (split transplantation). In 19 (4.5%) patients, bile duct strictures were diagnosed at different times after transplantation (0.2 to 97 months). These patients have been included in the present study. The study was approved by the ethics committee of the Center.

Immunosuppression

Immunosuppressive therapy included induction therapy with basiliximab, intravenous infusion of methylprednisolone at the time of graft reperfusion at 10 mg/kg (followed by minimization or withdrawal during the early postoperative period) and supportive therapy based on calcineurin inhibitors (tacrolimus); mycopholenic acid drugs were used optionally, in accordance with the clinical and laboratory picture. In cases of liver transplantation from blood group-incompatible related donors, the previously described preparation protocol used, which included the possibility of plasmapheresis with AB (IV) FFP replacement and rituximab administration.

Biliary reconstruction

Biliary reconstruction was performed after vascular revascularization of the graft with the Roux limb of the jejunum. The limb was 40–50 cm long. In the case of the preceding portoenterostomy, the previously formed limb was retained under the following conditions: confidence in the limb viability (absence of extensive deserosation, multiple perforations and circulatory disorders in the limb after enterolysis), limb length over 35 cm, no history of multiple recurrent cholangitis. The anastomosis was formed with separate PDS 6.0 interrupted stitches with 1–1.5 mm duct pitch. In case of two or more ducts at less than 4 mm distance, they were combined on a preparation table or immediately before the start of biliary reconstruction along the medial walls to form a common orientation. If the unit of the ducts was impossible, separate fistulas were formed. The anastomosis was performed with 3x binocular loupes. To prevent bile leakage, the original technique of peritonization of the biliodigestive anastomosis wall with the round graft ligament was used [8]. Since September 2017, Felker external stented drainage with a 22–16 Ga catheter (depending on the ducts diameter) has been routinely used.

Stricture diagnosis

At the transplantation center, follow-up of transplant cases is a standard practice. The protocol for inpatient and outpatient examination of children after liver transplantation includes physical examination and control of laboratory parameters as well as ultrasound of the abdominal organs. If the clinical and laboratory picture of cholestasis (including itching, GGT and bilirubin increase, stool hypocholia, etc.) or cholangitis symptoms were combined with the bile ducts expansion of more than 5 mm, the MR cholangiography was done as the basis for the biliodigestive anastomosis stricture diagnosis. At this, arterial blood flow disorders in history and characteristic MRI cholangiography and ultrasound patterns were the basis for the NAS diagnosis.

However, if the ducts dilatation was not accompanied by any clinical and laboratory changes, dynamic observation and conservative therapy, including choleretic therapy, were continued.

Description of the technique of percutaneous transhepatic external-internal drainage

The method used for percutaneous transhepatic external-internal drainage was based, with some minor assumptions, on the technique described in detail in Feier [5]. In our practice, a Chiba 18 Ga needle was used for percutaneous puncture. The puncture was performed in the X-ray operating room (Philips Allura Xper FD 20 OR Table, Netherlands and Shimadzu Bransist alexa, Japan) under ultrasound guidance (Fig. 1). The puncture point was usually located in the epigastrium along the midline. The 2nd segment duct was considered optimal for drainage. After the bile intake, with the mandrel removed, a small amount of a water-soluble contrast (Ultravist 370, Optiray 350 diluted with sterile saline solution 1:4) was injected, thus partially contouring the biliary tree of the graft. After that, the guidewire was inserted, the Chiba needle was changed for II 4 Fr, 5 Fr, 6F Terumo Radifocus Introducer and with the help of various catheters (Merit Medical Performa CB1 5F, USA, Merit medical Performa KA2 4-5F, USA, Terumo Radifocus Optitorque radial TIG II 3.5 5F, Japan), diagnostic guidewires (Asahi intecc UniQual Slip-Coat Guidewire 0.035″, Biometrix Angio-Line guidewire 0.35″) and coronary guidewires (Asahi intecc Prowaterflex 0.014″, Japan; Asahi intecc Fielder 0.014″, Japan; Boston Scientific PT2 LS

0.014″ USA), we attempted to pass the stricture. In case of successful stricture passage with characteristic signs of a guidewire and contrast entering the jejunal loop

Fig. 1. Ultrasound-guided punction of the bile ducts of a liver transplant

(guidewire-formed "large loops", contrasting circular folds of the small intestine mucosa), a Dawson-Muller drainage (Cook Medical, USA) with 8.5 Fr diameter was installed along the guidewire with additionally formed 2–3 holes on the straight part of the drainage. If drainage was impossible due to expressed strictures, the balloon dilatation was performed (Medtronic Sprinter Legend RX balloon catheters, USA, d 1.25 mm, l 10–12 mm; d 1.5 mm, l 12–15 mm; d 2.0 mm, l 15–20 mm. The distal loop was installed in the intestine with a fixation built in the drainage (Fig. 2).

For 2–3 days, to prevent reactive cholangitis, external bile diversion has been performed through the drainage, with the subsequent, in the absence of cholangitis signs and an improved laboratory picture, drainage block. The child was observed for several more days and discharged. Subsequently, the drainage was changed with an interval of about 3 months for large diameters (10.2; 12; 14 Fr) and upon reaching the maximum diameter, the drainage was removed with balloon control for angioplasty with a diameter of 5–7 mm (controlling the absence of a "waist" on the balloon).

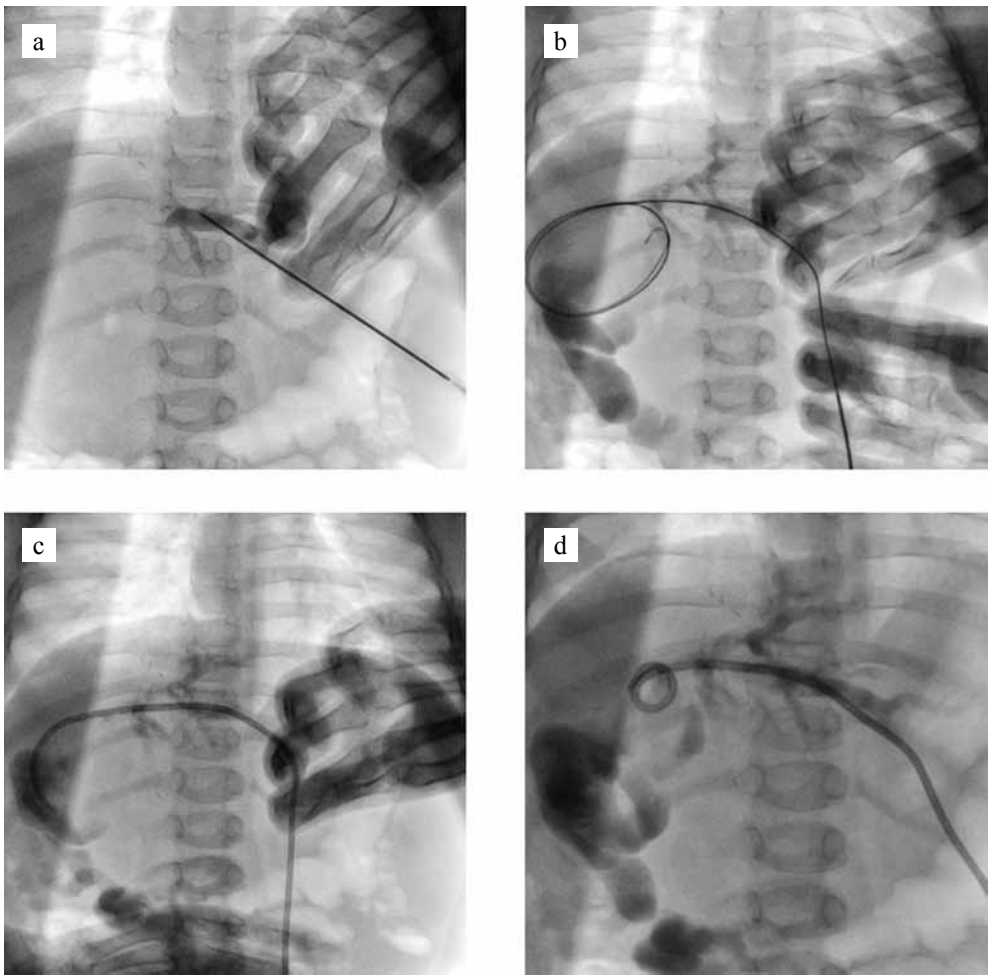

Fig. 2. The steps of an internal-external drainage set up: a – a contrast agent inserted to the dilated biliary duct; b – the guide conducted through the stricture into the Roux limb; c – the Dawson-Muller drainage passed into the Roux limb; d – the pig-tale of internal-external drainage placed behind the stricture and locked

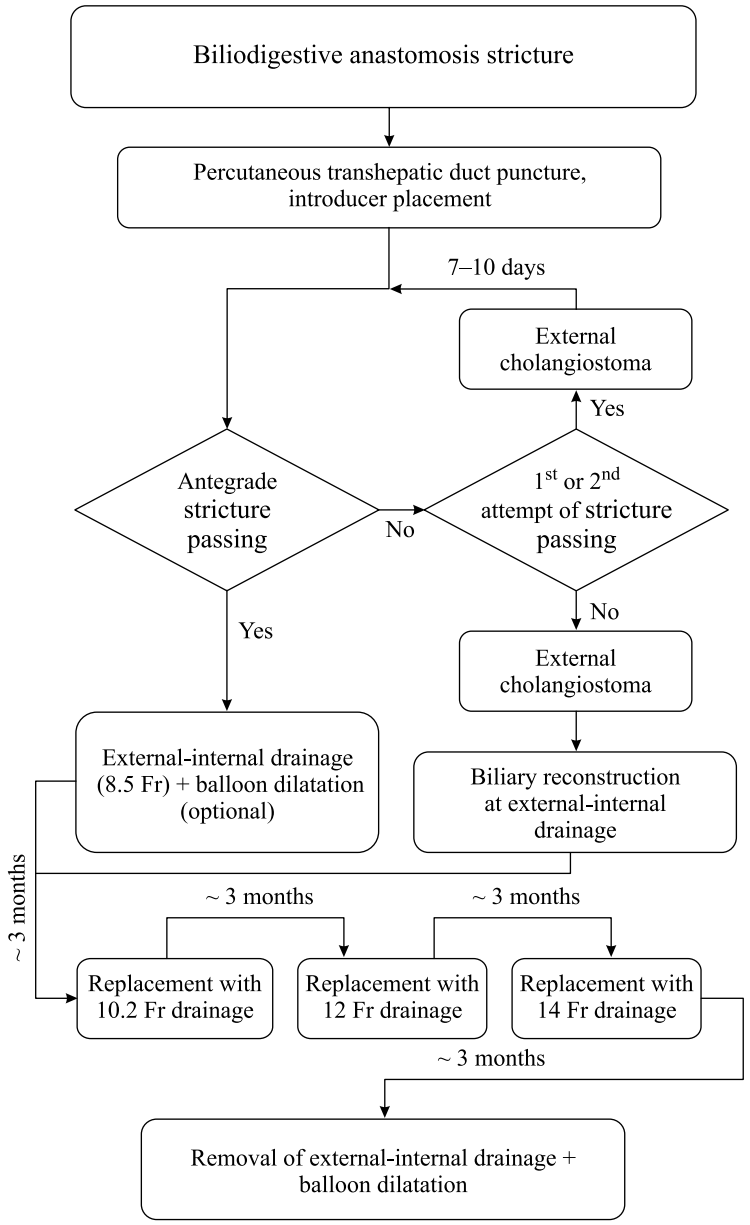

Fig. 3. The algorithm of biliary stricture management after LLS transplantation

If it was not possible to pass the stricture, an external cholangiostomy was left to decompress the bile ducts, and in 7–10 days an attempt was repeated to pass the stricture. If the stricture was not passed then, the need for the third attempt was decided individually, or biliary reconstruction was routinely performed. The algorithm is shown in Fig. 3 as a flowchart.

RESULTS

Table 1 shows the demographic and clinical characteristics of the recipients. The most frequent disease that led to the need for transplantation in the studied patients was biliary atresia (8 cases, 42.1%) and hepatic fibrosis, or Caroli syndrome (6 cases, 31.6%). In most cases (84.2%), a related LLS transplantation was performed. More often, biliary strictures developed in over a year after transplantation (17.8 ± 23.9 months), in most cases being anastomotic (n = 17; 89.5%).

Table 2 summarizes some features of staged treatment by the above algorithm. Thus, the antegrade passage of the stricture was successful in 14 of 19 observed cases. In this, the second attempt, i. e., after the formation of an external cholangiostomy, was more often successful (n = 7; 36.8%). At the time of the article submission, in 8 out of 14 patients (42.1%), the external-internal drainage was removed, i. e., the treatment cycle was completed. Of the five cases when the antegrade stricture failed to pass, biliary reconstruction was performed in four and in one – successful liver transplantation from a cadaver donor due to the formation of secondary biliary cirrhosis.

The results of treatment in patients with antegrade external-internal stenting are given in Table 3. The time

Table 1

Baseline demographic and clinical characteristics of LLS recipients with biliary stricture

Parameters	
Age*, months, mean ± SD	27.9 ± 30.1
Weight*, mean ± SD	11.3 ± 4.3
Gender, n (%)	
male	11 (57.6)
female	8 (42.1)
Diagnosis, n (%)	
Atresia	8 (42.1)
Byler	1 (5.3)
Caroli	6 (31.6)
Hypoplasia	1 (5.3)
Tyrosinemia	1 (5.3)
Galactosemia	1 (5.3)
Alpha1-Ab deficiency	1 (5.3)
PELD score, mean ± SD	21 ± 9.4
Transplantation, n (%)	
Relative LLS	16 (84.2)
Split LLS	3 (15.8)
Biliary anastomoses, n (%)	
1	13 (68.4)
2	5 (26.3)
3	1 (5.3)
Biliary stricture type, n (%)	
Anastomotic	17 (89.5)
Non-anastomotic	2 (10.5)
Stricture development after transplantation, months, mean ± SD	17.8 ± 23.9

Note. * – at the time of transplantation; PELD – Pediatric End-stage Liver Disease.

Table 2

Features of treatment of recipients with biliary stricture after liver transplantation

Parameters	
Stricture passing, n (%)	
At the 1st stage	5 (26.3)
At the 2nd stage	7 (36.8)
At the 3rd stage	2 (10.5)
Failed	5 (26.3)
Drainage replacement, n (%)	
1	2 (10.5)
2	2 (10.5)
3	2 (10.5)
Full cycle (removal)	8 (42.1)
Biliary reconstruction	4 (21.1)
Regrafting, n (%)	1 (5.3)

Table 3

The results of treatment in patients with percutaneous transhepatic antegrade external-internal drainage

Patients with interventional treatment (n = 14)	
Mean time between replacements, days, mean ± SD	
1st replacement (10.5 Fr)	101.8 ± 47.3
2nd replacement (12 Fr)	106 ± 41
3rd replacement (14 Fr)	110.6 ± 28
Drainage removal	115.7 ± 34.2
Follow-up*, months, mean ± SD	13 ± 8.7
Outcome, n (%)	
Favorable	7 (87.5)
Restenosis	–
Cholangitis episodes	1 (12.5)

Note. * – after removing the external-internal drainage.

between staged drainage replacements ranged from 101 to 116 days. The average follow-up period in 8 patients with fully completed treatment was more than a year (13 ± 8.7 months). During this period, only one of these patients developed cholangitis, which was relieved by systemic antibiotic therapy, and in no case there was a restenosis of the biliodigestive anastomosis.

DISCUSSION

According to numerous studies, biliary complications affect the survival of both grafts and recipients [9–12].

Also, for a number of reasons, endoscopic techniques are also not always optimal. Open reconstructions often become extensive surgical interventions, especially in the long term after transplantation, due to the intensive adhesion process. An effective minimally invasive technique for correcting complications is essential for transplantology. This applies to other aspects of the liver transplant program, which makes the presence of interventional radiology an important part of the transplantation center.

The percutaneous external-internal (antegrade) drainage with stenting has gained popularity in the treatment of various kinds of strictures of the hepato-pancreato-biliary zone. The basic principles and approaches were also transposed to the treatment of biliary strictures after transplantation of liver fragments.

The present article sets out the basic principles of antegrade treatment of biliary strictures in a rather narrow category of patients, liver LLS recipients. The state of permanent drug suppression, children's age, the type of transplanted fragment and biliodigestive option of bile diversion are the distinctive features of these patients.

The use of exclusively balloon dilation without prolonged formation of an anastomosis on the frame in the form of external-internal drainage is featured by a higher rate of restenosis [13–15]. In this regard, the presented technique allows the stricture to be resolved with a good long-term effect. Also, two cases of successful treatment of such a formidable and severe complication as NAS should be noted, which made it possible to avoid the need for regrafting these patients. In the present study, antegrade passage of the stricture was unsuccessful in five cases,

of which in four cases (21.1%) biliary reconstruction was required and in one case (5.3%) retransplantation. It should be noted that the presence of a cholangiostomy before the operation not only allowed stabilizing the patient by resolving jaundice and / or cholangitis, but also served as a convenient guide for navigation in conditions of a pronounced adhesive process. It was also made possible to comfortably form an anastomosis on the external-internal drainage.

The study was limited by a relatively small number of observations associated with the relatively low frequency of this complication (4.5%). Despite the fact that the study is single-center and non-randomized, the clinic's successful long-term experience may be useful for other medical institutions dealing with liver fragment transplantation.

CONCLUSION

Timely diagnosis and correction of biliary strictures after transplantation of liver fragments allows avoiding the graft loss. The minimally invasive approaches with interventional radiology can effectively eliminate biliary strictures in most children after transplantation of the left lateral sector of the liver. The proposed technique is effective and safe.

The authors declare no conflict of interest.

REFERENCES

1. *Pichlmayr R, Ringe B, Gubernatis G, Hauss J, Bunzendahl H.* Transplantation of a donor liver to 2 recipients (splitting transplantation) – a new method in the further development of segmental liver transplantation. *Langenbecks Archiv fur Chirurgie*. 1988; 373 (2): 127–130. PMID: 3287073.
2. *Strong RW, Lynch SV, Ong TH, Matsunami H, Koido Y, Balderson GA.* Successful liver transplantation from a living donor to her son. *N Engl J Med*. 1990; 322: 1505–1507. doi: 10.1056/NEJM199005243222106.
3. *Raia S, Nery JR, Mies S.* Liver transplantation from a live donors. *Lancet*. 1989; 8661: 497. doi: 10.1016/s0140-6736(89)92101-6.
4. *Yoshizumi T, Harada N, Mori M.* Biliary stricture: the achilles heel of pediatric living donor liver transplantation. *Transplantation*. 2019; 103 (9): 1758–1759. doi: 10.1097/TP.0000000000002573.
5. *Feier FH, da Fonseca EA, Seda-Neto J, Chapchap P.* Biliary complications after pediatric liver transplantation: Risk factors, diagnosis and management. *World J Hepatol*. 2015; 7 (18): 2162–2170. doi: 10.4254/wjh.v7.i18.2162.
6. *Jagannath S, Kalloo AN.* Biliary complications after liver transplantation. *Curr Treat Options Gastroenterol*. 2002; 5 (2): 101–112. doi: 10.1007/s11938-002-0057-3.
7. *Feier FH, Chapchap P, Pugliese R et al.* Diagnosis and management of biliary complications in pediatric living donor liver transplant recipients. *Liver Transpl*. 2014; 20 (8): 882–892. doi: 10.1002/lt.23896.
8. *Gautier SV, Monakhov AR, Tsiroulnikova OM, Dzhanbekov TA, Meshcheryakov SV, Semash KO.* Retrospektivnyj analiz primenenija modifikacii biliarnoj rekonstrukcii pri transplantacii levogo lateral'nogo sektora pecheni. *Russian Journal of Transplantology and Artificial Organs*. 2017; 19 (3): 6–230. [In Russ] https://doi.org/10.15825/1995-1191-2017-3-6-230.
9. *Darius T, Rivera J, Fusaro F et al.* Risk factors and surgical management of anastomotic biliary complications after pediatric liver transplantation. *Liver Transpl*. 2014; 20 (8): 893–903. doi: 10.1002/lt.23910.
10. *Chok KS, Chan SC, Chan KL et al.* Bile duct anastomotic stricture after pediatric living donor liver transplantation. *J Pediatr Surg*. 2012; 47 (7): 1399–1403. doi: 10.1016/j.jpedsurg.2011.12.014.
11. *Lüthold SC, Kaseje N, Jannot AS et al.* Risk factors for early and late biliary complications in pediatric liver transplantation. *Pediatr Transplant*. 2014; 18 (8): 822–830. doi: 10.1111/petr.12363.
12. *Feier FH, Seda-Neto J, da Fonseca EA et al.* Analysis of factors associated with biliary complications in children after liver transplantation. *Transplantation*. 2016; 100 (9): 1944–1954. doi: 10.1097/TP.0000000000001298.
13. *Okhotnikov OI, Jakovleva MV*. Radiosurgical antegrade transhepatic correction of the biliodigestive anastomosis stricture. *Annals of HPB Surgery*. 2012; 17 (3): 110–113 [In Russ].
14. *Kulezneva YV, Bruslik SV, Musaev GH, Israilov RE, Kirillova MS.* Percutaneous modalities of biliary decompression: development and disputable items. *Annals of HPB Surgery*. 2011; 16 (3): 35–43 [In Russ].
15. *Prajapati HJ, Kavali P, Kim HS.* Percutaneous interventional management of biliary complications after pediatric liver transplantation: A 16-year single-institution experience. *Pediatr Transplant*. 2017; 21 (1): 10.1111/petr.12837. doi: 10.1111/petr.12837.

The article was submitted to the journal on 17.06.2020

DOI: 10.15825/1995-1191-2020-3-26-35

PRIORITIZATION FOR LIVER TRANSPLANTATION

V.L. Korobka[1, 2], M.Y. Kostrykin[1], V.D. Passetchnikov[1, 3], E.S. Pak[1, 2]

[1] Rostov Regional Clinical Hospital, Rostov-on-Don, Russian Federation
[2] Rostov State Medical University, Rostov-on-Don, Russian Federation
[3] Stavropol State Medical University, Stavropol, Russian Federation

Objective: to determine the threshold MELD scores when prioritizing for liver transplantation. **Materials and methods.** We conducted a cohort study of 350 patients who were waitlisted for liver transplantation between 2015 and 2020. **Results.** A logistic regression model was used to identify the independent predictors of liver transplantation waitlist mortality. MELD scores and serum albumin at the time of listing were significant predictors of mortality ($p = 0.001$ and $p = 0.004$, respectively). Their predictive values were confirmed using ROC (Receiver Operating Characteristic) analysis. The area under the ROC curve (AUC) was 0.883 [95% confidence interval (CI) 0.828–0.939; $p < 0.001$] for MELD, and 0.841 [95% CI 0.775–0.907; $p < 0.001$] for serum albumin. Mortality odds ratio was 3.7778, 95% CI (1.619–7.765) provided that the listing MELD score was ≥25. Mortality odds ratio was 2.979 (95% CI 1.63–5.95) provided that the listing serum albumin concentration was ≤30.1 g/L. With a threshold MELD score of 25, there were significant differences between patient survival when comparing patient cohorts with MELD ≥25 and with MELD ≤25 (Log-rank, $p < 0.0001$). **Conclusion.** The MELD model has a high predictive ability in prioritization of waitlisted candidates for liver transplantation. The threshold MELD score and mortality predictors were determined. There were significant differences between patient survival among patient cohorts with MELD ≥25 and with MELD ≤25.

Keywords: liver transplant waiting list, MELD threshold, patient survival, prioritization for liver transplantation.

INTRODUCTION

Since the first liver transplant was performed by an American surgeon Thomas Earl Starzl [1], the operation has radically changed the treatment of severe liver diseases, significantly improving the survival of patients.

Currently, liver transplantation (LT) is a choice therapy for terminal liver diseases, fulminant hepatic failure and some types of hepatocellular carcinoma (GCC) [2]. The increased indications, the higher number of patients included in the waiting list (WL) for liver transplantation caused a severe shortage of donor livers in almost all countries [3–5].

In the Russian Federation, the need for LT in patients with various severe liver diseases far exceeds the resources of transplant centers. In 2018, according to the national register, 1,830 people were waitlisted, and in the same year LT was performed in 505 patients, thus reaching 3.4 per 1 million population [6].

Thus, the continued worldwide growth in the number of patients waitlisted for LT challenges healthcare organizers and transplant experts to determine the best ways to prioritize patients in need of this treatment. Many countries of the world have started the institutions to promptly regulate the distribution of donor organs for patients with the highest mortality risk. In the United States, such donor organs distribution tactics is performed by The United Network for Organ Sharing (UNOS) NGO [7].

The optimal time for LT has not yet been determined, as it is not clear at what stage of liver cirrhosis the need to perform this operation arises [8]. Besides, in conditions of significant excess of donor liver demand exceeding the supply, the primary task is not only to determine the timing of organ transplantation, but also to consider the correct selection of recipients [8, 9].

When the LT was just developing, such methods as the time in the WL, the disease severity, MELD score, etc. were used to prioritize patients [10, 12–14]. However, the transplant community has not yet come to consensus on what the ideal organ donation rate for LT should be. For example, some suggest that the prioritization of patients with LT should base on the difference between the survival rate after liver transplantation and the survival rate of patients that are still in WL [11].

An ideal indicator for organ allocation would help identify a relatively narrow group of patients, e. g., one similar in size to the number of available donors and adhere to the principle of prioritization according to medical needs. When prioritizing waitlisted patients, the MELD threshold above which LT will be most beneficial in reducing patient mortality should be considered.

Objective: to determine the threshold MELD scores when prioritizing the patients for liver transplantation.

Corresponding author: Victor Passetchnikov. Address: 21, Aviatsionnaya str., Stavropol, 355017, Russian Federation. Phone: (962) 447-75-13. E-mail: passetchnikov@mail.ru

MATERIALS AND METHODS

In the course of the cohort study of patients observed at the Center for Surgery and Donor Coordination of the Rostov Regional Clinical Hospital, 350 patients – candidates for LT were included in WL from 2015 to 2020. The study was approved by the Ethics Committee of the Rostov Regional Clinical Hospital.

Inclusion criteria

The absolute criteria for waitlisting the patients with terminal liver diseases was the lack of the effect of conservative therapy in the previous stages. Additional indications were the following: ascites or hepatic hydrothorax development, antibiotic relief of spontaneous bacterial peritonitis (SBP) in the disease history, the presence of cholestasis, hepatic encephalopathy (HE) and / or gastrointestinal varicose bleeding. The condition for inclusion in WL of the patients with alcoholic liver disease (ALD) was the abstinence for at least 3 months confirmed by the conclusions of experts in narcology and psychiatrists. At waitlisting, in the dynamics of the disease course and the development of any outcomes, the following indicators were calculated: the original and improved indices, MELD [14] and MELD-Na [15] as well as the Charlson comorbidity index (CCI) and Child-Turcotte-Pugh (CTP). The patients were waitlisted at MELD ≥16.

Exclusion criteria

Patients with severe pulmonary heart disease and those continuing alcohol ingestion at the time of the study were excluded. The study did not include HCC patients, the patients waitlisted due to decompensation and delisted due to reasons other than recompensation. The study excluded patients waitlisted for reasons other than decompensation (recurrent cholangitis at primary sclerosing cholangitis), as well as waitlisted patients for the following reasons: widespread thrombosis of portal vein and its main arteries; Budd-Chiari syndrome, sinusoidal obstruction syndrome; polycystic liver disease, and amyloidosis. The patients waitlisted for regrafting or with previous transplants of other organs and patients with acute liver failure were to be excluded from the study.

Diagnostic testing

At waitlisting, the patients underwent clinical examinations, laboratory tests of blood and urine, biochemical and hemostasis parameters studies. HBV and HCV screening and diagnosis were based on enzyme-linked immunosorbent assay (ELISA) for the corresponding markers and qualitative and quantitative determination of viruses in blood by polymerase chain reaction (PCR). All patients underwent elastography and in some cases, liver biopsy followed by morphological examination. Ascitic fluid analysis was made in some patients.

Therapy

Conservative therapy in the waitlisted patients was performed by syndromes, with non-selective β-blockers, diuretics, L-ornithine-L-aspartate combined with lactulose and rifaximin per os (if the overt or latent hepatic encephalopathy was present). Some patients underwent extracorporeal hemocorrection (plasma adsorption and prolonged veno-venous hemodiafiltration). If HCV and HBV infections were diagnosed, all patients received antiviral therapy, which included direct antiviral (HCV) drugs and nucleoside reverse transcriptase inhibitors (HBV). In patients with autoimmune diseases, therapy included immunosuppressants and glucocorticosteroids.

In connection with recurrent varicose bleeding, some patients received transjugular portosystemic shunts (TIPS) and azigo-portal disconnection (APD) surgery according to the original technique (RF patent 2412657) [16]. Orthotopic liver transplantation (OLT) was performed in 59 patients.

Study design

Depending on the disease outcome, the patients waitlisted at the Center for Surgery and Donor Coordination of the Rostov Regional Clinical Hospital were divided into 4 cohorts. The first cohort included 51 patients with LC recompensation due to the therapy. The criteria for the diagnosis of liver cirrhosis (LC) recompensation were the absence of ascites and / or hepatic hydrothorax; absence of peripheral edema (at diuretics discontinuation); absence of PE (without drugs aimed at stopping it); decrease in the MELD (≤15) and CTP for at least 6 months with confirmed steady compensation of liver function [17]. The second cohort (liver function subcompensation) consisted of 153 patients who failed to achieve CP recompensation and remained in WL. The third cohort included 87 patients with lethal outcomes. The fourth cohort consisted of 59 patients who underwent OLT.

The **primary endpoint** was a survival study for the waitlisted patients. The **secondary endpoint** of the study was the definition of the MELD threshold values to prioritize the selection of LT candidates.

Statistical data processing

The data was analyzed using the IBM SPSS Statistics software (v. 21). The type of distribution of the obtained data and the subsequent choice of parametric or nonparametric analysis was determined with Kolmogorov–Smirnov test. In case of normal distribution of samples, the data were represented by arithmetic means (M) and standard deviation (SD) with 95% confidence interval (CI). The statistical significance of the diffe-

rences between the compared parameters with normal distribution was determined by Student's t-test. If the sample showed the absence of the normal distribution, nonparametric tests were used: Wilcoxon for paired comparisons of dependent variables, Mann–Whitney (U test), Pearson's Chi-square for comparison of independent variables. Quantitative indicators in samples with a distribution other than normal were presented in the form of a median and an interquartile range (IQR), the interval between the 25th and 75th percentiles. Frequencies and proportions (%) were calculated to assess the qualitative data. Differences between the compared parameters were considered statistically significant with the error rate less than 0.05 ($p < 0.05$).

Mortality predictors were defined through regression analysis (logistic regression). The odds ratio was calculated for significant mortality predictors with 95% CI. To assess the quality of the regression model (predictive power of the model), ROC curves (Receiver Operating Characteristic) were plotted, and the AUC (Area Under Curve) was calculated. The statement that the AUC ROC does not differ from 0.5 [18] was taken as a null hypothesis.

The survival rate was assessed by Kaplan–Meier, the mean and median survival times were determined by criteria of Log-Rank (Mantel-Cox), Breslow, and Tarone-Ware.

RESULTS

In Kolmogorov–Smirnov test, patients' age, body mass index (BMI), leukocyte count, albumin concentration, MELD, MELD-Na at the time of waitlisting corresponded to the normal distribution and were analyzed with parametric statistics methods.

Such parameters as the severity of hepatic encephalopathy, alkaline phosphatase activity, Na, creatinine and bilirubin concentrations, INR, CCI and CTP at the time of waitlisting did not correspond to the normal distribution, and nonparametric statistical methods were used for their subsequent analysis (Mann–Whitney, U-test, Chi-square).

Tables 1 and 2 show demographic parameters, the results of clinical, laboratory studies, BMI, MELD, MELD-Na, CCI, and CTP in cohorts of patients with LC recompensation (n = 51), LC subcompensation (n = 153), the patients who died during their stay in WL (n = 87) and those who underwent OLT (n = 59).

Fig. 1 shows the MELD of the waitlisted patients of all cohorts. The MELD index in the group of patients with lethal outcomes significantly differed from the parameters of other compared cohorts. Patients with LC recompensation and lethal outcomes were subjected to regression analysis (logistic regression). MELD and blood plasma albumin ($p = 0.001$ and $p = 0.004$, respectively) were significant mortality predictors.

AUCs were calculated for MELD scores and albumin concentrations, and ROC curves for these parameters were plotted (Fig. 2).

AUC ROC for MELD was 0.883 [95% CI 0.828–0.939; $p < 0.001$]. AUC ROC for albumin concentration was 0.841 [95% CI 0.775–0.907; $p < 0.001$].

The odds ratio (OR) for the development of mortality, provided that at waitlisting MELD score ≥25, was 3.778, 95% CI (1.619–7.765). The OR for the development of mortality, provided that at waitlisting the concentration of plasma albumin ≤30.1 g/L, was 2.979 (95% CI 1.63–5.95).

The survival was analyzed depending on MELD scores with Kaplan–Meier and Log-rank (Mantel-Cox), Breslow, and Tarone-Ware criteria. The study showed that the survival rate of waitlisted patients depended on the MELD score. There were significant differences between patient survival when comparing cohorts of patients with MELD scores ≥25 and ≤25 (Log-rank, $p < 0.0001$; Breslow, $p < 0.0001$; Tarone-Ware, $p < 0.0001$). According to the developed model, the function of survival was identified with the development of mortality at certain times for specific patients (Fig. 3).

Table 1

Comparative characteristics of patient indices in study cohorts with normal distribution of the data sample

Parameters at waitlisting	Cohorts of patients			
	1 (n = 51) M ± SD	2 (n = 153) M ± SD	3 (n = 87) M ± SD	4 (n = 59) M ± SD
Age, years	48.35 ± 9.93*	51.85 ± 9.32	50.98 ± 11.35^{e}	45.02 ± 11.94^{a}
BMI, kg/m^2	27.72 ± 4.47	26.80 ± 4.46	24.50 ± 4.18^{e}	25.29 ± 4.13^{ad}
WBC, ×10^9/l	3.75 ± 0.49*	3.34 ± 0.69^{e}	2.69 ± 0.74^{m}	3.22 ± 0.70^{cd}
Plasma albumin, g/l	37.76 ± 4.73	33.27 ± 6.79	28.39 ± 7.67^{m}	31.69 ± 5.18^{acd}
MELD-Na	18.33 ± 1.93*	20.59 ± 4.46^{e}	25.97 ± 8.30^{m}	20.93 ± 5.64^{cd}

Note. 1 – LC recompensation; 2 – LC subcompensation; 3 – died in WL; 4 – OLT; * – $p < 0.05$ comparison between groups 1 and 2; ^{a} – $p < 0.05$ comparison between groups 2 and 4; ^{c} – $p < 0.05$ comparison between groups 3 and 4; ^{d} – $p < 0.05$ comparison between groups 1 and 4; ^{e} – $p < 0.05$ comparison between groups 2 and 3; ^{m} – $p < 0.05$ comparison between groups 1 and 3.

Table 2

Comparative characteristics of patient indices in study cohorts in the absence of normal distribution of the data sample

Parameters at waitlisting	Cohorts of patients			
	1 (n = 51) Median (IQR) or %	2 (n = 153) Median (IQR) or %	3 (n = 87) Median (IQR) or %	4 (n = 59) Median (IQR) or %
Male gender, %	64.7	50.3	55.2	57.6
Hepatic encephalopathy severity	2.0 (1.0–2.0)*	2.0 (2.0–2.0)^{e}	2.0 (3.0–3.0)^{m}	2.0 (2.0–3.0)^{d}
CCI	7.0 (5.0–8.0)*	9.0 (7.5–11.0)	14.0 (13.0–14.0)^{m}	9.0 (7.0–11.0)^{d}
CTP	14.0 (13.0–14.0)	14.0 (12.0–14.0)	14.0 (13.0–14.0)	14.0 (13.0–14.0)^{a}
PLT, $\times 10^9$/l	94.0 (78.0–126.0)*	67.0 (49.0–96.0)^{e}	45.0 (32.0–72.0)^{m}	43.0 (58.0–86.0)^{cd}
ALP, U/l	243.0 (167.0–365.0)	273.0 (148.5–383.5)^{e}	387.0 (286.0–500.0)^{m}	287.0 (217.0–401.0)^{c}
Na, mmol/l	139.0 (137.0–141.0)*	138.0 (136.0–140.0)^{e}	137.0 (136.0–139.0)^{m}	138.0 (136.0–140.0)^{cd}
Creatinine, μmol/l	109.0 (93.0–120.0)	112.0 (86.0–132.5)^{e}	139.0 (111.0–187.0)^{m}	120.0 (96.0–143.0)^{acd}
Bilirubin, μmol/l	79.0 (61.0–103.0)*	72.0 (51.0–95.0)^{e}	93.0 (58.0–198.0)^{m}	72.0 (48.0–96.0)^{cd}
IHR	1.4 (1.4–1.6)*	1.8 (1.6–2.0)^{e}	2.0 (1.6–2.5)^{m}	1.6 (1.4–1.8)^{ad}

Note. 1 – LC recompensation; 2 – LC subcompensation; 3 – died in WL; 4 – OLT; * – $p < 0.05$ comparison between groups 1 and 2; ^{a} – $p < 0.05$ comparison between groups 2 and 4; ^{c} – $p < 0.05$ comparison between groups 3 and 4; ^{d} – $p < 0.05$ comparison between groups 1 and 4; ^{e} – $p < 0.05$ comparison between groups 2 and 3; ^{m} – $p < 0.05$ comparison between groups 1 and 3.

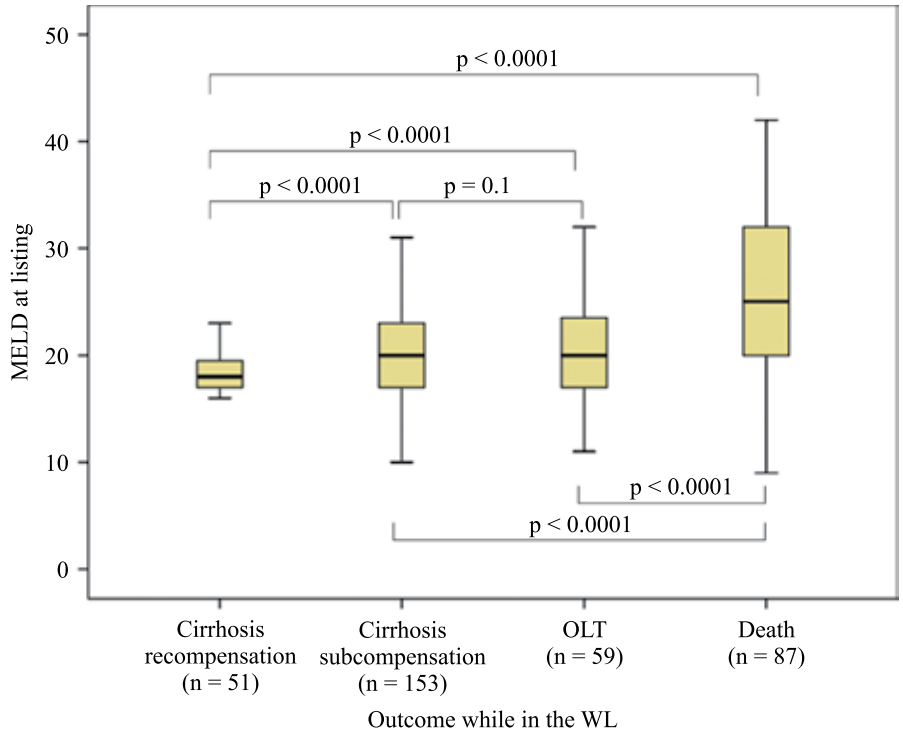

Fig. 1. MELD score in compared patient cohorts. Vertical bar on the box plot, the median; upper line, 75% of the quartile; lower line, 25% of the quartile; range, 95% CI; p, statistical significance of differences

DISCUSSION

LC is featured by high morbidity and mortality rates, reaching more than 48 thousand annually worldwide, or 2.4% of the total number of deaths. For 27 years in Russia, the number of patients with decompensated LC has almost doubled [19]. Decompensated LC is associated with poor prognosis and poor quality of life for patients. For the majority of patients with decompensated LC, LT remains the only treatment method [20], but in some patients there is a possibility of LC recompensation (stabilization of liver function) with subsequent delisting of patients [17, 21].

We found that in patients with LC recompensation, the level of leukocytes and the concentration of albumin were significantly higher in comparison with other stu-

died cohorts. At the same time, in this group, INR, the severity of hepatic encephalopathy, bilirubin, Na levels, platelets, MELD, MELD-Na, and CCI were significantly lower than in other cohorts.

Recompensation of terminal liver disease (TLD) of various etiologies is possible at a combination of factors. First, the preserved liver reserves and the presence of a "point of return" of the lost function after the damaging factors discontinue, which is confirmed by the better parameters of liver function in comparison with other cohorts during the listing, and second, the better response to the therapy.

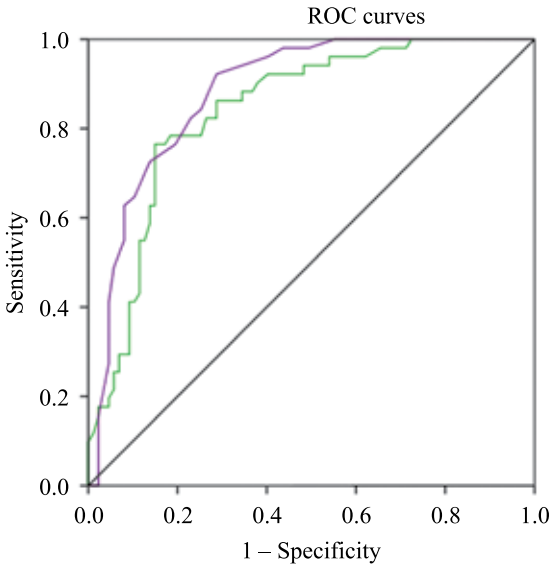

Fig. 2. ROC-curve for MELD and albumin in blood of the patients at waitlisting as mortality predictors. Diagonal segments are formed by matches. Curve source: green, albumin concentration at waitlisting; red, MELD at waitlisting; black, baseline

In 57% of cases, patients with LC recompensation underwent etiological and pathogenetic therapy (azathioprine for patients with autoimmune LC etiology, direct antiviral (HCV) drugs, sofosbuvir + daclatasvir and sofosbuvir/ledipasvir). In 71% of cases, patients received a non-selective β-blocker (carvedilol), in 100% of cases, diuretics and in 84% of cases, hepatic encephalopathy therapy (L-ornithine-L-aspartate intravenously in combination with lactulose and rifaximin per os). In addition to drug therapy, 31% of patients underwent APD, 47%, single endoscopic varicosity ligation, 22%, repeated ligations. Extracorporeal hemocorrection was performed in 16% of cases.

From the point of view of relieving the factors causing LC progression and complications development, significant advancements have been made recently. The use of vasopressors, antibiotics, and minimally invasive surgery techniques have significantly improved the prognosis for patients with acute variceal bleeding [22, 23]. The use of modern antimicrobial therapy has reduced the number of deaths from sepsis and septic shock [24]. Combined treatment of HRS with albumin and vasopressors also led to significant improvements in the outcome in TLD. Successful and timely HCV eradication with a subsequent decrease in LH and fibrosis can lead to the development of LC recompensation, thus making it possible to signi-

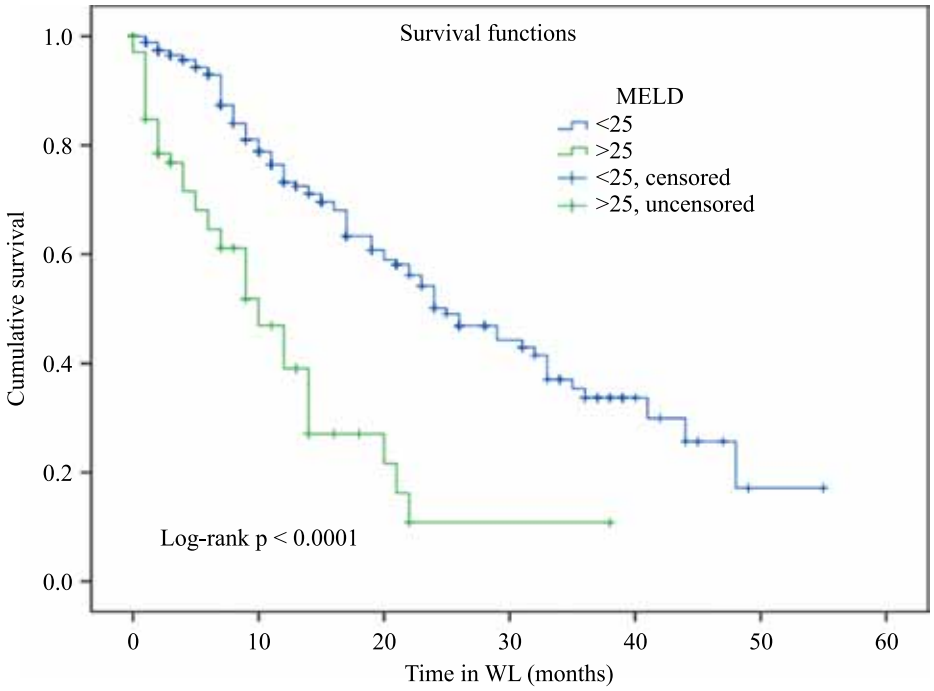

Fig. 3. Comparison of survival curves of patients with different MELD scores by log-rank. The time to death (time from waitlisting to death) is shown

ficantly "unload" WL, which is important in conditions of organ deficiency [21, 25, 26].

Antiviral therapy, AIH treatment with azathioprine and TIPS are counted as probable factors causing the development of LC recompensation with subsequent delisting of patients [17]. We believe that the development of recompensation in patients who left WL in the present study was determined by such factors as successful HCV antiviral therapy, the use of immunosuppressants in autoimmune diseases, treatment of hepatic encephalopathy, prescription of diuretics and nonselective β-blockers. Surgical treatment seems to have also made a certain contribution to the results of conservative treatment of the patients.

When prioritizing the waitlisted patients, it is worth relying on the CTP index, which was originally used to assess the severity of liver disease and predict the outcome of LC and has recently been used to stratify LC patients [20, 27].

In the present study, in all four cohorts, CTP did not significantly differ, thus showing its limited capabilities due to the subjectivity of ascites and hepatic encephalopathy indicators, frequent discrepancies between the clinical picture and the actual data of ultrasonography, psychometric testing, and electroencephalography [20, 28].

Other considered prognostic indices (MELD and its modification MELD-Na), in contrast to CTP, had significant differences in their values in the studied cohorts of patients: LC and OLT recompensation; LC recompensation and death; LC subcompensation and death; OLT and death. MELD and MELD-Na did not significantly differ between the cohorts of patients with LC and OLT subcompensation.

One of the most serious concerns for CRD patients awaiting transplantation is mortality the risk while in WL. In the present study, special attention was paid to the cohort of patients with LC subcompensation, since the therapy here did not allow achieving compensation of liver function in most cases. The patients in this group can move to other cohorts. Due to fluctuations in such laboratory parameters as creatinine and bilirubin, which inevitably occur during the treatment of LC patients, for example, with diuretic therapy or if the patient has sepsis or hemolysis, the use of the MELD index may be limited. A significant drawback of the clinical use of the index is its ability to predict only the short-term survival of LC patients, while the time spent in the LT WL in 63% of cases can be as long as one year; thus, when assessing a period of more than 3 months, the predictive accuracy of MELD significantly decreases [12, 14, 29, 30].

Despite its specificity in assessing the severity of LC, MELD does not take into consideration a number of other equally important clinical, instrumental and laboratory parameters, thus reduces the diagnostic value of the method and not providing full trust in the indicator when assessing an unfavorable outcome of the disease for a period of more than three months. The progress of TLD while in the WL can be unpredictable, and mortality grows exponentially [31] due to the development of an acute decompensating event (e. g., SBP and bleeding from esophageal varices) [30].

Thus, patients can live with a low MELD score (and therefore a low predicted mortality risk) for months or even years without realizing that a sudden breakdown in the SBP course may happen any time.

In our study, a fatal outcome occurred in 30% of the waitlisted patients. In this cohort of patients, the median WL stay was 10.8 ± 9.8 months. The MELD-Na index varied and exceeded 16 points in 84% of cases, averaging 25.97 ± 8.30. Significant predictors of mortality in regression analysis were MELD and blood plasma albumin at the time of inclusion in the WL ($p = 0.001$ and $p = 0.004$, respectively). The chosen model had high predictive power, sensitivity and specificity, as evidenced by AUC for both independent variables (0.883 and 0.841, respectively) and the ROC curves. This is confirmed by the OR calculation, which showed that in patients with MELD ≥25 at the time of inclusion in the WL, the probability of mortality increases by 3.778 times.

Despite the functioning system of patient prioritization with the MELD score [29] and the donor organ distribution system (UNOS), one in five patients (20%) in WL do not live to see this operation [30]. It can be assumed that the cause of death of these patients was the failure to perform LT due to improper stratification and / or deficiency of the donor organs, as well as the sudden TLD decompensation [30, 31]. This may indicate that the fate of the patient depends both on the correct tactics and the competence of the specialists managing the LT WL.

In the present study, hypoalbuminemia was another independent mortality predictor. This condition is a known independent risk factor for mortality in TLD patients as a malnutrition marker, and an increase in albumin concentration in blood plasma predicts the patient recompensation [17, 26]. This was confirmed by calculating the OR for the mortality development. If the concentration of blood plasma albumin at the time of waitlisting was ≤30.1 g/l, the probability of mortality increased by 2.979 times.

Noteworthy is our analysis of survival with Kaplan–Meier method and Log-rank (Mantel-Cox), Breslow, and Tarone-Ware criteria depending on MELD. It was found that the survival rate of patients in the WL is determined by MELD value, namely, its threshold value of 25 points, since there were significant differences between patient survival when comparing cohorts of patients with MELD ≥25 and MELD ≤25 (Log-rank, $p < 0.0001$).

Which of the patients in the LT WL should be given priority? This is an exceedingly difficult question, and many factors must be considered to answer it. For

the purposes of this study, we have shown that priority should be given to patients with MELD ≥25.

Adaptation of the MELD index to determination of the disease severity and prioritization of the patients access to LT made it possible to distribute donor organs to the most severe patients, regardless of the time of their inclusion in WL [14]. This approach has reduced mortality in patients awaiting LT in many countries [32]. Nevertheless, there are still limitations in the use of the MELD indicator, in particular in patients with cholestatic liver diseases [14, 15]. In this category of patients, until the latest TLD stages, MELD remains low due to the normal values of its constituent parts, i. e., IHR and creatinine level. Patients with refractory ascites, hepatopulmonary syndrome, and even chronic hepatic encephalopathy maintain liver function for a long time [32]. Thus, in these patients, in addition to MELD, other indicators must be considered for the timely implementation LT [33].

In the present study, mortality after OLT was 15% (9 deaths within 2 years after surgery). The average MELD score in this category of patients was close to but did not exceed 21. Merion et al. [9] showed that in patients with MELD scores of 18–20 after LT, the risk of mortality decreased by 38% compared to those patients who remained in WL. At the same time, in patients with MELD score of 15–17, the mortality risk was higher (21%) after LT than in patients remaining in the WL. This comparison highlighted the lack of LT efficacy at low MELD scores, despite the fact that in general, these patients had 79% lower mortality risk compared to those remaining in the WL [8]. The variability in assessing the results of LT has shown the need for additional requirements for selection of the patients and organs for LT to ensure its maximum efficacy [8, 34]. For this, it is proposed to use prioritization based not only on MELD, but also the deceased-donor risk index (DRI). It has been established that an organ with a high DRI index provides good survival of recipients after LT with high, not low MELD scores [35, 36]. Beal et al. [11] showed that at MELD <15, LT did not produce the expected effect. The present study also showed that LT was most effective with MELD scores of 21 or less.

CONCLUSION

Prioritizing certain patients on the waiting list as candidates for liver transplantation is a difficult choice for transplant surgeons. Our study showed that one approach to solving this problem, which would satisfy the set goals – to reduce the mortality of patients awaiting liver transplantation and are on a long-term waiting list, is to determine the threshold value of MELD. The MELD model turned out to be predictive in terms of mortality in patients in WL liver transplantation: significant predictors of mortality in regression analysis were MELD and plasma albumin at waitlisting ($p = 0.001$ and $p = 0.004$, respectively). The predictive value of the chosen model is confirmed by the AUC calculation for both independent variables (0.883 and 0.841, respectively) and ROC curves, as well as OR, which showed that in patients with MELD ≥25 at waitlisting, the probability of mortality increased by 3.778 times. The odds ratio for the mortality, provided that the plasma albumin concentration at waitlisting was ≤30.1 g/L, was 2.979 (95% CI 1.63–5.95).

MELD threshold score was 25, since there were significant differences between survival when comparing cohorts of patients with MELD ≥25 and MELD ≤25 (Log-rank, $p < 0.0001$).

The authors declare no conflict of interest.

REFERENCES

1. *Starzl TE, Marchioro TL, Vonkaulla KN et al.* Homotransplantation of the liver in humans. *Surg Gynecol Obstet*. 1963; 117: 659–676.
2. *Lee J, Lee JG, Jung I et al.* Advisory Committee on Improving Liver Allocation. Development of a Korean Liver Allocation System using Model for End Stage Liver Disease Scores: A Nationwide, Multicenter study. *Sci Rep*. 2019; 16; 9 (1): 7495. doi: 10.1038/s41598-019-43965-2.
3. Rapport médical et scientifique de l'Agence de la biomédecine 2017 n.d. https://www.agence-biomedecine.fr/Le-rapport-annuel-medical-et?lang=fr.
4. Organ Procurement and Allocation Transplant Network. National Data. Overall by Organ. Current U.S. Waiting List. Based on OPTN data as of December 7, 2017. https://optn.transplant.hrsa. gov/data/view-data-reports/national-data/#.
5. Organ Procurement and Allocation Transplant Network. National Data. Transplants by Donor Type. U.S. Transplants Performed January 1, 1988 – October 31, 2017. Based on OPTN data as of December 7, 2017. https://optn.transplant.hrsa.gov/data/viewdata-reports/national-data/#.
6. *Gautier SV, Khomyakov SM*. Organ donation and transplantation in Russian Federation in 2018. 11th report of National Register. *Russian Journal of Transplantology and Artificial Organs*. 2019; 21 (3): 7–32. [In Russ, English abstract]. doi: 10.15825/1995-1191-2019-3-7-32.
7. United Network for Organ Sharing / Organ Procurement and Transplantation Network Standard Transplant Analysis and Research Database; 2017. http://optn.transplant.hrsa.gov/data/about/OPTNDatabase.asp.
8. *Merion RM, Schaubel DE, Dykstra DM et al.* The survival benefit of liver transplantation. *Am J Transplant*. 2005; 5 (2): 307–313.
9. *Kim WR, Lake JR, Smith JM et al.* OPTN/SRTR 2013 Annual Data Report: liver. *Am J Transplant*. 2015; 15 Suppl 2: 1–28.
10. *Freeman RB, Wiesner RH, Edwards E et al.* Results of the first year of the new liver allocation plan. *Liver Transpl*. 2004; 10 (1): 7–15.

11. *Beal EW, Akateh C, Tumin D et al.* Defining a Liver Transplant Benefit Threshold for the Model for End-Stage Liver Disease-Sodium Score. *Exp Clin Transplant*. 2019 May 2. doi: 10.6002/ect.2018.0346. [Epub ahead of print] PubMed PMID: 31050611.
12. *Malinchoc M, Kamath PS, Gordon FD et al.* A model to predict poor survival in patients undergoing transjugular intrahepatic portosystemic shunts. *Hepatology*. 2000; 31 (4): 864–871.
13. *Kamath PS, Wiesner RH, Malinchoc M et al.* A model to predict survival in patients with end-stage liver disease. *Hepatology*. 2001; 33 (2): 464–470.
14. *Wiesner R, Edwards E, Freeman R et al.* Model for end-stage liver disease (MELD) and allocation of donor livers. *Gastroenterology*. 2003; 124 (1): 91–96.
15. *Leise MD, Kim WR, Kremers WK, Larson JJ et al.* A revised model for end-stage liver disease optimizes prediction of mortality among patients awaiting liver transplantation. *Gastroenterology*. 2011; 140: 1952–1960.
16. *Korobka VL, Shapovalov AM, Danil'chuk OYa, Korobka RV.* Sposob khirurgicheskogo lecheniya i profilaktiki retsidiva krovotecheniy pri varikoznom rasshirenii ven pishchevoda i kardial'nogo otdela zheludka. Patent RF № 2412657. http://www.freepatent.ru/images/patents/48/2412657/patent-2412657.pdf.
17. *Aravinthan AD, Barbas AS, Doyle AC et al.* Characteristics of liver transplant candidates delisted following recompensation and predictors of such delisting in alcohol-related liver disease: a case-control study. *Transpl Int*. 2017; 30: 1140–1149. https://doi.org/10.1111/tri.13008.
18. *Zweig MH, Campbell G.* Receiver-operating characteristic (ROC) plots: a fundamental evaluation tool in clinical medicine. *Clinical Chemistry.* 1993; 39: 561–577.
19. GBD 2017 Cirrhosis Collaborators. The global, regional, and national burden of cirrhosis by cause in 195 countries and territories, 1990–2017: a systematic analysis for the Global Burden of Disease Study 2017. *Lancet Gastroenterol Hepatol*. 2020; 5 (3): 245–266. doi: 10.1016/S2468-1253(19)30349-8.
20. *Christensen E.* Prognostic models including the Child-Pugh MELD and Mayo risk scores-where are we and where should we go? *J Hepatol*. 2004; 41: 344–350.
21. *Perricone G, Duvoux C, Berenguer M et al.* Delisting HCV-infected liver transplant candidates who improved after viral eradication: Outcome 2 years after delisting. *Liver Int*. 2018; 38: 2170–2177.
22. *de Franchis R.* Baveno VI Faculty. Expanding consensus in portal hypertension: Report of the Baveno VI Consensus Workshop: Stratifying risk and individualizing care for portal hypertension. *J Hepatol*. 2015; 63: 743–752. https://doi.org/10.1016/j.jhep.2015.05.022.
23. *Carbonell N, Pauwels A, Serfaty L et al.* Improved survival after variceal bleeding in patients with cirrhosis over the past two decades. *Hepatol Baltim Md*. 2004; 40: 652–659. https://doi. org/10.1002/hep.20339.
24. *Galbois A, Aegerter P, Martel-Samb P et al.* Improved prognosis of septic shock in patients with cirrhosis: a multicenter study. *Crit Care Med*. 2014; 42: 1666–1675.
25. *Roberts S, Gordon A, McLean C et al.* Effect of sustained viral response on hepatic venous pressure gradient in hepatitis C-related cirrhosis. *Clin Gastroenterol Hepatol*. 2007; 5: 932–937.
26. *Belli LS, Berenguer M, Cortesi PA et al.* Delisting of liver transplant candidates with chronic hepatitis C after viral eradication: A European study. *J Hepatol*. 2016; 65: 524–531.
27. *Pugh R, Murray-Lyon I, Dawson J.* Transsection of the oesophagus for bleeding oesophageal varices. *Br J Surg*. 1973; 60: 646–649.
28. *Durand F, Valla D.* Assessment of the prognosis of cirrhosis: Child-Pugh versus MELD. *J Hepatol*. 2005; 42 (Suppl): S100–S107.
29. *Freeman RB, Wiesner RH, Edwards E et al.* Results of the first year of the new liver allocation plan. *Liver Transpl*. 2004; 10: 7–15.
30. *Lai JC, Covinsky KE, Hayssen H et al.* Clinician assessments of health status predict mortality in patients with end-stage liver disease awaiting liver transplantation. *Liver Int*. 2015; 35 (9): 2167–2173. doi: 10.1111/liv.12792.
31. *Massie AB, Segev DL.* MELD trajectory prior to death on the liver transplant waitlist. *American journal of transplantation*. 2013; 13: 89–90.
32. *Samuel D, Coilly A.* Management of patients with liver diseases on the waiting list for transplantation: a major impact to the success of liver transplantation. *BMC Med*. 2018; 16: 113.
33. *Northup PG, Intagliata NM et al.* Mortality on the liver transplant waiting list: unintended policy consequences and model for end stage liver disease (MELD) inflation. *Hepatology*. 2015; 61: 285–291.
34. *Su F, Yu L, Berry K et al.* Aging of liver transplant registrants and recipients: trends and impact on waitlist outcomes, posttransplantation outcomes, and transplant-related survival benefit. *Gastroenterology*. 2016; 150 (2): 441–453.
35. *Schaubel DE, Sima CS, Goodrich NP et al.* The survival benefit of deceased donor liver transplantation as a function of candidate disease severity and donor quality. *Am J Transplant*. 2008; 8 (2): 419–425.
36. *Feng S, Goodrich NP, Bragg-Gresham JL et al.* Characteristics associated with liver graft failure: the concept of a donor risk index. *Am J Transplant*. 2006; 6 (4): 783–790.

The article was submitted to the journal on 30.06.2020

DOI: 10.15825/1995-1191-2020-3-36-42

EFFICACY OF ALBUMIN DIALYSIS AS A BRIDGE TO TRANSPLANTATION IN CHILDREN WITH END-STAGE LIVER DISEASE

A.G. Strokov[1, 2], I.L. Poz[1], A.R. Monakhov[1, 2], S.V. Meshcheryakov[1], M.A. Voskanov[1], S.V. Gautier[1, 2]

[1] Shumakov National Medical Research Center of Transplantology and Artificial Organs, Moscow, Russian Federation

[2] Sechenov University, Moscow, Russian Federation

Liver transplantation is the only effective treatment modality for end-stage liver disease. However, donor organs are not always available. In some cases, the gravity of the patient's condition makes transplantation impossible. In this regard, the use of artificial liver support systems helps in preparing a patient for transplant surgery. **Objective:** to conduct a retrospective study aimed at evaluating the efficiency of fractionated plasma separation and adsorption system. **Materials and methods.** From January 2019 to May 2020, 139 pediatric liver transplants were. We analyzed the data of 5 pediatric patients (2 girls and 3 boys, aged 12 to 17 years) who received fractionated plasma separation and adsorption (FPSA) sessions as a bridge to transplantation. The main clinical indication for FPSA was severe hepatic encephalopathy (grade 3 according to the West Haven Criteria), which was observed at 350–872 μmol/L (average 597 ± 98 μmol/L) serum bilirubin level. The FPSA sessions were conducted on a Prometheus device using AV-600 hemofilters as dialyzers (*Fresenius Medical Care, Germany).* **Results.** Depending on the extent of bilirubinemia in patients, it took from one (in one case) to three (in one case) daily FPSA sessions to restore clear consciousness, appetite and physical activity. Average bilirubin levels after treatment cycles decreased from 597 ± 98 to 236 ± 73 μmol/L. All patients successfully underwent liver transplant surgery within two to five days, two patients received a liver fragment from a living related donor. **Conclusion.** The FPSA system stabilizes the condition of potential recipients with acute liver failure. Further research is required to develop optimal regimens for albumin dialysis.

Keywords: cirrhosis, liver failure, albumin dialysis, liver transplantation, pediatric liver transplantation, extracorporeal liver support, hepatic encephalopathy, fractionated plasma separation and adsorption.

INTRODUCTION

Transplantation is the only radical method of treating patients with terminal liver diseases. However, the donor organ is not always available at the right time, and in some cases successful transplantation is hindered by the severity of the patient's condition. In such cases, the use of artificial liver support systems allows the patient to get prepared for transplantation. Over the last decades, a large number of such systems have been developed, both biological systems with hepatocytes and fully artificial [1–3]. Of the latter, systems based on albumin dialysis with membranes of high, up to 250 kDA, cutoff point, and containing a standard hemodialysis block for the injection of water-soluble substances [4]. Most of the studies of the past two decades focus on the use of albumin dialysis in cases of acute or acute chronic liver failure, are highly heterogeneous in the patients included, and therefore have hardly comparable results.

The purpose of the present retrospective study was to assess the efficacy and safety of one of the albumin dialysis systems, fractionated plasma separation and adsorption (FPSA) in the practice of the transplant center in the preparation of pediatric and adolescent patients with terminal hepatic failure for urgent liver transplantation.

MATERIALS AND METHODS

Patients

From January 2019 to May 2020, 139 transplants were performed in the pediatric patients (under 18 years of age). During this period, 5 children received at least one FPSA session in the preoperative period. Severe hepatic encephalopathy was the main clinical indication for the use of FPSA, assessed on the West-Haven Criteria [5]. The study was performed in compliance with the ethical principles of biomedical research as reflected in the World Medical Association Declaration of Helsinki. All medical interventions are envisaged by the standard protocols of the Center.

Corresponding author: Alexander Strokov. Address: 1, Shchukinskaya str., Moscow, 123182, Russian Federation. Phone: (499) 158-22-33. E-mail: medick@bk.ru

Fractionated plasma separation and adsorption sessions

The FPSA sessions were done on the Prometheus device (a schematic diagram of the extracorporeal circulation see Fig. 1). AV 600–1000 hemofilters (*Fresenius Medical Care, Germany*) were used as hemodialyzers. The standard session lasted for 6 hours at a blood flow rate of 180–250 ml/min and a circulation rate in the albumin circuit of 300–350 ml/min.

Vascular access was performed with standard 12F dual-lumen dialysis catheters implanted into the right IJV under ultrasound control. At this, coagulopathy and thrombocytopenia did not contraindicate vascular access.

The number of FPSA sessions was determined by the availability of a cadaver or live related donor for liver transplantation. Albumin dialysis sessions were carried out in the ICU every day until clear clinical improvements manifested by the elimination of manifestations of hepatic encephalopathy in the form of restored consciousness, physical activity and appetite.

A bicarbonate acetate-free dialyzing liquid of the following composition was used: Na^+ – 138–140, K^+ – 4.0; Ca^{++} – 1.75; Mg^{++} – 1.0; glucose – 10.0; bicarbonate – 32.0 (mmol/l) with a flow of 500 ml/min at 36.0–36.5 °C. Ultrafiltration was performed in volumes corresponding to transfusion therapy during the procedure. Anticoagulation in the extracorporeal circuit was carried out by dosed administration of heparin along two lines, before the plasma filter and along the additional line, before the hemodialyzer under the control of ABC and APTT.

Surgical techniques, immunosuppression protocols, and the principles of examination of related donors are detailed in previous publications [6–9].

Statistical analysis

Demographic and clinical data are expressed as frequency and percentage for qualitative variables and as mean and standard deviation (SD) for quantitative variables. To compare parametric indicators between groups, the Student's t-test was used and for comparison of non-parametric indicators Fisher's exact test. When testing statistical hypotheses, differences were considered statistically significant at $p < 0.05$. All calculations and data analysis were performed with SPSS version 23 software package (IBM, USA).

RESULTS

The clinical and demographic characteristics of patients are given in Table 1. Attention is drawn to the adolescence of patients in the study group (12.4 years, SD ± 3.4; $p = 0.004$), as well as diseases that led to terminal liver disease: Wilson disease (one case), autoimmune hepatitis (one case); in three cases the etiology of terminal liver damage has not been verified. The mean PELD/MELD level was higher than in the general group (34.2, SD ± 9.6; $p = 0.017$), and the UNOS status corresponded to 2a or 1. Of the five patients receiving FPSA, two patients were hospitalized directly in the ICU, three were transferred for treatment within two to three days after admission. The main clinical indication for FPSA was severe hepatic encephalopathy (grade 3 according to the West Haven Criteria). Similar symptoms were

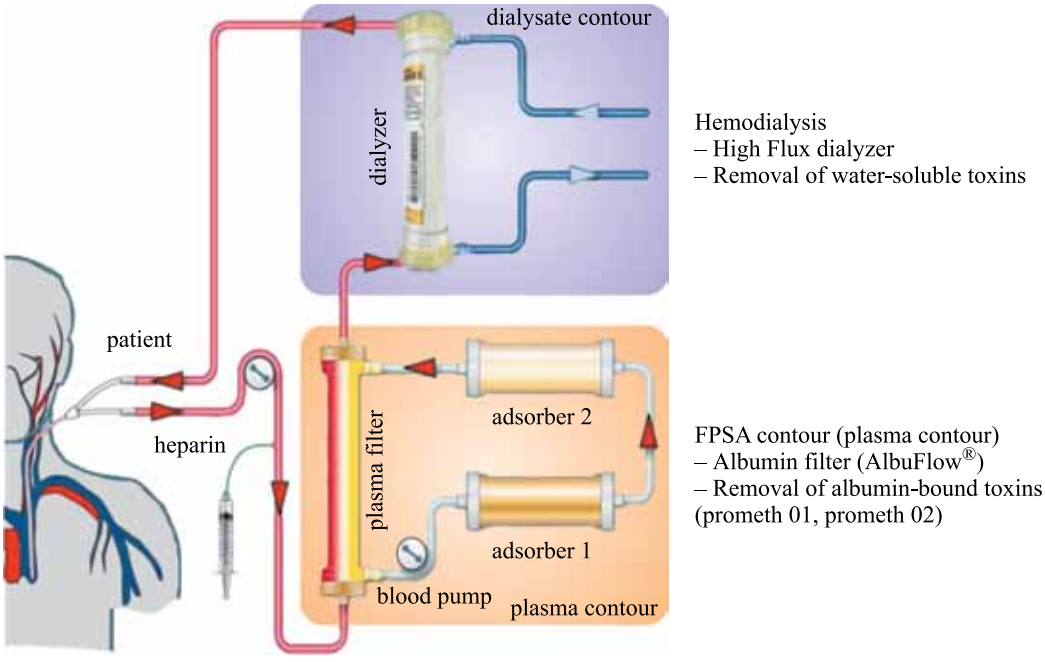

Fig. 1. Prometheus albumin dialysis. Schematic diagram of the extracorporeal circulation circuit [10]

Table 1

Baseline characteristics of patients

Parameters	No indications for FPSA, n = 134	Performed FPSA, n = 5	p
Age, years, mean ± SD	4.2 ± 5.1	12.4 ± 3.4	0.004
Gender, n (%)			0.661
Female	73 (54.5)	2 (40)	
Male	61 (45.5)	3 (60)	
Weight, kg, mean ± SD	17.6 ± 17	50.2 ± 17.7	0.014
PELD/MELD, mean ± SD	18 ± 9.9	34.2 ± 9.6	0.017
Encephalopathy, grade, n (%)			0.000
0–II	134 (100)	–	
≥III	–	5 (100)	
Diagnosis			–
Biliary atresia	47 (35.1)	–	
PFIC	14 (10.4)	–	
Biliary hypoplasia	12 (9.0)	–	
FCC	12 (9)	–	
Cirrhosis, undefined	11 (8.2)	3 (60)	
AIH	6 (4.5)	1 (20)	
PSC	5 (3.7)	–	
Wilson disease	4 (3)	1 (20)	
Graft disfunction	4 (3)	–	
Mucoviscidosis	4 (3)	–	
Alagille syndrome	3 (2.2)	–	
Glycogenosis	2 (1.5)	–	
Primary hyperoxaluria	2 (1.5)	–	
Tyrosinemia 1b	2 (1.5)	–	
Hepatoblastoma	1 (0.7)	–	
HCC	1 (0.7)	–	
Crigler-Najjer Syndrome, I	1 (0.7)	–	
Ketoacidemia	1 (0.7)	–	
Hemochromatosis	1 (0.7)	–	
Joubert syndrome	1 (0.7)	–	
GRWR %, mean ± SD	3 ± 1.3	2.1 ± 0.3	0.103
Transplant, n (%)			–
Full liver	5 (3.7)	3 (60)	
Left lobe	16 (11.9)	1 (20)	
LLS	91 (67.9)	–	
Right lobe	14 (10.4)	1 (20)	
Split-LLS	6 (4.5)	–	
Split-ERL	2 (1.5)	–	
Follow-up, months	9 ± 5.3	10.2 ± 4.2	0.583

Note. FPSA, Fractionated Plasma Separation and Adsorption; PELD, Pediatric End-Stage Liver Disease; MELD. Model of End-Stage Liver Disease; PFIC, Progressive familial intrahepatic cholestasis; FCC, Fibrocholangiocystosis; AIH. Autoimmune hepatitis; PSC, Primary sclerosing cholangitis; HCC, Hepatocellular carcinoma; GRWR, Graft-to-recipient weight ratio; LLS, Left lateral section; ERL, Extended right lobe.

observed at a bilirubinemia level of 350–872 with 597 ± 98 (μmol/L) average. The main laboratory parameters at admission are summarized in Table 2: marked hyperbilirubinemia, cytolytic syndrome, anemia, hypoproteinemia with low albumin levels, coagulopathy.

The number of FPSA sessions required to regress encephalopathy correlated with baseline bilirubinemia level. Thus, in a patient with a bilirubin concentration of 350 μmol/L, one session was sufficient, while a patient with a maximum level of 872 μmol/L needed three treatment sessions. The dynamics of the mean bilirubin concentration values during the FPSA treatment is shown in Fig. 2. At the end of the course of treatment, the mean bilirubin concentration decreased from 597 ± 98 to 236 ± 73 μmol/L. It should be noted that after the end of treatment, there was a tendency towards a regular increase in this parameter.

All five patients underwent liver transplantation within two to five days after FPSA treatment: in two cases, liver fragments were transplanted from live related donors, in three – from cadaver donors. The mean level of bilirubinemia before transplantation was 496 ± 108 μmol/L, while encephalopathy recurrence was not observed.

Of the technical complications during albumin dialysis, it is worth noting thrombosis of the extracorporeal circuit in one case, which was obviously associated with a low level of AT III (11%); in this case, an effective treatment session was performed after administration of two doses of fresh frozen plasma. The average heparin doses required for adequate anticoagulation in the extracorporeal circuit averaged 1122.2 ± 259.9 IU/h along the standard line before the plasma filter and 765.7 ± 287.2 IU/h along the additional line before the hemodialyzer. There were no clinical complications during the treatment sessions; hemodynamic parameters remained stable.

All patients were discharged from the clinic and are currently being followed up with functioning grafts.

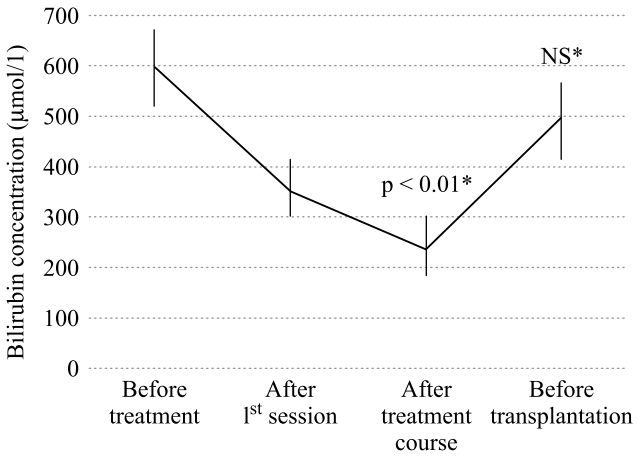

Fig. 2. Mean serum bilirubin change during FPSA sessions and before liver transplantation. * – compared to the concentration before treatment

Table 2

Characteristics of patients receiving FPSA

Parameters	n = 5
Age, years, mean ± SD	12.4 ± 3.4
Gender, n (%)	
Female	2 (40)
Male	3 (60)
Weight, kg, mean ± SD	50.2 ± 17.7
PELD/MELD, mean ± SD	34.2 ± 9.6
Laboratory indicators upon admission	
T. bil, μmol/l	553.6 ± 154.3
ALT U/L	193.2 ± 132.8
AST U/L	318.6 ± 158.5
Hb, g/L	73.2 ± 4.9
Total protein, g/L	63.6 ± 10.1
Albumin, g/L	29.0 ± 3.4
AT III,%	17.8 ± 11.5
PLT, 10^3/ μl	60.2 ± 27.5
PI, %	32.6 ± 11.0
APTT, C	58.0 ± 7.8
FPSA sessions, n, mean ± SD	2 ± 1
Complete encephalopathy regression with FPSA, n (%)	
Yes	60%
No	40%
Difference in total bilirubin level after FPSA session, μmol/L	
After 1st session (n = 5)	68.8 ± 159.9
After 2nd session (n = 5)	32.8 ± 89.4
After 3rd session (n = 1)	77
After 4th session (n = 1)	60
Survival,%	100
Follow-up after transplantation, months	10.2 ± 4.2

Note. PELD, Pediatric End-Stage Liver Disease; MELD, Model of End-Stage Liver Disease; T. bil., Total bilirubin; ALT – Alanine aminotransferase; AST, Aspartate aminotransferase; Hb, Hemoglobin; AT III, Antithrombin III; PI – Prothrombin index; APTT – Activated partial thromboplastin time.

DISCUSSION

Albumin dialysis systems aimed at maintaining liver function, and in particular the FPSA system, have been used in clinical practice for over twenty years. Already in the first studies, the ability of FPSA was shown to significantly reduce the concentrations of bilirubin, bile acids, and ammonia [11]. In subsequent studies, the effectiveness of the system was confirmed: there was a decrease in the activity of transaminases [12], as well as the concentration of amino acids [13], including those involved in the development of hepatic encephalopathy. The number of studies evaluating the clinical efficacy of FPSA is extremely limited. There are indications of regression of encephalopathy when using the system [14] and optimization of hemodynamic parameters [15]. In two studies evaluating the effectiveness of treatment by endpoints, there was no significant reduction in mortality with the FPSA [16, 17]. Moreover, a large randomized controlled trial in which FPSA was compared with standard therapy was terminated early [17], and only further analysis of patient subgroups revealed an improvement in the survival of the most severe patients with the use of FPSA. Such results can be explained by the extreme heterogeneity of the patients involved in the research and the lack of clear recommendations for therapy and its programs.

The present study, which used FPSA as a bridge to liver transplantation, came to quite encouraging results. Treatment courses, the duration of which was determined by the initial bilirubin concentration, made it possible to significantly reduce bilirubinemia and achieve a clear regression of encephalopathy. Interesting is the fact that at the end of treatment there was a regular increase in the level of bilirubinemia in the absence of encephalopathy recurrence. A plausible explanation for this phenomenon can be found in the literature. Thus, in the model of hepatic encephalopathy, a significant decrease in intracranial pressure was noted after FPSA sessions [18], which may contribute to the persistence of the clinical effect. In the present series of observations, the maximum period after the end of the course of treatment before liver transplantation did not exceed five days; possibly, with a longer waiting time for transplantation, it may be necessary to resume therapy.

CONCLUSION

The FPSA albumin dialysis system is an effective and safe method of preparing for transplantation in patients with terminal liver failure. If there is a real prospect of liver transplantation, this technique can be considered as lifesaving. Further research is needed to clarify the indications for initiating therapy and working out treatment programs when prolonging the waiting time for a transplant.

The authors declare no conflict of interest.

REFERENCES

1. *Saliba F, Samuel D.* Artificial liver support: a real step forward. *Minerva Med*. 2015; 106 (1): 35–43.
2. *Jain V, Dhawan A.* Extracorporeal Liver Support Systems in Paediatric Liver Failure. *J Pediatr Gastroenterol Nutr*. 2017; 64 (6): 855–863. doi: 10.1097/MPG.0000000000001500.
3. *Cucchiari D, Reverter E, Blasco M et al.* High cut-off membrane for *in vivo* dialysis of free plasma hemoglobin in a patient with massive hemolysis. *BMC Nephrol*. 2018; 19 (1): 250. Published 2018 Oct 4. doi: 10.1186/s12882-018-1051-x.
4. *García Martínez JJ, Bendjelid K.* Artificial liver support systems: what is new over the last decade? *Ann Intensive Care*. 2018; 8 (1): 109. Published 2018 Nov 15. doi: 10.1186/s13613-018-0453-z.
5. *Ferenci P, Lockwood A, Mullen K, Tarter R, Weissenborn K, Blei AT.* Hepatic encephalopathy: definition, nomenclature, diagnosis, and quantification: final report of the working party at the 11th World Congresses of Gastroenterology, Vienna, 1998. *Hepatology*. 2002; 35: 716–721. doi: 10.1053/jhep.2002.31250.
6. *Gautier SV, Konstantinov BA, Tsirulnikova OM*. Transplantatsiya pecheni. M.: Medicinskoe Informacionnoe Agentstvo, 2008. 248.
7. *Monakhov AR.* Prizhiznennoe donorstvo fragmentov pecheni dlya transplantacii detyam [Dissertation]. M., 2015.
8. *Akhaladze DG.* Revaskulyarizaciya transplantata levogo lateral'nogo sektora pecheni u detej. [Dissertation]. M., 2013.
9. *Gautier SV, Tsirulnikova OM, Moysyuk YG, Akhaladze DG, Tsirulnikova IE, Silina OV et al.* Transplantaciya pecheni detyam: analiz shestiletnego opyta. *Vestnik transplantologii i iskusstvennyx organov*. 2014; 16 (3): 54–62. doi.org/10.15825/1995-1191-2014-3-54-62.
10. Freseniusmedicalcare.com [Internet]. Prometheus® Therapy system for the support of liver function, Fresenius Medical Care. [updated 2007] Available from: https://www.freseniusmedicalcare.com/fileadmin/data/masterContent/pdf/Prometheus/Prometheus_Product_Range.pdf/.
11. *Evenepoel P, Alexander W, Wilmer A, Claes K, Kuypers D, Bammens B et al.* Prometheus versus molecular adsorbents recirculating system: comparison of efficiency in two different liver detoxification devices. *Artif Organs*. 2006; 30 (4): 276–284. doi: 10.1111/j.1525-1594.2006.00215.x.
12. *Grodzicki M, Kotulski M, Leonowicz D, Zieniewicz K, Krawczyk M.* Results of treatment of acute liver failure patients with use of the Prometheus FPSA system. *Transpl Proc*. 2009; 41 (8): 3079–3081. doi: 10.1016/j.transproceed.2009.08.024.

13. *Rifai K, Das A, Rosenau J, Ernst T, Kretschmer U, Haller H et al.* Changes in plasma amino acids during extracorporeal liver support by fractionated plasma separation and adsorption. *Artif Organs*. 2010; 34 (2): 166–170. doi: 10.1111/j.1525-1594.2009.00763.x.
14. *Senturk E, Esen F, Ozcan PE, Rifai K, Pinarbasi B, Cakar N et al.* The treatment of acute liver failure with fractionated plasma separation and adsorption system: experience in 85 applications. *J Clin Apher*. 2010; 25 (4): 195–201. doi: 10.1002/jca.20238.
15. *Komardina E, Yaroustovsky M, Abramyan M, Plyushch M.* Prometheus therapy for the treatment of acute liver failure in patients after cardiac surgery. *Kardiochir Torakochirurgia Pol*. 2017; 14 (4): 230–235. doi: 10.5114/kitp.2017.72226.
16. *Bergis D, Friedrich-Rust M, Zeuzem S, Betz C, Sarrazin C, Bojunga J.* Treatment of Amanita phalloides intoxication by fractionated plasma separation and adsorption (Prometheus®). PMID: 22720306.
17. *Kribben A, Gerken G, Haag S, Herget-Rosenthal S, Treichel U, Betz C et al.* Effects of fractionated plasma separation and adsorption on survival in patients with acute-on-chronic liver failure. *Gastroenterology*. 2012; 142 (4): 782–789. doi: 10.1053/j.gastro.2011.12.056.
18. *Ryska M, Laszikova E, Pantoflicek T, Ryska O, Prazak J, Koblihova E.* Fractionated plasma separation and adsorption significantly decreases intracranial pressure in acute liver failure: experimental study. *Eur Surg Res*. 2009; 42 (4): 230–235. doi: 10.1159/000208790.

The article was submitted to the journal on 6.07.2020

DOI: 10.15825/1995-1191-2020-3-43-52

ORGANIZATIONAL, MEDICAL AND EPIDEMIOLOGICAL PREREQUISITES FOR REVIEWING DONOR CRITERIA IN HEART TRANSPLANTATION

E.A. Tenchurina[1], *M.G. Minina*[1, 2]

[1] Moscow Coordinating Center for Organ Donation (Botkin City Clinical Hospital), Moscow, Russian Federation

[2] Shumakov National Medical Research Center of Transplantology and Artificial Organs, Moscow, Russian Federation

Organ donation and transplantation in Moscow have witnessed changes in the last decade. These changes have led not only to quantitative growth in the number of effective donors but also to fundamentally new (for Russian medical practice) characteristics of the donor pool. As a result, the selection criteria for organ donors have undergone some radical revisions. **Objective:** to analyze the medical and epidemiological characteristics of the pool of effective heart donors and assess their impact on selection of heart transplants. **Materials and methods.** In our study, we used the medical and epidemiological data of 650 brain-dead donors whose organs were procured from January 1, 2012 to December 31, 2017. **Results.** During the study period, the number of effective heart donors in Moscow increased from 4.4 (2012) to 11.2 (2017) per million population per year. The medical and epidemiological characteristics of the total pool of donors and the pool of heart donors underwent major changes. Among effective heart donors, there was a dynamic increase in the average age from 38.4 to 47 years, predominance of a proportion of donors with stroke 38.2 (2012) vs 83.2 (2017) and, accordingly, an increase in the frequency of such comorbid conditions, as hypertension and diabetes. **Conclusion.** The results presented in the study indicate a growing practice of working with expanded criteria donors. This practice is most effectively developed in the field of heart transplantation than in transplantation of other extrarenal organs. Undoubtedly, the experience under study is unique and relevant not only for the Russian Federation, but also for the world of transplantology, as it allows to provide vital assistance to patients with end-stage heart failure within a reasonable timeframe.

Keywords: effective heart donors, donor pool characteristics, expanded criteria heart donors.

INTRODUCTION

The transplant community continues to look for ways to reduce the shortage of donor organs for transplantation [1]. The use of organs from high-risk donors, including the older age group, without compromising the results of transplantation, is the most obvious and affordable way to increase the number of donor organs.

MATERIALS AND METHODS

The present study used clinical data on 650 brain death donors who underwent organ explantation between January 1, 2012 and December 31, 2017. The general dynamics of donor activity in Moscow in 2012–2017 has been investigated providing the basis for development of donation and heart transplantation, as well as the comparative dynamics of the use of the donor heart and other extrarenal organs for transplantation. To perform a comparative analysis of the effectiveness of using donor hearts in Moscow, the number of heart ED per million population per year was used, which was compared with a similar indicator in several countries of Europe. To represent the population characteristics of ED, including heart ED, mean age and median age of donors, gender ratio, and the proportion of nosological forms, causes of donor deaths (%) were used.

All organ donors were divided into two main groups. The first group included 452 donors (69.5%) from whom the heart was taken for transplantation either in isolation or in the format of multi-organ removal. The second group consisted of 198 (30.5%) donors with organ extractions in various formats, while heart explantation was not performed for various reasons. To identify the factors causing the donor heart refusal, a number of donor characteristics were selected that, in our opinion, could influence the decision to refuse. Among the factors that cannot be changed by any influence, there are age, cause of death, gender, history of hypertension, and diabetes mellitus. As for the factors featuring donor homeostasis and open for medical correction, mean arterial pressure (MAP), pH, lactate, Na and blood glucose, and the dose of vasopressor support were chosen. All explanted donor hearts included in this study were transplanted at the

Corresponding author: Elmira Tenchurina. Address: 5, Vtoroy Botkinsky proyezd, Moscow, 125284, Russian Federation. Phone: (967) 113-87-64. E-mail: arimle@inbox.ru

Shumakov National Medical Research Center of Transplantology and Artificial Organs (Ministry of Health of the Russian Federation, Moscow). Statistical analysis was made with Statistica 12.0 for Windows software.

SOME CONDITIONS AND FACTORS DEFINING CRITERIA FOR SELECTION OF HEART DONORS

In Moscow, since 2012, there has been stable growth dynamics of effective donors whose death was ascertained on the basis of neurological criteria, e. g., diagnosed brain death (BD) [2]. Fig. 1 shows the absolute number of effective donors diagnosed with BD per million population per year [3].

The progressive growth of donor activity became possible due to a number of organizational measures, so-called the "Moscow model" of organ donation, among which it is necessary to point out the improvement of the regional regulatory framework, the new position of a transplant coordinator in the practice of medical institutions with the definition of functional responsibilities of this position, formulation and normative consolidation of the so-called triggers for identifying potential organ donors, monitoring the neurological and somatic status of probable and potential donors, etc. [4, 5]. The taken organizational measures resulted in annual increase in the number of ED per million population per year that reached 15.5 in 2017, while over the same period, the total donor activity in Eurotransplant countries was 13.9 [6].

The growing dynamics of donor activity has become a crucial drive for the development of extrarenal transplant programs. At the same time, the difference in the indicators of the use of the donor pool for each type of clinical transplantation is quite significant. Fig. 2 shows the relative share of the use of donors with BD for heart, lung, liver, and pancreas transplantation. In 2012–2014, there has been sharp variations in the use of ED in heart, liver and pancreas transplantation. In this period, transplant programs have been obviously adapting to new working conditions, a growing number of BD donors, an increase in vascular diseases as the predominant cause of donor deaths, etc. then in 2015–2017, the rate of donor organs used for heart transplantation remained at an average level of 72.8%, while only in the year of 2017 the corresponding figure for the liver transplants was 67.2%. There is seen a slight positive trend in the use of the donor pool for lung transplantation. The most ineffective was the use of the donor pool for pancreas transplantation, where a progressive decrease was recorded.

Due to the high efficiency of using the donor pool for heart transplantation, the number of heart donors per million population in Moscow in 2017 was 11.2, which is shown in Fig. 3. A similar indicator in Europe in 2017 was at the level of 4.8 [6].

As noted above, the intensity of the use of the heart for transplantation took place in the conditions of radical changes in the donor pool: increased age of donors, the prevalence of vascular diseases in the structure of donor deaths, increase in the rate of comorbid risk factors, including hypertension (HT), diabetes mellitus (DM), systemic atherosclerosis, etc.

In a relatively short period, the average age of all EDs in Moscow increased by 7 years, from 42.15 in 2012 to 49.02 in 2017 (Fig. 4).

Even more significant changes are seen in the average age of donors among the heart ED pool. In 2012, relatively young donors were engaged, with the average age of 38.4, while in 2017 the average age of EDs in-

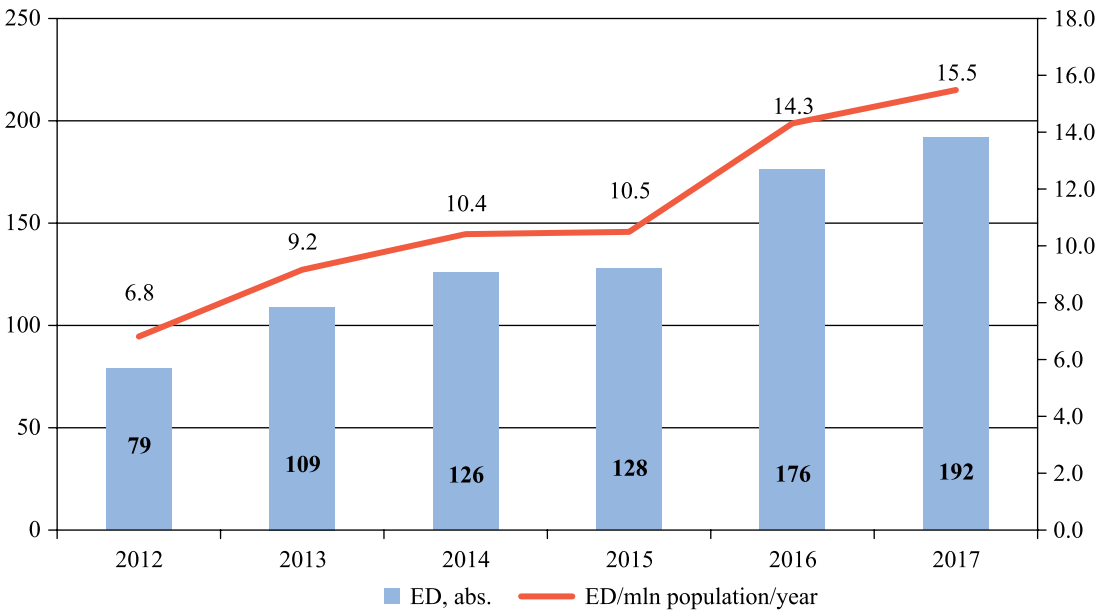

Fig. 1. Donor activity in Moscow in dynamics, 2012–2017

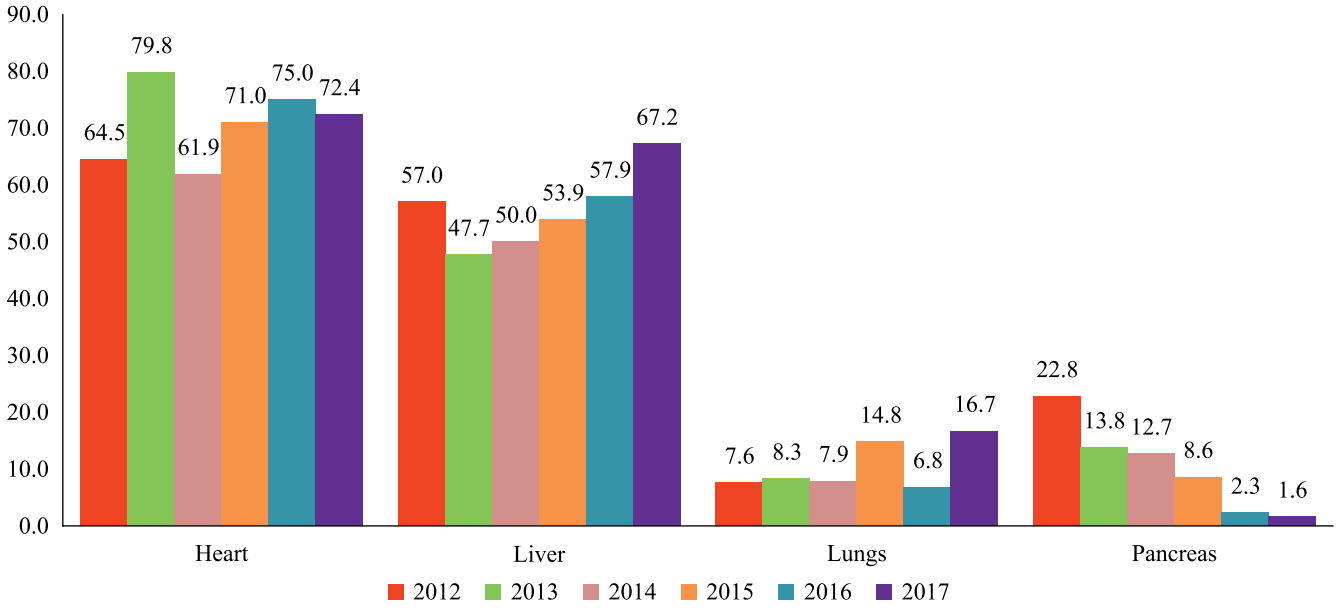

Fig. 2. Dynamics of the donor pool use for transplantation of extrarenal organs, 2012–2017

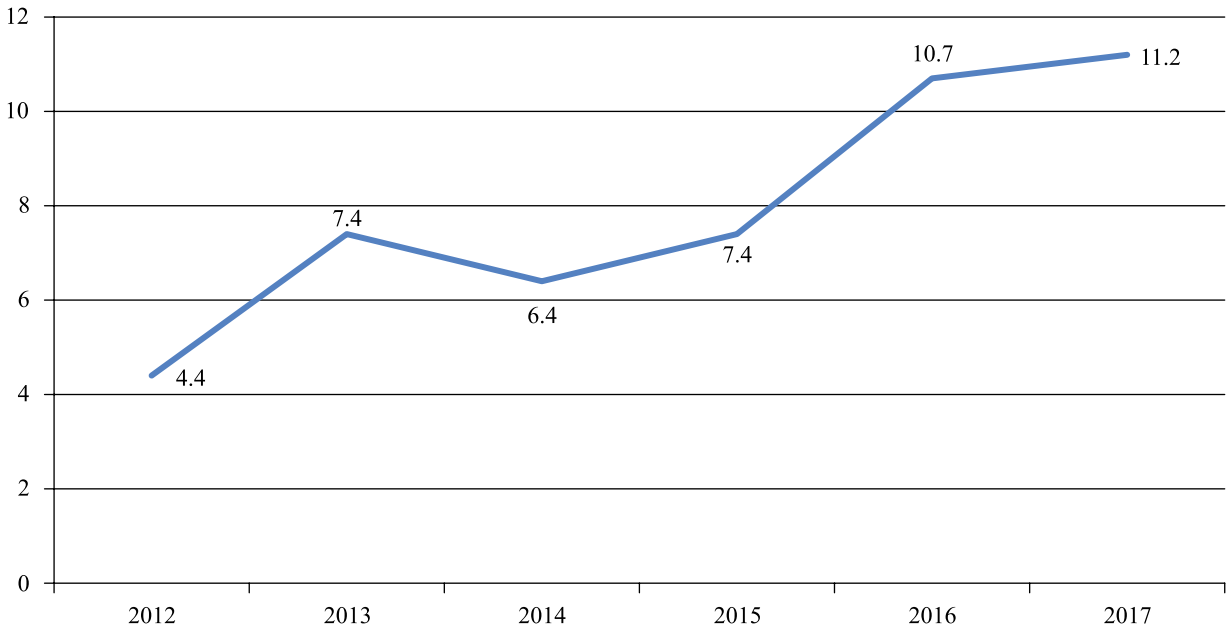

Fig. 3. The number of effective heart donors per million population per year, 2012–2017

creased to 47.0 (Fig. 5). For comparison, the average age of heart donors in Europe in 2017 was 43; in North America, for 30 years the median age of the donors has remained in the range of 25–27 [6, 7]. Accordingly, the greatest progress in engaging donors over 40 years of age has been achieved by European countries, including Russia, the experience of its city of Moscow is presented in this study.

Analysis of the main death causes of all EDs in Moscow revealed a significant predominance of donors who died of cerebrovascular diseases, in comparison with the number of donors who received traumatic injuries (Fig. 6). In the Eurotransplant countries, already in 2012, EDs with CVA dominated (78.3% of the total pool of all donors) [6]. Comparing foreign data with those obtained in this study, it is important to note that the appearance of similar donor tendencies in Russia testifies to the identical principles of organizing the donor process [5].

In the context of changes in Moscow donor pool, an extremely uneven transplantation activity of medical institutions performing heart transplantation was observed (Fig. 7). Only cases of heart donation sent for transplantation to Shumakov National Medical Research Center of Transplantology and Artificial Organs were included in the study, since heart transplantation is most

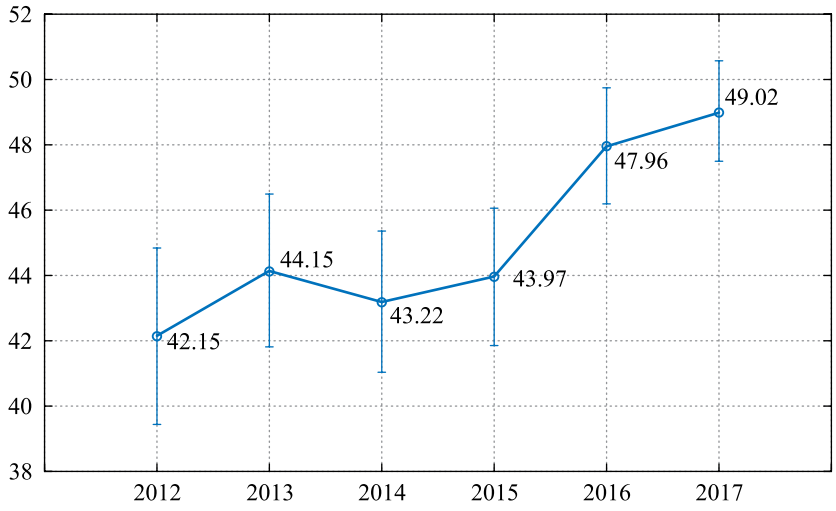

Fig. 4. Comparative dynamics of the average age of effective donors, 2012–2017. X axis, years; Y axis, age

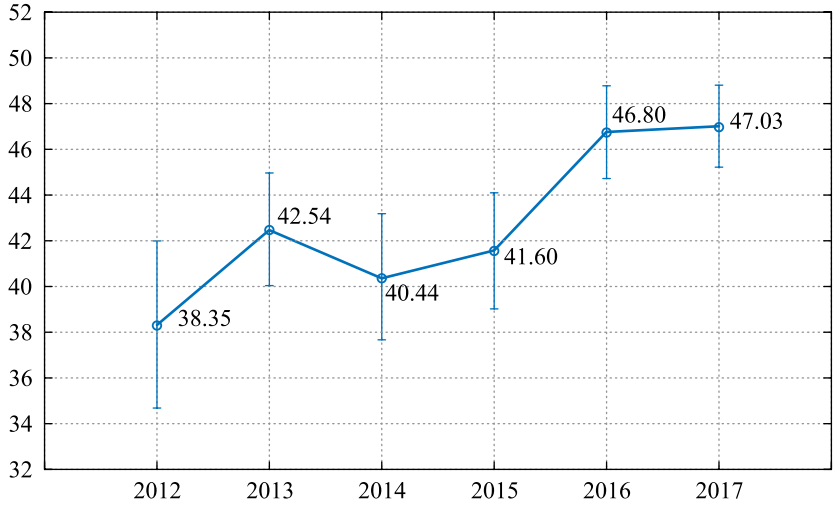

Fig. 5. Comparative dynamics of the average age of effective heart donors, 2012–2017. X axis, years; Y axis, age

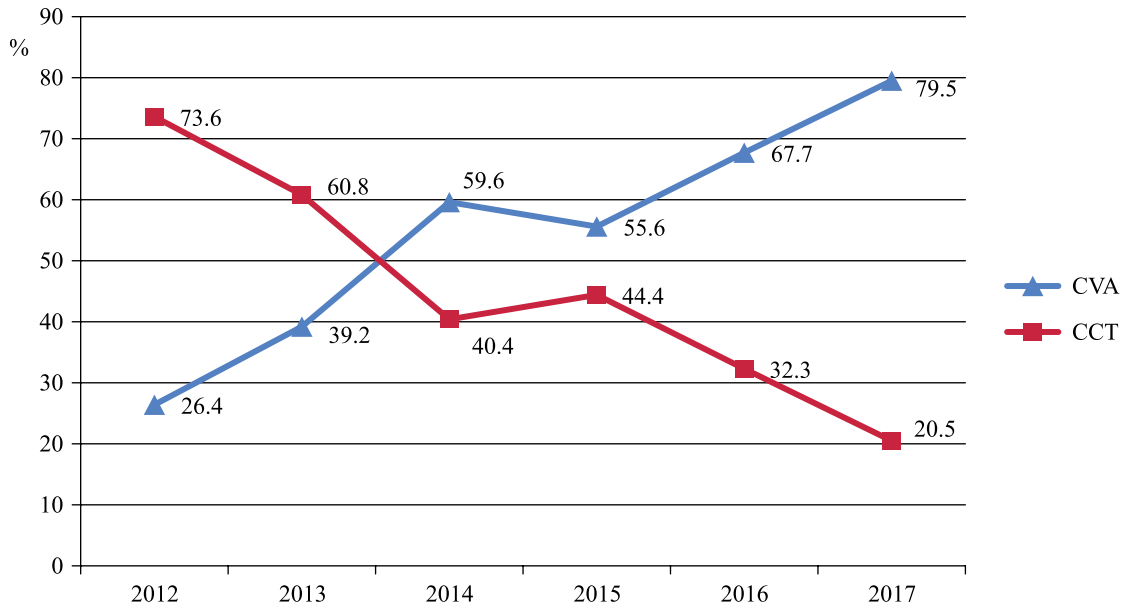

Fig. 6. The percentage of the major death causes in ED, 2012–2017

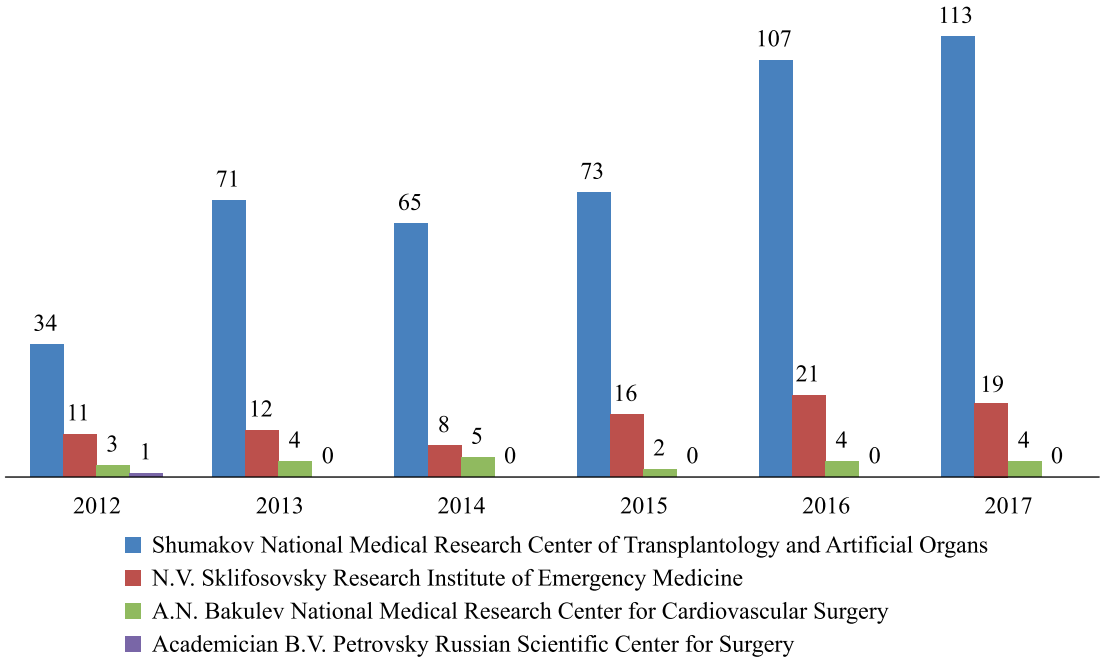

Fig. 7. Activity of heart transplant centers, 2012–2017

developed in this institution. By scientific publications of the Center, effective use of the changed donor pool in the city of Moscow seem to become possible primarily due to the timely revision of the donor selection criteria for heart transplantation [8, 9].

Organizational approaches in working with high-risk donors used in the joint work of the Moscow City Coordination Center for Organ Donation (MGKTsOD) and Shumakov National Medical Research Center of Transplantology and Artificial Organs have radically changed heart transplantation in the Russian Federation, making it more accessible in conditions when the number of "ideal" donors will only decrease.

MEDICAL AND EPIDEMIOLOGICAL CHARACTERISTICS OF EFFECTIVE HEART DONORS

Heart donors in 2012–2017, in line with the stated above trend of changes in the entire donor pool, also underwent changes. Fig. 8 shows the percentage of the main death causes of heart donors included in the study. In 2012, heart donors with CCTs predominated (61.8% versus 38.2% of donors who died from stroke). By 2015, the numbers of donors with both nosologies equaled, and in 2017 the number of donors who died of CCT has become 3.7 times less than in 2012, and the proportion of donors with CVA has increased to 83.2%.

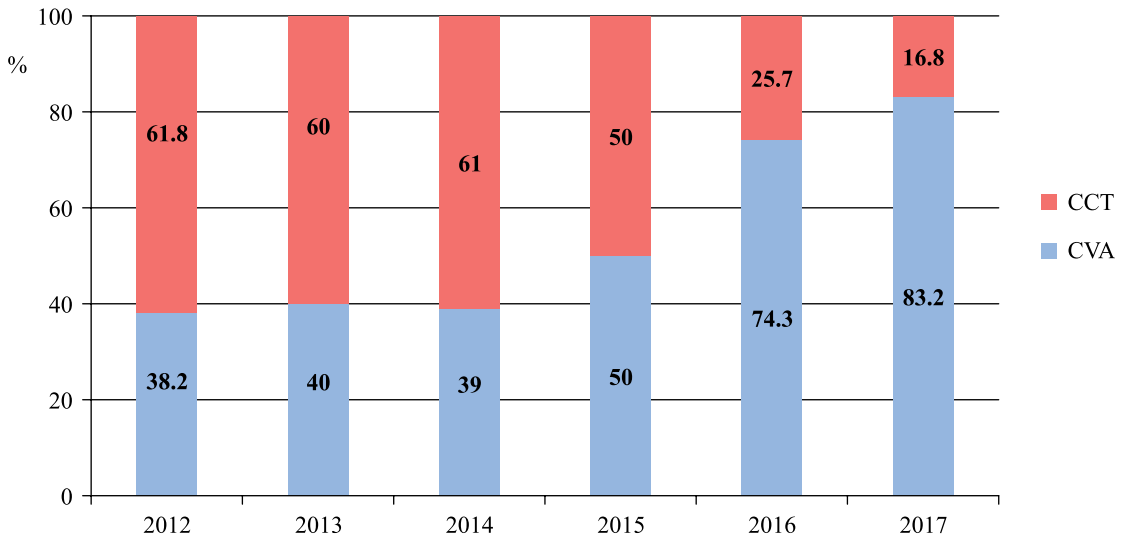

Fig. 8. Percentage of major death causes of heart donors, 2012–2017

According to the registry of the International Society for Heart and Lung Transplantation (ISLHT), in 2010–2018 there was a global decrease in the number of heart donors who died from CVA from 48.8 to 40.5%, and an increase in heart donors who died due to anoxic brain injuries from 7.7 to 21.5% [7].

The age of the heart EDs included in the present study corresponds to the aging trend of the entire pool of donors. If in 2012 85.3% of the total number of heart EDs were donors under 50, then in 2017, their share was 50.4%, along with an increase in the number of donors in the older age group (51–60) to 41.6 % vs 14.7% in 2012. In 2017, for the first time in the Russian Federation, heart donors whose age was in the range of 61–69 accounted for 7.1% of the total heart ED pool. Besides, in 2017, there was one case of heart explantation from a donor of the age group 70+. Over six years, the median age of heart EDs has increased from 41 to 50 years (Fig. 9.) In global practice, over the same period, there is also an increase in the number of donors in the older age group, but still a larger number, about 70% of the total number of heart EDs, were donors under 40. The median age of heart EDs in the world remained at the level of 32 in 2012–2017 [7].

If to speak of the gender distribution of effective heart donors, there is a persistent predominance of male donors. In 2017, there were 2.9 times more male donors than female donors; the proportion of male donors was 75.2% (Fig. 10). According to ISLHT, in 2009–2016 the male donors in Europe were 62.4%, 70.1% in North

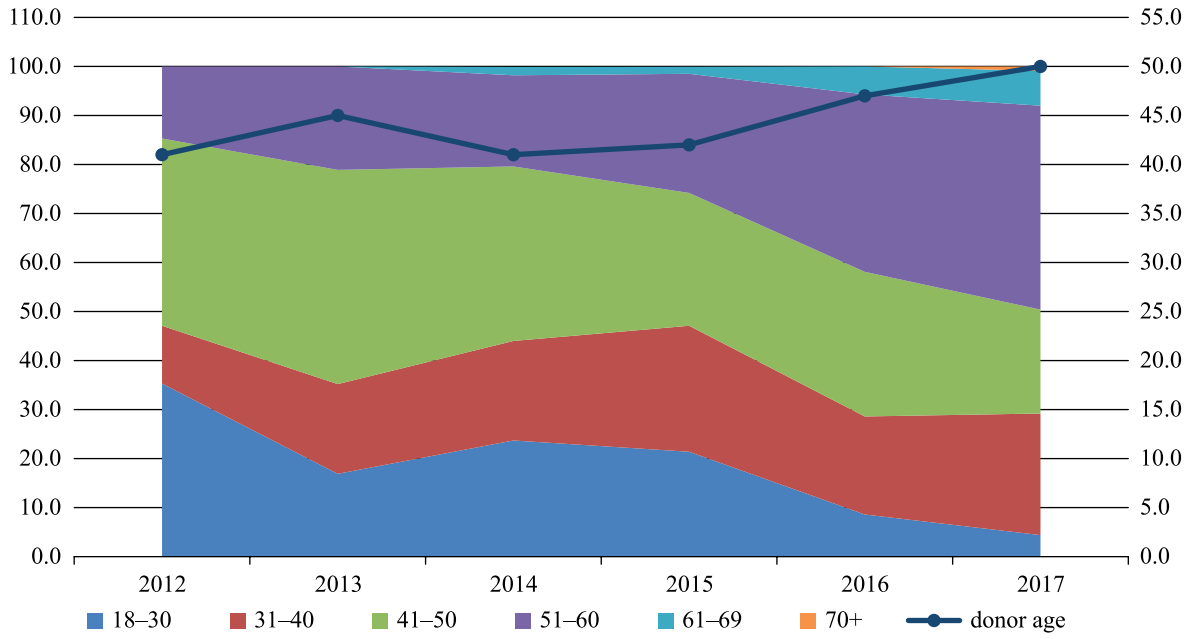

Fig. 9. Dynamics of the specific weight (%) of age groups of heart ED; median age (years) of heart ED in Moscow, 2012–2017

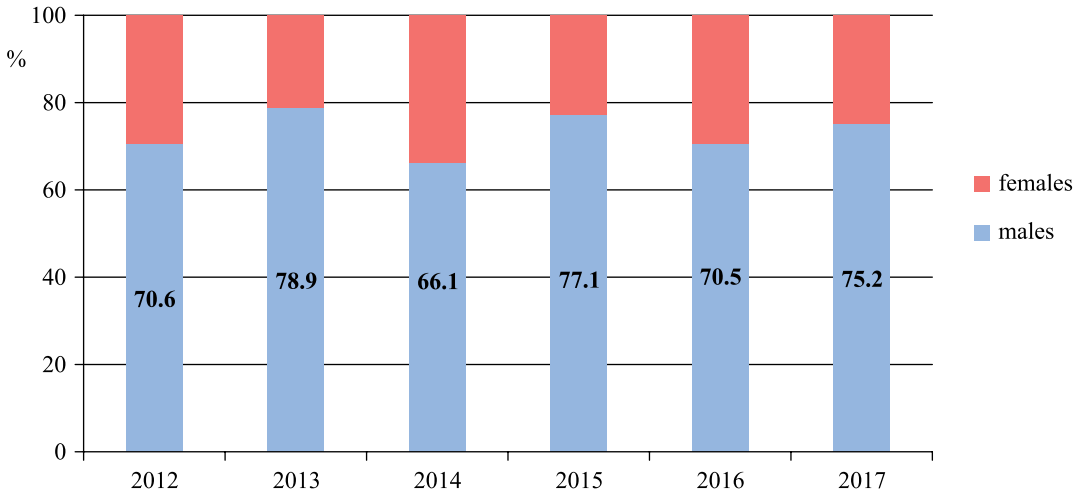

Fig. 10. Percentage of male and female heart donors, 2012–2017

America, 78.3% in other countries [7]. The predominance of male donors can be considered as a positive factor influencing the survival rate of male recipients, since, according to E.S. Weiss (2009), men who received hearts from male donors had the highest cumulative survival in 5 years [10].

In general, the given characteristics of heart donors in Moscow follow the trend of changes in the donor pool on a global scale, and even surpass it in a number of characteristics, in particular, in terms of the age of effective heart donors. Considering the data obtained, the development of a special tool (mathematical model) is becoming extremely urgent, as at the stage of organ donation it would allow to objectively assess the donor heart, considering the maximum number of donor factors available for research. Following the goal of developing such a model, we selected a number of donor risk factors that could cause the donor heart refusal.

ANALYSIS OF CAUSES OF DONOR HEART REFUSAL

For the study, donor factors were selected that were not amenable to correction, e. g., age, death cause, gender, HT, diabetes mellitus, and factors that determine the state of donor homeostasis: SBP, pH, lactate, blood Na and glucose, and dose of vasopressor support.

The Table shows the number of donor heart refusals (%) depending on the presence/absence of a donor factor. The analysis revealed a linear increase in the number of donor heart refusals with increasing age of the donor. In the 41–50 age group, the refusal rate is 27.5, in the 51–60 group 41.4, and in the 60+ age group it increases to 57.9%. The expansion of the selection criteria for heart donors contributed to a decrease in the number of refusals from donors who died of CVA, which made the difference in refusals from donors who died from CCT

Table

Studied donor factors and percentage of refusals from the donor heart

Donor factors	Total donors with BD	Group 1 (explanted heart)	Group 2 (not explanted heart)	Donor heart refusal, %
Donor age, years				
18–30	78	67	11	14.1
31–40	113	96	17	15.9
41–50	193	139	54	27.5
51–60	227	133	94	41.4
61–69	38	16	22	57.9
70+	1	1	0	0.0
Death cause				
CCT	239	179	60	25.1
CVA	411	273	138	33.6
Gender				
Male	464	329	135	29.1
Female	186	123	63	33.9
Hypertension				
Yes	364	231	133	36.5
No	286	221	65	22.7
Diabetes mellitus				
Yes	155	124	31	15.7
No	495	328	167	33.7
Mean arterial pressure (MAP), mm Hg				
≤60	46	31	15	32.6
≥61	604	421	183	30.3
pH, mmol/L				
≤7.0–7.2	31	21	10	32.3
≥7.3	582	414	168	28.9
n/a	37	17	20	
Lactate, mmol/L				
0.1–2.2	229	165	64	27.9
2.3–5.9	179	132	47	26.3
6.0–13.0	40	25	15	37.5
>13.0	5	3	2	40.0
n/a	197	127	70	

End of table 1

Donor factors	Total donors with BD	Group 1 (explanted heart)	Group 2 (not explanted heart)	Donor heart refusal, %
Na, mmol/L				
120–135	66	47	19	28.8
136–145	293	204	89	30.4
146–155	133	94	39	29.3
≥156	122	90	32	26.2
n/a	36	17	19	
Glucose, mmol/L				
≤8.3	213	153	60	28.2
8.4–10.9	161	118	43	26.7
>10.9	221	149	72	32.6
n/a	55	32	23	
Norepinephrine (NA), ng/kg/min				
<100	44	35	9	20.6
100–400	182	129	53	29.1
401–800	166	119	47	28.3
>800	111	72	39	35.2
n/a	11	7	4	

comparable (33.6 vs 25.1, respectively). The SBP parameter did not significantly affect the percentage of donor heart refusals, while the growth of the most important indicator of homeostasis, blood lactate, was associated with an increase in the number of donor heart refusals. In donors with blood lactate in the range of 6–13 mmol/L (3–6 times higher than the reference), heart failure was 37.5%. There was no significant difference in the rate of donor heart refusals depending on the pH The proportion of failures at low pH values is slightly higher (32.3%) than when it is normalized (28.9%). There was no significant difference in the number of donor heart refusals depending on the blood Na value, both with its normal and increased values, the proportion of refusals averaged 28.7%. Diabetes history of donors did not significantly affect the number of refusals. At the same time, in isolation, blood glucose values above 10.9 mmol/L were the reason for 32.6% of donor heart refusals. An increased number of donor heart refusals was revealed, associated with an increase in the dose of vasopressor support (NA), at its minimum values up to 100 ng/kg/min, a decision was made to refuse in 20.6% of cases, with an increase in the injection rate over 800 ng/min. kg/min the failure rate was 35.2%.

CONCLUSION

As the donor activity in the city of Moscow rises, there is an increase in the number of heart transplants. The most significant increase is seen in Shumakov National Medical Research Center of Transplantology and Artificial Organs. The results of the present study of the medical and epidemiological characteristics of donors show that without a balanced revision of the donor selection criteria, the effectiveness of the provision of transplant care not only for heart transplantation, but also for other types of transplantation, will be at a minimum level, and the number of recipients on the waiting list and the waiting time for donor organs will grow. To improve the provision of transplant care, a thorough analysis of donor characteristics and their impact on the suitability of the donor heart for transplantation is required. The article presents the initial results of such an analysis, which showed the identity of Russian and foreign practices and trends in heart transplantation, and the need to continue scientific research of donor criteria in order to create an objective tool for assessing donor heart.

The authors declare no conflict of interest.

REFERENCES

1. *Rudge C, Matesanz R, Delmonico FL, Chapman J.* International practices of organ donation. *Br J Anaesth.* 2012; 108: i48–55. https://doi.org/10.1093/bja/aer399.
2. Prikaz MZ RF ot 25.12.2014 № 908n “O poryadke ustanovleniya diagnoza smerti mozga cheloveka”, zaregistrirovan v Minyuste RF 12.05.15 № 37230, vstupil v silu s 01.01.2016. https://minjust.consultant.ru/documents/14630.
3. https://mosstat.gks.ru/folder/64634.
4. Prikaz Departamenta zdravookhraneniya goroda Moskvy ot 19.10.2017 № 737 “Ob organizatsii meditsinskoy deyatel’nosti, svyazannoy s donorstvom organov cheloveka i okazaniem meditsinskoy pomoshchi po profilyu “khirurgiya” (transplantatsiya organov i tkaney cheloveka) v gorode Moskve”. https://www.mos.ru/dzdrav/documents/department-acts/view/211382220/.

5. *Minina MG*. Razrabotka i vnedrenie v praktiku zdravookhraneniya innovatsionnoy modeli donorstva organov: Avtoref. dis. … d-ra med. nauk. M., 2016. 46.
6. www.Eurotransplant.org.
7. https://ishlt.org/.
8. *Poptsov VN, Spirina EA, Koloskova NN, Masyutin SA, Ukhrenkov SG, Dogonasheva AA*. Heart transplantation from older donors. *Russian Journal of Transplantology and Artificial Organs*. 2017; 19 (1): 89–102. [In Russ. English abstract]. https://doi.org/10.15825/1995-1191-2017-1-89-102.
9. *Poptsov VN, Spirina EA, Pchelnikov VV, Khatutsky VM, Aliev EZ, Voronkov VYu et al*. Heart transplantation from cardiac arrest-resuscitated donors. *Russian Journal of Transplantology and Artificial Organs*. 2019; 21 (2): 23–30. [In Russ, English abstract]. doi: 10.15825/1995-1191-2019-2-23-30.
10. *Weiss ES, Allen JG, Patel ND, Russell SD, Baumgartner WA, Shah AS et al.* The impact of donor-recipient sex matching on survival after orthotopic heart transplantation: analysis of 18.000 transplants in the modern era. *Cir Heart Fail*. 2009; 2 (5): 401–408.

The article was submitted to the journal on 13.07.2020

DOI: 10.15825/1995-1191-2020-3-53-61

FUNCTIONAL STATE OF THE CARDIORESPIRATORY SYSTEM AFTER ORTHOTOPIC HEART TRANSPLANTATION WITH PROLONGED COLD ISCHEMIA TIME

I.Yu. Loginova, O.V. Kamenskaya, A.V. Fomichev, D.V. Doronin, A.M. Chernyavskiy, V.V. Lomivorotov

Meshalkin National Medical Research Center, Novosibirsk, Russian Federation

Objective: to assess the functional state of the cardiorespiratory system in the long term after orthotopic heart transplantation (HT) with prolonged cold ischemia time. **Materials and methods.** The results of 60 orthotopic HTs performed at Meshalkin National Medical Research Center were analyzed. A comparison was made of the immediate and long-term outcomes of HTs in the group with cold ischemia time lasting for less than 240 minutes and in those with farther distance between donor and recipient sites with cold ischemia time of 240 minutes or more. In the long-term follow-up after HT, all patients underwent cardiopulmonary exercise testing, body plethysmography, assessment of the diffusing capacity of the lungs, and quality of life assessment. **Results.** Prolonged cold ischemia showed a negative effect on the early postoperative period – decreased myocardial contractility on postoperative day 1 and longer duration of inotropic support. At the same time, the survival rate and incidence of graft rejection reactions in the early and late post-HT periods in the studied groups did not differ significantly. Peak oxygen consumption in the general group in the long term after HT was 17 (14.7–21.0) mL/kg/min, VE/VCO_2 slope was 30 (29–36) at 100 (90–120) W threshold load power. All the parameters of pulmonary function tests did not differ significantly depending on cold ischemia duration. Quality of life also did not show significant differences depending on the duration of graft ischemia in terms of both physical and psycho-emotional health components of the SF-36 questionnaire. **Conclusion.** Long-term cold ischemia of the graft did not show any negative impact on the functional state of the cardiorespiratory system and quality of life in the long term after HT. The studied group of recipients was characterized by high efficiency of pulmonary ventilation and gas exchange, as well as high tolerance to physical activity in the long-term post-HT period.

Keywords: heart transplantation, cold ischemia time, cardiopulmonary exercise testing.

INTRODUCTION

Heart transplantation (HT) is the "gold standard" for terminal heart failure treatment [1]. According to international registries, the survival rate in the first year after HT is currently 85 to 93%, and the ten-year survival rate is 69% [2].

Despite the development of the legal framework for organ donation and an increase in the efficiency of the organization of the transplantation service, there remains a significant shortage of donor organs, forcing to come back to the issue of expanding the criteria for organ donation, in particular, the use of organs with prolonged cold ischemia [2, 3]. Thus, besides the publications of individual researchers [4–6], the report of the International Society for Heart and Lung Transplantation (ISHLT) in 2017 highlighted the topic of the duration of transplant ischemia as a priority for further study [2].

The transplant ischemia time depends on numerous logistic and technical factors. The recommended maximum duration of cold ischemia of the donor heart is 240 minutes [7, 8]. An increase in ischemic time affects the viability of the graft and, according to many authors, increases the risk of an unfavorable HT outcome [4, 7]. However, a number of studies have shown that prolonged time of cold ischemia does not significantly affect the early and long-term results of HT [9, 10]. The cases with extremely prolonged ischemia of the donor organ and satisfactory HT results in the long-term follow-up were described [5, 10].

Thus, the results of studies on the effect of graft ischemia duration on HT outcome are ambiguous. It is of interest to conduct further studies on this issue, including an assessment of the functional state of the organism of recipients in the long-term follow-up. The purpose of the present study is to assess the functional state of the cardiorespiratory system in the long term after orthotopic HT with prolonged cold graft ischemia.

MATERIALS AND METHODS

The study included 60 patients who underwent HT at the Meshalkin National Medical Research Center (Minis-

Corresponding author: Irina Loginova. Address: 15, Rechkunovskaya str., Novosibirsk, 630055, Russian Federation.
E-mail: i_loginova@meshalkin.ru

try of Health of Russia; Novosibirsk, Russian Federation) from 2013 to the present. The study was performed in accordance with Good Clinical Practice and the principles of the World Medical Association Declaration of Helsinki. The study protocol was approved by the local ethics committee. Written informed consent was obtained from all patients prior to inclusion.

The inclusion criterion was the HT in history. The exclusion criteria were refusal to participate, age under 18, musculoskeletal disorders that made it difficult to perform the cardiopulmonary exercise testing (CPT).

Orthotopic HT was performed by the common bicaval technique. The hearts were retrieved by the standard method, with conservation with "Custodiol" cold cardioplegic solution. In some cases, donor hearts from remote regions, Altai Kraj, Kemerovo Oblast, Krasnoyarsk Kraj were used.

In the postoperative period, all recipients received combined immunosuppressive therapy with calcineurin inhibitor (cyclosporin 4–6 mg/kg/day or tacrolimus 0.05–0.1 mg/kg/day), mycophenolate and prednisolone 1 mg/kg/day with a gradual dose reduction to 0.1–0.2 mg/kg/day. The target level of cyclosporine was 250–300 ng/ml, the concentration of tacrolimus was 15–20 ng/ml, with a gradual decrease in therapeutic concentration in the long term after HT.

The examination protocol after HT included virological and bacteriological examination, general clinical and biochemical blood analysis, determination of the concentration of tacrolimus and cyclosporine in blood, hemocoagulation parameters, and general urine analysis. Electro- and echocardiographic examination, CPT, endomyocardial biopsy with morphological and immunohistochemical analysis, coronary angiography were performed. Endomyocardial biopsy in the first 2 months after transplantation was performed every 10 days, then after 3 months, and later once a year. The graft rejection rate was determined in accordance with the ISHLT recommendations.

The analysis included anthropometric, demographic parameters, functional class (FC) of angina pectoris by NYHA, myocardial infarction in history, acute cerebrovascular accident, previous cardiac surgery, indicators of myocardial contractility, the presence of concomitant pathology. Intraoperative characteristics included the duration of cardiopulmonary bypass, aortic occlusion, the total surgery time, and the duration of graft cold ischemia. In the early postoperative period, the duration of stay in the intensive care unit (ICU), the need and duration of inotropic support, prolonged mechanical ventilation, the need for mechanical circulatory support, myocardial contractility (the first day after HT), and adverse outcomes including graft dysfunction and hospital mortality. In the long-term follow-up, survival, cases of cardiovascular accidents, repeated cardiac surgery, the presence and severity of graft rejection, myocardial contractility, parameters of pulmonary functional tests, including CPT, and quality of life were assessed.

CPT was performed on an OXYCON Pro bicycle ergospirometric system (Jaeger, Germany) with the RAMP protocol until maximum oxygen consumption or limiting symptoms followed by a recovery period. The analysis included the following CPT parameters: threshold load power (W), peak oxygen consumption (VO_2 peak, ml/min/kg) and its metabolic equivalent (MET, RVU), respiratory ratio (RER), ventilation equivalent by carbon dioxide (VE/VCO_2 slope), oxygen pulse at maximum load (O_2-pulse), partial pressure CO_2 in the final portion of expiration ($PetCO_2$, mmHg) at rest and at the anaerobic threshold level, recovery time of oxygen consumption, and heart rate. Anaerobic threshold level was determined by the V-slope. Arterial saturation (%) was measured using pulse oximetry.

Using the methods of body plethysmography and assessment of the diffusion capacity of the lungs (Master Screen, Jaeger, Germany), the absolute and assigned to due values (with accounting for anthropometric parameters and age) of respiratory function were studied. The analysis included the forced expiratory volume in the first second (FEV1, L), Tiffeneau index (%), and diffusive capacity of lungs (DLCO, mmol/L/kPa).

The quality of life was analyzed by the results of the SF-36 questionnaire; for the analysis, summary scales characterizing the physical component of health and the psychoemotional component of health were used.

The results were statistically analyzed with the Statistica 6.1 software package (StatSoft, USA). Quantitative variables are presented as median and interquartile range (Me (Q25–Q75), qualitative variables – as frequency of occurrence and / or percentage. Intergroup comparison of indicators was performed using the Mann – Whitney test or Fisher's exact test. Survival curves were plotted by the Kaplan–Meier method with an assessment of the significance of differences by the log-rank test. p value <0.05 was considered statistically significant for all kinds of analysis.

RESULTS

To assess the effect of the duration of cold graft ischemia on HT results, all patients were divided into two groups: in the first group, the duration of graft ischemia did not exceed 240 minutes, in the second, with remote removal, 240 minutes or more. The basic characteristics of the recipients are presented in Table 1. Average age, anthropometric parameters, the presence of concomitant pathology did not differ in the study groups. In both groups, male patients slightly predominated.

Percutaneous transluminal angioplasty with stenting of the affected coronary arteries prevailed in the previous cardiac surgeries. For health reasons, a left ventricular bypass system was installed in 8 patients prior to heart transplantation.

Table 1

Baseline recipient characteristics

Parameter		General group (n = 60)	Duration of graft cold ischemia		
			<240 min. (n = 35)	≥240 min. (n = 25)	p
Age, years		42 (33–50)	46 (40–51)	40 (30–48)	0.093
Male gender, n (%)		50 (83%)	31 (89%)	19 (76%)	0.062
BMI, kg/m^2		27 (19–33)	26 (19–31)	27 (20–34)	0.288
Etiology	ischemic, n (%)	24 (40%)	14 (40%)	10 (40%)	0.545
	non-ischemic, n (%)	36 (60%)	21 (60%)	15 (60%)	
Functional class by NYHA	III, n (%)	39 (65%)	20 (57%)	19 (76%)	0.324
	IV, n (%)	21 (35%)	15 (43%)	6 (24%)	
Acute myocardial infarction in history, n (%)		8 (13%)	5 (14%)	3 (12%)	0.683
Cerebrovascular accident in history, n (%)		9 (15%)	6 (17%)	3 (12%)	0.256
Diabetes mellitus, n (%)		3 (5%)	2 (6%)	1 (4%)	0.692
Chronic lung diseases, n (%)		2 (3%)	1 (3%)	1 (4%)	0.643
Chronic kidney disease >C3A, n (%)		1 (%)	1 (3%)	0 (0%)	0.380
Previous INCOR installation, n (%)		8 (13%)	4 (11%)	4 (16%)	0.150
Previous cardiac surgery, n (%)		23 (38%)	13 (37%)	10 (40%)	0.412
LVEF, %		22 (19–25)	20 (18–26)	22 (19–24)	0.443
Right ventricle FAC, %		30 (20–38)	31 (18–36)	33 (25–39)	0.267
Systolic pressure in the pulmonary artery, mm Hg		40 (33–48)	42 (35–50)	39 (30–48)	0.252
Time in WL, days		240 (48–376)	240 (143–359)	239 (24–368)	0.592

Table 2

Intraoperative characteristics and the early postoperative period after orthotopic heart transplantation

Parameter	General group (n = 60)	Duration of graft cold ischemia		
		<240 min. (n = 35)	≥240 min. (n = 25)	p
Duration of graft ischemia, min	210 (175–340)	180 (158–190)	350 (300–430)	<0.001
Duration of artificial blood circulation, min	191 (165–240)	182 (156–210)	193 (184–241)	0.624
Duration of aortic occlusion, min	105 (90–130)	102 (94–126)	105 (86–128)	0.814
Total operation duration, min	420 (360–525)	395 (360–510)	460 (330–540)	0.326
Duration of ICU stay, days	8 (6–10)	7 (6–10)	9 (5–10)	0.375
Duration of inotropic support, h	72 (34–96)	56 (34–77)	96 (57–139)	0.014
Duration of ventilation >24 h, n (%)	9 (15%)	4 (11%)	5 (20%)	0.245
MCS after surgery, n (%)	6 (10%)	1 (3%)	5 (20%)	0.032
Repeated surgical interventions, n (%)	8 (13%)	5 (14%)	3 (12%)	0.221
LVEF, %	59 (45–63)	62 (58–65)	56 (43–58)	0.030
Right ventricle FAC, %	40 (36–45)	46 (40–51)	37 (32–40)	0.017
Systolic pressure in the pulmonary artery, mm Hg	30 (26–35)	29 (24–33)	33 (27–38)	0.269
Primary graft dysfunction, n (%)	8 (13%)	3 (8.6%)	5 (20%)	0.163
Mortality associated with primary graft dysfunction, n (%)	1 (1.7%)	1 (2.9%)	0 (0%)	0.361
30-day mortality, n (%)	5 (8%)	2 (5.7%)	3 (12%)	0.502

Against the background of the absence of differences in the initial clinical and functional state of patients and the parameters of the intraoperative period, the differences in the characteristics of the early postoperative period are noteworthy (Table 2). Thus, in the group of remote graft removal, the duration of inotropic support was significantly higher. On day 1 after HT, a significant decrease in myocardial contractility was noted, followed by restoration to normal values by days 5–7 after surgery.

As a result of primary graft dysfunction, one patient died from the group with a graft ischemia duration of less than 240 minutes. The overall 30-day mortality rate was 8% (5 patients), with no significant differences between the groups. In 4 cases, mortality was not associated with graft dysfunction.

The long-term follow-up after HT averaged 3.0 (1.9–4.8) years (Table 3). Most of the patients were FC I – II by NYHA. Myocardial contractility in the long-term

Table 3

Clinical and functional characteristics of patients at long-term follow-up after orthotopic heart transplantation

Parameter		General group (n = 60)	Duration of graft cold ischemia		
			<240 min. (n = 35)	≥240 min. (n = 25)	p
Follow-up duration, years		3.0 (1.9–4.8)	3.0 (1.7–4.8)	3.1 (1.8–4.9)	0.845
Functional class by NYHA	I, n (%)	13 (25%)	7 (23%)	6 (27%)	0.413
	II, n (%)	37 (71%)	21 (70%)	16 (73%)	
	III, n (%)	2 (4%)	2 (7%)	0 (0%)	
Diabetes mellitus, n (%)		5 (10%)	3 (10%)	2 (9%)	0.828
Chronic kidney disease >C3A, n (%)		4 (8%)	1 (3%)	3 (14%)	0.126
Cardiac surgery, n (%)		1 (%)	1 (3%)	0 (0%)	0.551
Graft rejection reaction	1A–1B, n (%)	6 (11.5%)	3 (10%)	3 (14%)	0.236
	2A–2B, n (%)	7 (13.5%)	4 (13%)	3 (14%)	
	3A–3B, n (%)	1 (1.9%)	0 (0%)	1 (4.5%)	
Mortality, n (%)		8 (13%)	5 (14%)	3 (12%)	0.575
LVEF, %		65 (63–67)	65 (64–67)	65 (60–68)	0.501
Right ventricle FAC, %		46 (42–52)	47 (45–52)	46 (39–55)	0.523
Systolic pressure in the pulmonary artery, mm Hg		31 (28–35)	31 (28–35)	31 (30–34)	0.743

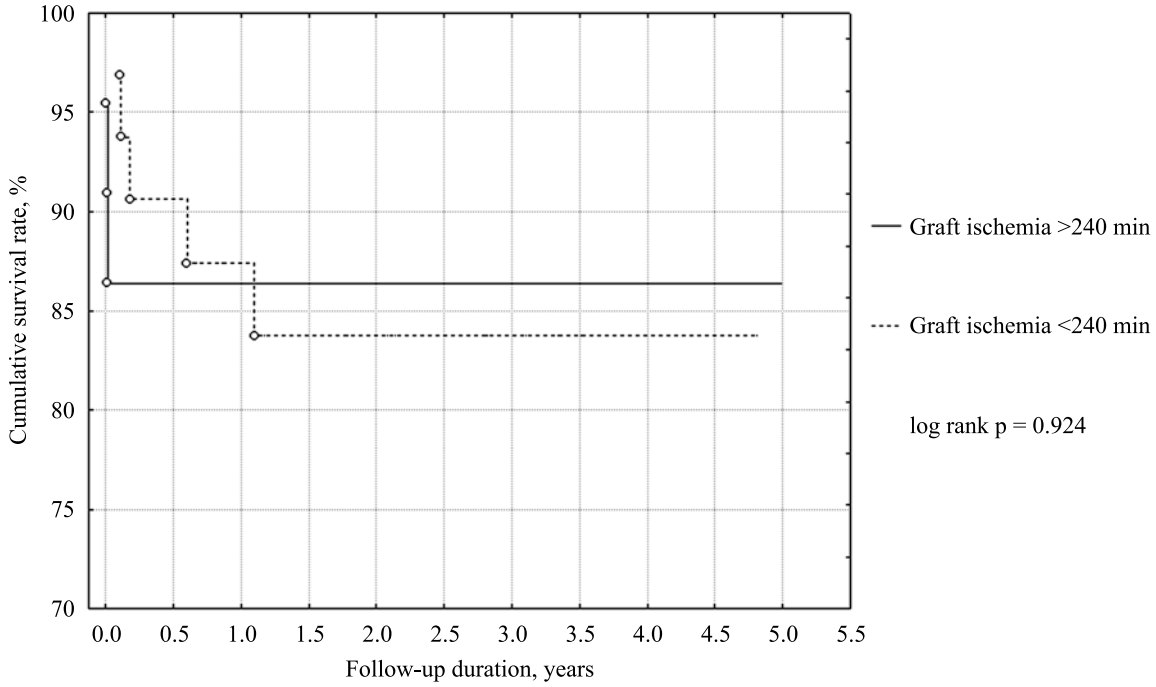

Fig. 1. Survival after orthotopic heart transplantation depending on the duration of cold transplant ischemia

period after HT corresponded to normal values, without significant differences between the groups.

During the follow-up, two patients developed diabetes mellitus, one – coronary artery disease of the transplanted heart, which required endovascular surgery.

Graft rejection grade 3A–3B was registered in 1 patient during the first year after HT, grade 2A–2B – in 7 patients. Rejection was successfully stopped after pulse therapy with methylprednisolone at a dose of 1000 mg/day for 3 days, followed by endomyocardial biopsy control. Graft rejection 1A–1B was registered in 6 patients and did not require radical correction of immunosuppressive therapy. The overall mortality rate was 13%, with no significant differences between the groups (Fig. 1). All mortality cases in the long-term follow-up period were not associated with graft dysfunction.

With improved hemodynamics after HT, all patients showed a high exercise tolerance (Table 4).

The parameters of pulmonary ventilation and gas exchange, including those during provoking physical activity, did not differ in patients with remote transplant removal. The peak oxygen consumption in the general group averaged 17 (14.7–21.0) ml/min/kg, 5.2 (4.2–6.0) MET, with a threshold load power of 100 (90–120) W.

Table 4

The results of pulmonary functional tests in the long-term follow-up after orthotopic heart transplantation

Parameter	General group (n = 60)	Duration of graft cold ischemia		
		<240 min. (n = 35)	≥240 min. (n = 25)	p
Load threshold power, W	100 (90–120)	110 (100–140)	100 (90–110)	0.146
VO_2 peak, ml/min/kg	17 (14.7–21.0)	19 (15.6–21.0)	16 (14.1–21.5)	0.269
VE/VCO_2 slope	30 (29–36)	32 (29–36)	30 (29–36)	0.458
RER peak	1.15 (1.05–1.18)	1.11 (1.06–1.16)	1.06 (1.02–1.18)	0.433
O_2-pulse peak	11.4 (9.6–12.7)	11.5 (9.6–12.6)	10.9 (10.5–12.8)	0.922
MET, conv. units	5.2 (4.2–6.0)	5.5 (4.5–6.0)	4.6 (4.0–6.1)	0.270
$PetCO_2$ at the level of the anaerobic threshold, mm Hg	37 (35–39)	36 (35–38)	38 (33–39)	0.775
$PetCO_2$ gain during exercise, mm Hg	6.3 (5.2–8.5)	5.8 (5.2–7.7)	7.0 (3.1–9.5)	0.628
VO_2 recovery time, min	6 (5–8)	7 (5–8)	6 (4–7)	0.536
HR recovery time, min	9 (7–10)	7 (6–10)	9 (8–10)	0.268
Arterial saturation, %	96 (95–97)	96 (95–97)	95 (94–97)	0.182
FEV1, % of reference	95 (84–103)	98 (92–106)	93 (76–100)	0.136
Tiffeneau Index, %	81 (77–89)	82 (75–90)	81 (76–87)	0.979
DLCO, % of reference	77 (64–85)	72 (61–80)	81 (67–87)	0.859

Note. VO_2 – oxygen consumption; VO_2 peak – peak oxygen consumption; VE/VCO_2 – ventilation coefficient of carbon dioxide; RER peak – respiratory coefficient during exercise; O_2 pulse – oxygen pulse during exercise; MET – metabolic equivalent; $PetCO_2$ – end tidal carbon dioxide partial pressure; HR – heart rate; FEV_1 – forced expiratory volume in 1 second; DLCO – lung diffusion capacity.

The absence of significant differences in the study groups was also seen for the main parameters of the quality of life, which was assessed using the SF-36 questionnaire in the long term after HT (Fig. 2).

The level of quality of life in the general group for the physical and psychoemotional components of health of the SF-36 questionnaire was above average and amounted to 53 (50–55) and 52 (50–56) points, respectively.

Thus, in the studied group of patients, long-term cold ischemia of the graft did not show a significant effect on the functional state of the cardiorespiratory system and quality of life in the long term after HT.

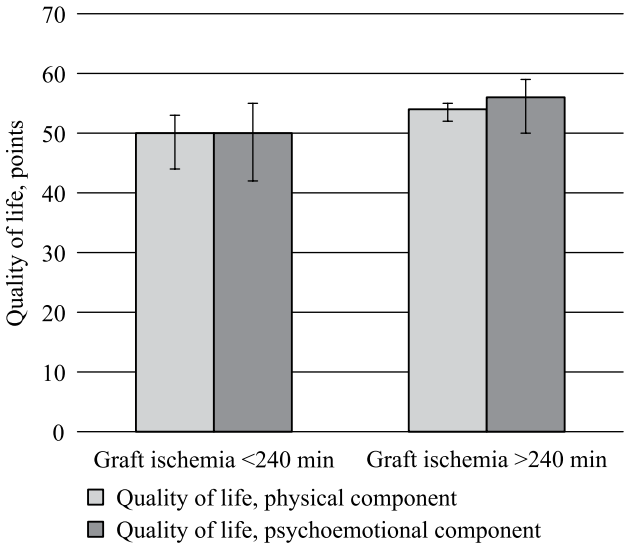

Fig. 2. Quality of life in the long-term follow-up after heart transplantation, SF-36 questionnaire results

DISCUSSION

The duration of graft cold ischemia is considered one of the most important factors determining the effectiveness of HT [2, 11, 12]. According to many authors, exceeding the safe time threshold increases the risk of postoperative allograft dysfunction and the death of the recipient [4, 13]. Destabilization of biological membranes, generation of reactive oxygen species, disturbances in electrolyte balance, energy supply, coagulation hemostasis that occur during hypoxia and subsequent tissue reperfusion play a great role in the mechanisms of allograft damage [13, 14].

However, the increase in the number of patients on the HT waiting list dictates the need to change strategies to increase the donor pool. Our study analyzed the results of long-term follow-up after HT in two groups: with allograft ischemia duration less than 4 hours, on average 180 (158–190) minutes, and exceeding the safe ischemia threshold (average ischemia time 350 (300–430) minutes).

The results of the study showed that the adverse effect of long-term cold ischemia of the allograft affects the early postoperative period after HT. Myocardial injury during prolonged cold ischemia and its subsequent reperfusion injury led to contractile dysfunction of the donor heart on the first day after HT, which required more prolonged inotropic support in the group with graft ischemia of more than 4 hours. It should be noted that by the end of hospitalization the myocardial contractili-

ty in this group corresponded to normal values and did not differ from the group with the duration of allograft ischemia less than 4 hours. Mortality in the study groups in the early postoperative period also had no significant differences, including cases associated with primary graft dysfunction. These data are comparable with the results of other researchers [15].

Numerous studies show improvements in physical performance, peak oxygen consumption and other parameters of pulmonary ventilation and gas exchange in the general cohort of patients undergoing HT [16–19]. However, when analyzing the effect of long-term allograft ischemia, the authors, as a rule, use only the main characteristics of clinical outcomes, such as graft rejection reactions, survival [4–6, 15]. In particular, the current international recommendations do not analyze the potential interactions between the ischemic time of the allograft and the characteristics of the clinical and functional state of the recipient's body and do not assess the role of the ischemic time of the allograft in any specific subgroups [2].

The advantage of the present study was a comprehensive assessment of the functional state of the cardiorespiratory system in the long term after HT, depending on the duration of graft ischemia.

Patients of both studied groups in the long term after HT corresponded mainly to FC I–II by NYHA and were characterized by normal myocardial contractility. There were no differences in the incidence of graft rejection reactions and patient survival.

The effect of the duration of graft cold ischemia on exercise tolerance and other CPT parameters was not noted. All patients in the long term after HT were characterized by high efficiency of pulmonary ventilation and gas exchange, high physical performance. The level of peak oxygen consumption in the general group, equal to 17 (14.7–21.0) ml/min/kg and VE/VCO_2 slope equal to 30 (29–36), as well as an increase in $PetCO_2$ during exercise over 5 mm Hg. Art. obtained in our study indicate a good long-term prognosis in patients undergoing HT. The kinetics of heart rate recovery and oxygen consumption after stress testing also did not depend on the duration of graft ischemia.

Quality of life, being an important indicator of the effectiveness of treatment, in our study did not show significant differences depending on the duration of graft ischemia and corresponded in the long term after HT to a level above the average for both physical and psychoemotional health components of the SF-36 questionnaire.

The findings are comparable to those of large studies. Despite the fact that the overall risk of graft dysfunction increases with an increase in the duration of ischemia beyond 4 hours, many authors believe that it is possible to safely increase the threshold to at least 5 hours without compromising HT results [20]. According to other authors, exceeding the safe time threshold has a negative value only for an allograft obtained from an older donor, since, due to age-related changes, the heart of an elderly donor may be especially susceptible to hypoxic and reperfusion damage and have a lower ability to regenerate [6, 21]. In addition, in the future, the role of the ischemic time of the allograft may change as a result of the possible introduction of new perfusion systems for the preservation of donor organs [22].

The limitation of this study was the relatively small number of observations after HT with prolonged cold ischemia of the allograft. However, the results obtained in this cohort of patients indicate the need for further study of this issue from the standpoint of a comprehensive assessment of the functional state of the organism of recipients after HT.

CONCLUSION

The study showed that long-term cold ischemia of the donor heart has a negative effect on the early postoperative period of HT in the form of a decrease in myocardial contractility on the first day after surgery and an increase in the duration of inotropic support. The survival rate and the incidence of graft rejection reactions in the early and late periods after HT were comparable in the groups with graft ischemia of less than 240 minutes and with prolonged ischemia of more than 240 minutes.

Long-term cold ischemia of the graft did not show a negative effect on the functional state of the cardiorespiratory system and quality of life in the long term after HT. The study group of recipients was characterized by high efficiency of pulmonary ventilation and gas exchange, as well as high exercise tolerance in the long term after HT.

The authors declare no conflict of interest.

REFERENCES

1. *Gautier SV.* Innovations in transplantology: heart transplantation program development in Russian Federation. *Patologiya krovoobrashcheniya i kardiokhirurgiya.* 2017; 21 (3S): 61–68. doi: 10.21688/1681-3472-2017-3s-61-68.
2. *Chambers DC, Yusen RD, Cherikh WS, Goldfarb SB, Kucheryavaya AY, Khusch K et al.* The registry of the International Society for Heart and Lung Transplantation: Thirty-fourth adult lung and heart-lung transplantation report – 2017; Focus Theme: Allograft ischemic time. *The Journal of Heart and Lung Transplantation.* 2017; 36 (10): 1047–1059. doi: 10.1016/j.healun.2017.07.016.
3. *Chernyavskiy AM, Fomichev AV, Doronin DV, Alsov SA.* Experience of the heart transplantation with prolonged cold transplant ischemia. *Russian Journal of Transplantology and Artificial Organs.* 2019; 21 (5): 35–35. (In Russ.).
4. *Russo MJ, Chen JM, Sorabella RA, Martens TP, Garrido M, Davies RR et al.* The effect of ischemic time on survival after heart transplantation varies by donor age: An analysis of the United Network for Organ Sharing

database. *The Journal of Thoracic and Cardiovascular Surgery.* 2007; 133 (2): 554–559. doi: 10.1016/j.jtcvs.2006.09.019.
5. *Currie ME, Shudo Y, Woo YJ.* Successful outcome following orthotopic heart transplantation with a donor half way across the country. *Transplantation Proceedings.* 2018; 50 (10): 4062–4063. doi: 10.1016/j.transproceed.2018.09.014.
6. *Reich HJ, Kobashigawa JA, Aintablian T, Ramzy D, Kittleson MM, Esmailian F.* Effects of older donor age and cold ischemic time on long-term outcomes of heart transplantation. *Texas Heart Institute Journal.* 2018; 45 (1): 17–22. doi: 10.14503/thij-16-6178.
7. *Fernandez J, Aranda J, Mabbot S, Weston M, Cintron G.* Overseas procurement of donor hearts: ischemic time effect on postoperative outcomes. *Transplantation Proceedings.* 2001; 33 (7–8): 3803–3804. doi: 10.1016/s0041-1345(01)02610-0.
8. *Erasmus M, Neyrink A, Sabatino M, Potena L.* Heart allograft preservation. *Current Opinion in Cardiology.* 2017; 32 (3): 292–300. doi: 10.1097/hco.0000000000000395.
9. *Mitropoulos FA, Odim J, Marelli D, Karandikar K, Gjertson D, Ardehali A et al.* Outcome of hearts with cold ischemic time greater than 300 minutes. A case-matched study. *European Journal of Cardio-Thoracic Surgery*. 2005; 28 (1): 143–148. doi: 10.1016/j.ejcts.2005.01.067.
10. *Alsov SA, Fomichev AV, Doronin DV, Shmyrev VA, Osipov DE, Chernyavskiy AM.* Heart transplantation with extremely extended cold ischemia time of the donor heart. *Russian Journal of Transplantology and Artificial Organs.* 2018; 20 (1): 110–113. (In Russ.) doi: 10.15825/1995-1191-2018-1-110-113.
11. *Stehlik J, Edwards LB, Kucheryavaya AY, Aurora P, Christie JD, Kirk R et al.* The registry of the International Society for Heart and Lung Transplantation: Twenty-seventh official adult heart transplant report – 2010. *The Journal of Heart and Lung Transplantation*. 2010; 29 (10): 1089–1103. doi: 10.1016/j.healun.2010.08.007.
12. *Nicoara A, Ruffin D, Cooter M, Patel CB, Thompson A, Schroder JN et al.* Primary graft dysfunction after heart transplantation: Incidence, trends, and associated risk factors. *American Journal of Transplantation.* 2017; 18 (6): 1461–1470. doi: 10.1111/ajt.14588.
13. *Yellon DM, Hausenloy DJ.* Myocardial Reperfusion Injury. *New England Journal of Medicine.* 2007; 357 (11): 1121–1135. doi: 10.1056/nejmra071667.
14. *Sologub TV, Romancova MG, Kremen NV, Aleksandrova LM, Anikina OV, Suhanov DS et al.* Svobodnoradikal'nye processy i vospalenie (patogeneticheskie, klinicheskie i terapevticheskie aspekty). Uchebnoe posobie dlja vrachej. M.: Akademija estestvoznanija (2008).
15. *Marasco SF, Esmore DS, Richardson M, Bailey M, Negri J, Rowland M et al.* Prolonged cardiac allograft ischemic time – no impact on long-term survival but at what cost? *Clinical Transplantation*. 2007; 21 (3): 321–329. doi: 10.1111/j.1399-0012.2007.00644.x.
16. *Guazzi M, Arena R, Halle M, Piepoli MF, Myers J, Lavie CJ.* 2016 Focused Update: Clinical Recommendations for Cardiopulmonary Exercise Testing Data Assessment in Specific Patient Populations. *Circulation.* 2016; 133 (24): e694–e711. doi: 10.1161/cir.0000000000000406.
17. *Tsai WJ, Tsai HY, Kuo LY, Lin YS, Chen BY, Lin WH et al.* VE/VCO_2 Slope and Functional Capacity in Patients Post-Heart Transplantation. *Transplantation Proceedings.* 2018; 50 (9): 2733–17377. doi: 10.1016/j.transproceed.2018.05.010.
18. *Uithoven K, Smith J, Medina-Inojosa J, Squires R, Van Iterson E, Olson T.* Clinical and Rehabilitative Predictors of Peak Oxygen Uptake Following Cardiac Transplantation. *Journal of Clinical Medicine*. 2019; 8 (1): 119. doi: 10.3390/jcm8010119.
19. *Loginova IY, Kamenskaya OV, Chernyavskiy AM, Doronin DV, Alsov SA, Lomivorotov VN.* Dynamic of end-tidal carbon dioxide pressure during cardiopulmonary exercise testing before and after heart transplantation. *Russian Journal of Transplantology and Artificial Organs.* 2019; 21 (2): 16–22. (In Russ.) doi: 10.15825/1995-1191-2019-2-16-22.
20. *Yeen W, Polgar A, Guglin M, Downes K, Faber C, Roy A et al.* Outcomes of Adult Orthotopic Heart Transplantation With Extended Allograft Ischemic Time. *Transplantation Proceedings.* 2013; 45 (6): 2399–2405. doi: 10.1016/j.transproceed.2013.04.003.
21. *Slegtenhorst BR, Dor FJ, Elkhal A, Rodriguez H, Yang X, Edtinger K et al.* Mechanisms and consequences of injury and repair in older organ transplants. *Transplantation.* 2014; 97 (11): 1091–1099. doi: 10.1097/tp.0000000000000072.
22. *Chew HC, Macdonald PS, Dhital KK.* The donor heart and organ perfusion technology. *Journal of Thoracic Disease.* 2019; 11 (S6): S938–S945. doi: 10.21037/jtd.2019.02.59.

The article was submitted to the journal on 30.04.2020

DOI: 10.15825/1995-1191-2020-3-62-68

PERSONALITY FACTORS IN HEART TRANSPLANT RECIPIENTS

M.A. Simonenko[1], P.A. Fedotov[1], P.V. Shirobokova[2], Yu.V. Sazonova[1], M.A. Bortsova[1], A.V. Berezina[1], M.A. Karpenko[1]

[1] Almazov National Medical Research Centre, St. Petersburg, Russian Federation
[2] Pavlov First St. Petersburg State Medical University, St. Petersburg, Russian Federation

Objective: to assess the personal psychological profile of heart transplant recipients as the first stage in the development of post-transplant personalized rehabilitation programs. **Materials and methods.** From January 2010 to July 2019, 129 HTs were performed (mean age 46.6 ± 14.1 years; 74% (n = 95) were men, 26% (n = 34) were women). All patients in the heart transplant waiting list were examined by a clinical psychologist and a psychotherapist to exclude contraindications to transplant surgery. To assess personal traits, we used the standard multifactorial questionnaire by Cattell R., 16 PF (version A), which included 187 questions. Heart transplantation and absence of post-transplant severe cognitive impairments were the selection criteria for this study. Patients were surveyed before they were discharged from the hospital – 30–60 days following HT: during the period of complete recovery after surgery. In the present study, a retrospective assessment of the results was performed in 107 patients (n = 76 – men; n = 31 – women). **Results.** Analysis of the personality portrait revealed that over half of recipients were reserved, distant (factor A – schizothymia) and restrained (factor F – restraint; F2 – introvert; F4 – conforming) with lower mental capacity (factor B), and were shy, timid (factor H), with low super ego (factor G: irresponsible, tolerates disorder, flexible, open to change). Our results showed that 47% of patients (n = 18 out of 38 patients, n = 22 are pensioners) with a weak degree of factor C (reactive, affected by feelings) are workers to 42% (n = 29 out of 69, n = 28 – retirees) with a strong degree of the same factor. One year after HT, the number of physically active patients was higher among those with low anxiety compared with high anxiety (41% (18 of 44) and 32% (20 of 63), respectively, p = 0.41). **Conclusion.** Personality factors are non-modifiable characteristics of patients. They affect human behavior, return to work and to social life, as well as physical and psychological recovery from HT. Knowing the personal traits of recipients would allow to develop a personalized approach to their rehabilitation and a technique for timely examination after HT.

Keywords: heart transplantation, psychological well-being, personality factors, quality of life.

INTRODUCTION

Psychological and social factors in patients with chronic heart failure (CHF) and recipients before heart transplantation (HT) take on special significance and determine the patients' compliance at the stage of waiting for the operation, during reconstructive postoperative treatment and rehabilitation, which is related directly to the overall clinical prognosis, including their survival [1]. Despite the fact that every year the number of HT increases [2] and there are studies reflecting the dynamics of quality of life (QL) after surgery, at present there are no publications on the peculiarities of personal characteristics of recipients after a heart transplantation.

Purpose: to assess the personal psychological profile of heart transplant recipients as the first stage in the development of post-transplant personalized rehabilitation programs

MATERIALS AND METHODS

January 2010 to July 2019, 129 HT were performed (mean age 46.6 ± 14.1 years; 74% (n = 95) men, 26% (n = 34) women), of which six were children (median age 15, range 10 to 16); 5 girls, 1 boy). Mechanical circulatory support (MCS) was implanted as a bridge to HT in 14% (n = 18) patients: 11 – extracorporeal membrane oxygenation (ECMO) system, 8 – Berlin Heart "EXCOR" biventricular system, 1 – left ventricular assist circulatory system (and LV "AVK-N"). While on the waiting list for heart transplantation (HT WL), 46 patients were working or studying (school, institute) and 83 were not working, including retirees. One of the points of examination at HT WL was a consultation with a clinical psychologist and a psychotherapist to rule out contraindications for surgery. If necessary, patients were recommended to take antidepressants. After HT, consultations with a clinical psychologist or a psychotherapist were performed only by indications or personal requests of patients: two patients continued to take the drugs recommended by the HT WL, and 5 drugs were first prescribed within 1 month to 5 years after HT.

To assess personal characteristics, we used the standard multifactorial questionnaire by Cattell R., 16 PF

Corresponding author: Maria Simonenko. Address: 2, Akkuratova str., Saint-Petersburg, 197341, Russian Federation. Phone: (921) 952-43-55. E-mail: dr.maria.simonenko@gmail.com, simonenko_ma@almazovcentre.ru

(version A), which includes 187 questions and is designed to examine adults with an education of at least 8–9 grades. The results of the questionnaire allow us to assess the primary and secondary factors of various personality traits, which have a double (bipolar) title characterizing the degree of development of a trait: strong or weak [3]. This study was conducted in accordance with the principles of the Declaration of Helsinki.

The selection criteria for this study were HT performed and the absence of severe cognitive impairments that developed in the post-transplant period. Patients were questioned before they were discharged from the hospital on days 30–60 after HT: during the period of complete recovery after surgery. Patients under 18 completed the questionnaires only after they reached the age of 16–17. In the present study, a retrospective assessment of the results was performed in 107 patients (76 men, 31 women). The analysis did not include 22 recipients (17%): 10% (13 of 129) died in the early postoperative period, 3% (4 of 116) were not questioned due to severe cognitive impairments developed after HT, and five were not included in the present study due to HT performed less than 30 days ago.

After discharge from the hospital, all recipients were put on dispensary registration in the Center, including regular observation, laboratory and instrumental research and specialist consultations.

Data were statistically processed with the SPSS 21.ORU software. Mean values and standard deviation (M ± SD) were calculated. In case of a small sample (<20), the data were presented as medians (Me) [minimum and maximum values]. Statistical significance criterion was $p < 0.05$. Correlation analysis was also performed.

RESULTS

In the described population, the psychological personality profile of patients after HT in most of them is presented by strong features: the frequency of occurrence of personal factors of more than 50% was 13 strong degrees and 7 weak degrees out of 20 (Table 1). According to our results, only one third of patients who underwent HT had high intelligence. When analyzing the personality portrait, it was revealed that more than half of the recipients were secretive, distrustful (factor A – schizothymia) and restrained (factor F – restraint; F2 – introvert; F4 – conformity) with low intelligence (factor B), indecisive (factor H – trektia), with a low superego (factor G: irresponsible, disorganized, fickle, changeable). Among the personal factors, the majority of patients showed emotional stability (factor C – strength I), self-will and stubbornness (factor E – dominance), restlessness and fussiness (factor I – premission), internal tension and egocentricity (factor L – resistance), idealism and dreaminess (factor M – autism), insight (factor N – diplomacy), depression and self-flagellation (factor O – hypothymia), good awareness and tolerance for in-

Table 1

Results of P. Cattell's a6 PF questionnaire in heart transplanted patients (version A)

	Determining factors	Personal characteristics			
		"–"		"+"	
I	Factor A	Schizothymia	60% (n = 64)	Affectothymia	40% (n = 43)
II	Factor B	Low intelligence	65% (n = 70)	High intelligence	35% (n = 37)
III	Factor C	Weak I	36% (n = 38)	Strong I	64% (n = 69)
IV	Factor E	Conformity	33% (n = 35)	Dominance	67% (n = 72)
V	Factor F	Reservedness	61% (n = 65)	Expressiveness	39% (n = 42)
VI	Factor G	Low superego	60% (n = 64)	High superego	40% (n = 43)
VII	Factor H	Trektia	62% (n = 66)	Parmia	38% (n = 41)
VIII	Factor I	Harria	41% (n = 44)	Premsia	59% (n = 63)
IX	Factor L	Alaxia	39% (n = 42)	Protensia	61% (n = 65)
X	Factor M	Praxernia	37% (n = 40)	Autia	63% (n = 67)
XI	Factor N	Straightforwardness	27% (n = 29)	Diplomacy	73% (n = 78)
XII	Factor O	Hyperthymia	48% (n = 51)	Hypothymia	52% (n = 56)
XIII	Factor Q1	Rigidity	43% (n = 46)	Radicalism	57% (n = 61)
XIV	Factor Q2	Group dependence	12% (n = 13)	Self-sufficiency	88% (n = 94)
XV	Factor Q3	Low self-righteousness	30% (n = 32)	High self-righteousnes	70% (n = 75)
XVI	Factor Q4	Low ego tension	32% (n = 34)	High Low ego tension	68% (n = 73)
Secondary factors					
I	Factor F1	Low anxiety	41% (n = 44)	High anxiety	59% (n = 63)
II	Factor F2	Introvert	64% (n = 69)	Extrovert	36% (n = 38)
III	Factor F3	Sensitivity	48% (n = 51)	Reactive balance	52% (n = 56)
IV	Factor F4	Conformity	82% (n = 88)	Independence	18% (n = 19)

conveniences (factor Q1 – radicalism) and reactive balance (factor F3 – stability, cheerfulness, determination).

The primary factor "C" is responsible for 2 degrees of development: "–" weakness of the I (weakness, emotional instability, changeable, easily upset, refuses to work, unwavering in interests) and "+" strength of the I (strength, emotional stability, mature, realistic configured, workable). According to our results, 47% (18 patients out of 38; 22 are retirees) with a weak degree of factor C are working, compared to 42% (29 out of 69; 28 are retirees) with a strong degree of this factor ("I Power").

The primary factor "B" has 2 degrees of development of traits: "–" – low intelligence (unfocused, disorganized with rigid thinking and low mental abilities) and "+" – high intelligence (focused, quick-witted, high mental abilities). The number of obese patients (BMI >30 kg/m^2) prevailed among patients with weak factor B (low intelligence) compared with those with high intelligence (11% (8 out of 70) and 5% (2 out of 37), respectively, p = 0.49). Factor Q4 levels, low ego tension and high ego tension, reflect personality characteristics ranging from relaxation, apathy, low motivation and laziness to focus, energy, increased motivation and activity: 35% (12 of 34) of patients with low ego returned to work after HT versus 44% (32 of 73) with high ego (p = 0.53).

One year after HT, the number of physically active patients was higher among those with low anxiety compared with highly anxious (41% (18 of 44) and 32% (20 of 63), respectively, p = 0.41). According to our results, the personal characteristics of patients did not affect the parameters of cardiopulmonary testing (VO_{2peak}, VO_{2peak} (% MV), Ve/VCO_2) 1 year after HT (p > 0.05).

When comparing personality characteristics depending on gender, it was revealed that in men 9 out of 20 factors had a weak degree of development, while in women – 10 out of 20 (Table 2). In men, among the factors, harria prevailed (severity, realistic judgments, does not pay attention to physical ailments, practicality) and extension (great conceit, irritability, the requirement from others to be responsible for their mistakes), while in women – a premium (sensitivity, hypochondria, anxiety, over-caution) and alaxia (gullibility, agreement with the proposed conditions, tolerance). Hypothymia (anxiety, anxiety, depression, feelings of loneliness, hypochondria) prevailed among women, and hyperthymia (carelessness, self-confidence, serenity, thoughtlessness) among men. Both sexes had high self-esteem, self-sufficiency, high ego-tension and anxiety (>50%). 62% of men and 71% of women in the analyzed population were characterized by shyness, secrecy, restraint (factor F2 – introvert) and passivity, the need for support (factor F4 – conformity).

Table 2

Results of personality factors in patients after heart transplantation regarding their gender

Nos.	Factors "–"			Factors "+"		
		Men (n = 76)	Women (n = 31)		Men (n = 76)	Women (n = 31)
Primary factors						
I	Schizothymia	62% (n = 47)	55% (n = 17)	Affectothymia	38% (n = 29)	45% (n = 14)
II	Low intelligence	64% (n = 49)	68% (n = 21)	High intelligence	36% (n = 27)	32% (n = 10)
III	Weak I	33% (n = 25)	42% (n = 13)	Strong I	67% (n = 51)	58% (n = 18)
IV	Conformity	28% (n = 21)	45% (n = 14)	Dominance	72% (n = 55)	55% (n = 17)
V	Reservedness	59% (n = 45)	65% (n = 20)	Expressiveness	41% (n = 31)	35% (n = 11)
VI	Low superego	59% (n = 45)	61% (n = 19)	High superego	41% (n = 31)	39% (n = 12)
VII	Trektia	61% (n = 46)	65% (n = 20)	Parmia	39% (n = 30)	35% (n = 11)
VIII	Harria	57% (n = 43)	3% (n = 1)	Premsia	43% (n = 33)	97% (n = 30)
IX	Alaxia	34% (n = 26)	52% (n = 16)	Protensia	66% (n = 50)	48% (n = 15)
X	Праксерния	41% (n = 31)	29% (n = 9)	Autia	59% (n = 45)	71% (n = 22)
XI	Straightness	29% (n = 22)	23% (n = 7)	Diplomacy	71% (n = 54)	77% (n = 24)
XII	Hyperthymia	58% (n = 44)	23% (n = 7)	Hypothymia	42% (n = 32)	77% (n = 24)
XIII	Conservatism	38% (n = 29)	55% (n = 17)	Radicalism	62% (n = 47)	45% (n = 14)
XIV	Group dependence	15% (n = 11)	6% (n = 2)	Self-sufficiency	85% (n = 65)	94% (n = 29)
XV	Low self-righteousness	29% (n = 22)	32% (n = 10)	High self-righteousness	71% (n = 54)	68% (n = 21)
XVI	Low ego tension	34% (n = 26)	26% (n = 8)	High ego tension	66% (n = 50)	74% (n = 23)
Secondary factors						
I	Low anxiety	47% (n = 36)	26% (n = 8)	High anxiety	53% (n = 40)	74% (n = 23)
II	Introvert	62% (n = 47)	71% (n = 22)	Extrovert	38% (n = 29)	29% (n = 9)
III	Sensitivit	33% (n = 25)	84% (n = 26)	Reactive balance	67% (n = 51)	16% (n = 5)
IV	Conformity	80% (n = 61)	87% (n = 27)	Independence	20% (n = 15)	13% (n = 4)

There were no correlations between personality characteristics and mortality after heart transplantation ($p > 0.05$).

The following correlations between the factors of personal characteristics have been determined (Table 3). In 51% (n = 54) patients, a relationship was found between two factors: restraint, caution (factor F) and self-sufficiency, independence in decision-making (Q2). Moreover, 11% (6 out of 54) of patients with the above factors died within 3 months to 3 years after HT, compared with 15% (n = 8 out of 53) of patients who died without the personality characteristics F and Q2 (2 – sudden cardiac death, 1 – acute cerebrovascular accident (CVA) and 5 – progression of chronic diseases). In 5 out of 6 recipients, lethal outcomes (3 – crises of allograft rejection with graft dysfunction, 1 – myocardial infarction, transplanted heart coronary artery disease (ACVD), 1 – CVA) occurred due to complications for which they did not timely report complaints.

Moreover, 57% (n = 61) of patients had a combination of factors F1 + Q4 (irritability and aggressiveness), 13% (8 of 61) of which died, compared with 8.7% (7 of 46) of patients, not having these personality factors.

DISCUSSION

Patients after heart transplantation use different types of defense mechanisms, and more active use of defense mechanisms leads to psychological readiness for transplantation [4, 5]. Quality of life (QL) levels in physical well-being in patients after HT are improved, results are better in physically active patients [6]. QL and the incidence of depression after transplant have been studied in various works [7–10], but there are currently no publications on personality characteristics in recipients who received HT.

Personal characteristics are features that occur in all patients and do not change regardless of the operation. Depending on certain personal factors, the behavior of the recipient may differ and lead to different reactions to complications and coping mechanisms to negative dynamics of the state [4, 5]. Emotionally labile, or vice versa, reserved patients may underestimate the emergence of new complaints and untimely seek medical attention. While determined, radical patients with extroverted thinking will be motivated to improve their quality of life, perform regular physical activity and

Table 3

Correlations between personality factors in patients after heart transplantation

Nos.	Factor correlations	Value	Deciphered personality factors	Patients
Positive correlations				
1	E and F2	r = 0.390 (p < 0.001)	Being a dominant, unyielding, conflicting, wayward and extrovert who is good at establishing and maintaining social contacts	34% (n = 36)
2	E and F4	r = 0.304 (p = 0.002)	Being dominant and independent and aggressive	15% (n = 16)
3	F and F2	r = 0.393 (p < 0.001)	Being expressive, impulsive and extroverted	27% (n = 29)
4	H and F2	r = 0.595 (p < 0.001)	Being bold, adventurous, light-hearted and extroverted	26% (n = 28)
5	M and F4	r = 0.310 (p < 0.001)	Being dreamy, distracted, unbalanced and independent	16% (n = 17)
6	Q1 and F4	r = 0.365 (p < 0.001)	Being radical and critical, with intellectual interests, and aggressive, quick-witted	16% (n = 17)
7	F1 and Q4	r = 0.757 (p < 0.001)	Being irritable, motivated and aggressive, but quick-witted	57% (n = 61)
Negative correlations				
8	F and Q2	r = –0.377 (p < 0.001)	Being reserved, cautious, pessimistic and self-sufficient, independent in making decisions	51% (n = 54)
9	H and F1	r = –0.371 (p < 0.001)	Being indecisive, irritable, strictly adhering to rules and guidelines and satisfied with life, but with little motivation to strive for new goals and better quality of life	13% (n = 14)
10	H and Q4	r = –0.329 (p < 0.001)	Being emotionally labile and calm with a lack of motivation to take additional actions	12% (n = 13)
11	I and F3	r = –0.546 (p < 0.001)	Being realistic, practical, who doesn't pay attention to physical ailments	19% (n = 20)
12	M and F3	r = –0.324 (p < 0.001)	Being practical, attentive to small things, conscientious and calm, but having difficulty making quick decisions on their own	25% (n = 27)
13	N and F2	r = –0.302 (p = 0.002)	Being straightforward, emotionally labile and at the same time secretive, reserved and shy	19% (n = 20)

outpatient examination according to the protocol after heart transplantation.

The stress associated with HT can also occur long after transplant. The types of psychological disorders and associated risk factors confirm the need for ongoing psychological and clinical support of recipients after HT [11]. Symptoms of depression and post-traumatic stress disorder (PTSD) can also increase mortality and morbidity among patients in HT WL and after HT [11, 12]. Factors influencing the development of stress and psychological disorders after surgery: young age, female sex, orthopedic diseases and lack of psychological support [11]. But personality traits are not modifiable factors due to HT or other surgical interventions, but only reflect the personal character of patients. It is important to organize social support for patients both in HT WL and after heart transplantation [12]. Currently, there is no unified system of social and psychological support for recipients after HT in the Russian Federation; each center chooses its own protocol for working with them. In the conditions of our Center, we adhere to a personalized approach to working with patients at HT WL and after HT. All recipients are regularly monitored and have the opportunity of telephone contact with the attending physician when complaints or changes in their state of health appear, which made it possible to form a patient-physician relationship and increased the number of cases of timely access to medical institutions, examination and treatment initiation. We also recommend conducting training on the peculiarities of life after HT not only for recipients, but also for their relatives (parents, spouses, children). In informed consent for observation, patients with heart transplants always indicated the closest contact for communication, the closest relatives reported a deterioration in the patients' well-being, including with the appearance of febrile fever, shortness of breath, neurological disorders, etc., which made it possible to start treatment on time and unscheduled them hospitalize. Formation of communication "patient–doctor" can be especially useful in relation to secretive and restrained patients, and in relation to anxious and hypochondriacal patients, knowledge of the anamnesis of the disease and long-term observation will make it possible to verify the disease in a shorter time.

Gender differences also affect the types of stress and coping mechanisms and the tactics of their treatment after heart transplantation [13]. According to our results, male transplanted patients were more secretive, decisive and inclined to ignore difficulties (factors F2 – introvert, F3 – reactive balance), while patients after HT were dominated by hypochondria, hypercaution, sensitivity, anxiety, anxiety and depression. (factors I – premium, O – hypothymia, F3 – sensitivity).

According to L. Petrucci et al., 87% (n = 131) of recipients worked before transplant, and only 39% (n = 51) returned to work after surgery [14]. In our analyzed population, 36% (46 of 129) of patients worked or studied during their stay at HT WL and 43% (47 of 107) returned to work/school after a heart transplant. Moreover, some employers approached the patients' attending physicians to clarify their professional suitability and obtain a written work permit, considering their state of health.

In the future, a large study is required to assess the frequency of hospitalizations and post-transplant complications, as well as to search for risk factors for the development of psychological problems and failure to achieve psychological well-being after HT.

CONCLUSION

Personality characteristics are non-modifiable traits of patients that affect their behavior, return to work and social life, and their physical and psychological recovery after HT. Rehabilitation of patients should include the formation of a trusting relationship "patient–doctor", the possibility of unscheduled telephone contact with the attending physician in the event of new complaints or the development of complications. Knowledge of the personal characteristics of recipients will allow to develop a personalized approach to their rehabilitation and an algorithm for timely examination after HT.

The authors declare no conflict of interest.

REFERENCES

1. *Shindrikov RYu, Schelkov OYu, Demchenko EA, Sitnikova MYu*. Psychosocialnii status pacientov s hronicheskoi nedostatochnostiu, ojidauschih transplantaciu serdca. *RUDN Journal of Psychology and Pedagogics*. 2019; 16 (2): 163–180. doi: 10.22363/2312-1683-2019-16-2-163-180.
2. Heart Transplantation: overall. JHLT. 2018 Oct; 37 (10): 1155–1206.
3. *Cattell HEP, Mead AD.* The Sixteen Personality Factor Questionnaire (16PF), The SAGE Handbook of personality theory and assessment: Volume 2 – Personality Measurement and Testing, Chapter 7. 2008; 135–159. doi: 10.4135/9781849200479.n7.
4. *Pfeifer PM, Ruschel PP, Bordignon S.* Coping strategies after heart transplantation: psychological implications. *Rev Bras Cir Cardiovasc*. 2013; 28 (1): 61–68. doi: 10.5935/1678-9741.20130010.
5. *Trevizan FB, de Oliveira Santos Miyazaki MC, Silva YLW, Roque CMW.* Quality of life, depression, anxiety and coping strategies after heart transplantation. *Braz J Cardiovasc Surg*. 2017; 32 (3): 162–170.
6. *Simonenko MA, Berezina AV, Fedotov PA, Sazonova YuV, Pervunina TM, Lelyavina TA et al.* Dynamic of physical capacity and quality of life after heart transplantation. *Journal of Transplantology and Artificial organs*. 2018; 20 (1): 32–38. doi: 10.15825/1995-1191-2018-1-32-38.
7. *Albert W, Hudalla A, Traue K, Hetzer R.* Impact of heart transplantation in infancy and adloscence on quality of life and compliance. *HSR Proceedings in Intensive Care and Cardiovascular Anestesis*. 2012; 4 (2): 125–129.

8. *Shevchenko AO, Khalilulin TA, Mironkov BL, Saitgareev RSh, Zakharevich VM, Kormer AYa et al*. Quality of life assessment in cardiac transplant recipients. *The Journal of Transplantology and Artificial organs*. 2014; 16 (4): 11–16. doi: 10.15825/1195-1191-2014-4-11-16.
9. *Epstein F, Parker MM, Lucero A, Chaudhary R, Song E, Weisshaar D*. Association of depression and anxiety before heart transplant with mortality after transplant: a single-centre experience. *Transplant Research and Risk Management*. 2017; 9: 31–38. doi: 10.2147/TRRM.S132400.
10. *Saeed I, Rogers C, Murday A.* Health-related quality of life after cardiac transplantation: results of a UK National survey with norm-based comparison. *The Journal of Heart and Lung Transplantation*. 2008; 27 (6): 675–681. doi: 10.1016/j.healun.2008.03.013.
11. *Grady KL, Wang E, White-Williams C, Naftel DC, Myers S, Kirklin JK et al.* Factors associated with stress and coping at 5 and 10 years after heart transplantation. *J Heart Lung Transplant*. 2013; 32 (4): 437–446. doi: 10.1016/j.healun.2012.12.012.
12. *Rosenberger EM, Dew MA, Crone C, DiMartini AF.* Psychiatric disorders as risk factors for adverse medical outcomes after solid organ transplantation. *Curr Opin Organ Transplant*. 2012; 17 (2): 188–192. doi: 10.1097/MOT.0b013e3283510928.
13. *Grady KL, Andrei AC, Li Z, Rybarczyk B, White-Williams C, Gordon R et al.* Gender differences in appraisal of stress and coping 5 years after heart transplantation. *Heart Lung*. 2016; 45 (1): 41–47. doi: 10.1016/j.hrtlng.2015.09.009.
14. *Petrucci L, Ricotti S, Michelini I, Vitulo P, Oggionni T, Cascina A et al.* Return to work after thoracic organ transplantation in a clinically-stable population. *The European Journal of Heart Failure*. 2007; 9: 1112–1119. doi: 10.1016/j.ejheart.2007.08.002.

The article was submitted to the journal on 6.02.2020

DOI: 10.15825/1995-1191-2020-3-69-78

CORRELATION BETWEEN MICRORNA EXPRESSION LEVELS AND PLASMA CONCENTRATIONS OF BIOMARKERS OF POST-TRANSPLANT COMPLICATIONS IN HEART TRANSPLANT RECIPIENTS

D.A. Velikiy[1], O.E. Gichkun[1, 2], A.A. Ulybysheva[1, 3], S.O. Sharapchenko[1], A.V. Marchenko[1], O.P. Shevchenko[1, 2], A.O. Shevchenko[1–3]

[1] Shumakov National Medical Research Center of Transplantology and Artificial Organs, Moscow, Russian Federation
[2] Sechenov University, Moscow, Russian Federation
[3] Pirogov Medical University, Moscow, Russian Federation

Objective: to analyze the correlation between the expression levels of microRNA-101, microRNA-142, microRNA-27, microRNA-339, and microRNA-424 and the plasma concentrations of biomarkers that are potentially significant for the diagnosis of post-transplant complications in heart recipients. **Materials and methods.** The study enrolled 72 heart recipients, among whom were 56 men (77.8%). The average age of recipients was 48.6 ± 10.9 (16 to 70) years. There were 38 patients with severe chronic heart failure, among whom were 29 men (76.3%). Patients' mean age was 48.8 ± 9.9 (26 to 70) years. The control group consisted of 12 healthy individuals who did not differ significantly by sex and age. microRNA expression levels in blood plasma were measured via quantitative polymerase chain reaction. Plasma concentrations of VEGF-A, PLGF, MCP-1, and sCD40L were determined using a multiplex method. ST2 and Galectin-3 concentrations were measured via enzyme-linked immunosorbent assay. **Results.** Patients with end-stage chronic heart failure were found to have significantly higher expression levels of microRNA-27, microRNA-339 and microRNA-424 in blood plasma compared with the healthy individuals. In potential heart recipients, the expression le vels of microRNA-339 and microRNA-424 correlated with serum galectin-3 concentrations, microRNA-101 expression levels correlated with PLGF-1 concentrations, while microRNA-27 expression levels correlated with plasma MCP-1 concentrations. In the early post-transplant period, the expression levels of microRNA-101, microRNA-339, and microRNA-424 in heart recipients were significantly lower than in patients with severe chronic heart failure. In the early post-transplant period (one year or more after transplantation), microRNA-101 and microRNA-27 expression levels were significantly higher than in heart recipients. A year or more after transplantation, the following correlations were found in heart recipients: microRNA-142 expression level correlated with serum levels of galectin-3 ($p = 0.05$), microRNA-27 and microRNA-424 expression levels correlated with ST2 concentrations ($p = 0.02$), microRNA-27 expression level correlated with PLGF-1 concentrations ($p = 0.02$), while microRNA-101 expression level correlated with serum levels of PAPP-A ($p = 0.05$). **Conclusion.** In heart recipients, the expression levels of microRNA-142, microRNA-27, microRNA-424, and microRNA-101 correlate with the concentration levels of biomarkers of fibrosis (Galectin-3), rejection (ST2), neoangiogenesis (PLGF), and tissue destruction (PAPP-A). A comprehensive analysis of pre- and post-translational markers may open up new perspectives in diagnosis, assessment of the risks of post-transplant complications, and in understanding the processes leading to their development.

Keywords: heart transplantation, rejection, microRNA, ST2, Galectin-3, placental growth factor (PLGF), pregnancy-associated plasma protein A (PAPP-A).

INTRODUCTION

Timely diagnosis of post-transplant complications is necessary to select and adjust the optimal dosages of immunosuppressive therapy and restore the function of the transplanted organ. To date, the standard for determining the degree and nature of acute rejection of a transplanted heart is endomyocardial biopsy (EMB), which is performed after transplantation, within the time frame stipulated by the protocol, as well as when signs of graft dysfunction are manifested [1]. Due to the fact that the innervation of the transplanted heart is disturbed, post-transplant complications in heart recipients are not accompanied by pain and may develop asymptomatically. To ensure long-term functioning of the transplanted organ, early diagnosis of complications after transplantation and the appointment of well-timed treatment are necessary [2].

Corresponding author: Dmitriy Velikiy. Address: 1, Shchukinskaya str., Moscow, 123182, Russian Federation. Phone: (499) 193-87-62. E-mail: dim_vel@mail.ru

The participation of a number of biomarkers in the development of cardiovascular complications in patients with heart failure and in patients with heart transplants has been recently shown, as well as the possibility of exploiting the assessment of their concentration to predict and diagnose acute rejection, coronary artery disease, cardiac graft fibrosis [3–6].

A separate group of signaling molecules considered as promising candidates for the role of biomarkers of post-transplant complications in heart recipients is made up of microRNAs – small non-coding RNAs that regulate gene expression. It is believed that microRNAs play an important role in the regulation of the functions of both healthy and damaged cells. Changes in the expression of some miRNAs are associated closely with a number of pathological processes, such as autoimmune diseases, malignant neoplasms, and rejection of transplanted organs [7–9].

In this work, we analyzed the relationship between the expression level of miRNA-27, miRNA-101, miRNA-142, miRNA-339 and miRNA-424, determined in the blood plasma of cardiac recipients, with the concentration of biomarkers that are potentially significant for the diagnosis of post-transplant complications.

MATERIALS AND METHODS

The study included 72 patients who underwent heart transplantation (HT) in 2013–2016 at the Shumakov National Medical Research Center of Transplantology and Artificial Organs (Ministey of Health of Russia, Moscow, Russian Federation), among them men 56 (77.8%), the average age of recipients was 48.6 ± 10.9 (16 to 70), and 38 patients with severe chronic heart failure (III and IV functional class by NYHA), including 29 men (76.3%), the average age of patients was 48.8 ± 9.9 (26 to 70). Dilated cardiomyopathy (DCMP) was diagnosed in 20 (52.6%) patients with severe chronic heart failure, and coronary heart disease (IHD) in 18 (47.4%) patients. Follow-up of recipients after transplantation included: early period, the first month after HT (median 35 [15; 69] days); long-term period, a year or more after HT (median 404 [346.7; 783.5] days). The comparison group consisted of 12 healthy individuals, which did not differ significantly in gender and age.

All patients with indications for HT underwent a routine examination according to the National Clinical Guidelines "Heart transplantation and mechanical support of blood circulation" and the protocol for managing patients at the Shumakov National Medical Research Center. After transplantation, routine examinations of the recipient included: clinical assessment of the state, general and biochemical blood tests to determine the concentration of tacrolimus, 24-hour blood pressure monitoring (to correct antihypertensive therapy), echocardiographic examination, repeated myocardial biopsies, annual coronary angiographic examination. All recipients received three-component immunosuppressive therapy, including a combination of calcineurin inhibitors (tacrolimus) and cytostatics (mycophenolate mofetil or mycophenolic acid), as well as varying doses of oral prednisolone, depending on the time after surgery and the frequency of episodes of transplant rejection and adjuvant medication if required [1].

The material for the study of miRNA expression was venous blood plasma (1 to 3 samples from each patient, 1.44 on average). Patients' peripheral blood samples were collected in disposable tubes with the anticoagulant ethylenediamineacetic acid (EDTA), centrifuged for 10 minutes at 3000 rpm, after which the blood plasma was separated from the cell sediment and immediately frozen at –20 °C. Total RNA was isolated from 100 μL of blood plasma using Serum Plasma kits (Qiagen, USA) with preliminary addition of 1.6×10^8 copies of synthetic miRNA cel-miR-39 (Qiagen) after plasma incubation with Qiazol phenolic mixture. Cel-miR-39 was used as an internal control of the efficiency of RNA isolation, synthesis of complementary DNA (cDNA), and quantitative polymerase chain reaction (PCR) in real time. The intensity of miRNA expression was calculated using the $2^{-\Delta CT}$ method [10] and was expressed in relative units equivalent to $\log_2(2^{-\Delta Ct})$, where ΔCt are the working values of the change in the production cycle relative to the internal control of miRNA cel-miR-39 expression.

The concentration of VEGF-A, PlGF, MCP-1, and sCD40L in blood plasma was determined using a multiplex method that combines the principle of flow fluorimetry and enzyme immunoassay using polystyrene magnetic microspheres marked with red and infrared fluorophores, loaded with specific antibodies. The multiplex panel was generated based on the Simplex ProcartaPlex™ reagent kits. Determination of ST2 concentration in blood plasma was carried out by the method of enzyme-linked immunosorbent assay using the Critical Diagnostics Presage® ST2 Assay reagent kit (USA). The concentration of galectin-3 in blood plasma was measured by enzyme immunoassay using Human Galectin-3 Platinum ELISA reagent kits (Bender MedSystems GmbH, Vienna, Austria). Optical density at a wavelength of 450 nm was measured on a spectrophotometer.

Statistical data processing. Statistical analysis of the results was performed with the IBM SPSS Statistics 20 software package (IBM SPSS Inc., USA). The data obtained were statistically processed by nonparametric methods: when comparing dependent samples, the paired Wilcoxon test, and the Mann–Whitney U test to compare the independent variables. To assess the relationship between quantitative and qualitative ordered signs, the Spearman's rank correlation coefficient was calculated. The critical level of significance was taken equal to 5%, i. e., the null hypothesis was rejected at $p < 0.05$.

RESULTS AND DISCUSSION

Comparative analysis of the expression level of miRNA-101, miRNA-142, miRNA-27, miRNA-339 and miRNA-424 in healthy individuals and patients with terminal chronic heart failure is given in Table 1. Data are presented as a median of concentrations [interquartile range] with an indication of the significance of the differences, which is due to the distribution of values different from normal.

In patients with terminal chronic heart failure, the expression level of miRNA-27, miRNA-339, and miRNA-424 was significantly higher than in healthy individuals (Fig. 1).

The expression level of miRNA-101 and miRNA-142 in these groups did not differ significantly (p = 0.08 and p = 0.77, respectively).

In patients with severe chronic heart failure, the expression levels of miRNA-101, miRNA-142, miRNA-27, miRNA-339, and miRNA-424 did not differ between men and women (p = 0.93, p = 0.98, p = 0.63, p = 0.97 and p = 0.26, respectively). Indicators of miRNA expression did not depend on the patient's age (r = –0.304, p = 0.16; r = –0.236, p = 0.35; r = –0.361, p = 0.08; r = 0.146, p = 0.44 and r = –0.054, p = 0.82, respectively).

The expression level of miRNA-339 in patients with severe chronic heart failure caused by ischemic heart disease was significantly higher than in patients diagnosed with dilated cardiomyopathy (Fig. 2).

Table 1

Comparative analysis of miRNA expression in healthy individuals and patients with severe chronic heart failure

MiRNA ($\log_2(2^{-\Delta Ct})$)	Healthy individuals	CHF patients	Confidence, p
MiRNA-101	–5.66 [–6.85; –4.97]	–4.29 [–6.86; –3.21]	0.08
MiRNA-142	–7.39 [–10.26; –6.36]	–7.35 [–8.19; –6.25]	0.77
MiRNA-27	–5.79 [–6.70; 4.6]	–5.3 [–6.37; –1.22]	**0.02**
MiRNA-339	–11.14 [–11.75; –11.03]	–6.06 [–7.89; –4.86]	**0.0001**
MiRNA-424	–8.3 [–9.34; –7.41]	–5.46 [–7.54; –1.46]	**0.001**

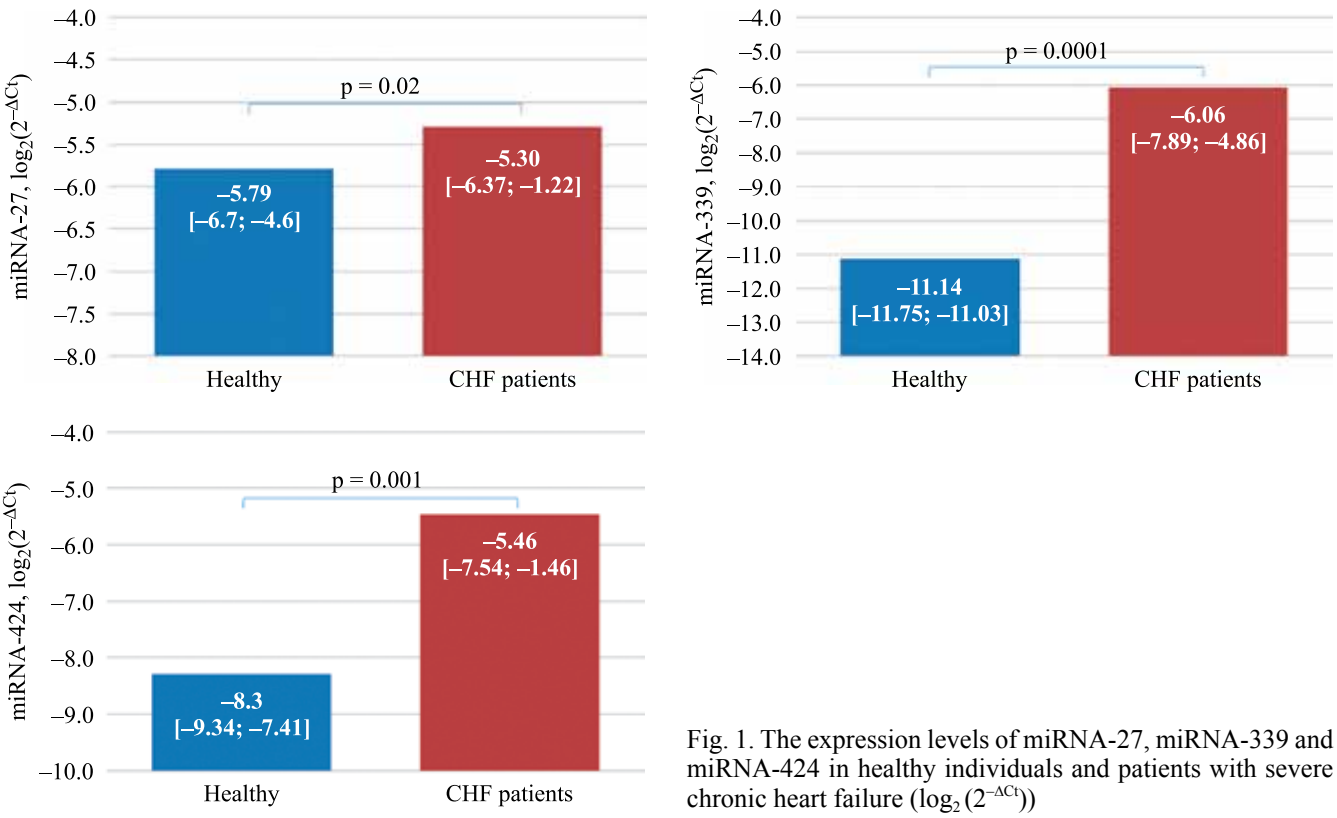

Fig. 1. The expression levels of miRNA-27, miRNA-339 and miRNA-424 in healthy individuals and patients with severe chronic heart failure ($\log_2(2^{-\Delta Ct})$)

There were no significant differences in the expression level of miRNA-101, miRNA-142, miRNA-27, and miRNA-424 depending on the initial diagnosis (DCMP or IHD) that caused the development of severe chronic heart failure (p = 0.6, p = 0.52, p = 0.87, p = 0.57 and p = 0.12, respectively).

The following biomarkers were included in the present study:

– vascular endothelial growth factor A (VEGF-A), produced by macrophages, fibroblasts, endothelial and other cells; involved in the activation, proliferation, migration and differentiation of endothelial cells of blood and lymphatic vessels [12];
– placental growth factor (PLGF), a biomarker of neoangiogenesis involved in the initiation of inflammatory processes in the vascular wall [13];
– macrophage chemoattractant protein (MCP-1) produced by vascular endothelial and smooth muscle cells, fibroblasts, lymphocytes and other cells; MCP-1 activates the migration of leukocytes into the vascular wall, is involved in the activation and degranulation of leukocytes, myelopoiesis, angiogenesis and fibrogenesis [14];
– soluble form of ligand CD40 (sCD40L), a component of the CD40 / CD40L lymphocyte costimulation system; participates in the processes of inflammation, thrombus formation, causes the activation and proliferation of smooth muscle cells [15];
– stimulating growth factor (ST2), the soluble form of which is the circulating form of the receptor for interleukin-33 and is a biomarker of acute rejection of a heart transplant; the secretion of interleukin-33 mainly occurs in response to mechanical stretching of fibroblasts and cardiomyocytes, leading to the activation of signaling pathways and preventing the development of myocardial hypertrophy [16];
– galectin-3, belonging to the family of β-galactoside-binding proteins that play an important role in the regulation of inflammation, immune response and fibrosis; at the site of injury, galectin-3 is able to be secreted into the extracellular space, which stimulates the process of fibrosis through the activation and reproduction of fibroblasts [17].

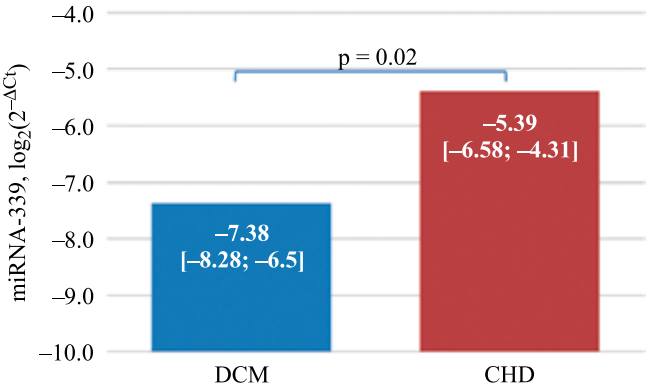

Fig. 2. The expression levels of miRNA-339 in patients with severe chronic heart failure depending on the initial diagnosis: DCM or CHD ($\log_2(2^{-\Delta Ct})$)

A comparative analysis of the correlation between the level of miRNA expression in the blood plasma of patients with end-stage heart failure and the content of protein (post-translational) biomarkers of post-transplant complications is given in Table 2.

In patients with terminal chronic heart failure, the expression level of miRNA-339 and miRNA-424 had an inverse correlation with the concentration of galectin-3 (Fig. 3).

The expression level of miRNA-101 had a direct correlation with the concentration of PLGF-1, and the level of expression of miRNA-27 was inversely correlated with the concentration of MCP-1 (r = 0.783, p = 0.01 and r = –0.717, p = 0.03, respectively).

No correlations were found between the expression level of miRNA-101, miRNA-142, miRNA-27, miRNA-339, and miRNA-424 and the concentration of VEGF-A, sCD40L, and PAPP-A in patients with end-stage chronic heart failure.

Table 2

Comparative analysis of the correlation between of the miRNA expression levels in the blood plasma of the patients with severe chronic heart failure and the concentration of biomarkers potentially significant for the diagnosis of post-transplant complications

MiRNA	Galectin-3	VEGF-A	PlGF-1	MCP-1	sCD40L	PAPP-A
MiRNA-101	r = 0.174, p = 0.55	r = 0.4, p = 0.29	**r = 0.783, p = 0.01**	r = –0.017, p = 0.97	r = 0.324, p = 0.28	r = 0.0182, p = 0.96
MiRNA-142	r = 0.321, p = 0.48	r = 0.5, p = 0.67	r = 0.5, p = 0.67	r = –0.5, p = 0.67	r = 0.314, p = 0.54	r = –0.6, p = 0.4
MiRNA-27	r = –0.139, p = 0.62	r = –0.183, p = 0.64	r = –0.417, p = 0.26	**r = –0.717, p = 0.03**	r = 0.0813, p = 0.78	r = –0.248, p = 0.49
MiRNA-339	**r = –0.519, p = 0.03**	r = –0.115, p = 0.75	r = 0.336, p = 0.31	r = 0.176, p = 0.63	r = –0.012, p = 0.97	r = 0.385, p = 0.19
MiRNA-424	**r = –0.714, p = 0.01**	r = 0.286, p = 0.49	r = 0.690, p = 0.06	r = 0.476, p = 0.23	r = 0.0091, p = 0.98	r = 0.238, p = 0.57

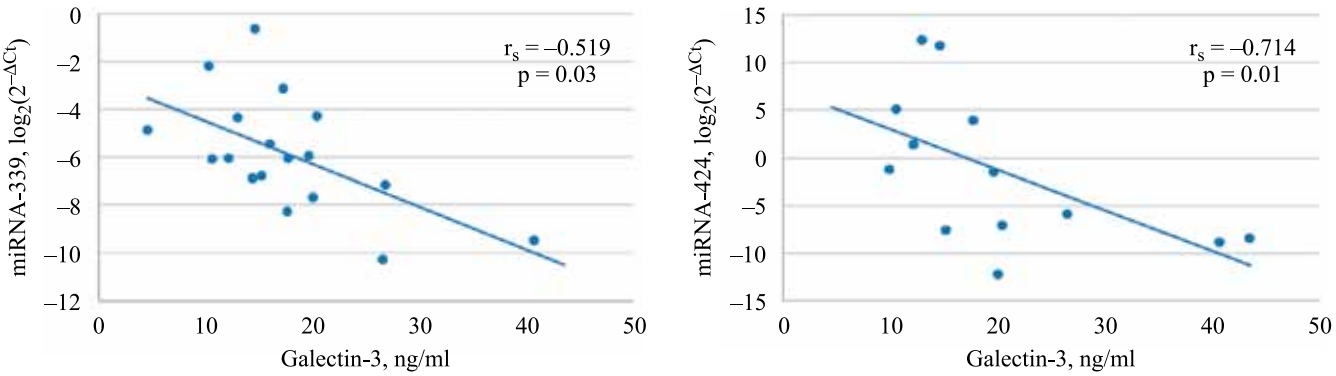

Fig. 3. Correlation between the expression level of miRNA-339, miRNA-424 and the concentration of Galectin-3 in patients with severe chronic heart failure ($\log_2(2^{-\Delta Ct})$)

Table 3

Comparative analysis of microRNAs expression in patients with chronic heart failure and heart transplant recipients at early and long-term after transplantation

MiRNA ($\log_2(2^{-\Delta Ct})$)	CHF patients	Heart recipients		Confidence, p	
		1 month after HT	1 year after HT		
MiRNA-101	–4.29 [–6.86; –3.21]	–8.28 [–9.74; –5.77]	–6.12 [–7.39; –4.61]	**0.005***	**0.03****
MiRNA-142	–7.35 [–8.19; –6.25]	–7.03 [–8.35; –6.01]	–6.52 [–7.39; –5.09]	0.89*	0.25**
MiRNA-27	–5.3 [–6.37; –1.22]	–5.76 [–6.24; –4.08]	–3.85 [–4.88; –1.73]	0.19*	**0.02****
MiRNA-339	–6.06 [–7.89; –4.86]	–9.91 [–11.29; –5.94]	–9.02 [–10.56; –5.80]	**0.02***	0.44**
MiRNA-424	–5.46 [–7.54; –1.46]	–7.21 [–8.25; –6.13]	–6.41 [–7.60; –5.50]	**0.01***	0.09**

Note. * – comparison between groups of patients with CHF and recipients after 1 month after HT; ** – comparison between groups of recipients after 1 month and 1 year after HT.

A comparative analysis of the expression level of miRNA-101, miRNA-142, miRNA-27, miRNA-339, and miRNA-424 in patients with chronic heart failure and heart recipients showed a tendency for a decrease in expression in the early stages after transplantation and a gradual increase in the long term (Table 3).

Fig. 4 shows the dynamics of the studied miRNAs in patients with severe chronic heart failure and recipients at different times after transplantation.

In heart recipients, 1 month after transplantation, the expression level of miRNA-101, miRNA-339, and miRNA-424 was significantly lower than in patients with terminal chronic heart failure.

The expression level of miRNA-101 and miRNA-27 in heart recipients 1 year or more after transplantation was significantly higher than after 1 month after HT.

There were no differences in the expression of the studied miRNAs in patients with severe chronic heart failure and long-term recipients after transplantation ($p \geq 0.05$).

In the early stages after transplantation, the expression level of miRNA-101, miRNA-339, and miRNA-424 is lower than in patients with end-stage chronic heart failure. A year or more after transplantation, the expression level of miRNA-101 and miRNA-27 in cardiac recipients increases as compared to those at early stages, which may reflect the development of fibrosis in the graft.

The presented data, obtained in the study of a larger number of heart recipients, confirm the results of our previous work [11] regarding the significance of differences in the level of miRNA-101 expression in patients with end-stage CHF and recipients in the early stages after HT, as well as the level of miRNA-101 and miRNA-27 in early and late periods after transplantation. At the same time, new results were shown regarding the reliability of differences in the expression levels of miRNA-339 and miRNA-424 in patients with end-stage CHF and recipients in the early stages after HT.

Analysis of the correlation between the level of miRNA expression in the blood plasma of recipients 1 year or more after transplantation with the content of biomarkers potentially significant for the diagnosis of post-transplant complications is given in Table 4.

In cardiac recipients 1 year or more after transplantation, the level of miRNA-142 expression had an inverse correlation with the concentration of galectin-3 (Fig. 5).

There is evidence that miRNA-142 is expressed by T-lymphocytes and is involved in the regulation of acute cellular rejection of the transplanted heart [18]. The correlation between the level of miRNA-142 expression and the concentration of galectin-3 suggests the involvement of immune mechanisms in the processes of myocardial fibrosis in cardiac recipients.

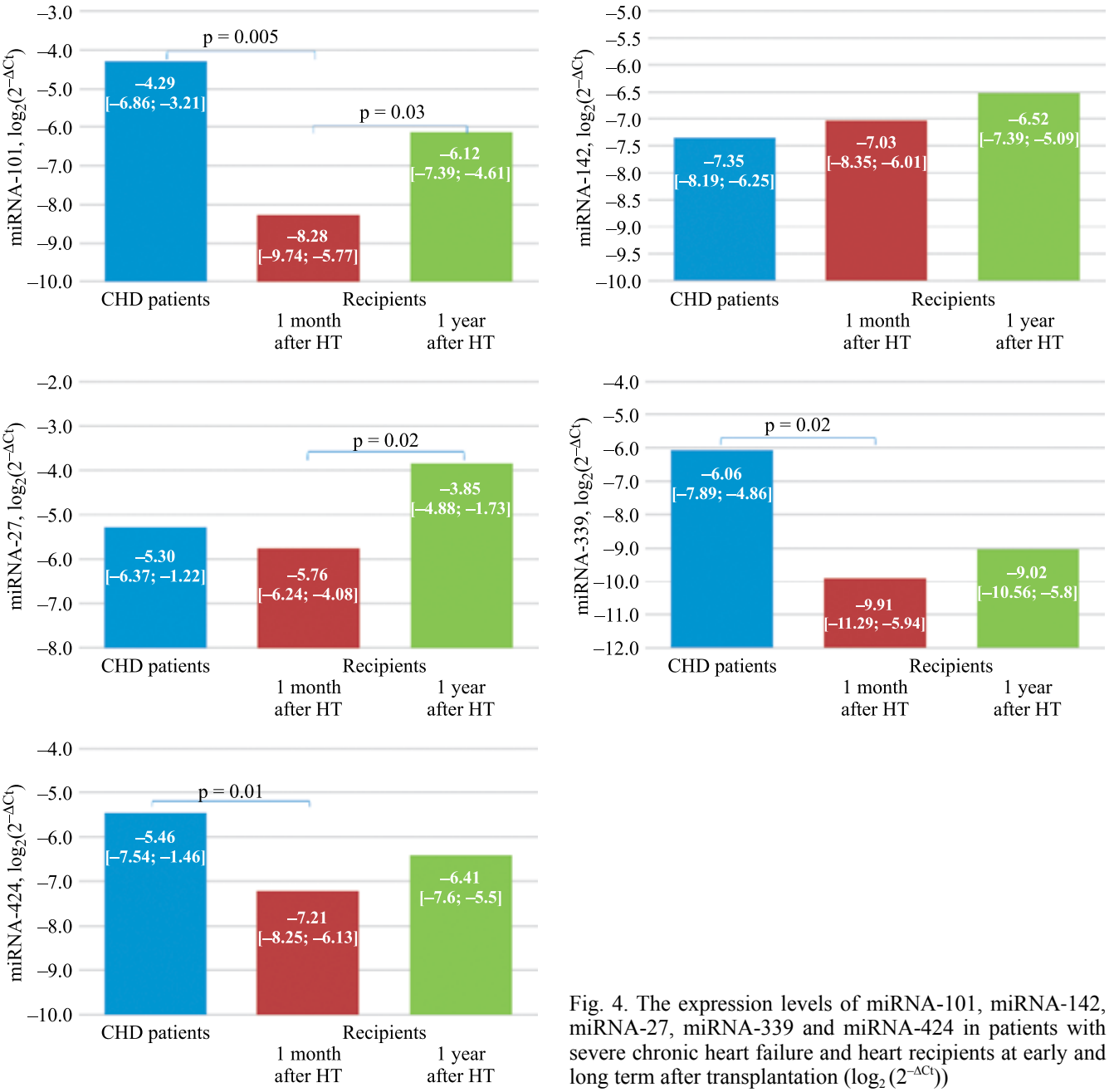

Fig. 4. The expression levels of miRNA-101, miRNA-142, miRNA-27, miRNA-339 and miRNA-424 in patients with severe chronic heart failure and heart recipients at early and long term after transplantation ($\log_2(2^{-\Delta Ct})$)

Table 4

Comparative analysis of the correlation between of the miRNA expression levels in the blood plasma of the recipients at long-term after transplantation and the concentration of biomarkers potentially significant for the diagnosis of post-transplant complications

MiRNA	Galectin-3	ST2	VEGF-A	PlGF-1	MCP-1	sCD40L	PAPP-A
MiRNA-101	r = 0.0673, p = 0.73	r = –0.209, p = 0.44	r = 0.119, p = 0.78	r = 0.491, p = 0.22	r = 0.143, p = 0.74	r = –0.429, p = 0.34	**r = –0.557, p = 0.05**
MiRNA-142	**r = –0.534, p = 0.05**	r = 0.1, p = 0.87	r = 0.5, p = 0.67	r = 0.9451, p = 0.21	r = 0.5, p = 0.67	н/д	r = –0.4, p = 0.6
MiRNA-27	r = 0.133, p = 0.51	**r = –0.585, p = 0.02**	r = 0.429, p = 0.34	**r = 0.847, p = 0.02**	r = 0.679, p = 0.09	r = –0.143, p = 0.79	r = –0.321, p = 0.34
MiRNA-339	r = 0.0433, p = 0.83	r = –0.041, p = 0.88	r = 0.0303, p = 0.93	r = 0.377, p = 0.28	r = –0.03, p = 0.93	r = –0.405, p = 0.32	r = –0.303, p = 0.29
MiRNA-424	r = 0.0148, p = 0.94	**r = –0.542, p = 0.02**	r = 0.286, p = 0.49	r = 0.539, p = 0.17	r = –0.381, p = 0.35	r = 0.2746, p = 0.55	r = –0.099, p = 0.76

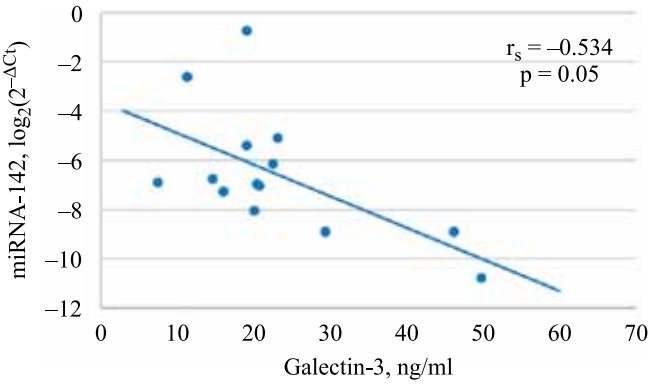

Fig. 5. Correlation between the expression level of miRNA-142 and the concentration of Galectin-3 in heart recipients at long-term after transplantation ($\log_2(2^{-\Delta Ct})$)

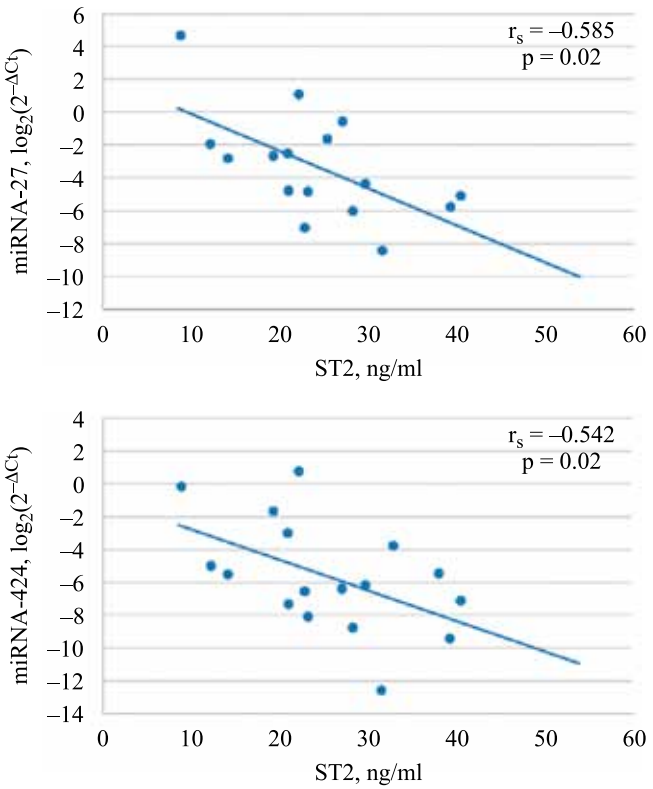

Fig. 6. Correlation between the expression level of miRNA-27, miRNA-424 and the concentration of ST2 in heart recipients at long-term after transplantation ($\log_2(2^{-\Delta Ct})$)

Expression levels of miRNA-27 and miRNA-424 in cardiac recipients 1 year or more after transplantation had an inverse correlation with the ST2 concentration (Fig. 6).

It has been shown that miRNA-424 plays an important role in the pathogenesis of pulmonary hypertension and subsequent right ventricular hypertrophy through inhibition of the function of the SMURF specific regulatory factor [19].

The expression level of miRNA-101 was inversely correlated with the concentration of PAPP-A, and the expression level of miRNA-27 was directly correlated with the concentration of PLGF-1 (r = –0.557, p = 0.05 and r = 0.847, p = 0.02, respectively). Changes in the expression profile of miRNA-101 and miRNA-27 are associated with the participation of these molecules in the regulation of myocardial fibrosis through interaction with the transcription factor RUNX1 and transforming growth factor β receptor 1 (TGFBR1) [20, 21].

No correlations were found between the expression level of miRNA-101, miRNA-142, miRNA-27, miRNA-339, and miRNA-424 and the concentration of VEGF-A, MCP-1, and sCD40L in heart recipients 1 year or more after transplantation.

In heart recipients a year or more after transplantation, there is a correlation between the level of expression of miRNA-142 and the concentration of galectin-3, the level of expression of miRNA-27, miRNA-424 and the concentration of ST2, the level of expression of miRNA-27 and the concentration of PLGF-1, the level of miRNA-101 expression and PAPP-A concentration. The relationship between the level of miRNA expression and the concentration of biomarkers potentially significant for the diagnosis of post-transplant complications in cardiac recipients not only confirms the available data on the involvement of these signaling molecules in the regulation of various pathological processes, including the graft, but also suggests their diagnostic potential for risk assessment. development of rejection and the possibility of minimizing immunosuppressive therapy. In this regard, the combined use of miRNAs with biomarkers of post-transplant complications for the formation of complex tests (multimarker panels) that make it possible to diagnose changes at various translational levels may become especially promising. Further comprehensive studies of pre- and post-translational markers can open up new perspectives both in diagnosis, assessment of the risks of post-transplant complications, and in understanding the processes leading to their development.

The study was funded by the grant of the President of the Russian Federation NSh-2598.2020.7 for state support of the leading scientific schools of the Russian Federation.

The authors declare no conflict of interest.

REFERENCES

1. *Gautier SV, Shevchenko AO, Popcov VN*. Pacient s transplantirovannym serdcem: rukovodstvo dlya vrachej po vedeniyu pacientov, perenesshih transplantaciyu serdca. M.: Triada, 2014; 144.
2. *Crespo-Leiro MG, Barge-Caballero G, Couto-Mallon D.* Noninvasive monitoring of acute and chronic rejection in heart transplantation. *Curr Opin Cardiol*. 2017 Mar 16. doi: 10.1097/HCO.0000000000000400. [Epub ahead of print].

3. *Kransdorf EP, Kobashigawa JA.* Novel molecular approaches to the detection of heart transplant rejection. *Per Med*. 2017 Jul; 14 (4): 293–297.
4. *van Gelder T.* Biomarkers in solid organ transplantation. *Br J Clin Pharmacol*. 2017 Dec; 83 (12): 2602–2604.
5. *Starling RC, Stehlik J, Baran DA et al.* Multicenter analysis of immune biomarkers and heart transplant outcomes: results of the clinical trials in organ transplantation-05 study. *American Journal of Transplantation*. 2016; 16: 121–136.
6. *Savic-Radojevic A, Pljesa-Ercegovac M, Matic M et al.* Novel biomarkers of heart failure. *Advances in Clinical Chemistry*. 2017; 79: 93–152.
7. *Di Francesco A, Fedrigo M, Santovito D, Natarelli L, Castellani C, De Pascale F et al*. MicroRNA signatures in cardiac biopsies and detection of allograft rejection. *J Heart Lung Transplant*. 2018 Nov; 37 (11): 1329–1340.
8. *Shah P, Bristow MR, Port JD.* MicroRNAs in Heart Failure, Cardiac Transplantation, and Myocardial Recovery: Biomarkers with Therapeutic Potential. *Curr Heart Fail Rep*. 2017 Dec; 14 (6): 454–464.
9. *Khush K, Zarafshar S.* Molecular Diagnostic Testing in Cardiac Transplantation. *Curr Cardiol Rep*. 2017 Oct 13; 19 (11): 118.
10. *Livak KJ, Schmittgen TD.* Analysis of relative gene expression data using real-time quantitative PCR and the 2(-Delta Delta C(T)) Method. *Methods*. 2001 Dec; 25 (4): 402–408.
11. *Velikiy DA, Gichkun OE, Sharapchenko SO, Shevchenko OP, Shevchenko AO*. Uroven' ekspressii mikroRNK v rannie i otdalennye sroki posle transplantacii u recipientov serdca. *Vestnik transplantologii i iskusstvennyh organov*. 2020; 22 (1): 26–34.
12. *Daly KP, Stack M, Eisenga MF, Keane JF, Zurakowski D, Blume ED, Briscoe DM.* Vascular endothelial growth factor A is associated with the subsequent development of moderate or severe cardiac allograft vasculopathy in pediatric heart transplant recipients. *J Heart Lung Transplant*. 2017 Apr; 36 (4): 434–442.
13. *Albonici L, Giganti MG, Modesti A, Manzari V, Bei R.* Multifaceted Role of the Placental Growth Factor (PlGF) in the Antitumor Immune Response and Cancer Progression. *Int J Mol Sci*. 2019 Jun 18; 20 (12): 2970.
14. *Abe T, Su CA, Iida S, Baldwin WM 3rd, Nonomura N, Takahara S, Fairchild RL.* Graft-derived CCL2 increases graft injury during antibody-mediated rejection of cardiac allografts. *Am J Transplant*. 2014 Aug; 14 (8): 1753–1764.
15. *Michel NA, Zirlik A, Wolf D.* CD40L and Its Receptors in Atherothrombosis-An Update. *Front Cardiovasc Med*. 2017 Jun 20; 4: 40.
16. *Grupper A, AbouEzzeddine OF, Maleszewski JJ et al.* Elevated ST2 levels are associated with antibody-mediated rejection in heart transplant recipients. *Clin Transplant*. 2018; 32 (9): e13349.
17. *Coromilas E, Que-Xu EC, Moore D, Kato TS, Wu C, Ji R et al*. Dynamics and prognostic role of galectin-3 in patients with advanced heart failure, during left ventricular assist device support and following heart transplantation. *BMC Cardiovasc Disord*. 2016 Jun 14; 16: 138.
18. *Sukma Dewi I, Hollander Z, Lam KK, McManus JW, Tebbutt SJ, Ng RT et al.* Association of Serum MiR-142-3p and MiR-101-3p Levels with Acute Cellular Rejection after Heart Transplantation. *PLoS One*. 2017; 12 (1): e0170842.
19. *Baptista R, Marques C, Catarino S, Enguita FJ, Costa MC, Matafome P et al.* MicroRNA-424(322) as a new marker of disease progression in pulmonary arterial hypertension and its role in right ventricular hypertrophy by targeting SMURF1. *Cardiovasc Res*. 2018 Jan 1; 114 (1): 53–64.
20. *Li X, Zhang S, Wa M, Liu Z, Hu S.* MicroRNA-101 Protects Against Cardiac Remodeling Following Myocardial Infarction via Downregulation of Runt-Related Transcription Factor 1. *J Am Heart Assoc*. 2019 Dec 3; 8 (23): e013112.
21. *Zhang XL, An BF, Zhang GC.* MiR-27 alleviates myocardial cell damage induced by hypoxia/reoxygenation via targeting TGFBR1 and inhibiting NF-κB pathway. *Kaohsiung J Med Sci*. 2019 Oct; 35 (10): 607–614.

The article was submitted to the journal on 22.07.2020

DOI: 10.15825/1995-1191-2020-3-79-85

MATHEMATICAL EVALUATION OF HEMOLYSIS IN A CHANNEL CENTRIFUGAL BLOOD PUMP

A.P. Kuleshov[1], G.P. Itkin[1, 2], A.S. Buchnev[1], A.A. Drobyshev[1]

[1] Shumakov National Medical Research Center of Transplantology and Artificial Organs, Moscow, Russian Federation

[2] Moscow Institute of Physics and Technology, Moscow, Russian Federation

The objective of this work is to conduct research on a mathematical model to assess hemolytic characteristics in a channel centrifugal blood pump developed by us with 2000–3400 rpm impeller speed range and 100–250 mmHg pressure drop in different parts of the pump flow path. Hemolysis index was measured at 1 to 10 L/min flow rate. The result was an estimate of the average magnitude of the shear stress (SS), taking into account the distribution in the pump, which ranged from 40 to 60 Pa. The most critical areas of the pump in terms of blood injury were evaluated. The maximum SSs were determined: 456 Pa in the impeller wheel zone and 533.3 Pa in the adjacent area of the body, with an exposure time of 0.0115 s and 0.0821 s respectively. In these zones, maximum hemolysis index values were 0.0420 and 0.0744 respectively. Based on the data obtained, these zones were optimized in terms of minimizing hemolysis.

Keywords: 3D modeling, mechanical circulatory support, channel centrifugal blood pump, shear stress, exposure time, hemolysis index.

INTRODUCTION

In the development of modern pumps for auxiliary circulation, one of the main stages is a preliminary theoretical assessment of the influence of the pump on the hemocompatibility parameters in terms of minimizing conditions leading to blood injury [1, 2]. To solve this problem, modern software systems are used, which in the process of designing pumps will allow determining the directions for optimizing the design of pumps. In this work, a theoretical analysis of the channel centrifugal pump (CCP) developed by us is carried out from the point of view of minimizing blood trauma when using the pump when bypassing the left ventricle of the heart (LV) and extracorporeal membrane oxygenation (ECMO) with the results of calculations of the shear stress (SS) and exposure time (ET), which are the main parameters determining blood trauma. Based on the data obtained, the calculated hemolysis indices (HI) for the main working zones of the pump were estimated.

Fig. 1. Calculation model of the channel centrifugal pump

MATERIALS AND METHODS

The studies were carried out on the CCP model developed by us with a detailed calculation of the pump components – inlet path, impeller (I), spiral casing (SC) and outlet channel, as well as transition zones described in more details in [3]. The general view of the pump is shown in Fig. 1.

The geometrical parameters of the I flow path represent an updated model of a closed-type blade structure. The inner diameter of the entrance cannula is 10 mm. The 46 mm outer diameter I disc has four tubular channels with a constant cross section of 5 mm in diameter. Each channel is formed along a logarithmic spiral and has a circular cross-section, providing conditions for a laminar flow. The main elements of the pump are shown in Fig. 2. I rotation is performed by means of a magnetic coupling, which is a mechanism for contactless transmission of rotational energy from the pump drive to I. The outlet is terminated with a 10 mm fitting (8). The gaps between I and the inner surface were 500 μm. In this work, SS was evaluated for seven main pump zones, critical from the point of view of blood injury and shown in Fig. 2: upper zone UZ (1726.9 mm^2), spiral casing zone SC (1449.2 mm^2), lateral zone LZ (1135.0 mm^2), channel zone CZ (3152.3 mm^2), lower zone LZ (1688.9 mm^2), impeller zone IZ (4435.1 mm^2) and diffuser zone DZ (473.3 mm^2).

Corresponding author: Arkady Kuleshov. Address: 1, Shchukinskaya str., Moscow, Russian Federation. Phone: (915) 292-47-98. E-mail: ilovemylene@yandex.ru

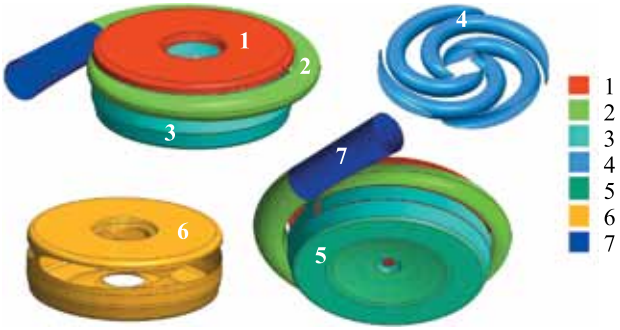

Fig. 2. Pump areas for investigation. 1, upper zone; 2, spiral outlet; 3, lateral zone; 4, channel zone, 5, lower zone, 6, impeller zone; 7, diffuser zone

Based on preliminary computer studies, a 3D CCP model was built with the Solid Works Corporation (Concord, MA) software, which served as the basis for building the CCP structure. The resources of the Fluent v16.0 software package (ANSYS inc., Canonsburg, Pennsylvania) were used to simulate the CCP computational grid. The software package uses the SST turbulent flow model adapted for calculations near the wall. The working fluid was assumed to be incompressible and Newtonian with a viscosity of 4.0 SP, a density of 1.050 kg/m^3, which reflects the picture of an expected hematocrit of 35%. In this case, the concentration and size of the particles were selected in accordance with the physiology of the blood cells. The choice of boundary conditions reflected the parameters for applying CCP in LV and ECMO procedures. The rotational speed range of the CCP I is from 2000 to 3400 rpm in 200 increments. Five test points for analysis were selected to cover the clinically relevant working area: 1.0 L/min (low flow), 2.5; five; 7.5 l/min (nominal flow) and 10.0 l/min (high flow). The roughness of the surface was chosen as 10 microns.

Calculation of shear stress and hemolysis index

Pa cause platelet activation, and uncontrolled hemolysis occurs at values above 150 Pa [4], which we have taken as a threshold value. The investigated SS τ at a steady speed of fluid movement υ changes according to a linear law depending on the distance from the wall y, regardless of the nature of the movement [5]:

$$\tau = \mu \frac{d\upsilon}{dy}, \quad (1)$$

where μ – dynamic viscosity coefficient.

Exposure time (ET) is an important factor. In this study, t was calculated from the mean travel time of a particle obtained in a software calculation. ET is calculated as the time average of 10 particle tracks. In this case, ET is calculated as the distance between the start and end points along the area of interest, divided by the average speed for the segment.

One important aspect of flow-induced blood damage is hemolysis, defined as the release of hemoglobin into plasma due to damage to the erythrocyte membrane. Pump-induced NNC and Bt are the main factors causing hemolysis. It is still considered useful for engineering problems a power-law equation for estimating the amount of increase in released hemoglobin ΔHb, expressed in concentration units, relative to the baseline ΔHb value [4, 6]:

$$\frac{\Delta Hb}{Hb} = A \times t^{\alpha}\tau^{\beta}, \quad (2)$$

where τ – shear stress acting on blood, t – ET in the shear stress area. Goubergrits and Affeld model, which uses Euler's numerical model for hemolysis, is calculated using the coefficients of the equation $A = 3.62 \times 10^{-7}$, $\alpha = 0.785$, $\beta = 2.416$. The constants are successfully used, despite the fact that their validity has been questioned by many researchers for the fact that they overestimate hemolysis to a large extent [7–9].

CALCULATION RESULTS

The calculations were performed on particles comparable in size to the size of an erythrocyte. ET averaged 0.6 to 0.08 seconds over the entire input range with increasing pump flow. In Fig. 3 shows the change in SS in the channels, on the impeller and on the inner surface of the pump. The maximum values of SS for each area are highlighted, shown in Fig. 4 for each zone, which are an evaluation criterion for hemolysis. For these purposes, the regions above the threshold voltages were considered. The critical SS was based on the value of 150 Pa.

The calculations showed a stable increase in the maximum value of SS with an increase in the rotation speed from 2000 to 3400 and the transition from the LVC mode to ECMO. The average SS value did not exceed the critical threshold. The highest values were obtained in the IZ and LZ. There is also a tendency for the SS values to increase with increasing flow rates, which stress the volute and diffuser. Based on the data obtained and calculations of t, the dependences of the average hemolysis index (HI) were derived (Fig. 5).

HI increases with increasing flow rate and with increasing rotation speed I, however, it is within the permissible norm. Since the estimate of the average HI reflects only the general trend of changes in the parameters of the effect of the pump cavity on the blood, the most reliable sign of hemolysis is a zone of high SS above 150 Pa. In

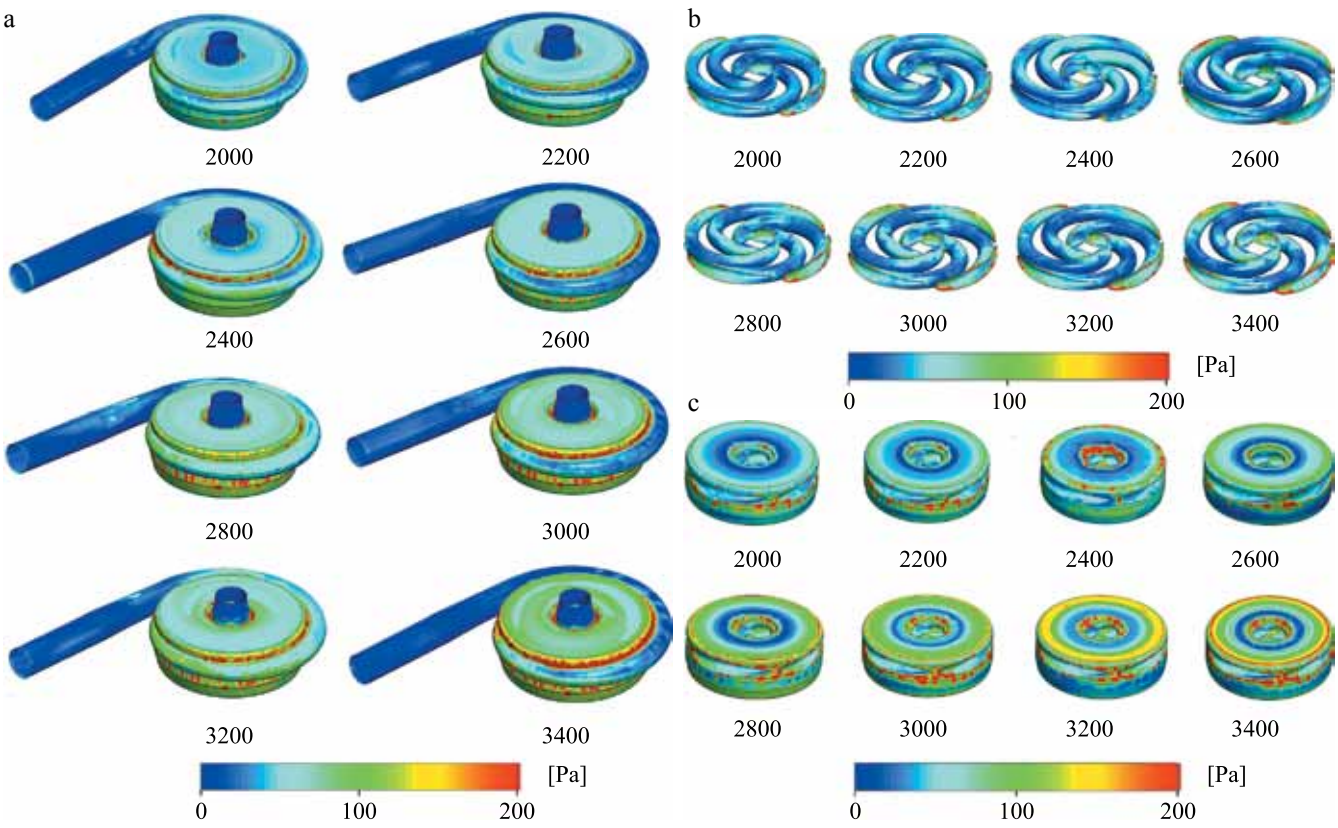

Fig. 3. Change of shear stress in the pump cavity (a), in the channels (b) and on the surface of the impeller (c) with an increase of the impeller's speed and a fixed flow rate of 5 l/min

this case, the maximum SS values in each considered pump zone were analyzed. It should be borne in mind that the SS values exceeding the critical threshold have a high scatter of values, from 150 to 500 Pa. In view of this, an estimate of HI for each value above 150 Pa is impractical. Therefore, an assumption was made, as a result of which the calculation of HI was made based on the maximum values of SS and *t* observed in a separate study area. As a result, it can be assumed that the calculation of the maximum HI will be somewhat overestimated, but nevertheless it reflects the main values of hemolysis. In addition to SS, to assess the effects of the pump on the blood, a numerical assessment of the surface area causing hemolysis of erythrocytes was carried out for each zone. In this case, the area is the sum of areas of high SS over 150 Pa. Fig. 6 shows the average and maximum values of the hemolysis index in each zone. These calculations objectively show the importance of optimizing IZ and LZ. The rest of the areas do not require significant improvement.

For example, the most critical pump operation mode in ECMO systems is considered, at an impeller speed of 3400 rpm. The average and maximum values of HI in the zones under consideration, the area of impact on erythrocytes and *t* for each zone were registered. The values have been recorded in the Table for a flow rate of 5 l/min.

DISCUSSION

The results of CFD modeling and mathematical calculation made it possible to analyze the design of the CCP with the assessment of SS and hemolysis under

Table

Distribution of parameters in the pump areas at the flow rate of 5 L/min and 3400 rpm

Zone	UZ	LZ	LZ	CZ	WWZ	SC	DZ
Mean SS, Pa	87.0	170.1	60.1	42.5	140.7	50.2	14.3
Max SS, Pa	189.2	533.3	189.2	185.3	359.0	157.1	100.7
Index by max SS	0.0083	0.042	0.0091	0.0037	0.0744	0.0105	0.0022
Zone area, mm^2	1726	1135	1688	3152	4435	1449	473
Zone area of high SS >150 Pa, mm^2 (% of zone)	100 (5.8%)	566 (49.8%)	302 (17.9%)	60 (1.9%)	788 (17.8%)	103 (7.1%)	0 (0%)
ET, s	0.0321	0.0115	0.0411	0.0352	0.0821	0.0832	0.0240

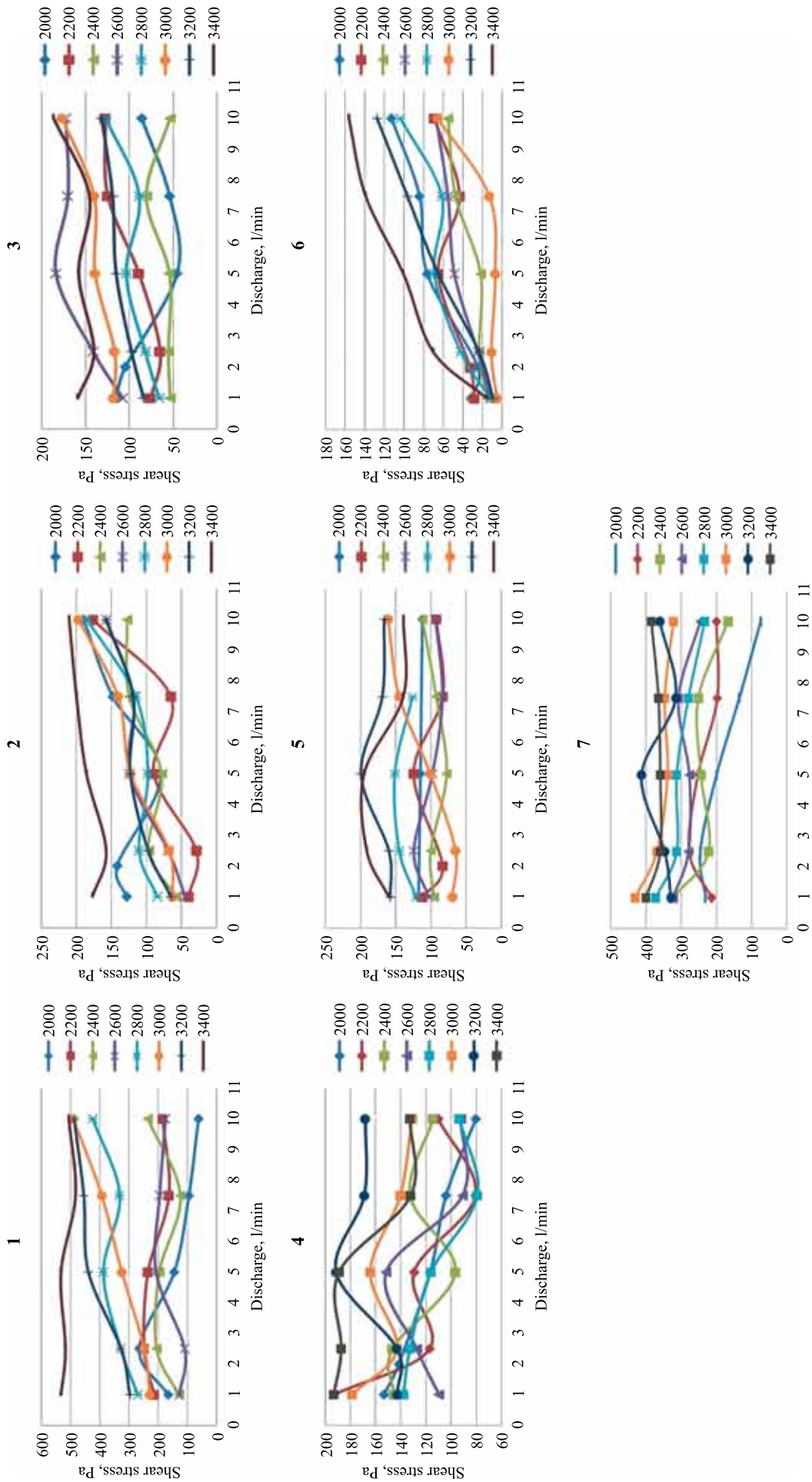

Fig. 4. Maximum shear stress in the studied zones: lateral (1), channel (2), SS (3), lower (4), upper (5), diffuser (6), and impeller (7)

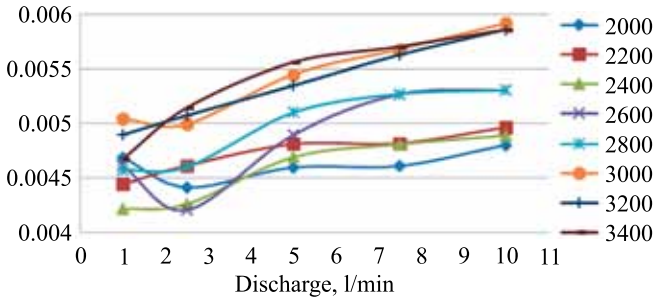

Fig. 5. Change in the calculated average hemolysis index of the channel centrifugal pump

conditions of its operation in LVC and ECMO systems in a wide range of blood flow rates. One of the main results of the calculation performed is the assessment of ET in various areas of the pump, which determines the duration of exposure to blood cells. The zones are characterized by a decrease in HI with increasing flow, which can be explained by a decrease in ET. It was shown that the calculated exposure time of blood for the zones does not exceed 0.09 s, which, together with SS in the range of 150–200 Pa, determines a low level of hemolysis for such zones as UZ, LZ, CZ and DZ. The SC zone has one of the highest ET, but low SS, which also provides a low I.I. In critical regions, such as LZ and I, the maximum ID values are 0.0420 and 0.0744. This is due to the high SS – 533.3 Pa on the inner side surface and 456 Pa on the side surface I, with a corresponding *t* of 0.0115 and 0.0821.

At maximum I speed, the area of influence on the blood corpuscles with SS above 150 Pa increases. On the example of the pump operating mode in the ECMO systems UZ, CZ, SC and LZ practically do not affect the blood. In LZ, there is a moderate spread of high SS. A significant predominance of high SS areas is seen in LZ and I.

It is also worth noting an increase in voltage in the spiral bend, especially in the area of transition to the diffuser at low and high liquid flows. This can be explained by the high pressure in this area and the high speed. High-velocity zones are associated with an increase in hydraulic resistance during the development of turbulent flow and an increase in fluid viscosity. This fact causes a sharp increase in the shear stress in the region of the transition of the helix to the diffuser for each I rotation speed.

The results obtained provide grounds for optimization of SC, LZ and WWZ, critical in terms of the impact on the blood of the pump zones. The most important decision seems to be to expand the SC area by increasing its throughput. Since the channels of constant cross-section provide optimal SS parameters, expanding the channel diameter by 5–7 percent will maintain flow at lower RPM I. This will reduce the radial flow velocity when leaving the channel, which in accordance with equation (1) will provide a decrease in SS. Increasing the lateral clearances between I and LZ will also decrease SS.

CONCLUSION

Computer-aided analysis of CFD in CAD systems is becoming the main tool for researching a variety of medical device designs for IPC. However, this tool has its limitations. The calculated SS ranges in the pumps are necessary to preliminary assess the hemocompatibility of the pumps in terms of the likelihood of blood injury and will serve as a basis for pump optimization.

The authors declare no conflict of interest.

REFERENCES

1. *Wiegmann L, Thamsen B, de Zélicourt D, Granegger M, Boës S, Schmid Daners M, Kurtcuoglu V*. Fluid dynamics in the HeartMate 3: Influence of the artificial pulse feature and residual cardiac pulsation. *Artif Organs*. 2019 Apr 7; 43 (4): 363–376. Epub 2018 Nov 7. doi: 10.1111/aor.13346.
2. *Thamsen B, Gülan U, Wiegmann L, Loosli C, Schmid Daners M, Kurtcuoglu V et al.* Assessment of the Flow Field in the HeartMate 3 Using Three-Dimensional Particle Tracking Velocimetry and Comparison to Computational Fluid Dynamics. ASAIO Journal. 2019; 1. doi: 10.1097/mat.0000000000000987.
3. *Kuleshov AP, Itkin GP, Baybikov AS.* Razrabotka tsentrobezhnogo nasosa kanal'nogo tipa. *Vestnik transplantologii i iskusstvennykh organov*. 2018; 20 (3): 32–39.
4. *Thamsen B, Blümel B, Schaller J, Paschereit CO, Affeld K, Goubergrits L, Kertzscher U*. Numerical Analysis of Blood Damage Potential of the HeartMate II and HeartWare HVAD Rotary Blood Pumps. *Artificial Organs*. 2015; 39 (8): 651–659. doi: 10.1111/aor.12542.
5. *Lomakin AA.* Tsentrobezhnye i osevye nasosy. 2-e izd., pererab. i dop. M.–L.: Mashinostroenie, 1966. 364.
6. *Taskin ME, Fraser KH, Zhang T, Gellman B, Fleischli A, Dasse KA et al.* Computational Characterization of Flow and Hemolytic Performance of the UltraMag Blood Pump for Circulatory Support. *Artificial Organs*. 2010; 34 (12): 1099–1113. doi: 10.1111/j.1525-1594.2010.01017.x.
7. *Paul R, Schügner F, Reul H, Ray G.* Recent findings on flow induced blood damage: critical shear stresses and exposure times obtained with a high shear stress Couette system. *Artif Organs.* 1999; 23: 680.
8. *Schima H, Müller MR, Tsangaris S et al.* Mechanical blood traumatization by tubing and throttles *in vitro* pump tests: Experimental results and implications for hemolysis theory. *Artif Organs*. 1993; 17: 167–170.
9. *De Wachter D, Verdonck P, Verhoeven R, Hombrouckx R.* Red cell injury assessed in a numerical model of a peripheral dialysis needle. *ASAIO J.* 1996; 42: M524–29.

The article was submitted to the journal on 17.06.2020

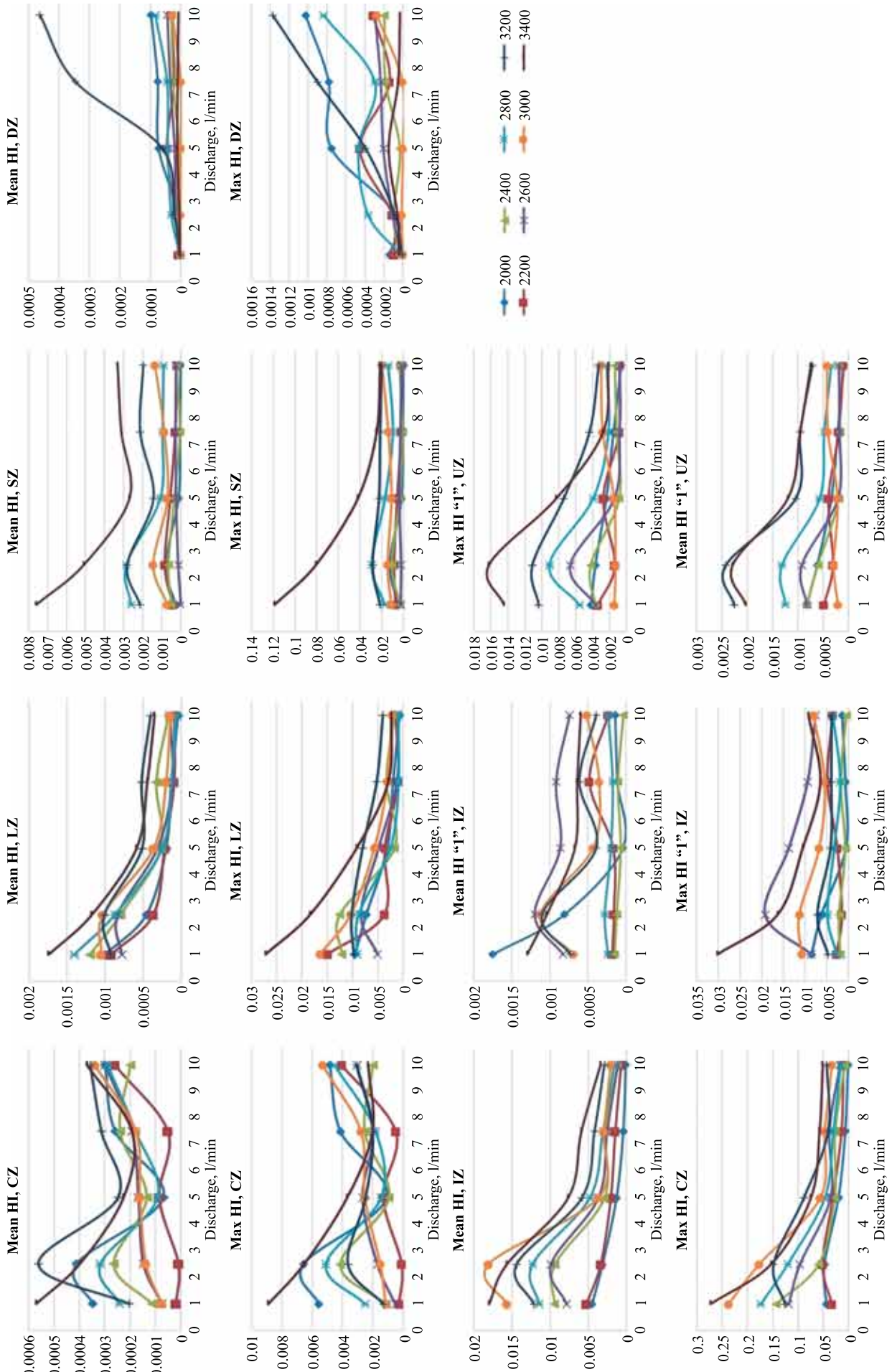

Fig. 6. Dependences of the mean and maximum hemolysis index (HI) in the studied zones of channel centrifugal pump

DOI: 10.15825/1995-1191-2020-3-86-98

CADAVERIC KIDNEY ALLOGRAFT TRANSPLANTATION USING THE DA VINCI ROBOTIC SURGICAL SYSTEM. INITIAL EXPERIENCE IN THE RUSSIAN FEDERATION

V.L. Medvedev, V.A. Porkhanov, K.E. Chernov, S.N. Volkov, G.A. Palaguta, O.V. Arepyeva, E.V. Gerdel

Ochapovsky Regional Clinical Hospital No. 1, Krasnodar, Russian Federation

Kidney transplantation is the treatment of choice for patients with end-stage renal disease. In order to reduce the number of postoperative complications following open surgeries, a number of clinics in the USA and Europe are currently developing robot-assisted surgical techniques. Studies have shown that robotic surgery facilitates kidney transplantation under optimal ergonomic position for the surgeon, with functional results and patient safety comparable to those obtained under an open approach. We herein present our initial experience (in the Russian Federation) on heterotopic cadaveric kidney transplantation by laparoscopic surgery using the Da Vinci robotic surgical system.

Keywords: kidney transplantation, Da Vinci robotic surgical system.

INRODUCTION

Minimally invasive surgery can reduce postoperative pain syndrome and the number of early postoperative complications in comparison with traditional open surgery, which, in turn, contributes to earlier activation of patients [1–5]. The role of minimally invasive surgery is especially important in a number of patients who have undergone kidney transplantation, since they often have severe concomitant pathology, accompanied by immunodeficiency after surgery. Such patients have a very high risk of postoperative complications, which undoubtedly affects not only the duration of rehabilitation, but also endangers both the viability of the graft and the life of the patient himself [6–9].

The technique of minimally invasive operations in kidney transplantation has been described quite recently [10–12]. In 2010 Modi et al. developed a laparoscopic method of kidney transplantation [10]. Giulianotti et al. first performed and described the technique of robotic transplantation [11]. Nevertheless, the authors noted a slower recovery of graft function compared to open surgery [13, 14]. Initially, a surgical technique was used without cooling the renal graft. To reduce the time of thermal ischemia, a number of authors modernized the technique [15] and began to use all kinds of devices for intraoperative, intraperitoneal graft cooling, which we also used in the operation. In total, clinics in the USA and Europe have accumulated experience of up to 500 such operations. In the domestic literature, it was not possible to find publications on the conduct of this type of surgical intervention. In our clinic, kidney transplants have been performed since 2009, as of 01.01.2020 467 kidney operations have been performed. Since December 2014 at the Ochapovsky Regional Clinical Hospital No. 1 (Krasnodar, Russian Federation), it became possible to perform operations using the Da Vinci Si robotic system. From that moment to January 2020, more than 900 robotic-assisted surgical interventions of various complexity categories were performed: radical prostatectomy with extended pelvic lymphadenectomy, kidney resection in case of tumor lesion, with a high RENAL index, radical cystectomy with orthotopic and heterotopic intestinal urine diversion in men and women, plastic surgery of the pelvic-ureteric segment, ureterocystoanastomosis, adenomectomy and other surgical interventions. Thanks to the extensive experience of Professor V.L. Medvedev and his team, performing both open and laparoscopic and robotic operations, as well as performing kidney transplantation, it became possible to successfully perform this operation.

MATERIALS AND METHODS

Clinical case 1

The recipient, a woman, 55, body mass index (BMI) 36.9 (Fig. 1). In 2000, the patient was diagnosed with autosomal dominant polycystic kidney disease. Since 2004, renal failure has occurred, and therefore conservative treatment was цукformed. In February 2008, terminal renal dysfunction was diagnosed, which required renal replacement therapy by hemodialysis 3 times a week for 5 h. Due to the large size of the kidneys, to prepare for transplantation in 2013, nephrectomies were performed sequentially on the right and left with the lumbotomic approaches. The patient is on the WL for transplantation.

Corresponding author: Kirill Chernov. Adress: 167, Pervaya Maya str., Krasnodar, 350086, Russian Federation. Phone: (861) 252-87-32; mobile phone: (967) 302-33-30. E-mail: chernov_ke@mail.ru

Fig. 1. The appearance of patient № 1 before surgery

The recipient was called from the waiting list for a kidney transplant, according to the tiping protocol (03.19.16). Blood group A (II). No hemotransfusions. Laboratory data upon admission to the hospital: urea 11.65 mmol/l, creatinine 487 mmol/l. The donor, a man, 50, and the recipient are identical by AB0 and HLA system antigens (I and II classes).

Clinical case 2

The recipient, a man, 28, BMI 37.8 with alimentary obesity (Fig. 2). Since 2012, the patient has noted an increase in blood pressure (BP) up to 200/120 mm Hg. Since July 2017, he has been feeling a worsening of his condition in the form of uncontrolled hypertension, severe general weakness and shortness of breath. On August 10, 2017, the patient was admitted to the central district hospital for hypertensive crisis. The examination revealed azotemia (urea – 26.8 mmol/l, creatinine – 800 μmol/l). The clinical diagnosis of chronic glomerulonephritis, hypertensive variant. The patient began to receive renal replacement therapy using programmed hemodialysis. From 23.01.2018 he was included in the WL for kidney transplant, on 11.10.18 was called from the waiting list according to the tiping protocol. Blood group (0) 1. No hemotransfusions. Laboratory indicators upon admission to the hospital: urea 14.16 mmol/l, creatinine 612.9 mmol/l. The donor, a woman, 27, and the recipient are identical by AB0 system and HLA system antigens (I and II classes).

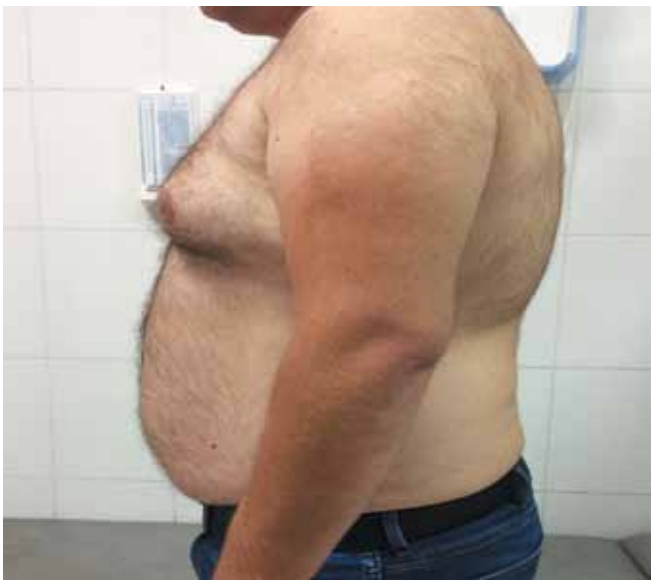

Fig. 2. The appearance of patient № 2 before surgery

TECHNIQUE AND STAGES OF OPERATION

Patient position and port location

Patients on the operating table were in the position, as in a standard developed intervention on the pelvic organs, lying on the back with legs apart [16, 17]. In the first patient, a vertical skin incision up to 4 cm long was made 4–5 cm above the navel along the midline, and an open entrance to the abdominal cavity was made under visual control (considering the previously performed ventral hernia repair). In the second patient, the main telescopic trocar was installed in a closed way. Other ports, including three 8mm robotic ports and one 12mm assistant port were installed as shown in Fig. 3 [16, 18].

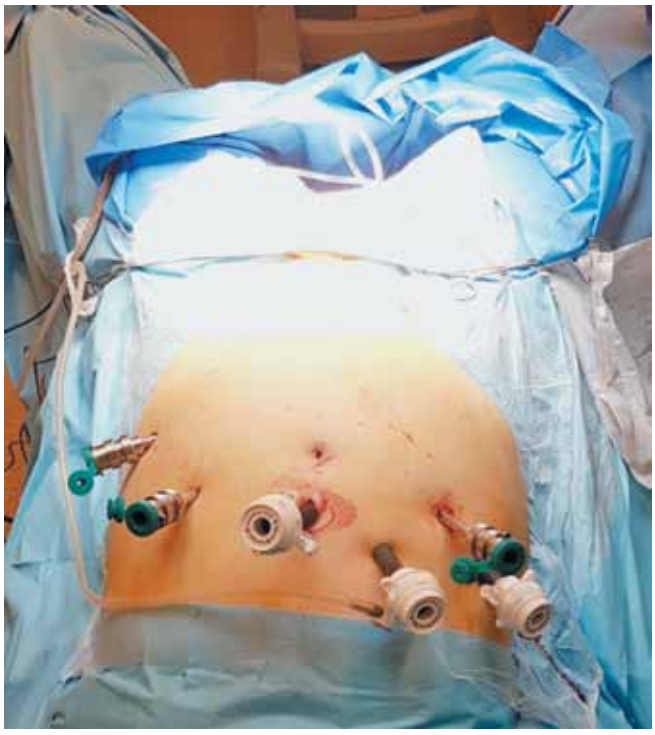

Fig. 3. The position of the ports (trocars)

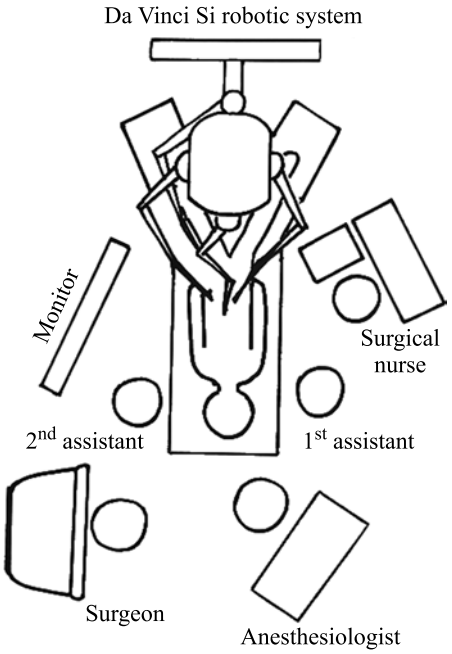

Fig. 4. The location of the patient, the operating team and the robot system in the operating room

Then the operating table was moved to the Trendelenburg position, and the Da Vinci Si robotic system (Intuitive Surgical, Sunnyvale, CA, USA) was located at the foot end of the table and the manipulators were fixed (Fig. 4).

Preparation of vessels

In both cases, the initial stages of the operation were the same. Laparoscopy and revision of the abdominal cavity with 30 ° camera lens was performed. No pathological changes were found in the abdominal cavity. The right external iliac vessels were identified; the parietal peritoneum was dissected above their projection. The right common, external, internal arteries and veins were identified, after which the vessels were taken to the turnstiles (Fig. 5, 6).

Renal graft preparation

Simultaneously with the preparation of the recipient and the beginning of the robotic stage, a cadaveric kidney was collected in the adjacent operating room and the renal graft was dissected. In each case, the cadaveric kidney was isolated from the perirenal tissue, the renal vessels were dissected (1 artery and 1 vein in both cases), and the ureter with the mesentery was mobilized. The kidney transplant was wrapped in several rounds of gauze napkin, pre-soaked with ice crumbs and saline sodium chloride solution, and placed in a sterile polyethylene container with ice, into which a 12 cm long, 16Ch diameter vinyl chloride tube was inserted. The latter was connected to an ice-cold saline infusion system to maintain further intraperitoneal cooling. The renal

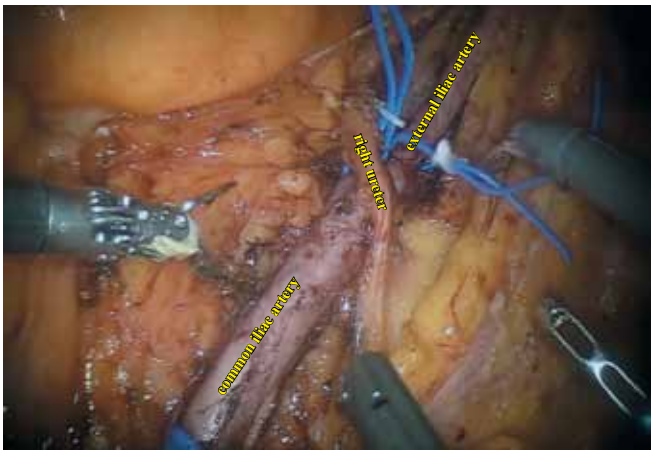

Fig. 5. Right iliac (common, external and internal) arteries

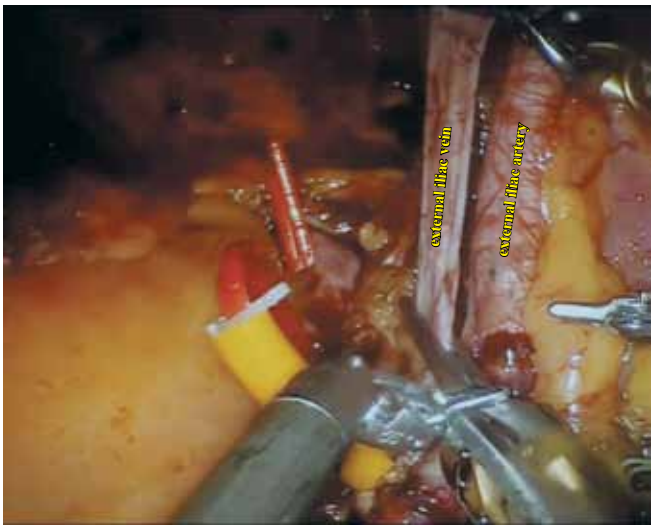

Fig. 6. Right external iliac artery and vein

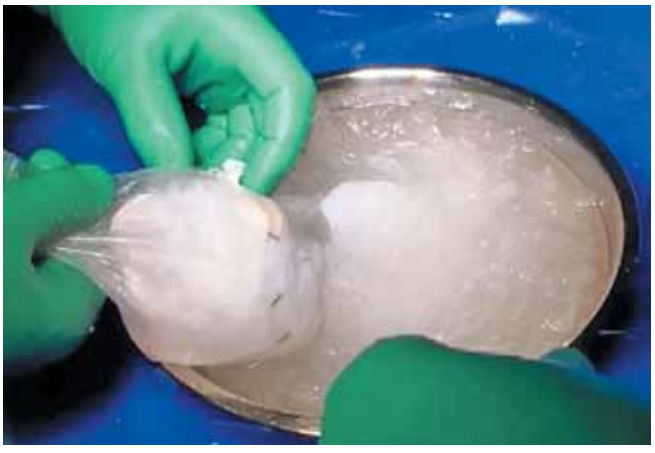

Fig. 7. Renal transplant preparation

vessels of the graft were taken out through the opening in the container (Fig. 7).

In the first case, the patient's uterus was taken on holders with separate sutures and laid forward and upward to the anterior abdominal wall. In the rectouterine pouch, in

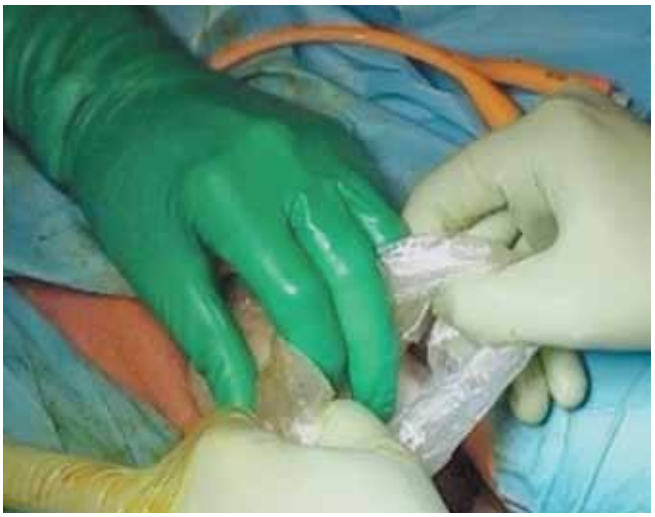

Fig. 8. The stage of transvaginal input of renal transplant

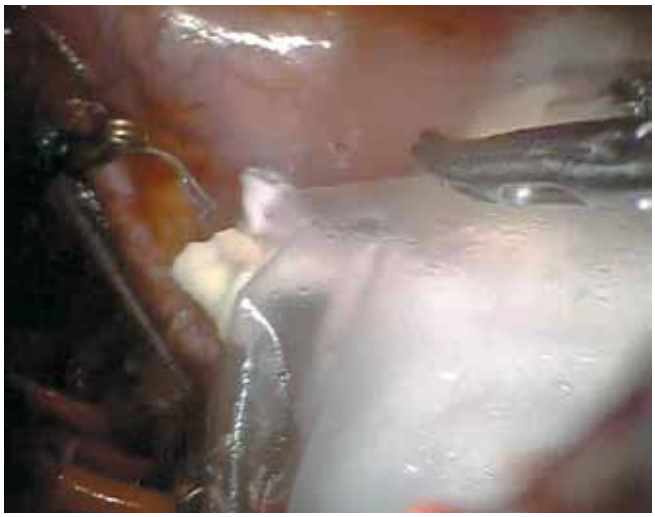

Fig. 9. The position of the transplant container in the abdominal cavity

the projection of the posterior fornix of the vagina up to 5 cm wide, a transverse incision of the peritoneum was made, and the wall of the vagina was dissected to the full depth, and a polyethylene sleeve was passed through the vagina, along which a graft in a container was inserted into the abdominal cavity and placed in the right iliac region (Figs. 8–11).

The vaginal vault was sutured continuously with a resorbable suture. The peritoneum is sutured.

In the second case, a mini laparotomy was performed with Pfannenstiel approach. A renal graft in a container is immersed in the pelvic cavity through a polyethylene sleeve. The laparotomic wound was sutured tightly in layers.

Through a separate puncture in the right iliac area, a system was inserted into the abdominal cavity for supplying and irrigating the graft with physiological sodium chloride solution +2 ° C in order to minimize the time of renal warm ischemia (Fig. 12).

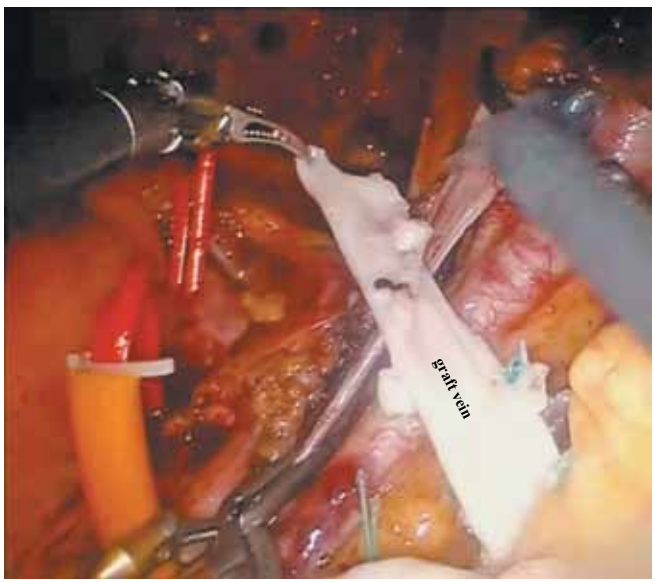

Fig. 10. The position of the renal vein of the graft relative to the iliac vessels of the recipient before performing the anastomosis

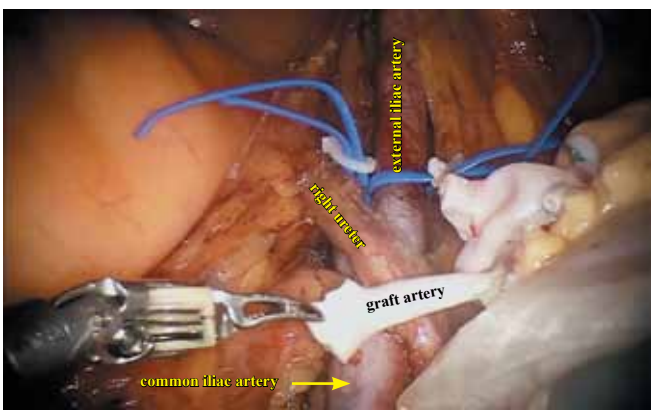

Fig. 11. The position of the renal artery transplant relative to the iliac vessels of the recipient before performing anastomosis

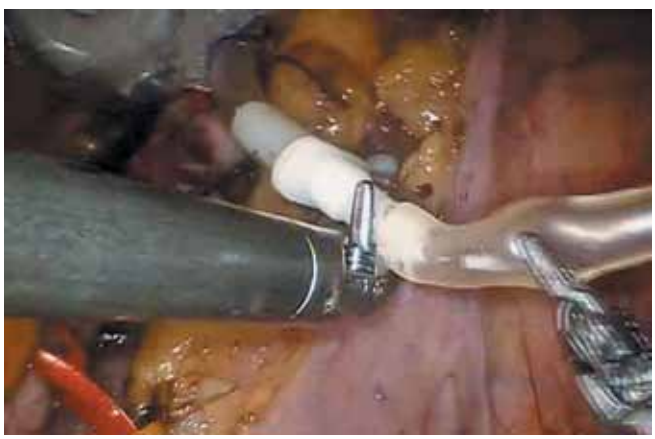

Fig. 12. Connecting the transplant irrigation system with ice-cold saline

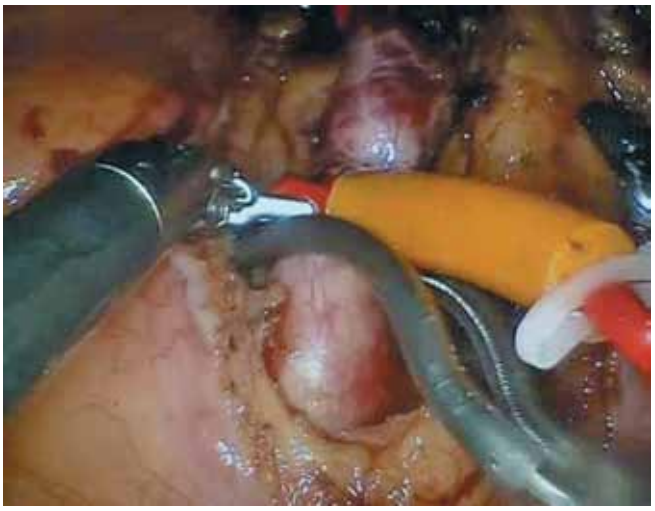

Fig. 13. The application of the vascular clamp type “bulldog” on the right common iliac artery

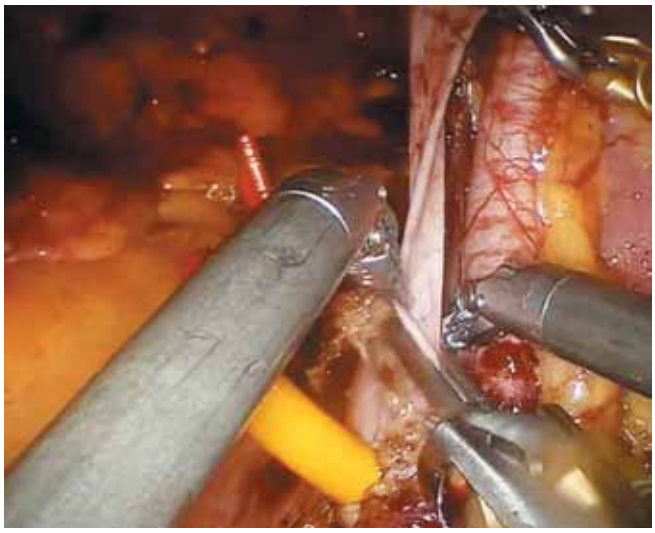

Fig. 14. The application of the vascular clamp type “bulldog” on the right external iliac vein

Venous anastomosis

The vascular stage of the operation began with a venous anastomosis. Bulldog-type vascular clamps were applied to the proximal and distal ends of the previously isolated iliac vessels (arteries and veins) in order to stop the blood flow (Fig. 13, 14).

Initially, the wall of the external iliac vein was opened and resected in size slightly wider than the diameter of the graft vein (about 12 mm). The lumen of the iliac vein was flushed with a heparin solution (5000 units of heparin per 100.0 physiological sodium chloride solution) through a 6Ch catheter. An end-to-side anastomosis was made with a continuous suture using Gore-Tex 5/0 suture material (WL Gore & Associates Inc, Flagstaff, AZ, USA) (Fig. 15, 16), while a needle holder was used in the “right hand” of the robotic system , and in the left hand is a bipolar forcept “Maryland forceps” Da Vinci (Intuitive Surgical, Sunnyvale, CA, USA). Before completing the venous anastomosis, the lumen of the vein is flushed again with heparinized saline sodium chloride solution in an amount of 20 ml.

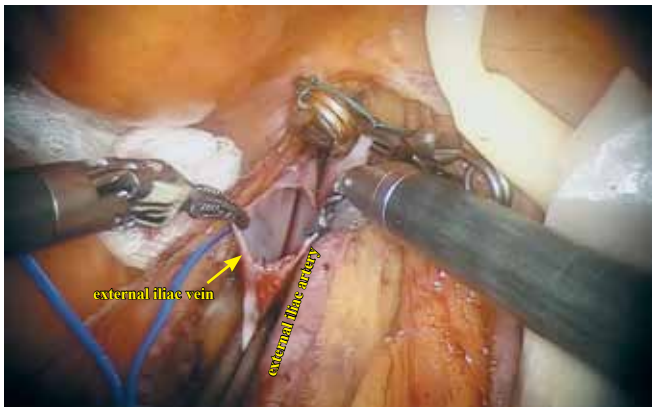

Fig. 15. Dissection of the lumen of the right external iliac vein

Arterial anastomosis

A circular arteriotomy with a diameter of up to 10 mm was performed in the wall of the right common iliac artery using robotic scissors. The lumen of the artery is also flushed with heparinized sodium chloride solution 20 ml. An end-to-side anastomosis was made with a renal graft artery, which was about 6 mm in diameter, with a continuous suture using Gore-Tex 5/0 suture material (Fig. 17, 18). Similarly, before completing the arterial anastomosis, the lumen of the vessels is flushed again with heparinized sodium chloride solution 20 ml.

A layer of BioGlue® for additional suture sealing (CryoLife USA) was applied to the area of vascular ana-

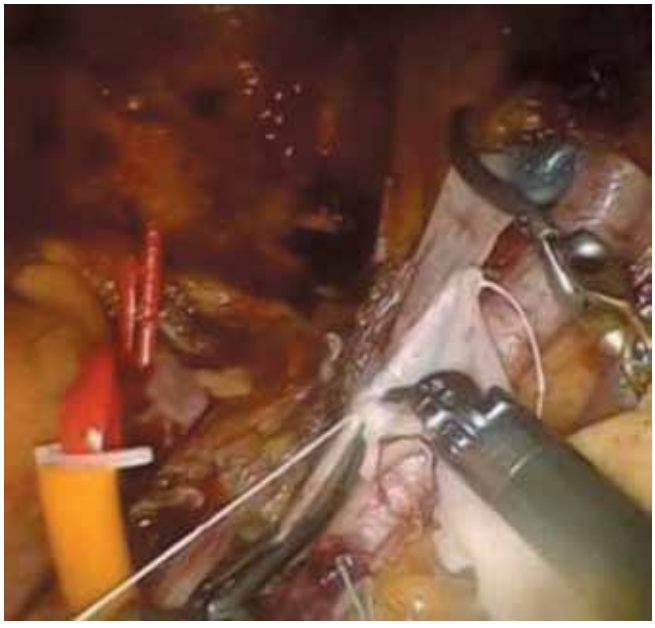

Fig. 16. Performing a vascular anastomosis between the renal vein and the right external iliac vein

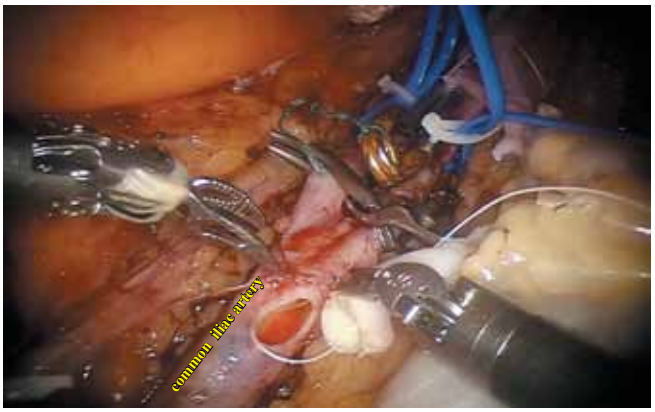

Fig. 17. Performing a vascular anastomosis between the renal artery and the right common iliac artery (beginning)

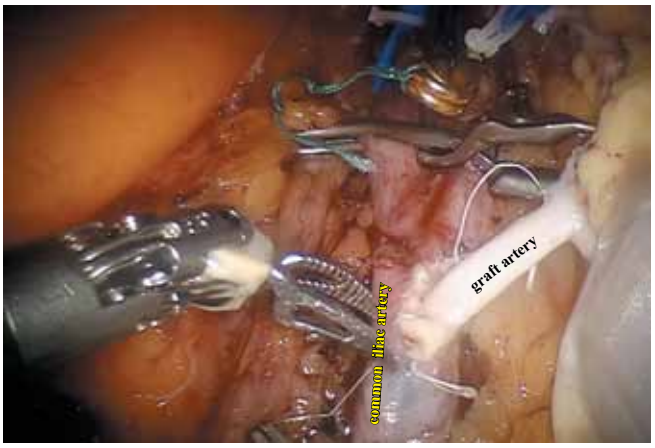

Fig. 18. Performing a vascular anastomosis between the renal artery and the right common iliac artery (completion)

stomoses. According to the standard protocol for kidney transplantation, methylprednisolone 1000 mg is injected intravenously into the recipient before starting the blood flow in the graft. Vascular clamps were removed one by one, starting from the distal venous, then cranial, then arterial. After the resumption of blood flow and control of the tightness of the anastomoses, the vascular clamps were removed from the abdominal cavity (Figs. 19, 20).

It should be noted that during the resumption of blood flow into the renal graft, it is necessary to be ready for immediate hemostasis. For this purpose, a gauze napkin was placed in the area of vascular anastomoses for 2–3 minutes. In case of ongoing bleeding, diastasis and / or perforation in the vessels are sutured with separate Z-shaped sutures using Prolene 5/0 suture (Ethicon, USA). The pulsation of the artery and blood filling of the graft were visually assessed. At this stage of the operation, it is extremely important to medically increase the recipient's blood pressure to high numbers – 130–140 mm Hg. From the distal end of the graft ureter, approximately 3–5 minutes after the start of the blood flow, light urine was dripped. After control of patency, tightness of vascular anastomoses, hemostasis, the graft irrigation system with ice solution was disconnected. The container and gauze pad, which was wrapped around the kidney graft, were cut with scissors and removed from the abdominal cavity through the assistant's 12 mm port.

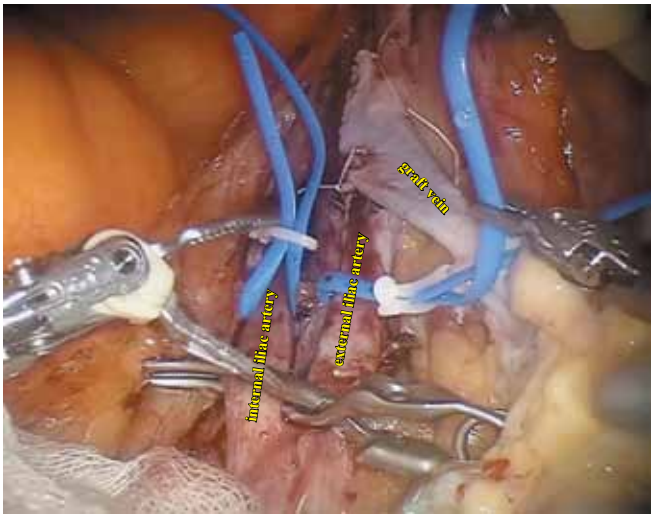

Fig. 19. Removing the clamp from the external iliac vein

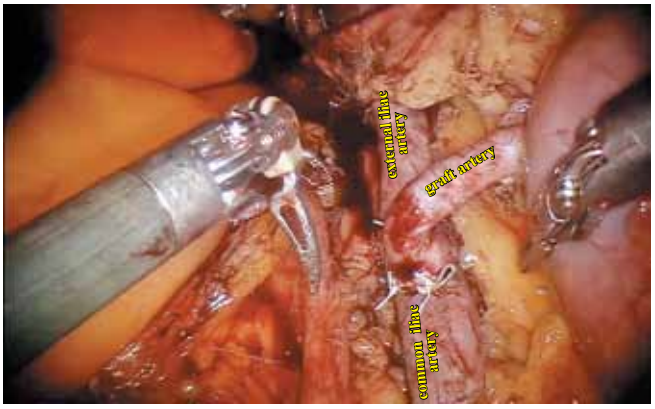

Fig. 20. Restoring blood flow to the graft

Ureterocystoanastomosis

Into the bladder of recipients through a pre-installed urethral catheter under sterile conditions, 200 ml of physiological sodium chloride solution was introduced. In the area of the bottom of the bladder, a longitudinal section of its wall up to 2.5 cm long was made using monopolar electric shears of a robotic system. The distal end of the graft ureter was spatulated for 2 cm. Ureterocystoanastomosis was placed with a continuous suture with Biosyn 4-0 thread (Covidien, USA). After suturing the lateral lip of the anastomosis, a Ch 7/22 double J stent (RuschGmbh, Germany) was inserted into the abdominal cavity through the 12-mm assistant port. The stent was installed at one end into the pelvis of the graft, with the other into the bladder cavity, after which the medial lip

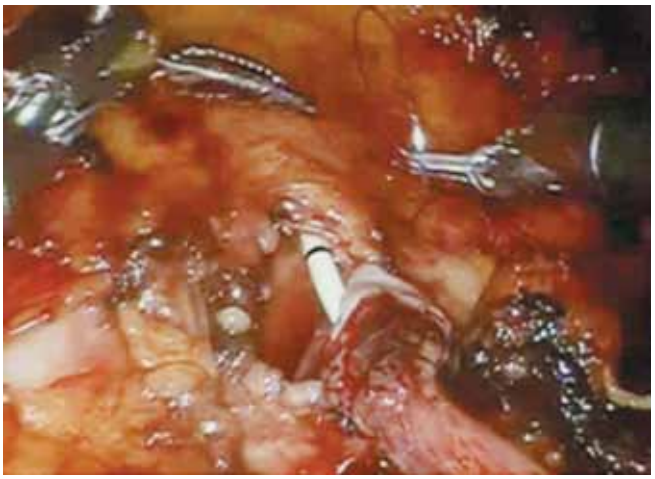

Fig. 21. Performing ureterocystoanastomosis (beginning)

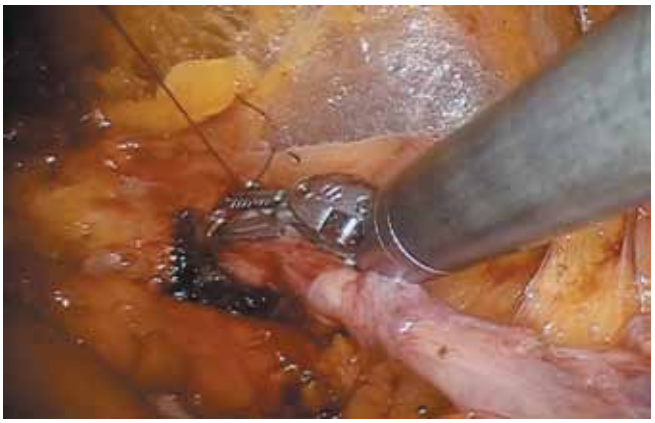

Fig. 22. Performing ureterocystoanastomosis (completion)

of the ureterocystoanastomosis was sutured. Analogous to open surgery, an important point in this stage of the operation is the creation of an antireflux mechanism of the ureter. In our clinical cases, we did this by suturing the detrusor fibers over the distal end of the ureter with the Leach – Gregoire technique [19, 20] (Figs. 21, 22).

Final stage, retroperitonization and drainage

The renal graft was immersed in a pocket that had previously been formed in the right iliac fossa between the retroperitoneal fascia and the peritoneum. The integrity of the peritoneal leaf over the graft was restored with a continuous suture with V-Loc™ 3-0 suture (Covidien, USA). Final hemostasis was performed. Through a robotic port in the right iliac region, a safety tubular silicone drainage with a diameter of 20Ch was installed into the newly formed retroperitoneal space on the right to the renal graft. The manipulators are disabled, the robotic stage of the operation is completed. Trocar holes were sutured under visual control using a furrier needle. Intradermal sutures to the skin. Aseptic stickers.

The operation time in the first case was 405 minutes, in the second observation, taking into account the accumulated experience of the first operation, the operation time was 190 minutes. The main stages of the operation in time intervals are presented in the Table. A longer time of some stages of the operation, in comparison with open ones, is associated with the development of the technique. The volume of blood loss did not exceed 80 ml in the first observation and 50 ml in the second.

Immunosuppressive therapy was carried out intraoperatively according to the standard scheme: induction with basiliximab 20 mg intravenously before the start of the incision 10 min. Before starting the blood flow in the graft, administration of methylprednisolone 1000 mg. From the first day after the operation, the scheme of immunosuppressive therapy was as follows: in the first observation – cyclosporine 300 mg/day, methylprednisolone 14 mg/day, mycophenolate mofetil 360 mg 2 r/day; in the second observation – methylprednisolone 4 mg 4 r/day, from the 3rd day after the operation, tacrolimus 5.5 mg 2 times a day, and from the 10th day – 5.5 + 4.5 mg per day.

Postoperative period

After the end of the operation, the recipients were taken to the boxed ward of the intensive care unit, where they were kept for 7 days. The next day after the transplantation, the patients became more active and began to walk within the ward. Anesthesia with narcotic analgesics was not required. The graft function is urgent. In the first observation, the diuresis on the first day was 4000 ml, in the second – 2200 ml. As can be seen from the presented graph (Fig. 23, 24), from the 3rd day after the operation, the first patient established a certain stable volume of diuresis, which was about 3000 ml/day. In the second patient, on the 10th and 12th days of the postoperative period, polyuria was noted up to 7500 and 5700 ml per day, respectively.

In both patients, there were no clinical manifestations of postoperative intestinal paresis, which made it possible to prescribe food for the next day after the operation and to fully feed the patients from the second day after the surgery. The insurance drains were removed on the 2nd day after the operation. There were no infectious, wound complications during the entire observation period. Controlled blood concentration of immunosuppressive drugs at 2 times a week was adequate. According to the ultrasound of the graft, which was periodically performed in patients, there were no abnormalities in the echostructure of the grafts and signs of impaired urodynamics. Blood flow data from day 10 after surgical treatment stabilized and averaged the following indicators: total Vmax 58 cm/s, RI 0.7; segmental Vmax 40 cm/s, RI 0.6, arc Vmax 22 cm/s, RI 0.6 (Figs. 25–28).

According to laboratory blood tests for a 30-day follow-up period, the level of blood leukocytes did not exceed 9.0×10^9/l, erythrocytes and hemoglobin did

Table

Stages of operation in time intervals

Operation stages	Time, min	
	Case 1 (19.03.2016)	Case 2 (11.10.2018)
Installing ports	15	12
Opening the peritoneum, isolating the iliac vessels	25	20
Graft preparation	35	25
Opening of the posterior vaginal fornix, transvaginal graft insertion	20	–
Pfannenstiel laparotomy, transplant placement, wound closure	–	35
Венозный анастомоз	25	20
Arterial anastomosis	25	15
Starting blood flow, hemostasis	20	10
Ureterocystoanastomosis with stent placement	40	25
Drainage installation, peritonization	35	30
Removing, suturing ports	15	15
Warm ischemia time	10	10
Cold ischemia time	120	90
Console running time	315	155
Total operation duration	405	190
Anesthesia duration	435	220

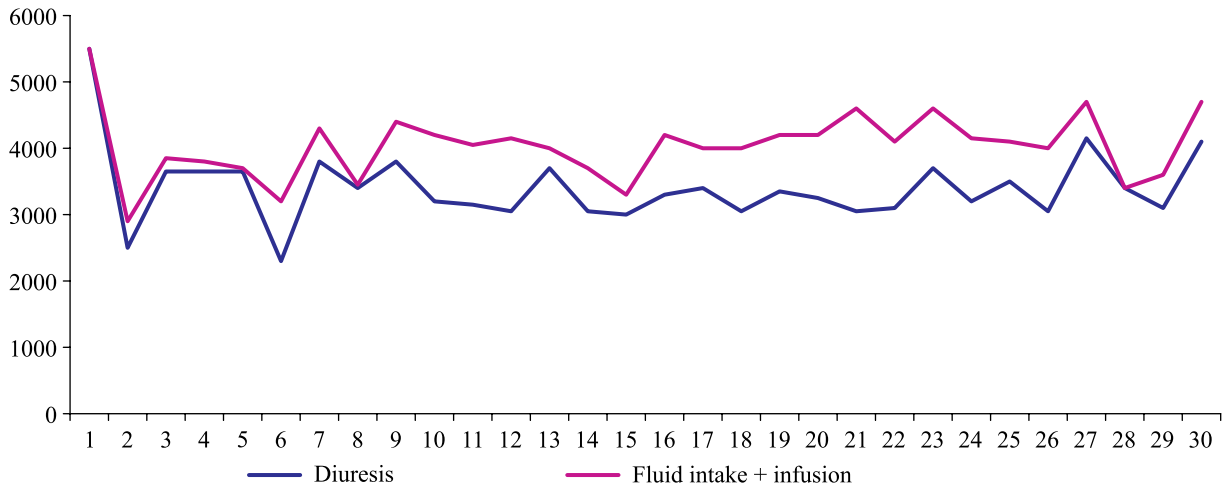

Fig. 23. Dynamics of diuresis and fluid intake with infusion therapy (ml) in the postoperative period in observation No. 1

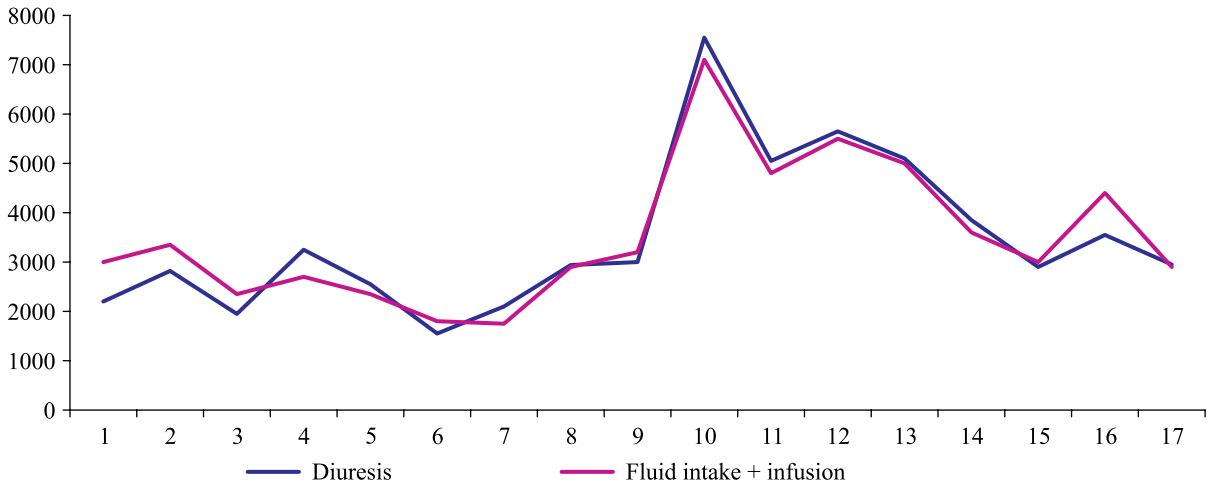

Fig. 24. Dynamics of diuresis and fluid intake with infusion therapy (ml) in the postoperative period in observation No. 2

not decrease below 3.0×10^{12}/l and 94 g/l, respectively. In the biochemical blood test, as shown in the graph (Fig. 29, 30), the urea and creatinine values in the first patient decreased steadily and remained relatively stable from 5–6 days after kidney transplantation (on average 4.64 mmol/L – for urea and 115 μmol/l – for creatinine).

The urethral catheter was removed on the 7th and 10th days (in the 1st and 2nd observation, respectively), and the ureteral stent – on the 21st day after surgery. On the 30th day, the patients were discharged from the hospital in a satisfactory condition.

Patients are regularly (once every 3 months) examined by a nephrologist. Throughout the entire period of observation and to this day, the state of health of the patients is satisfactory, they have the opportunity to travel freely. Renal transplants are functioning satisfactorily. There are no data for renal failure in terms of blood urea and creatinine (Fig. 31).

At the moment, the woman is receiving immunosuppressive therapy in the amount of: mycophenolic acid – 360 mg 2 times a day, cyclosporine – 50 mg in the morning and 75 mg in the evening, methylprednisolo-

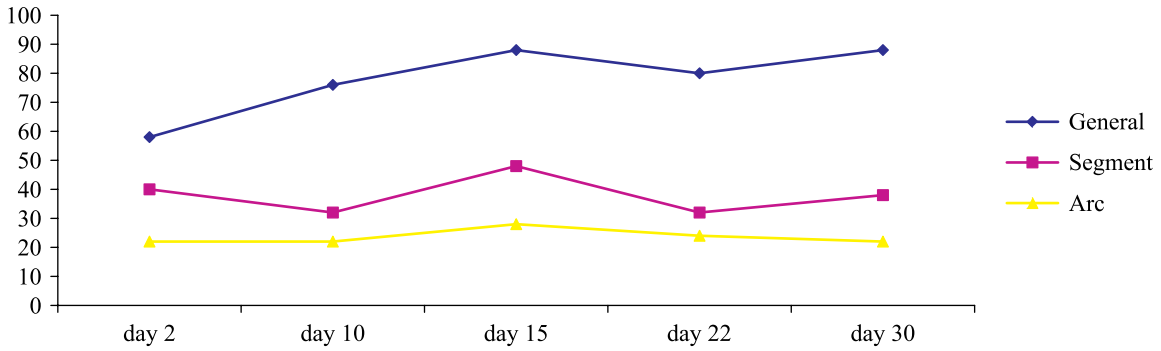

Fig. 25. Transplant blood flow data in the 1st observation Vmax (cm/s)

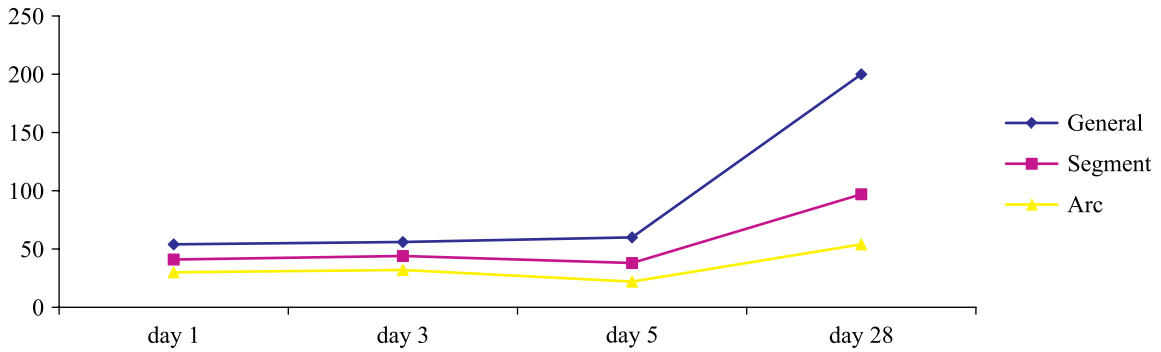

Fig. 26. Transplant blood flow data in the 2nd observation Vmax (cm/s)

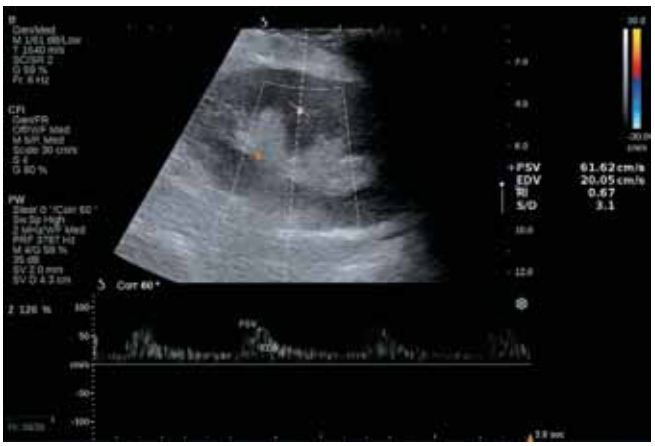

Fig. 27. Ultrasound image of a renal transplant of clinical case № 1

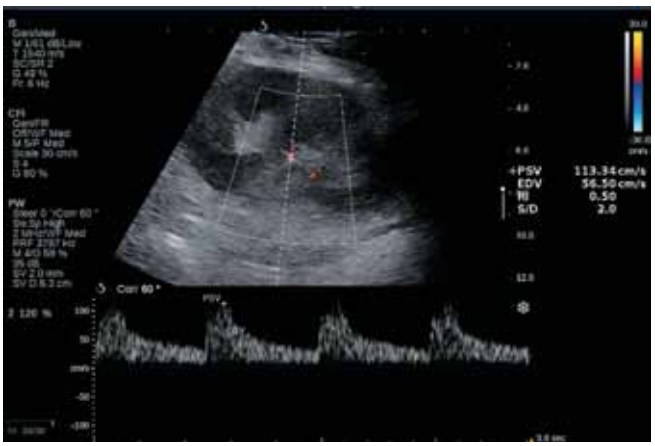

Fig. 28. Ultrasound image of a renal transplant of clinical case № 2

ne – 4 mg once a day. The second patient was prescribed the following therapy: mycophenolic acid – 360 mg 2 times a day, tacrolimus – 1.5 mg in the morning and 2.0 mg in the evening, and methylprednisolone – 4 mg in the morning.

CONCLUSION

The advantages of kidney transplantation using the Da Vinci robotic system in comparison with open surgery include a significant reduction in surgical trauma and, as a result, minimal postoperative pain syndrome

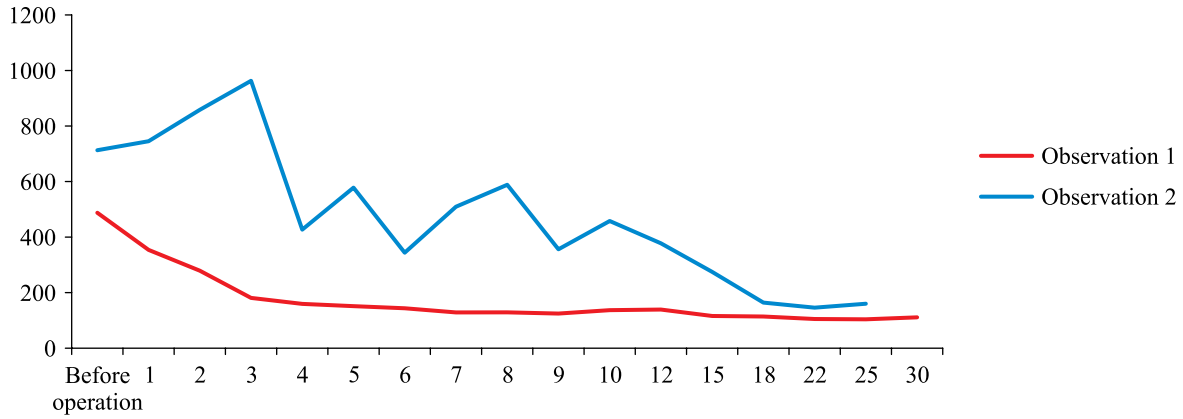

Fig. 29. Indicators of blood creatinine in the postoperative period (μmol/l)

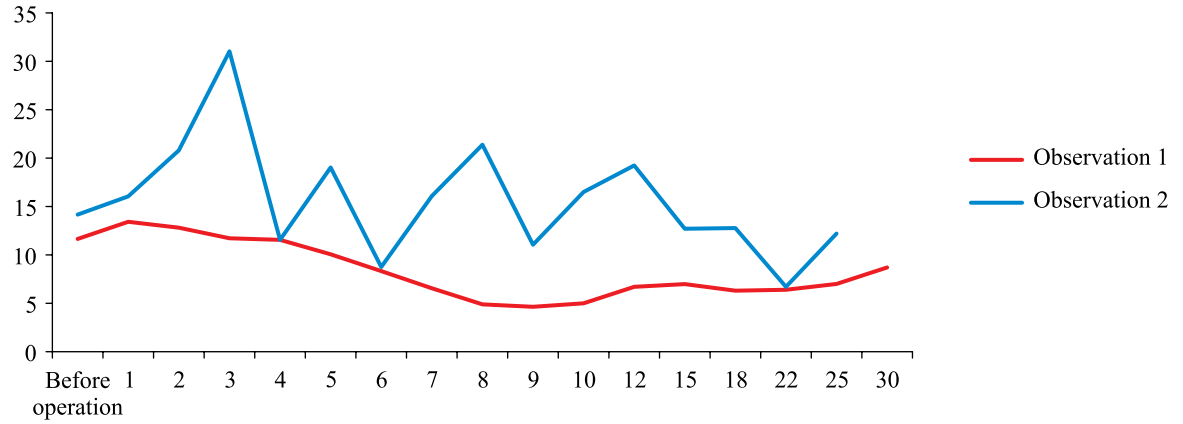

Fig. 30. The indicators of blood urea in the postoperative period (mmol/l)

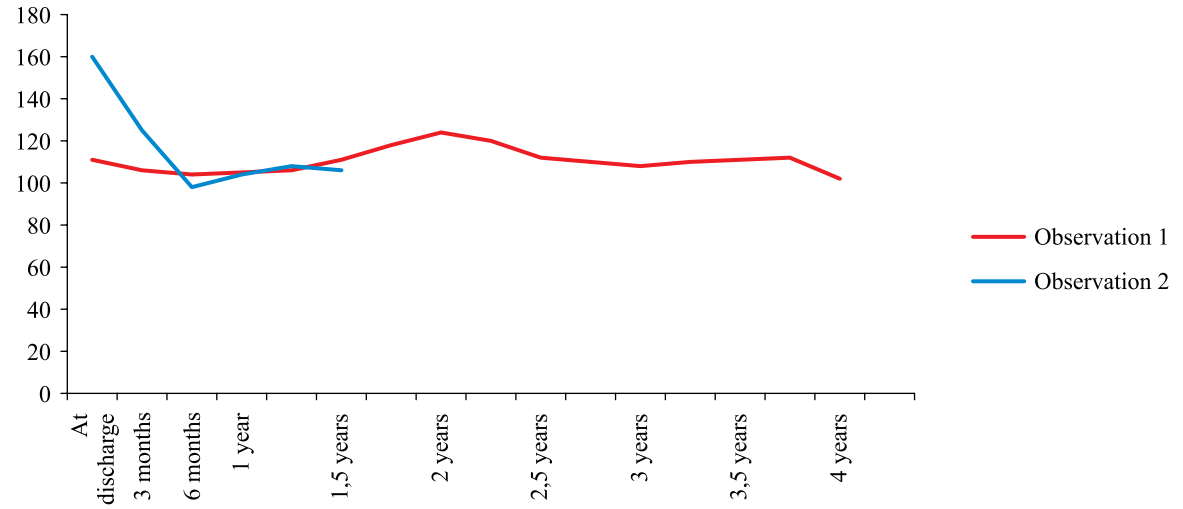

Fig. 31. Indicators of creatinine in the blood of patients during dynamic observation (μmol/l)

that does not require the use of narcotic analgesics, the convenience of visualization for the surgeon when manipulating in the pelvic cavity, the possibility of precise imposition anastomoses.

Besides, this type of surgery allows minimizing the risk of wound infectious complications, activating patients the next day after surgery, which is especially important for patients with diabetes and obesity due to the risk of thrombotic complications and hypoventilation changes in the lungs.

Among the disadvantages of the technique, it is necessary to note the long duration of the operation at the stage of development, the rather high cost of tools and equipment.

However, if the surgeon has sufficient experience in working with the Da Vinci robotic system, the equipment of the hospital, highly qualified specialists and the well-coordinated work of the team, the operation is technically feasible.

Compliance with all the rules of conservative treatment by experienced personnel, constant laboratory and instrumental control allow achieving satisfactory functional results in the treatment of patients who underwent kidney transplantation using minimally invasive technology.

To obtain statistically reliable results, it is necessary to perform a greater number of such operations, which will improve the surgical technique, reduce the time of surgical intervention and shorten the time of recipient stay in the hospital, thereby improving the quality of life of this category of patients and reducing material costs for rehabilitation.

The authors declare no conflict of interest.

REFERENCES

1. *Trinh QD, Sammon J, Sun M et al.* Perioperative outcomes of robotassisted radical prostatectomy compared with open radical prostatectomy: results from the nationwide inpatient sample. *Eur Urol*. 2012; 61: 679–685.
2. *Nguyen NT, Goldman C, Rosenquist CJ et al.* Laparoscopic versus open gastric bypass: a randomized study of outcomes, quality of life, and costs. *Ann Surg.* 2001; 234: 279–289.
3. *Park A, Birch DW, Lovrics P.* Laparoscopic and open incisional hernia repair: a comparison study. *Surgery*. 1998; 124: 816–821, discussion 821–822.
4. *Park Y, Ha JW.* Comparison of one-level posterior lumbar interbody fusion performed with a minimally invasive approach or a traditional open approach. *Spine*. 2007; 32: 537–543.
5. *Romy S, Eisenring MC, Bettschart V, Petignat C, Francioli P, Troillet N.* Laparoscope use and surgical site infections in digestive surgery. *Ann Surg*. 2008; 247: 627–632.
6. *Giral-Classe M, Hourmant M, Cantarovich D et al.* Delayed graft function of more than six days strongly decreases long-term survival of transplanted kidneys. *Kidney Int*. 1998; 54: 972–978.
7. *Lynch RJ, Ranney DN, Shijie C, Lee DS, Samala N, Englesbe MJ.* Obesity, surgical site infection, and outcome following renal transplantation. *Ann Surg*. 2009; 250: 1014–1020.
8. *Matas AJ, Gillingham KJ, Payne WD, Najarian JS.* The impact of an acute rejection episode on long-term renal allograft survival (t1/2). *Transplantation*. 1994; 57: 857–859.
9. *Osman Y, Shokeir A, Ali-el-Dein B et al.* Vascular complications after live donor renal transplantation: study of risk factors and effects on graft and patient survival. *J Urol*. 2003; 169: 859–862.
10. *Modi P, Rizvi J, Pal B et al.* Laparoscopic kidney transplantation: an initial experience. *Am J Transplant*. 2011; 11: 1320–1324.
11. *Giulianotti P, Gorodner V, Sbrana F et al.* Robotic transabdominal kidney transplantation in a morbidly obese patient. *Am J Transplant*. 2010; 10: 1478–1482.
12. *Boggi U, Vistoli F, Signori S et al.* Robotic renal transplantation: first European case. *Transpl Int*. 2011; 24: 213–218.
13. *Modi P, Pal B, Modi J et al.* Retroperitoneoscopic living-donor nephrectomy and laparoscopic kidney transplantation: experience of initial 72 cases. *Transplantation*. 2013; 95: 100–105.
14. *Oberholzer J, Giulianotti P, Danielson KK et al.* Minimally invasive robotic kidney transplantation for obese patients previously denied access to transplantation. *Am J Transplant*. 2013; 13: 721–728.
15. *Menon M, Abaza R, Sood A et al.* Robotic kidney transplantation with regional hypothermia: evolution of a novel procedure utilizing the IDEAL guidelines (IDEAL phase 0 and 1). *Eur Urol*. 2014; 65: 1001–1009.
16. *Menon M, Shrivastava A, Kaul S et al.* Vattikuti Institute prostatectomy: contemporary technique and analysis of results. *Eur Urol*. 2007; 51: 648–658, discussion 657–658.
17. *Jeong W, Sood A, Ghani KR et al.* Bimanual examination of theretrieved specimen and regional hypothermia during robot assisted radical prostatectomy: a novel technique for reducing positive surgical margin and achieving pelvic cooling. *BJU Int*. In press. http://dx.doi.org/10.1111/bju.12573.
18. *Menon M, Tewari A, Peabody J.* Vattikuti Institute prostatectomy: technique. *J Urol*. 2003; 169: 2289–2292.
19. *Riedmiller H, Gerharz EW.* Antireflux surgery: Lich-Gregoir extravesical ureteric tunnelling. *BJU Int*. 2008; 101: 1467–1482.
20. *Hoznek A, Zaki SK, Samadi DB et al.* Robotic assisted kidney transplantation: an initial experience. *J Urol*. 2002; 167: 1604–1606.

The article was submitted to the journal on 19.05.2020

DOI: 10.15825/1995-1191-2020-3-99-106

INITIAL EXPERIENCE IN DIRECT GRAFT PERFUSION ASSESSMENT FOLLOWING ORTHOTOPIC LIVER TRANSPLANT

A.V. Moiseenko, A.A. Polikarpov, P.G. Tarazov, D.A. Granov

Granov Russian Scientific Center of Radiology and Surgical Technology, St. Petersburg, Russian Federation

Objective: classical methods of determining arterial blood supply of the graft following orthotopic liver transplantation (OLT) reflect the presence of blood flow in the trunk and large branches of the *A. hepatica*, without the characteristic of completeness of blood filling of peripheral sections, which is very important for objective evaluation of function. The aim of this study is to establish the diagnostic value of a direct perfusion study (IFlow) of the graft. **Materials and methods**. From 1998 to 2019, 245 OLTs were conducted. From 2015 to 2019, arterial changes were detected in 24 (23%) patients after 104 OLTs. A perfusion study was performed in 9 patients with suspected arterial graft failure. According to the IFlow study, liver hypoperfusion due to stenosis and/or splenic steal syndrome was detected in 8 cases and became an indication for therapeutic intervention. **Results.** Hepatic stenting and/or splenic artery embolization was performed to improve arterial blood supply to the liver. Endovascular procedures performed restored the perfusion index from 0.24 (0.01–0.89) to 0.61 (0.35–0.98). **Conclusion**. Absence of ultrasound and multispiral computed tomography signs of arterial complications does not rule out the need for perfusion angiography. Perfusion angiography allows to objectify the angiography data and perform corrective intervention in good time.

Keywords: orthotopic liver transplantation, blood flow, stenting, splenic artery embolization, graft perfusion angiography.

INTRODUCTION

The main indication for orthotopic liver transplantation (OLT) is terminal cirrhosis of various etiologies. The formation of cirrhosis leads to hemodynamic changes in the pancreatobiliary zone: depletion of the arterial flow to the liver and its simultaneous increase in the left gastric, gastroduodenal and splenic arteries. This creates unfavorable conditions for the blood supply to the donor organ [1].

During OLT, ligation of aberrant hepatic arteries is performed, leaving the common hepatic artery as the only source of blood supply to the organ parenchyma and bile ducts. Classical methods for determining the arterial blood supply of the graft after OLT (ultrasound, ultrasound, computed tomography, CT and angiography) display the presence of blood flow in the trunk and large branches of *A. hepatica*, without characterizing the completeness of blood filling in its peripheral parts, which seems to be quite important for an objective assessment of the graft function [2].

The **purpose** of the present study is to establish the diagnostic value of direct perfusion investigation of the graft by the IFlow program of the angiographic complex in patients with clinical, laboratory and radiological suspicion of liver hypoperfusion.

MATERIALS AND METHODS

In the Granov Russian Scientific Center of Radiology and Surgical Technology (St. Petersburg, Russian Federation) from 1998 to 2019, 245 OLTs were conducted. In 1998–2014, classical subtraction diagnostic angiography was performed only when vascular complications were detected using non-invasive (CT and / or ultrasound) methods (Fig. 1).

Fig. 1:

– a–c: MSCT of the abdominal organs with intravenous contrast, arterial phase: the diameters of the splenic (white arrow) and common hepatic arteries (black arrow) are comparable, = 3 mm (a); the right hepatic artery (arrow) is patent (b); segmental liver arteries (arrow) are defined (c);
– d: celiacography 2 days after MSCT; depleted intrahepatic arterial architectonics: no segmental vascular pattern as a sign of insufficient inflow (thick white arrows); the diameter of the dilated splenic artery (black arrow) is twice the common hepatic artery (white arrow): steal syndrome;
– e: control celiacography after embolization of the splenic artery trunk (under the same conditions for the introduction of a contrast agent); restored intrahepatic arterial architectonics, the vascular pattern can be traced to the subsegmental level (white arrows); stenosis of the common hepatic artery, the hemodynamic significance of which cannot be assessed without

Corresponding author: Andrey Moiseenko. Address: 70, Lenigradskaya str., St. Petersburg, 197758, Russian Federation. Phone: (981) 837-78-19. E-mail: med_moiseenko@mail.ru

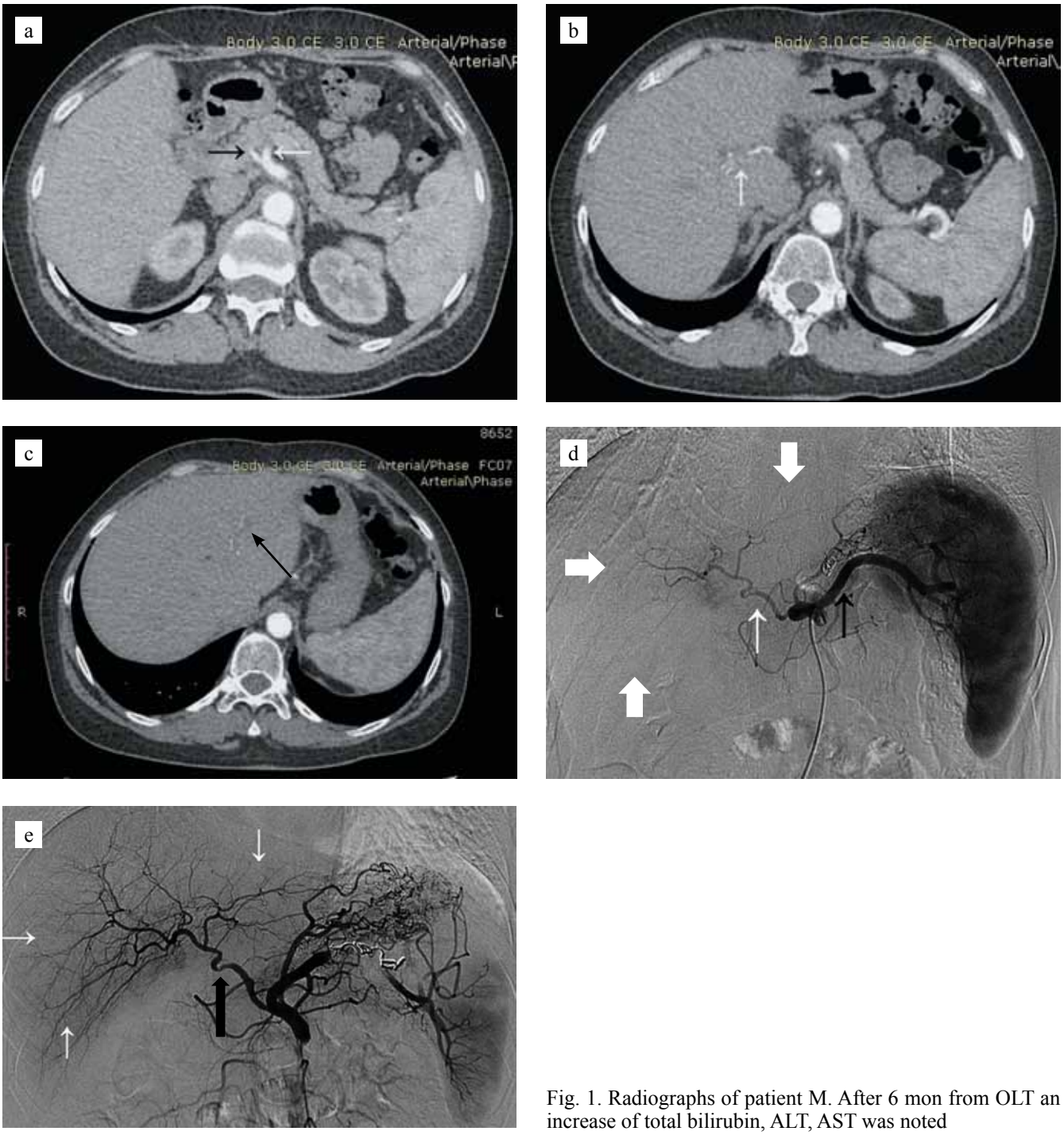

Fig. 1. Radiographs of patient M. After 6 mon from OLT an increase of total bilirubin, ALT, AST was noted

iFlow (black arrow); after 2 weeks. after endovascular intervention, biochemical parameters returned to normal, observed 4 years after OLT without biliary complications.

Since 2015, all patients with suspected liver hypoperfusion according to clinical and laboratory data have underwent angiography. In 2015–2019, arterial changes after 104 OLT were detected in 24 (23%) patients.

Classical diagnostic angiography was performed on a modern angiographic complex Siemens Artis Zee Biplane (Germany) with the IFlow function. Femoral artery puncture was performed under local anesthesia with 1% lidocaine solution using a 5F (1F = 0.33 mm) introducer sheath. Next, a Hook 5F catheter (Cook/Cordis, USA) was sequentially placed in the superior mesenteric artery and celiac trunk, subtraction angiography was performed using a syringe injector and 35 ml of contrast agent (Omnipak-350 or Ultravist-370) was injected at a rate of 4 ml/s.

The perfusion study was performed in 9 patients (Table). The difference in contrast agent concentration in the reference area (Ref AUC) and control areas (ROI AUC) was determined, where Ref AUC (referral area under curve) is the area of reference value under the curve,

Table

Analysis of perfusion values after OLT

Nos., age (years)	Timing of angiography after OLT	Interventions	Initial perfusion in S_{VI}, S_{VIII}, S_{II}	Final perfusion in S_{VI}, S_{VIII}, S_{II}	Ischemic biliary complications
1. K., 49	47 months	SAE SAE	0.08 0.10 0.22	0.40 0.65 0.40	–
2. S., 26	19 days	DA DA	0.89 0.81 0.89	0.89 0.81 0.89	–
3. K., 29	2 months	SAE + St SAE + St	0.20 0.25 010	0.55 0.50 0.53	+
4. Ch., 36	2 months	St St	0.15 0.20 0.10	0.60 0.28 0.33	+
5. K., 50	1 days	St St	0.01 0.02 0.01	0.45 0.40 0.35	+
6. S., 47	1 months	BAp BAp	0.50 0.55 0.30	0.70 0.75 0.65	–
7. K., 38	3 months	SAE + St SAE + St	0.02 0.30 0.25	0.45 0.55 0.35	+
8. Ch., 53	4 days	SAE + St SAE + St	0.12 0.11 0.35	0.80 0.81 0.83	–
9. G., 49	9 days	SAE SAE	0.08 0.05 0.16	0.81 0.89 0.98	–

Note. OLT – orthotopic liver transplantation, DA – diagnostic angiography, SAE – splenic artery embolization, St – stenting, BAp – balloon angioplasty.

and ROI AUC (region of interest area under curve) – the area of the control area under the curve. The reference area is the vessel (usually the celiac trunk) with maximum contrast medium filling during angiography. The control areas are the areas of the liver segments of interest (the most peripheral: SVI, SVIII, SII). The obtained angiograms were evaluated in the IFlow program. For this purpose, celiacography was selected at the workstation for 6–8 s of the series, when the vascular pattern of the liver was traced as far as possible along the segments. In the image tab, we switched to the IFlow mode, in the appeared dialog box, the duration video was set at the second when the subtraction celiacography was stopped. Then we went to the total contrast ROI selection dialog box with the subsequent selection of the circle value of the control area (circle ROI). The reference area was installed in the celiac trunk, giving it a value equal to the cross-sectional area of the vessel. Three control areas for measuring blood flow were set in the projection of the donor organ with the same values of their area, within 150–400 mm^2, and were located in the segments farthest from the reference point (SVI, SVIII, SII). The obtained tabular and graphical images displayed the completeness of filling the parenchyma with a contrast agent and the rate of reaching the peak concentration of the contrast agent, which in numerical value objectified the results obtained (Fig. 2, observation No. 1, Table). Adequate perfusion index (ROI AUC/REF AUC) was considered to be ≥0.65, the reference value was 1.0.

Fig. 2:

– a: celiacography, picture of depleted intrahepatic arterial architectonics. The diameter of the enlarged splenic artery (black arrow) is twice the common hepatic artery (white arrow): steal syndrome;
– b: perfusion study; the reference area, the size of which is equal to the cross-sectional area of the celiac trunk (value = 1) – circle Ref; areas of interest, areas of all circles in mm^2 – white circles 2, 3 and 4 (arrows in the upper table); the graph (at the bottom of the figure) displays the degree of filling of the studied areas (circles 2, 3 and 4) with a contrast agent over time, at 7 s: 5, 10 and 10%, respectively (thick arrow); the perfusion parameters of the studied areas are reduced (curved arrows);
– c: control celiacography after embolization of the splenic artery trunk to eliminate steal syndrome: in-

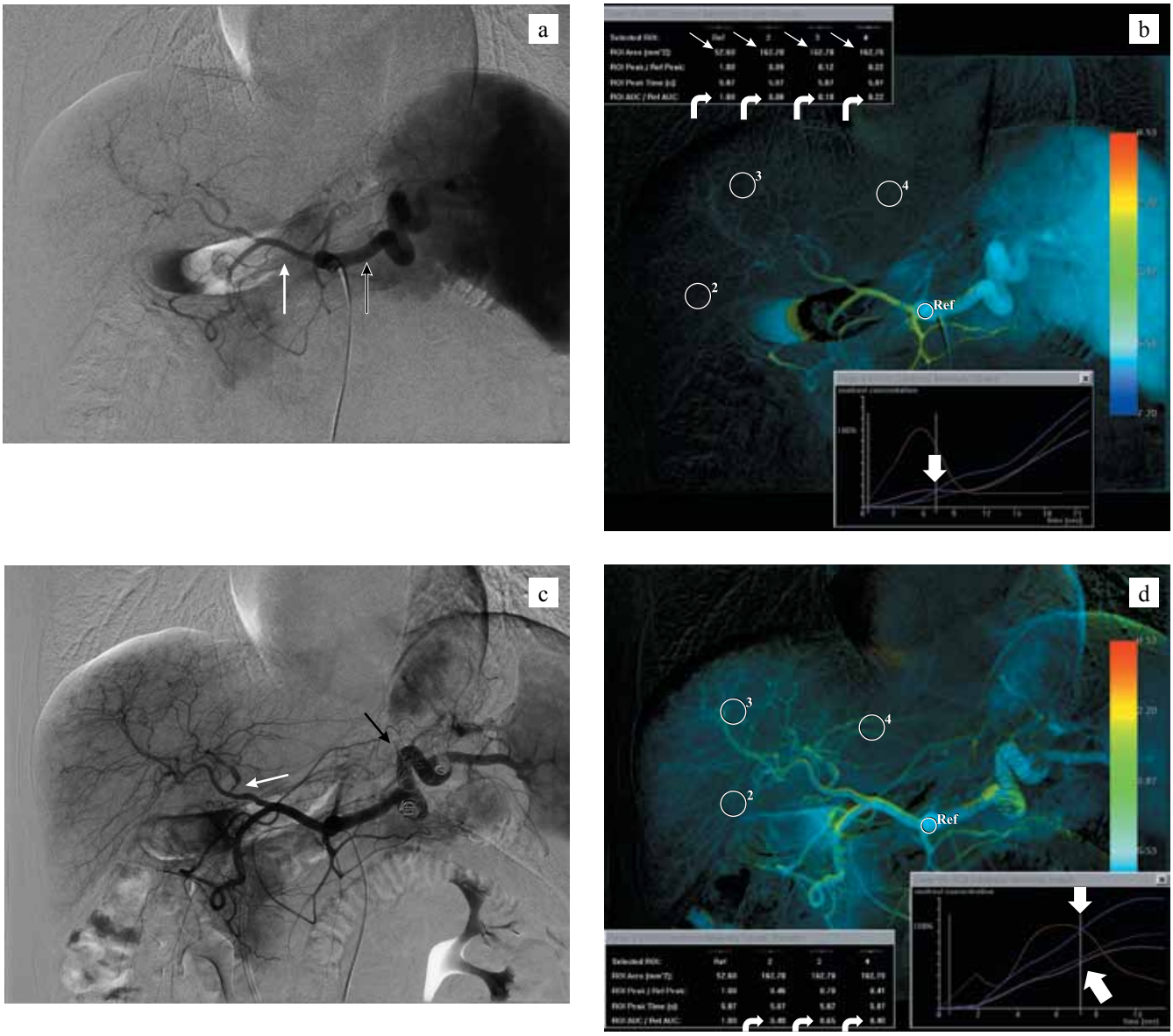

Fig. 2. Angiograms of patient K. 47 mon after OLT (case 1). The increase of ALT and AST was noted against adequate immunosuppressive therapy

trahepatic arterial architectonics can be traced in all segments; stenosis of the left hepatic artery (white arrow); metal coils in the trunk of the splenic artery (black arrow).

– d: perfusion study of the same patient after embolization, the perfusion index increased by 5, 6 and 2 times, respectively (curved arrows); the filling of the areas under study with a contrast agent increased by 7 s to 40, 40 and 70% (thick arrows); despite the unevenness of the contours of the left hepatic artery, the perfusion index of the left lobe of the liver is satisfactory, additional intervention is not required; the patient is observed 5.5 years after OLT without biliary complications.

RESULTS

There were no complications associated with diagnostic angiography. Initial angiograms and liver perfusion were satisfactory in one case (Fig. 3, observation No. 2, Table). Based on the obtained angiographic and perfusion data, therapeutic intravascular interventions were required in 8 patients (Table).

Fig. 3:

– a: cholangiography; X-ray picture of “burnt tree” of the left lobe of the liver, class C according to C. Buis (black arrows); complete block at the level of the biliary anastomosis (white arrow); cholangiostomy (thick white arrow);
– b: at celiacography, the contours of the hepatic artery are even, the diameters of the splenic and common hepatic arteries are comparable, arterial architectonics

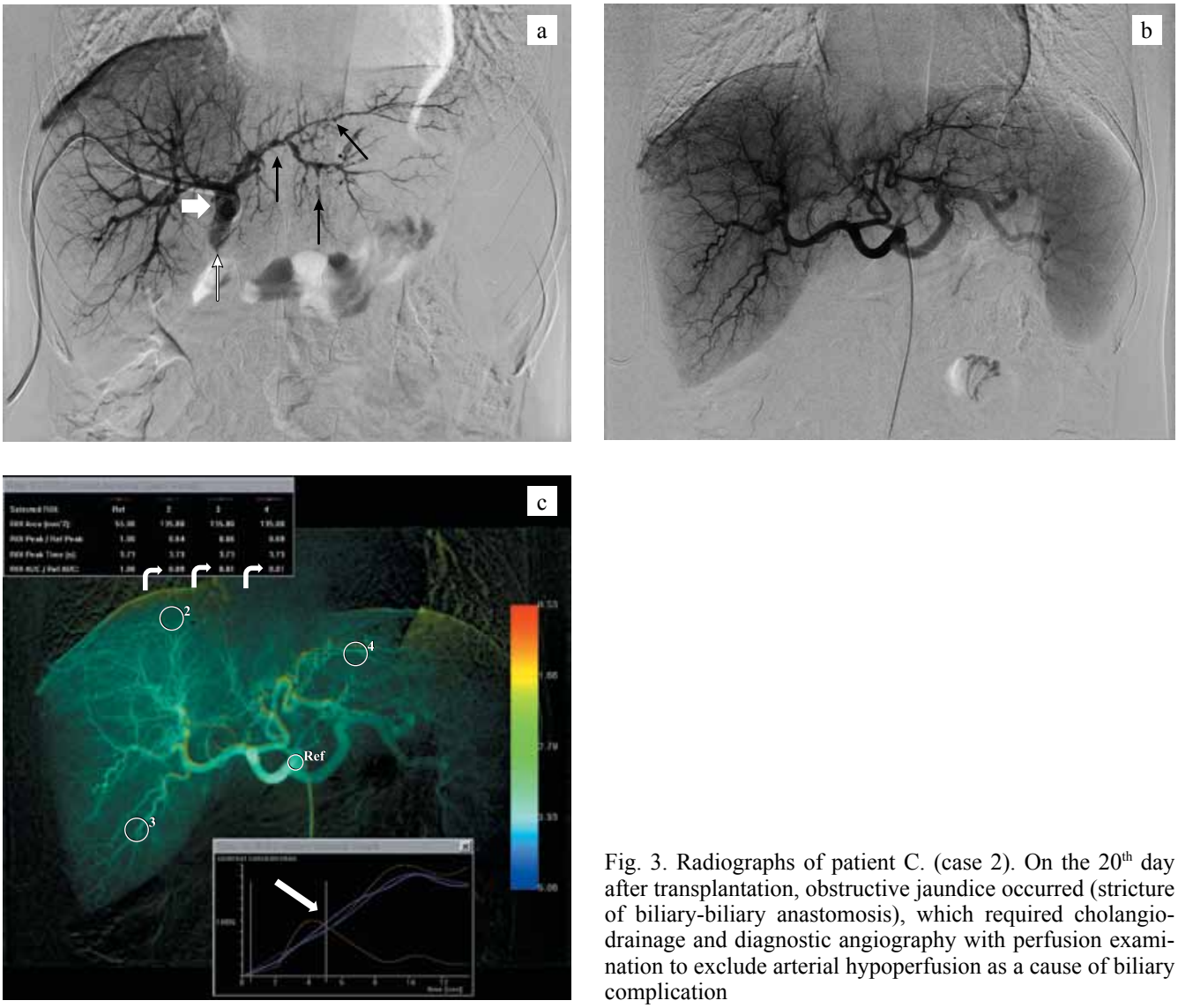

Fig. 3. Radiographs of patient C. (case 2). On the 20th day after transplantation, obstructive jaundice occurred (stricture of biliary-biliary anastomosis), which required cholangiodrainage and diagnostic angiography with perfusion examination to exclude arterial hypoperfusion as a cause of biliary complication

can be traced to the subsegmental level; there were no angiographic signs of hypoperfusion;

– c: perfusion study; a reference area, the size of which is equal to the cross-sectional area of the celiac trunk (value = 1) – circle Ref; the areas under study (white circles 2, 3, 4), the perfusion index of which in SVI, SVIII, SII = 0.89; 0.81; 0.81 (curved arrows); the graph (at the bottom of the figure) displays the percentage of filling the areas under study with a contrast agent over time, for 5 s: up to 45% (white arrow); perfusion indicators are more than 0.65, and the curve of filling the studied areas with a contrast agent over time is equated to the reference value; hypoperfusion was not detected; the biliary stricture is recognized as anastomotic, balloon plasty of the biliary-biliary anastomosis is performed.

The mean baseline perfusion value in the presence of splenic artery steal syndrome and / or hepatic artery stenosis was 0.24 (0.01–0.89). As a result of the therapeutic measures (stenting of the hepatic artery and / or embolization of the splenic artery trunk), the segmental perfusion index was restored to 0.61 (0.35–0.98) in all 8 patients. In four patients, the perfusion index did not exceed 0.6; later, biliary non-anastomotic strictures of class C and D according to Buis developed [3, 4]. The perfusion study avoided embolization of the left gastric artery to enhance the flow to the liver and objectified the need for hepatic artery stenting despite a satisfactory angiographic picture in one patient (Fig. 4, observation 8). Upon reaching a perfusion value of ≥0.65, no therapeutic actions were performed.

Fig. 4:

– a: celiacography: steal syndrome of the liver by the splenic artery (black arrow); kink of the non-anastomotic part of the hepatic artery (white arrow) was regarded as hemodynamically insignificant; depleted intrahepatic arterial architectonics;
– b: perfusion study; the reference area, the size of which is equal to the cross-sectional area of the celiac trunk (value = 1) – circle Ref; the areas under study

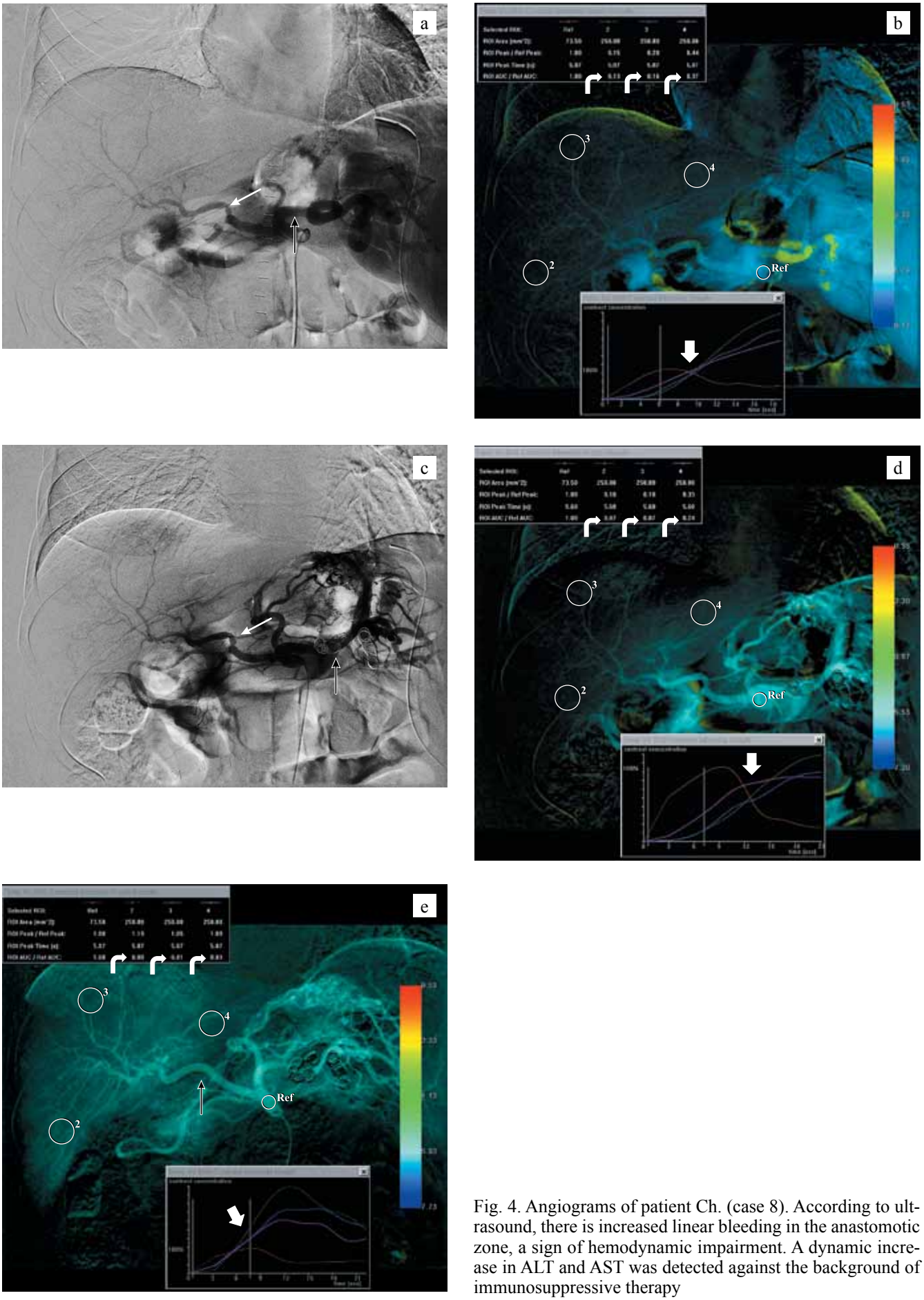

Fig. 4. Angiograms of patient Ch. (case 8). According to ultrasound, there is increased linear bleeding in the anastomotic zone, a sign of hemodynamic impairment. A dynamic increase in ALT and AST was detected against the background of immunosuppressive therapy

(white circles 2, 3, 4), the perfusion index of which in SVI, SVIII, SII = 0.13; 0.16; 0.37 (curved arrows); the graph (at the bottom of the figure) displays the percentage of filling the areas under study with a contrast agent over time, for 9 s: up to 30% (thick arrow); IFlow picture of pronounced hypoperfusion;

– c: celiacography after embolization of the splenic artery trunk: depleted intrahepatic arterial pattern is preserved, with moderately positive dynamics, bending of the hepatic artery (white arrow); reduced blood flow in the trunk of the splenic artery (black arrow);
– d: perfusion index in the studied areas 0.07; 0.07; 0.24, below original values (curved arrows); the filling of the studied areas with a contrast agent only for 13 s reaches 30–35% (thick arrow); IFlow picture of pronounced hypoperfusion, negative dynamics despite embolization of the splenic artery; the decision was made to stent the hepatic artery;
– e: perfusion study after hepatic artery stenting (black arrow); the perfusion index in the studied areas increased by 11, 11 and 4 times and amounted to 0.80; 0.81; 0.83 respectively (curved arrows); the filling of the study areas with a contrast agent decreased to 7 s and increased to 40, 40 and 50%, respectively (thick arrows); endovascular treatment was found to be effective, ALT and AST indices returned to normal on the 10th day.

DISCUSSION

We share the opinion of the authors who consider angiography a priority method for detecting vascular changes after OLT. Complications associated with diagnostic angiography do not exceed 1%, we did not have such complications [5, 6].

The present study showed that the presence of ultrasound and / or CT signs of intrahepatic arterial blood supply does not exclude transplant hypoperfusion [7].

The programs available in modern angiographic complexes help not only to suspect, but also to objectively identify the cause of the hypoperfusion state of the graft, which, with its timely and adequate elimination, can reduce the risk of biliary ischemic complications [2].

The obtained data are of great importance in the choice of tactics for the restoration of adequate graft perfusion. Embolization of the splenic or left gastric arteries performed without indications can lead to septic complications leading to a cascade of pathological mechanisms, especially against the background of mandatory immunosuppressive therapy [8]. Unnecessary stenting of the hepatic artery condemns the patient to lifelong antiplatelet therapy, and in case of thrombosis leads to the death of the organ and the patient [5]. According to D. Seehofer et al. [4], the formation of nonanastomotic strictures of the bile ducts in the graft is based on arterial hypoperfusion at all levels. It is associated either with a defect in the collection of the organ, or with its inadequate perfusion after the start of arterial blood flow. According to our data, there is a clear relationship between low perfusion values (<0.65) and ALT and AST indices with the subsequent development of biliary strictures.

CONCLUSION

The absence of ultrasound and CT signs of arterial complications does not exclude the need for angiography in case of suspected transplant hypoperfusion according to clinical and laboratory data. Angiography in combination with IFlow supplements the data of non-invasive diagnostic methods, allowing an objective assessment of the indications and efficacy of endovascular X-ray interventions in patients after OLT. Further study of graft hypoperfusion is required using the results of IFlow and MSCT perfusion.

The authors declare no conflict of interest.

REFERENCES

1. *Guan Y-S, Hu Y.* Clinical application of partial splenic embolization. *The Scientific World Journal*. 2014; 1–9. doi: 10.1155/2014/961345/.
2. *Prieto M, Gastaca M, Valdivieso A et al.* Does low hepatic artery flow increase rate of biliary strictures in deceased donor liver transplantation? Letter. The author's reply Kim PT., Fernandez H., Gupta A. et al. *Transplantation*. 2017; 101 (2): 332–340. doi: 10.1097/TP.0000000000001564.
3. *Buis CI, Verdonk RC, Van der Jagt EJ et al.* Nonanastomotic biliary strictures after liver transplantation, part 1: Radiological features and risk factors for early *vs* late presentation. *Liver Transplantation*. 2007; 13: 708–718. doi: 10.1002/lt.21166.
4. *Seehofer D, Eurich D, Veltzke-Schlieker W et al*. Biliary complications after liver transplantation: old problems and new challenges. *American Journal of Transplantation*. 2013; 13: 253–265. doi: 10.1111/ajt.12034.
5. *Goldsmith LE, Wiebke K, Seal J et al*. Complications after endovascular treatment of hepatic artery stenosis after liver transplantation. *Journal of Vascular Surgery*. 2017; 66 (5): 1488–1496. doi: 10.1016/j.jvs.2017.04.062.
6. *Dariushnia SR, Gill AE, Martin LG et al*. Quality improvement guidelines for diagnostic arteriography. *Journal of Vascular and Interventional Radiology*. 2014; 25 (12): 1873–1881. doi: 10.1016/j.jvir.2014.07.020.
7. *Granov DA, Polikarpov AA, Tileubergenov II et al*. A case report of successful liver retransplantation in patient with early hepatic artery thrombosis complicated by bile ducts necrosis. *Russian Journal of Transplantology and Artificial Organs*. 2019; 21 (3): 76–83. doi: 10.15825/1995-1191-2019-3-76-83.
8. *Aiolfi A, Inaba K, Strumwasser A et al*. Splenic artery embolization versus splenectomy. *Journal of Trauma and Acute Care Surgery*. 2017; 83 (3): 356–360. doi: 10.1097/ta.0000000000001550.

The article was submitted to the journal on 1.06.2020

DOI: 10.15825/1995-1191-2020-3-107-114

VALVE-IN-VALVE TRANSCATHETER AORTIC VALVE REPLACEMENT ON A SELF-EXPANDABLE NITINOL FRAME DUE TO DEGENERATION OF PRIMARY BIOPROSTHETIC VALVE CUSPS. CLINICAL CASE OF A HIGH-RISK SURGICAL FEMALE PATIENT

L.S. Kokov[1, 2], V.V. Sokolov[1], M.V. Parkhomenko[1, 2], R.Sh. Muslimov[1], M.V. Bulanova[1], N.M. Bikbova[1]

[1] Sklifosovsky Research Institute of Emergency Care, Moscow, Russian Federation
[2] Sechenov University, Moscow, Russian Federation

Introduction. We present the clinical observation of a 72-year-old female patient with high surgical risk and structural degeneration of a bioprosthetic aortic valve (AV) cusps in the form of stenosis, accompanied by severe dysfunction. Transcatheter implantation of bioprosthesis Medtronic CoreValve™ Evolut™ R-23 was performed using the valve-in-valve technique. The choice of minimally invasive treatment tactics is substantiated, a preoperative examination algorithm and a specific bioprosthesis model for such intervention are provided. **Materials and methods.** Imaging – echocardiography (Echo), electrocardiography, multispiral computed tomography, coronary angiography. Bioprosthetic valve calcification and stenosis with critical parameters of the bioprosthetic AV peak pressure gradient according to Echo data were the indications for minimally invasive surgery. **Results.** Dynamic observation revealed a progressive deterioration in the function of the previously implanted bioprosthetic heart valve in the aortic position, and a critical deterioration in the patient's condition. After additional examination of the patient and selection of a new prosthesis, valve-in-valve transcatheter aortic valve replacement was done. The positive dynamics of the general state of the patient was noted in the early postoperative period. Echo data showed that the bioprosthetic AV peak systolic pressure gradient decreased from 90 to 29 mmHg, average gradient – from 42 to 19 mmHg. **Conclusion.** The minimally invasive valve-in-valve transcatheter aortic valve replacement used to correct the dysfunction of a bioprosthetic AV that was previously implanted during an open surgery was shown to be safe and effective and can be considered as one of the options for repeat valve replacement.

Keywords: valve-in-valve transcatheter aortic valve replacement, aortic valve, aortic valve bioprosthesis, structural valve degeneration.

INTRODUCTION

Stenosis of the aortic valve (AV) is the most common acquired disease among all valvular heart diseases, requiring surgical treatment – open under artificial circulation (CP) or minimally invasive endovascular intervention. In view of the increasing tendency of population aging every year in the world, and in particular in Russia, the number of uses of biological prostheses for the correction of AV failure in case of its stenotic lesion is increasing [1].

The use of a biological prosthesis (BP) allows to abandon lifelong anticoagulant therapy [2, 3–7]. At the same time, among its significant drawback are the limited period of normal functioning associated with the degeneration of the biomaterial of the leaflets and dysfunction of the valve prosthesis as a whole, which necessitates a repeated intervention in the long term (after 5–10 years) [1, 3–7].

Today there are two possible ways to solve this problem. The first one is to perform re-implantation of the prosthesis in a standard way on an "open heart" in AC conditions. This path is associated with the risk of complications and mortality due to the elderly and senile age of patients, the presence of concomitant diseases in patients of this category and the trauma of the intervention itself. The second method – minimally invasive – is the transcatheter aortic valve implantation (TAVI). In the case of placing a new prosthesis in the frame of an old invalid one, this technique is called "valve-in-valve" [1, 3, 4].

Currently, in the world and especially in Russia, a small number of observations of reprosthetics using TAVI using the valve-to-valve technique have been published. Therefore, we consider it possible to offer our own experience of such an operation.

CLINICAL CASE

Patient K., 72, was routinely hospitalized in the emergency cardiac surgery department of the N.V. Sklifo-

Corresponding author: Marina Bulanova. Address: 3, Bolshaya Sukharevskaya Ploshchad, Moscow, 129090, Russian Federation. Phone: (916) 456-67-80. E-mail: marellabmv@mail.ru

sovsky Research Institute for Emergency Medicine in November 2019. Upon admission, she complained of shortness of breath with minimal physical exertion (walking a distance of 50–100 m), episodes of tachycardia, and weakness.

The anamnesis showed that 11 years ago (in 2008), the patient underwent AV prosthetics with a Carpentier-Edwards 21 xenoaortic bioprosthesis, linear resection and exoprosthetics of the ascending aorta with a synthetic InterGard prosthesis, due to bicuspid AV stenosis and expansion of the ascending aorta up to 5 cm under AC conditions. 10 years after AV prosthetics, angina attacks began to recur, and therefore the patient was examined in June 2018. According to the results of coronary angiography, hemodynamically significant stenoses were not found. Echocardiography (EchoCG) revealed moderate dysfunction of the AV prosthesis (peak gradient 45–50 mm Hg), which did not require surgical treatment.

The patient has begun to notice a significant deterioration in her condition from February 2019 in the form of shortness of breath, weakness, and tachycardia attacks. Upon re-hospitalization six months later, the following data were obtained during the examination. ECG showed no pathological changes. According to echocardiography: ejection fraction (EF) of the left ventricle (LV) – 65%, local myocardial contractility is not impaired. AV: the contours of the previously implanted prosthesis are determined, the valves are compacted, thickened, their opening is sharply limited, the peak gradient is 90 mm Hg. Art., the average gradient is 42 mm Hg, regurgitation of the 0–1st degree. Mitral valve: grade 1 regurgitation, average diastolic gradient 2.6 mm Hg. Tricuspid valve: 2nd degree regurgitation. The systolic pressure in the pulmonary artery is 40 mm Hg.

Coronary angiography did not detect any hemodynamically significant stenoses.

From the anamnesis, it is known that the patient suffers from arterial hypertension for a long time (maximum BP values 160/80 mm Hg, adapted to BP values 110/60 mm Hg), type 2 diabetes mellitus, bronchial asthma, chronic obstructive pulmonary disease, obliterating atherosclerosis of the vessels of the lower extremities, chronic heart failure.

A consultation was held by a multidisciplinary team consisting of a cardiologist, cardiac surgeon, X-ray endovascular surgeon, anesthesiologist. When discussing the options for correcting the pathology, the following factors were considered, which determine the high risk of repeated open surgery in AC conditions: previous surgery – AV prosthetics and intervention on the ascending aorta, older age, the presence of concomitant pathology. Surgical risk stratification indices EuroSCORE II >10% and STS >10% were determined, exceeding the maximum allowable level for open surgery. In connection with all of the above, it was decided to carry out transcatheter endovascular AV reprosthetics using the valve-to-valve technique. An additional examination is scheduled.

Multispiral computed tomography (MSCT) of the heart with ECG synchronization and the introduction of a contrast agent (Iopromide 370 mg iodine / ml in a volume of 100 ml intravenous bolus). In the AV projection, an X-ray-positive frame of a previously installed bioprosthesis with signs of asymmetric calcification of its valves is visualized (it is not possible to objectively assess the volume and degree of calcification due to the presence of a metal frame of the prosthesis) (Fig. 1). In the projection of the ascending aorta – a vascular prosthesis. The sizes at the levels that are fundamental for the preoperative planning of TAVI were determined (Tables 1, 2). According to preliminary estimates, the diameter of the passage hole of the previously installed Carpentier Edwards 21 bioprosthesis was 19 mm.

High bifurcation of both common femoral arteries (CFA), left CFA aneurysm (up to 20 mm) were also revealed. The wall of the aorta and main branches throughout the entire length is unevenly thickened with the presence of multiple calcifications, the contrasting of the lumen is uniform. In the projection of the coronary arteries and the base of the posterior cusp of the mitral valve, calcifications of various sizes were also revealed. Below the renal arteries – a moderate deviation of the aorta to the right. There was a deficit in the diameter of the external iliac arteries (APA) on both sides.

After the examination, it was decided to implant a Medtronic CoreValve Evolut R23 transcatheter biopros-

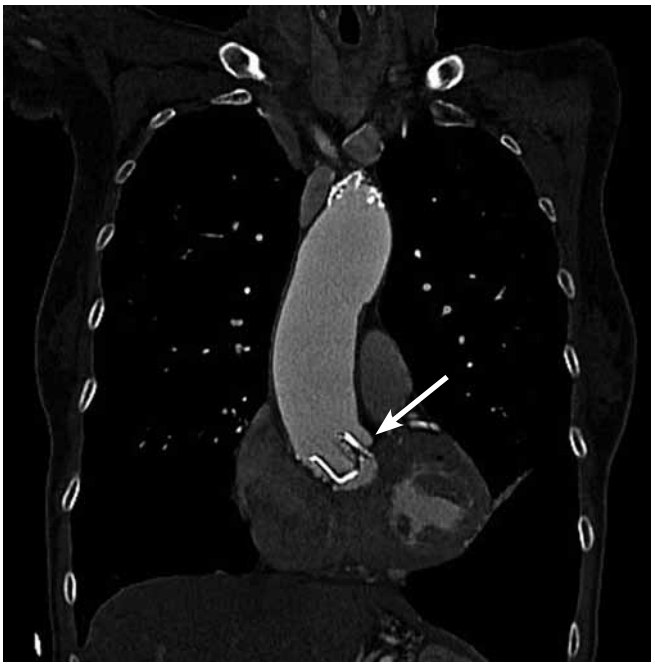

Fig. 1. MSCT of the heart before transcatheter AV bioprosthesis implantation; coronary projection; metal frame of the "prior" bioprosthesis Carpentier Edvards 21 (white arrow)

Table 1

MSCT data of the aortic valve elements and the left ventricle outflow tract

Analysis component	Diameter (mm)	Perimeter (mm)	Area (mm^2)	Height (mm)
Passage opening of the AV prosthesis	16.3	52.1	211.6	–
LV outlet	18.1	67.2	345.8	–
Sinuses of Valsalva	32.4	–	–	Right – 19 Left – 23
Sinotubular ridge	31–33	–	–	–
Distance from the annulus fibrosus to the orifices of the coronary arteries	–	–	–	To LCA – 15.7 To RCA – 13.2

thesis on a self-expanding nitinol framework through a transfemoral approach on the left.

Endovascular AV reprosthetics was performed in December 2019. Under endotracheal anesthesia, the left common femoral artery (CFA) was exposed and catheterized in the femoral triangle, and sheath 7F was installed. An electrode for temporary pacing was passed through the right jugular vein into the right ventricular cavity.

Through the puncture access of the right BOTH, a Pig tail 6F catheter was inserted into the aortic root. From the left-sided femoral approach, a diagnostic catheter was passed into the LV cavity, and a 0.035" Confida guidewire was inserted through it. The 7F introducer was replaced by the 12F introducer. Through its lumen, the previously implanted AV prosthesis was predilated with an Atlas Gold balloon catheter 18 × 40 mm with high-frequency pacemaker up to 180 per minute. Further, the 12F introducer was replaced with the 18F delivery system. The AV Medtronic CoreValve Evolut R23 prosthesis on a self-expanding nitinol framework was implanted in the aortic position.

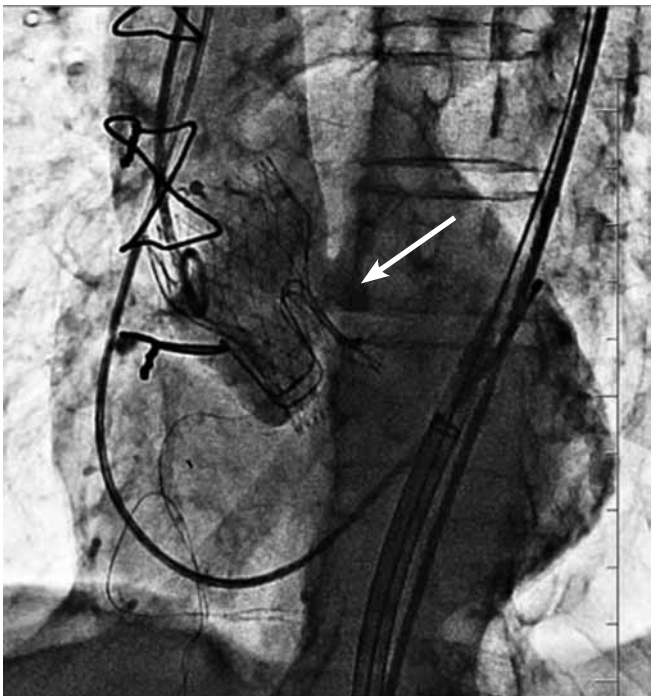

Fig. 2. Control aortogram after transcatheter aortic valve-in-valve bioprosthesis implantation; the position of the Medtronic CoreValve Evolut R23 prosthesis is optimal (white arrow); regurgitation is not determined

Table 2

MSCT data on the aorta diameter at different levels and its main branches

Analysis component	Diameter (mm)
Ascending aorta	33.9
Descending aorta	23
Abdominal aorta region in suprarenal area	20
At the level of renal arteries	13
Infrarenal area	12
Common iliac arteries	Right 4.6–6.3 Left 7.5–8.4
External iliac arteries	Right 4.4–4.7 Left 4.0–4.2
Common femoral arteries	Right 5.4–6.1 Left 5.4–5.7

Control aortography showed no regurgitation into the LV cavity (Fig. 2). Delivery system removed. Control transthoracic echocardiography was performed intraoperatively. The new prosthesis is located in the frame of the previously implanted one, paraprosthetic regurgitation of the 0–1st degree.

No events in the early postoperative period. There was a noticeable positive dynamics, both in the patient's objective condition and according to the data of instrumental examination.

ECG showed no signs of ischemic changes in the myocardium. The control echocardiography was performed (Table 3): LVEF – 65%, local contractility is not impaired. In the study in the color Doppler mapping mode, AV regurgitation of the 0–1st degree (Fig. 3, a), in the pulse-wave Doppler mode, the peak pressure gradient at the level of the AV prosthesis is 29 mm Hg. Art., the average gradient is 19 mm Hg. Art. (Fig. 3, b). Regurgitation on the mitral valve – grade 1–2, on the tricuspid valve – grade 2, systolic pressure in the pulmonary artery – 39 mm Hg. Art.

To assess the structures of the aortic root and the position of bioprostheses, MSCT of the heart with ECG

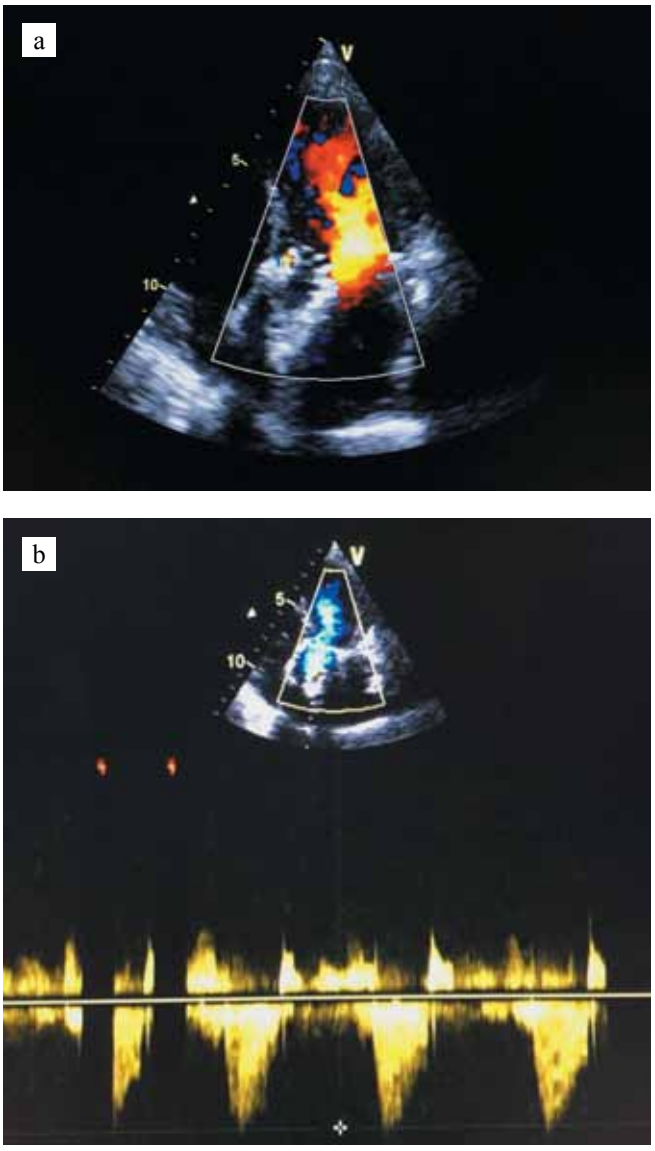

Fig. 3. Control Echo-CG after transcatheter aortic valve-in-valve bioprosthesis implantation: a – apical 5-chamber view, color Doppler mapping mode-regurgitation on the AV 0–1 degree; b – pulse-wave Doppler mode, peak pressure gradient at the prosthesis level AV – 29 mm Hg, mean pressure gradient – 19 mm Hg

Table 3

Echo-CG indicators before and after implantation of the AV bioprosthesis

Parameter	At admission	At discharge
LVEF	65%	65%
Peak gradient	90 mm Hg	29 mm Hg
Mean gradient	42 mm Hg	19 mm Hg
Regurgitation	0–1 grade	0–1 grade (interprosthetic)
Mitral valve	Regurgitation 1 grade	Regurgitation 1–2 grade
Tricuspid valve	Regurgitation 2 grade	Regurgitation 2 grade
mPAP	40 mm Hg	39 mm Hg

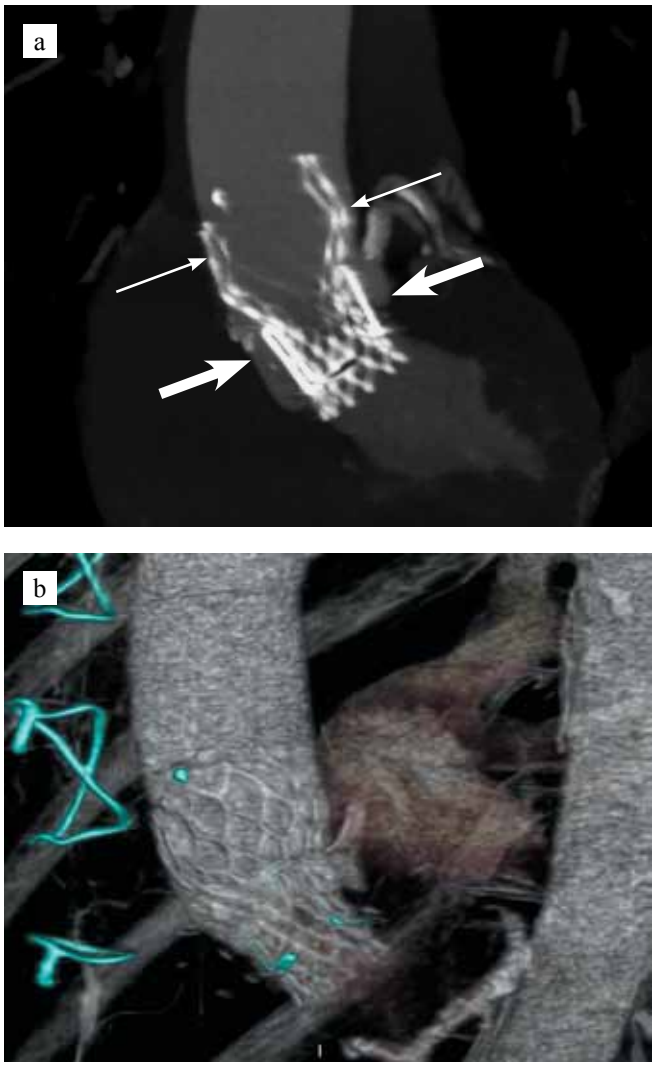

Fig. 4. MSCT of the heart after transcatheter aortic valve-in-valve bioprosthesis implantation: a – coronary plane, MIP view, bioprosthesis frame Medtronic CoreValve Evolut R23 (thin arrows) inside the bioprosthesis Carpentier Edvards 21 (thick arrows); b – 3D volume reconstruction of the aortic root with visualization of both prostheses

synchronization was performed on the 5th day (Fig. 4). In the AV projection, aortic root, sinotubular ridge, an implanted prosthesis is visualized, located in the frame of a previously installed biological prosthesis. There were no signs of valve dislocation. The position of the implanted valve complies with established standards. Contrasting of the trunks of the coronary arteries was preserved.

The patient was discharged on the 7th day after the operation with recommendations to control blood pressure, heart rate, control ECG, echocardiography, outpatient observation by a physician, cardiologist, pulmonologist.

DISCUSSION

When choosing the type of implantable prosthesis in the aortic position, bioprostheses are now more often

preferred, a significant advantage of which is the absence of the need for lifelong intake of anticoagulants and the associated risk of bleeding, constant laboratory monitoring of blood clotting. In addition, biological prostheses have a higher effective valve opening area, which leads to a low residual pressure gradient and a good hemodynamic effect. At the same time, a significant disadvantage of the bioprosthesis is the relatively short period of its normal functioning [1–7]. According to various studies, up to 60% of prostheses require replacement after 15–20 years. At the same time, according to the Global Valve-in-Valve Registry, the median life of bioprostheses is 9 years (interquartile range is 7–13 years) [1, 8, 9].

Dysfunction of the bioprosthesis is caused by degenerative changes in the structure of the valves (calcification and damage). This eventually leads to the need for reprosthetics [2, 5–9].

The standard method of bioprosthesis restenosis correction is repeated surgical implantation, as a rule, of a similar prosthesis, which is associated with a high risk of complications and mortality, which is primarily due to the high trauma of the intervention itself, as well as the advanced age of patients and the presence of concomitant diseases [1, 3–5].

In such difficult situations, a new alternative to open AV interventions is a minimally invasive operation – transcatheter implantation of AV bioprostheses with a sutureless fixation method [1, 3–7].

The presented clinical observation of a patient with dysfunction of a previously implanted AV bioprosthesis due to its calcification and stenosis and a high surgical risk showed the high efficiency of transcatheter implantation of the prosthesis by the "valve-in-valve" technique. The use of a bioprosthesis manufactured by Medtronic CoreValve Evolut R (Medtronic Inc., USA) with a self-opening function and the possibility of repositioning made it possible to implant it exactly into the frame of a previously implanted prosthesis. According to postoperative echocardiography, interprosthetic regurgitation was grade 0–1. Dislocation of prostheses in the early postoperative period was not revealed.

A distinctive feature of this clinical observation is the need for careful selection of a "new" bioprosthesis and delivery device of appropriate parameters, taking into account the size of the "old" bioprosthesis and individual anatomical features (small lumen) of the patient's iliac arteries. The complexity of endovascular intervention consisted in pronounced calcification of the walls of the aorta and its branches, and a deficit in the diameter of both APA, which increased the risk of dangerous complications. A bioprosthesis was used, used, according to the literature, in addition to the standard TAVI by "valve-in-valve" technique. This device is a percutaneous delivery system and porcine pericardial valve housed on a self-expanding nitinol mesh structure. The delivery system provides controlled and portioned repositioning. Radiopaque design allows for optimal positioning. The framework is designed to maintain coronary perfusion. An intraannular position and a sealed valve skirt reduce paraprosthetic regurgitation. The diameter of the delivery catheter at 18F is the smallest among those known today, its use was the only acceptable option for passing instruments through the ABP in the patient under discussion, and in combination with other features of the device determined our choice.

Currently, various models of transcatheter bioprostheses are widely used for valve-in-valve implantation: the first generation – Sapien, Sapien XT, Sapien 3 (Edwards LifeScience, USA), CoreValve, CoreValve Evolut R, Melody (Medtronic Inc., USA); second generation – Portico (St. Jude Medical, USA), Lotus (Boston Scientific, USA), Accurate TA (Symetis SA, Switzerland), Engager (Medtronic Inc., USA) [1]. In our observation, a Medtronic CoreValve Evolut R bioprosthesis with a diameter of 23 mm was successfully used.

Today, transcatheter heart valve reprosthesis is the only method that can significantly reduce the likelihood of complications of surgical treatment in high-risk patients with severe stenosis of the previously installed AV bioprosthesis [2, 3–7].

Based on the analysis of literature sources, various types of intra- and postoperative complications are possible limitation of the application of the valve-in-valve technique: the formation of a high transprosthetic pressure gradient, para- and transprosthetic regurgitation, device dislocation, obstruction of the coronary arteries with exfoliated calcifications, heart rhythm disturbances, as well as complications associated with the operational features of the procedure itself [1, 6, 7]. To prevent the occurrence of such complications, a thorough preoperative examination of the patient using echocardiography, coronary angiography, MSCT of the heart, the entire aorta and arteries of the lower extremities up to the level of the ilio-femoral segment is necessary. This allows making an accurate selection of the model of the AV transcatheter prosthesis, considering the anatomical features of the access arteries, the parameters of the aortic root, the design and size of the "old" bioprosthesis.

The X-ray endovascular technique of re-implantation of a bioprosthesis in the aortic position using the valve-in-valve technique is a rational treatment option, especially in elderly patients with a high surgical risk due to existing concomitant pathology [10]. The use of surgical risk scales known in cardiac surgery (EuroSCORE, STS-score) [11, 12] made it possible not only to predict the likelihood of complications, but also to prevent them in the postoperative period in the high-risk patient we described and, refraining from surgical AV reprosthetics, to successfully carry out transcatheter intervention.

CONCLUSION

The presented clinical case of successful transcatheter aortic valve replacement using the valve-in-valve technique demonstrates the safety and effectiveness of this treatment method. It can be argued that this method is a real alternative to the classical open intervention. This type of surgical intervention, of course, can be considered as one of the options for reprosthetics in patients with high surgical risk, for whom reoperation is indicated due to dysfunction of previously implanted biological prostheses of heart valves.

The authors declare no conflict of interest.

REFERENCES

1. *Klyshnikov RYu, Ovcharenko EA, Kudryavtseva YuA, Barbarash LS.* "Valve-in-valve" reprosthesing of cardiac artificial valves. *Russ J Cardiol.* 2016; 11 (139): 73–80. [In Russ, English abstract]. doi: 10.15829/1560-4071-2016-11-73-80.
2. *Imaev TE, Komlev AE, Kolegaev AS, Lepilin PM, Akchurin RS.* The current status of transcatheter heart valve replacement, using the valve-in-valve technique. *Consilium Medicum*. 2016; 18 (5): 89–92. [In Russ, English abstract].
3. *Nagaraja V, Raval J, Eslick GD, Denniss AR*. Approaches for transcatheter aortic valve replacement: a systematic review and meta-analysis. *Online J Health Allied Scs*. 2013; 12 (4): 3.
4. *Spaziano M, Mylotte D, Thériault-Lauzier P, Ole De Backer, Sndergaard L, Bosmans J et al*. Transcatheter aortic valve implantation versus redo surgery for failing surgical aortic bioprostheses: a multicentre propensity score analysis. *EuroIntervention.* 2017; 13 (10): 1149–1156.
5. *Hisato Takagi, Shohei Mitta, Tomo Ando*. Meta-analysis of valve-in-valve transcatheter versus redo surgical aortic valve replacement. *Thorac Cardiovasc Surg.* 2019; 67: 243–250.
6. *Duncan A, Moat N, Simonato M, de Weger A, Kempfert J, Eggebrecht H et al*. Outcomes following transcatheter aortic valve replacement for degenerative stentless versus stented bioprostheses. *JACC Cardiovasc Interv.* 2019 Jul 8; 12 (13): 1256–1263.
7. *Gurvitch R, Cheung AYeJ, Wood DA Willson AB, Toggweiler S, Binder R et al*. Transcatheter valve-in-valve Implantation for failed surgical bioprosthetic valves. *J Am Coll Cardiol.* 2011; 58 (21).
8. *Dvir D, Webb JG, Bleiziffer S, Pasic M, Waksman R, Kodali S et al*. Transcatheter aortic valve implantation in failed bioprosthetic surgical valves. *JAMA*. 2014; 312 (2): 162–170.
9. *Dvir D, Webb JG, Brecker S, Bleiziffer S, Hildick-Smith D, Colombo A et al*. Transcatheter aortic valve replacement for degenerative bioprosthetic surgical valves: results from the Global Valve-in-Valve Registry. *Circulation.* 2012; 126: 2335–44.
10. *Grubitzsch H, Zobel S, Christ T, Holinski S, Stangl K, Treskatsch S et al.* Redo procedures for degenerated stentless aortic xenografts and the role of valve-in-valve transcatheter techniques. *European Journal of Cardio-Thoracic Surgery.* 2017; 51 (4): 653–659. doi: 10.1093/ejcts/ezw397.
11. *Kofler M, Sebastian J, Stastny L, Dumfarth J, Reindl M, Wachter K et al*. EuroSCORE II and the STS score are more accurate in transapical than in transfemoral transcatheter aortic valve implantation. *Interactive CardioVascular and Thoracic Surgery*. 2018; 26 (3): 413–419. doi: 10.1093/icvts/ivx343.
12. *Aziz M, Simonato M, Webb J, Abdel-Wahab M, McElhinney D, Duncan A et al.* Mortality prediction after transcatheter treatment of failed bioprosthetic aortic valves utilizing various international scoring systems: Insights from the Valve-in-Valve International Data (VIVID). *Catheter Cardiovasc Interv.* 2018; 00: 1–8. doi: 10.1002/ccd.27714.

The article was submitted to the journal on 2.04.2020

DOI: 10.15825/1995-1191-2020-3-115-122

MANDIBULAR ENDOPROSTHESIS WITH SUPPORT ZONES AS AN ARTIFICIAL ORGAN

A.I. Shaikhaliev, P.S. Petruk, I.M. Shpitser, A.S. Migachev, L.D. Arasashvili, T.R. Davydova, G.A. Gasbanov, R.S. Korgoloev

Sechenov University, Moscow, Russian Federation

Mandibular reconstruction after partial or complete resection is a prerequisite for restoring normal facial aesthetics, articulation and chewing function. We present a clinical case of lower jaw reconstruction in a female patient with acquired extensive bone defect while taking pervitin and desomorphine. Detailed descriptions of the stages of planning and performing surgery, manufacture of an individual endoprosthesis, as well as preoperative preparation of the patient are presented. Clinical and radiological data in the postoperative period were analyzed and an objective assessment of the effectiveness of the technique was given. Adequate restoration of the main functions of the lost organ was achieved thanks to the use of an individual titanium mandibular endoprosthesis with integrated dental implants and a full-arch denture.

Keywords: mandibular reconstruction, prostheses and implants, artificial organs, virtual planning, computer-assisted design.

INTRODUCTION

Mandible (M) is the only movable and most massive bone of the facial skull, which is the support and place of attachment of functionally important muscle groups. M plays one of the main roles in ensuring the functions of chewing, swallowing, articulation and, in some cases, breathing.

Extensive M defects lead to asymmetry of the lower face zone, cause functional disorders, and are also accompanied by the loss of a person's aesthetic appearance [1]. Recently, a large number of scientific works have dealt with the correspondence of the hysteresis behavior of the endoprosthesis system to the hysteresis behavior of tissues. Many works are devoted to the advantages of manufacturing individual endoprostheses [2, 3]. Nevertheless, it seems unlikely to achieve a stable functionally and aesthetically satisfactory result after arthroplasty of extensive defects of the lower jaw in the absence of dental prosthetics. Fixation of jawbone fragments with a standard titanium plate and subsequent removable prosthetics should be considered a relatively satisfactory solution. The development and implementation of more durable and physiological structures is required. Currently, the development of CAD/CAM technologies allows the manufacture of individual implants for craniomaxillofacial prosthetics.

We present a clinical observation of the stages of planning and performing surgery that describes the method of manufacturing an individual endoprosthesis of the lower jaw, as well as the features of the patient's preoperative preparation.

CLINICAL CASE

Patient A., born in 1985. In history, drug addiction based on desomorphine and pervitin. 6 years кemission. In 2004, she was operated on in the city of Ukhta, a sequestrnecrectomy was performed, and the anterior teeth were removed in the lower jaw. In 2006, a second sequestrnecrectomy was performed, removal 43, 44. In 2009, "Konmet" serial reconstructive plate was installed in Ukhta. The patient addressed the clinic of maxillofacial surgery of the Sechenov First Moscow State Medical University. In February 2012, complaints of exposure of the reconstructive plate in the oral cavity, violation of chewing and speech, deformity of the face (Fig. 1). A sanitizing operation was performed, which consisted in the removal of the incompetent metal structure and revision of the pathological focus.

At the council, it was decided to make an individual endoprosthesis with the inclusion of support zones for subsequent prosthetics in order to restore the chewing function. Preliminarily, the erupted metal structure was removed, and inflammation was relieved. In September 2012, a surgical intervention was performed in the amount of endoprosthetics of the lower jaw.

***Preoperative planning**. The patient underwent multispiral computed tomography of the skull with volumetric reconstruction of the image, on which the subtotal defect of the lower jaw is determined, as well as the defect of the left maxillary bone with complete edentulousness in the second segment. Stereolithographic models were made according to MSCT data. A team of authors, together with engineers of the Konmet company, has developed*

Corresponding author: Pavel Petruk. Address: 2, buld. 4, Bolshaya Pirogovskaya str., Moscow, 119991, Russian Federation. Phone: (926) 275-91-75. E-mail: petruk_pavel@yahoo.com

an individual titanium endoprosthesis with shafts for implants [4]. The implants were fixed into the body of the endoprosthesis in the factory (Figs. 2, 3).

***Operation**. Typical submandibular incisions were made on the right and left, as well as a preauricular approach using the Bramley-Al-Kayat technique [5]. In the area of the preserved area of the lower jaw body, on the right and on the left, an osteotomy of the cortical layer was performed, a groove 2 mm wide was formed for laying the anterior part of the endoprosthesis fragment.*

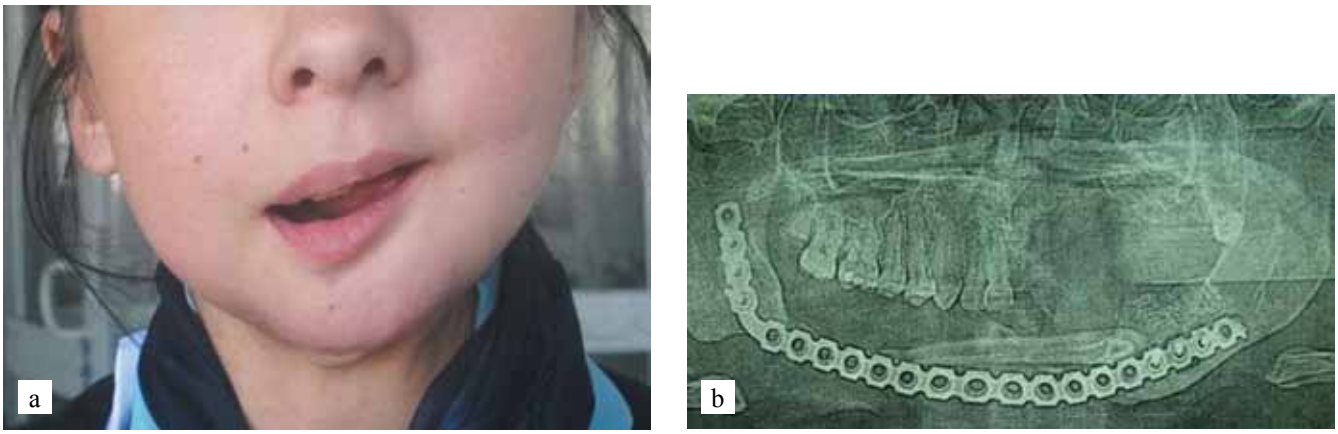

Fig. 1: a – appearance of the patient when applying to the clinic of maxillofacial surgery of the Sechenov First MSMU; b – orthopantomogram, condition after resection of the mandible and fixation the reconstructive plate of mass production

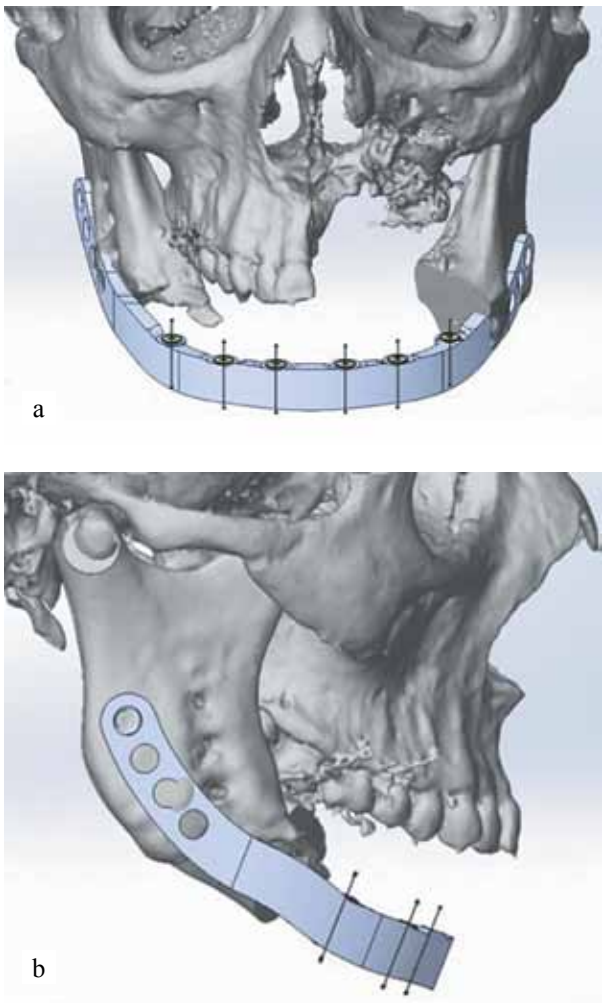

Fig. 2. Analysis of the virtual model of the visceral cranium. Modeling an individual endoprosthesis of the mandible

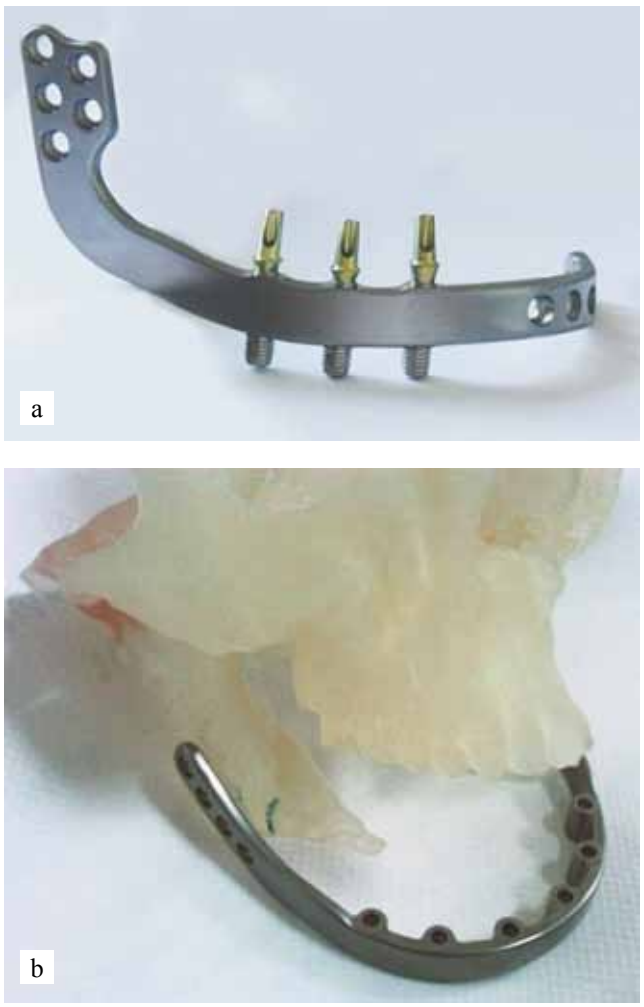

Fig. 3. Planning the stages of the operation. Fitting an individual endoprosthesis with supporting zones for dental implants on a stereo model

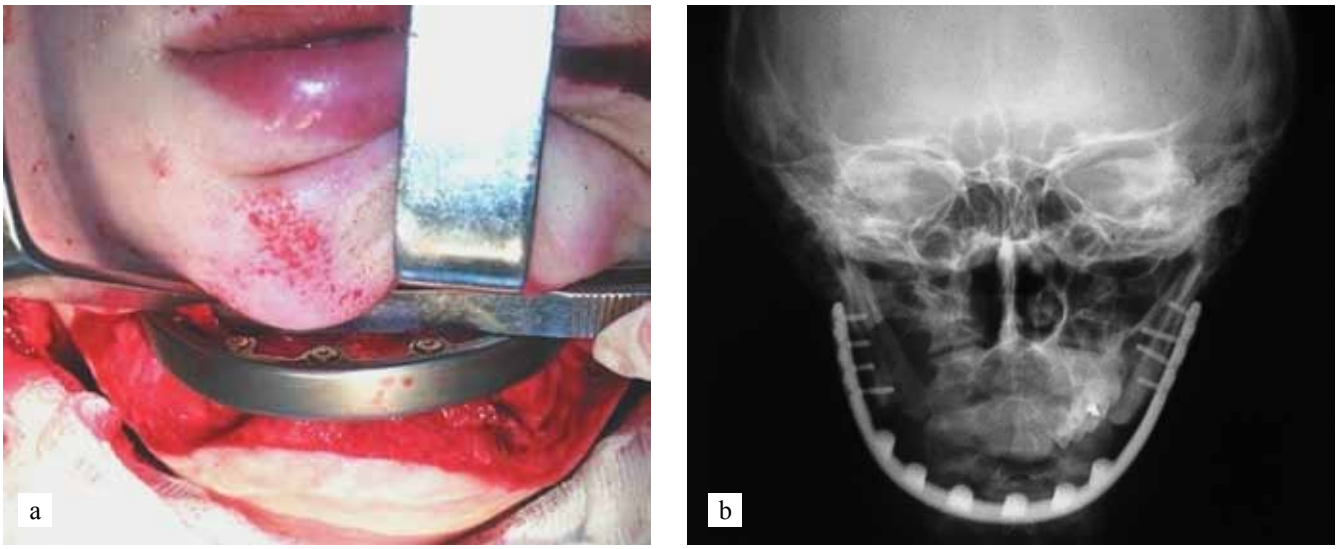

Fig. 4. Implantation and fixation of the endoprosthesis: a – stage of the surgery; b – postoperative roentgenogram

The endoprosthesis was installed and fixed with screws in the area of the corner and branch of the lower jaw on the right and left.

The wound was sutured in layers, latex drains were left for 2 days (Fig. 4). The patient underwent complex antibacterial, anti-inflammatory, symptomatic therapy.

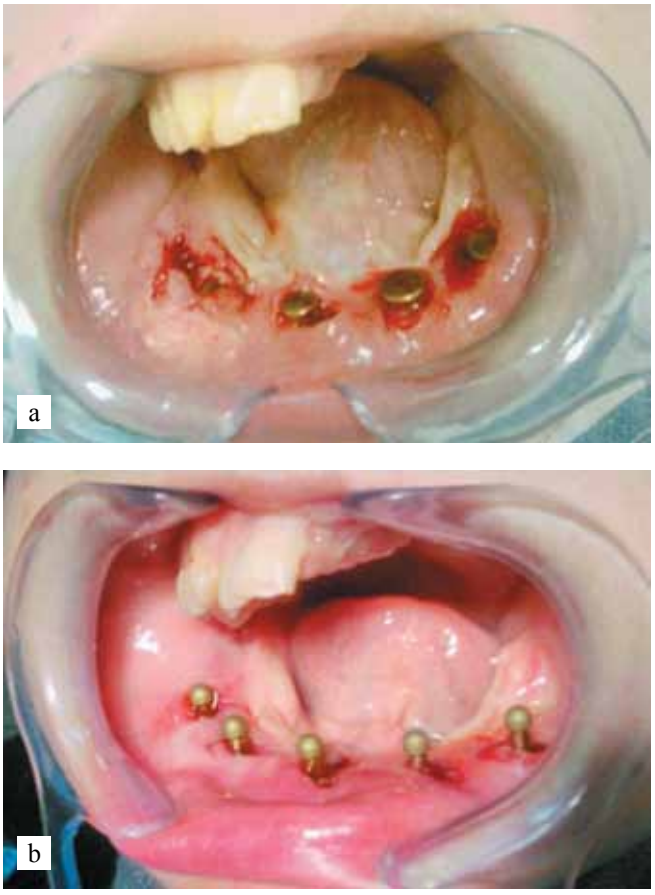

Fig. 5. The condition of the tissues in the oral cavity: a – gingival formers are installed; b – transfers are established to obtain a working impression of the mandible

The early postoperative period was uneventful. Wounds were healed by primary intention, without complications. Removal of sutures on the skin was performed on the 7th day, sutures in the oral cavity – after 14 days.

In 6 months, the gingival margin formers were installed. After 14 days, an impression was taken using transfers (Fig. 5). Prosthetics was performed with the manufacture of a conditionally removable prosthesis of a bar construction on individual abutments (Fig. 6, 7). The cosmetic and functional results were assessed as satisfactory by the specialists and the patient herself. The restoration of the shape and size of the lower jaw, the contours of the face in general, an increase in the amplitude of movements of the lower jaw were noted. A positive result persists for 6 years after the operation (Fig. 8).

The advantage of the endoprosthesis used is that after installation, it is completely covered with mucous membrane, and individual abutments are placed on a delayed basis. This fact reduces the risk of postoperative infection and increases the rate of healing.

***Recommendations**. After implantation of the endoprosthesis, the mucous membrane must be completely sutured to avoid infection. Impression taking and prosthetics should be delayed. After the end of the regeneration of the tissues surrounding the endoprosthesis, prosthetics can be performed using individual abutments. The flushing zone of the denture should be 1.8–2 mm to ensure satisfactory oral hygiene [6].*

DISCUSSION

One of the important anatomical features of the jaws is the presence of teeth that perform a number of functions, which imposes a certain specificity not only on the course of diseases of the maxillofacial region, but also on the approaches to their treatment and rehabilitation

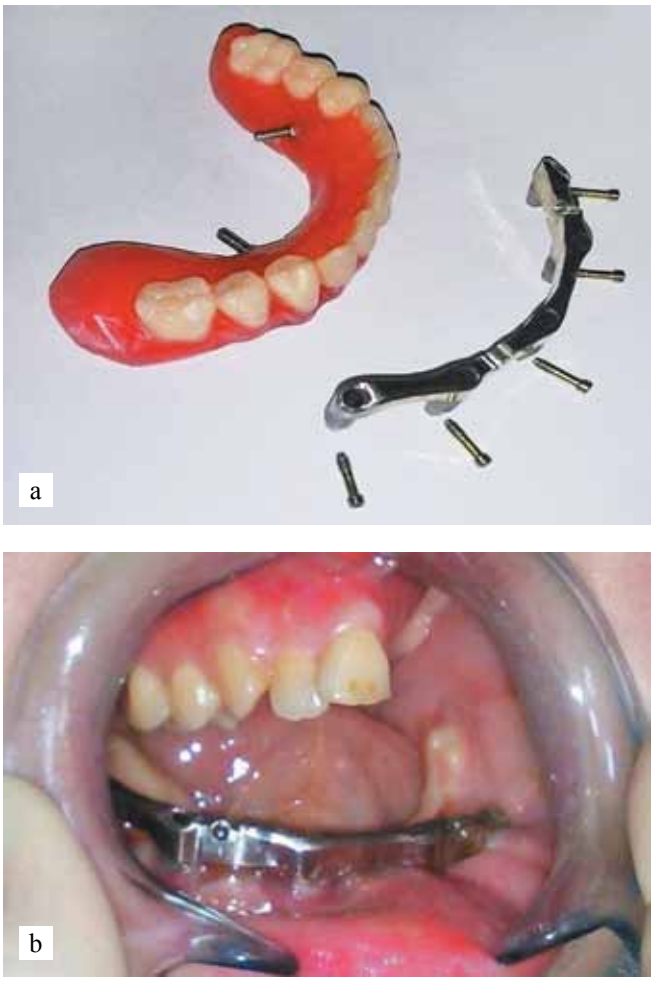

Fig. 6. Production of a conditionally removable denture on a beam construction

[7, 8]. Loss of a fragment of the lower jaw with the loss of the chewing function on the affected side leads to uneven work of the group of masticatory muscles with the development of secondary asymmetry of the face. In addition, additional trauma to the mucous membrane in the absence of dental prosthetics leads to the eruption of the endoprosthesis. In addition, the absence of antagonist teeth in the teeth of the opposite segment leads to a decrease in their functional load, the development of the Popov – Godon phenomenon [9], periodontal diseases and early loss of intact teeth. The absence of teeth leads to pathology of the temporomandibular joint (TMJ), which is one of the important organs involved in postural control of the human body [10].

D.A. Nikitin et al. [11] developed a clinical classification of defects in the bone structures of the lower jaw, considering the possibility of using the method of dental implantation in reconstructive operations. The authors identified three groups of patients. According to this classification, extensive defects of the lower jaw with disruption of its continuity in the frontal and lateral parts were attributed to the 3rd class.

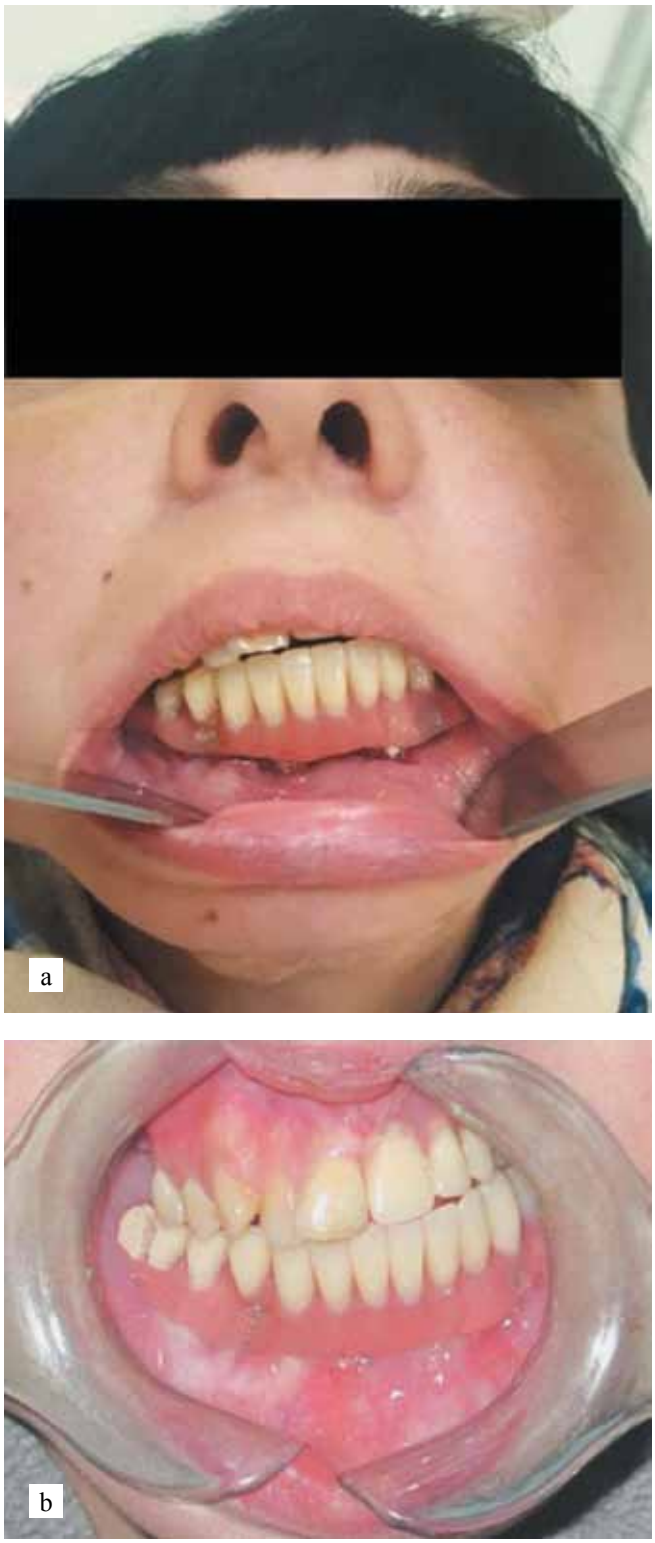

Fig. 7. Appearance of the patient after conditionally removable prosthetics

Currently, the most common reconstructive operations in patients with extensive acquired defects of the maxillofacial area (MFA) are performed using allografts, revascularized and nonvascularized autografts, endoprostheses. Based on the analysis of the properties of the above groups of grafts (Table), there is reason to

Table

Pros and cons of various reconstructive materials

Reconstructive material	Advantages	Disadvantages
Allograft	Does not require the creation of an additional operating field; there is a possibility of replacing combined defects of the face and jaws; the possibility of transplantation in patients with cancer in remission (more than five years) and in HIV-positive patients [12]	The need to create a bone bank [13], technological complexity, differences in the size and geometry of the donor site and the defect [14], it is impossible to exclude the possibility of infection of the recipient; ethics committee approval required
Nonvascularized autograft	Less technically complex and costly operation compared to the use of a vascularized graft, there are more sites to choose; reducing the risk of graft rejection	Donor site trauma; limited available volume for sampling [15]; resorption [16, 17]; it is not always possible to make up for an extended defect [14]; risk of infection [18]
Revascularized autograft	Possibility of replacing extended jaw defects (up to 8 cm); used after radiation therapy and in soft tissues with cicatricial changes; the possibility of implantation (there are both positive and negative results) [18, 19]; preventing the risk of graft rejection	Injury of the donor site, expensive equipment and high qualification of the surgeon are required, it is not always possible to fill the defect; long operation time; the need for two specialized surgical teams; morbidity; longer hospital stay [20–23]
Endoprosthesis	Does not require the creation of an additional operating field; the ability to manufacture an individual endoprosthesis with pre-calculated optimal geometric parameters, which can significantly reduce the operating time; the possibility of prosthetics when using an endoprosthesis with support zones	Fracture of the fixing part of the endoprosthesis, intrusion of its head into the cavity of the middle cranial fossa during arthroplasty; eruption [24]; risk of infection or infection; the thickness of the endoprosthesis, which does not provide a sufficient volume of reconstruction [14]; material fatigue, which imposes restrictions on the duration of operation

Fig. 8. Oral cavity examining (September 2019)

believe that endoprosthetics is one of the most promising techniques.

Most authors positively assess the experience of using endoprostheses of the lower jaw, emphasizing its prospects [7, 24]. In cases of removal of the TMJ with the M branch as a single block, one should not forget about the preservation of the above function in the intact joint. It should be noted that the use of the temporal bone glenoid fossa prosthesis prevents the recurrence of ankylosis and the penetration of the articular head of the endoprosthesis into the cavity of the middle cranial fossa [25].

Historically, for M and temporomandibular joint (TMJ) arthroplasty, alloys resistant to corrosion in body fluids have been used: stainless steel, an alloy of cobalt (vitalium), chromium, molybdenum, and tantalum [26]. The most popular were endoprostheses of the Vitalium M branch, proposed by B.S. Freeman (1948) [27]. In subsequent years, materials from titanium and its alloys were actively introduced into medical practice. In particular, R.W. Christensen (2004) developed numerous variants of titanium prostheses, described the methods of surgical interventions for prosthetics of the glenoid cavity and the M branch [2].

Positive properties of titanium and its alloys include high biocompatibility; bioinertness in body tissues; corrosion resistance due to the formation of an oxide film that is stable in the environment of the body; modulus of elasticity close to the modulus of elasticity of the bone; non-magnetic; low thermal conductivity; low coefficient of linear expansion; no clinically significant toxicity [28]. In addition, experimental experimental studies on animals have shown that titanium structures are more resistant to fatigue loading compared to other materials [7].

Nevertheless, the development and introduction into clinical practice of more advanced material [28, 29] does not exclude the development of both early and late complications, which can be associated, among other reasons, with the insufficient physiological nature of the replacement construct.

According to the specialized literature, the most optimal current method of rehabilitation in patients with partial and complete edentulousness in patients is dental implantation [30]. Nevertheless, this method of restoration of the dentition is, for obvious reasons, practically impracticable during a standard metal endoprosthesis [31]. Based on the anatomical, functional and aesthetic significance of M, we can say that the operation to implant the proposed metal structure is equivalent to the creation of an artificial organ, which is especially important for maintaining an acceptable standard of living for the patient.

CONCLUSION

Thus, due to the proposed technique, it is possible to solve the main tasks of reconstructive surgery in patients with extensive defects of the lower jaw: to restore functions, as well as to recreate the facial aesthetics as closely as possible, which, in turn, has a significant effect on the patient's quality of life. This clinical case clearly demonstrates that the use of an individual endoprosthesis of the lower jaw with integrated dental implants, followed by the manufacture of a conditionally removable orthopedic structure, allows to obtain a predictable stable result and is quite promising in terms of patient rehabilitation.

The authors declare no conflict of interest.

REFERENCES

1. *Goiato MC, Ribeiro AB, Dreifus Marinho ML.* Surgical and prosthetic rehabilitation of patients with hemimandibular defect. *J Craniofac Surg*. 2009; 20: 2163–2167. doi: 10.1097/scs.0b013e3181bf014a.
2. *Christensen RW.* The History of the Christensen Mandibular end TMJ Alloplastic Reconstruction. *TM Journal*. 2004; 3 (6): 1–19.
3. *Muraev AA, Ivanov SYu, Ivashkevich SG, Gorshenev VN, Teleshev AT, Kibardin AV et al*. Orthotopic bone implants for bone regeneration. *Stomatologiya*. 2017; 96 (3): 36–39. [In Russ, English abstract]. doi: 10.17116/stomat201796336-39.
4. Patent RU 146000 U1, Ustrojstvo dlya ustraneniya defektov i deformacij kosti nizhnej chelyusti na osnove ispol'zovaniya modeli licevoj chasti cherepa s vklyuchenny'mi v nee dental'ny'mi implantatami dlya ustraneniya funkcional'nogo i kosmeticheskogo defektov, 2014.03.05, Shaikhaliev A.I. et al. Available at: https://yandex.ru/patents/doc/RU146000U1_20140927.
5. *Braimah R, Taiwo A, Ibikunle A, Oladejo T, Adeyemi M, Adejobi F, Abubakar S.* Clinical experience in managing temporomandibular joint ankylosis: five-year appraisal in a Nigerian subpopulation. *Journal of the Korean Association of Oral and Maxillofacial Surgeons*. 2018; 44 (3): 112. doi: 10.5125/jkaoms.2018.44.3.112.
6. *Nikolskiy VD, Zhuruli GN, Tsalikova NA.* Vybor konstruktsii protezov pri protezirovanii na zubnykh implantatakh pri polnoy adentii. *Stomatologiya dlya vsekh*. 2015; 4: 48–52. [In Russ, English abstract].
7. *Sirak SV, Sletov AA, Elizarov AV, Meboniya TT, Arutyunov AV*. Rekonstruktsiya obyemnykh defektov nizhney chelyusti s pomoshchyu implantata-endoproteza. *Meditsinskiy vestnik Severnogo Kavkaza*. 2014; 9 (1): 87–91. [In Russ, English abstract]. doi: /10.14300/mnnc.2014.09024.
8. *Bak M, Jacobson AS, Buchbinder D, Urken ML.* Contemporary reconstruction of the mandible. *Oral Oncol*. 2010; 46: 71–76. doi: /10.1016/j.oraloncology.2009.11.006.
9. *Akhmedova NA.* Analiz zubochelyustnykh narusheniy u patsiyentov s chastichnoy vtorichnoy adentiyey i patsiyentov bez narusheniya tselostnosti zubnykh ryadov. *Nauka molodykh – Eruditio juvenium*. 2018; 6 (3): 347–353. [In Russ, English abstract].
10. *Carlson JE.* Physiologic occlusion. MidWest Press; 2009.
11. *Nikitin DA, Mirgazizov MZ, Nikitin AA*. Lecheniye i reabilitatsiya bolnykh posle kostno-rekonstruktivnykh i vosstanovitelnykh operatsiy na nizhney chelyusti s ispolzovaniyem endoprotezirovaniya i dentalnykh implantatov. *Almanakh klinicheskoy meditsiny*. 2011; 24: 15–21. [In Russ, English abstract].
12. *Kasiske BL, Cangro CB, Hariharan S et al.* The evaluation of renal transplant candidates: clinical practice guidelines. *Am J Transplant*. 2001; 2 (Suppl 1): 5–95. doi: 10.1034/j.1600-6143.2001.0010s2001.x.
13. *Rochanawutanon S, Suddhasthira S, Pairuchvej V, Vajaradul Y.* Long term follow-up of reconstruction with allogeneic mandibular bone crib packed with autogenous particulate cancellous bone marrow. *Cell and Tissue Banking*. 2002; 3 (3): 183–197. doi: 10.1023/a:1023602717328.
14. *Bayat M, Naji S, Motlagh M.* Bone Allograft: An Option for Total Mandibular Reconstruction. *Craniomaxillofacial Trauma & Reconstruction*. 2017; 10 (04): 306–313. doi: 10.1055/s-0036-1593474.
15. *Rocchietta I, Simion M, Hoffmann M, Trisciuoglio D, Benigni M, Dahlin C.* Vertical bone augmentation with an autogenous block or particles in combination with guided bone regeneration: A clinical and histological preliminary study in humans. *Clin Implant Dent Relat Res*. 2016; 18: 19–29. doi: 10.1111/cid.12267.
16. *Toker H, Ozdemir H, Ozer H, Eren K.* Alendronate enhances osseous healing in a rat calvarial defect model. *Arch Oral Biol*. 2012; 57: 1545–1550. doi: 10.1016/j.archoralbio.2012.06.013.
17. *Li P, Honda Y, Arima Y, Yasui K, Inami K, Nishiura A, Hashimoto Y, Matsumoto N.* Interferon-γ enhances the efficacy of autogenous bone grafts by inhibiting postoperative bone resorption in rat calvarial defects. *J Prosthodont*. 2016; 60: 167–176. doi: 10.1016/j.jpor.2016.01.002.

18. *Khachatryan L, Khachatryan G, Hakobyan G.* The Treatment of Lower Jaw Defects Using Vascularized Fibula Graft and Dental Implants. *J of Craniofacial Surgery*. 2018: 1. doi: 10.1097/scs.0000000000005015.
19. *Anne-Gaelle B, Samuel S, Julie B et al.* Dental implant placement after mandibular reconstruction by microvascular free fibula flap: current knowledge and remaining questions. *Oral Oncol*. 2011; 47: 1099–1104. doi: 10.1016/j.oraloncology.2011.07.016.
20. *Van Germet JT, Van Es RJ, Van Cann EM, Koole R.* Non-vascularized bone grafts for segmental reconstruction of the mandible – a reappraisal. *J Oral Maxillofac Surg*. 2009; 67: 1446–1452. doi: 10.1016/j.joms.2008.12.052.
21. *Van Germet JT, Van Es RJ, Rosenberg AJ, Van der Bilt A, Koole R, Van Cann EM.* Free vascularized flaps for reconstruction of the mandible: complications, success, and dental rehabilitation. *J Oral Maxillofac Surg*. 2012; 70: 1692–1698. doi: 10.1016/j.joms.2011.08.024.
22. *Desai SC, Sclaroff A, Nussenbaum B.* Use of recombinant human bone morphogenetic protein 2 for mandible reconstruction. *JAMA Facial Plast Surg*. 2013; 15: 204–209. doi: 10.1001/jamafacial.2013.650.
23. *Tatara AM, Kretlow JD, Spicer PP, Lu S, Lam J, Liu W et al*. Autologously Generated Tissue-Engineered Bone Flaps for Reconstruction of Large Mandibular Defects in an Ovine Model. *Tissue Engineering, Part A*. 2012; 21 (9–10): 1520–1528. doi: 10.1089/ten.tea.2014.0426.
24. *Kropotov MA, Sobolevskij VA, Dikov YuYu, Yakovleva LP, Lysov AA.* Rekonstrukciya visochno-nizhnechelyustnogo sustava pri segmentarnoj rezekcii nizhnej chelyusti s ekzartikulyaciej po povodu pervichnyh i vtorichnyh opuholej nizhnej chelyusti. *Al'manah klinicheskoj mediciny*. 2017; 45 (6): 486–94. [In Russ, English abstract].
25. *Dikov YuYu, Yakovleva LP, Lysov AA.* Temporomandibular joint's reconstruction after segmental mandibulectomy in patients with primary and secondary tumors of the mandible. *Journal Almanac of Clinical Medicine*. 2017; 45 (6): 486–494. [In Russ, English abstract]. doi: 10.18786/2072-0505-2017-45-6-486-494.
26. *Sysolyatin PG, Sysolyatin SP, Baydik OD, Ilyenok OV.* Istoriya razvitiya khirurgii visochno-nizhnechelyustnogo sustava. *Byulleten sibirskoy meditsiny*. 2016; 15 (2): 98–111. [In Russ, English abstract].
27. *Freeman BS.* The use of vitallium plates to maintain function following resection at the mandible. *Plastic Reconstr Surg*. 1948; 10 (1): 985. doi: 10.1016/0030-4220(48)90126-1.
28. *Trofimov VV, Fedchishin OV, Klimenov VA*. Titan, splavy titana i ikh primeneniye v stomatologii. *Sibirskiy meditsinskiy zhurnal*. 2009; 90 (7): 10–12. [In Russ, English abstract].
29. *Epifanov SA, Polyakov AP, Skuredin VD*. Protezirovaniye visochno-nizhnechelyustnogo sustava. *Vestnik Natsionalnogo mediko-khirurgicheskogo tsentra im. N.I. Pirogova*. 2014; 9 (4): 17–22. [In Russ, English abstract].
30. *Aliyev A.M.* Obosnovaniye primeneniya dentalnoy implantatsii v komplekse lecheniya patsiyentov s defektami zubnykh ryadov (obzor literatury). *Molodoy uchenyy*. 2016; 26 (130): 193–196. [In Russ, English abstract].
31. *Hayden RE, Mullin DP, Patel AK.* Reconstruction of the segmental mandibular defect: current state of the art. *Curr Opin Otolaryngol Head Neck Surg*. 2012; 20: 231–236. doi: 10.1097/moo.0b013e328355d0f3.

The article was submitted to the journal on 15.05.2020

DOI: 10.15825/1995-1191-2020-3-123-133

EXPERIMENTAL APPROACHES TO CREATING A TISSUE-SPECIFIC MATRIX FOR A BIOARTIFICIAL LIVER

A.M. Grigoriev[1], Yu.B. Basok[1], A.D. Kirillova[1], L.A. Kirsanova[1], N.P. Shmerko[1], A.M. Subbot[2], E.A. Nemets[1], I.A. Miloserdov[1, 3], M.Yu. Shagidulin[1, 3], V.I. Sevastyanov[1]

[1] Shumakov National Medical Research Center of Transplantology and Artificial Organs, Moscow, Russian Federation

[2] Research Institute of Eye Diseases, Moscow, Russian Federation

[3] Sechenov University, Moscow, Russian Federation

Shortage of donor organs for liver transplantation in the treatment of end-stage liver disease dictates the need to develop alternative methods that include technologies on tissue engineering and regenerative medicine. **Objective:** to study the ability of a tissue-specific matrix from decellularized human liver fragments (DHLF) to maintain adhesion and proliferation of human adipose tissue-derived mesenchymal stem cells (hAT-MSCs) and HepG2 under static conditions and in a flow-through bioreactor. **Materials and methods**. Treatment with surfactants (SAS) – sodium dodecyl sulfate, Triton X-100 – followed by exposure to DNase was used for decellularization of human liver fragments (no more than 8 mm^3). Biochemical screening included the determination of DNA quantity in the test samples. Efficiency of surfactant washing was assessed by the cytotoxicity of the matrix in the NIH 3T3 fibroblast culture. Viability and metabolic activity of cells were assessed via vital staining with a complex of fluorescent dyes LIVE/DEAD® and PrestoBlue™ (Invitrogen, USA). Morphological examination of the liver cell-engineered constructs was carried out through histological staining and scanning electron microscopy with lanthanide contrast. **Results.** It was shown that the liver decellularization method used allows to obtain a biocompatible matrix with a residual DNA quantity <1%, which is capable of maintaining adhesion and proliferation of hAT-MSCs and HepG2. On day 7 of cultivation in the bioreactor, there was formation of a single conglomerate of the DHLF matrix with numerous groups of viable cells with a high nuclear-cytoplasmic ratio. The urea content in the culture medium is 1.5 ± 0.1 mmol/L, exceeding that of samples obtained under static conditions. This indicates the metabolic activity of HepG2 in the composition of the obtained culture systems. It was shown that constant flow of the culture medium in the perfusion bioreactor increased the proliferative activity of HepG2 and allowed to provide a more uniform colonization by matrix cells in comparison with static cultivation conditions. **Conclusion.** The conditions for uniform colonization of DHLFs in a flow-through bioreactor with cell cultures were established. The ability of the matrix to maintain adhesion and proliferation of hADSCs and HepG2 for 11 days indicates that it could be used in liver tissue engineering.

Keywords: liver, decellularization, mesenchymal stem cells, HepG2, cell-engineered construct, tissue engineering, bioreactor.

INTRODUCTION

Shortage of donor organs for liver transplantation in the treatment of terminal stages of liver failure dictates the need to develop alternative methods, which include technologies of tissue engineering and regenerative medicine [1, 2].

Tissue decellularization is a promising method for creating matrices for regenerative medicine due to the removal of immunogenic factors (DNA, galactose-α-1,3-galactose) and preservation of morphology that is largely specific for organs and tissues and the natural extracellular matrix (ECM), which includes the necessary sites for adhesion, migration and proliferation of cells [3, 4].

Tissue decellularization is a promising method for creating matrices for regenerative medicine due to the removal of immunogenic factors (DNA, galactose-α-1,3-galactose) and preservation of morphology that is largely specific for organs and tissues and the natural extracellular matrix (ECM), which includes the necessary sites for adhesion, migration and proliferation of cells [3, 4].

Significant progress has now been achieved in decellularization of the whole liver by perfusion with surface acting agent (SAA) solutions [5, 6]. The attractiveness of this method of decellularization lies in the potential for obtaining whole organs when populated with cells using perfusion and transplantation of the obtained tissue-engineered structures in vivo by creating anastomoses with preserved vascular structures [7, 8]. However, decellularization of the whole liver has a number of disadvantages: low efficiency of removal of cells and

Corresponding author: Alexey Grigoriev. Address: 1, Shchukinskaya str., Moscow, 123182, Russian Federation. Phone: (499) 193-86-62. E-mail: Bear-38@yandex.ru

their fragments and recellularization due to microcirculation disorders and the difficulty of transporting sufficient amounts of oxygen and nutrients to cells in the thickness of the organ. In this regard, the most rational approach seems to be the decellularization of not the whole organ, but its fragments. Earlier, we developed a method for decellularization of human liver fragments, which made it possible to obtain a matrix with a complete absence of cellular debris and a preserved tissue structure [9]. Note that the interaction of cells with the resulting tissue-specific matrix has not been studied.

The inherent immunomodulatory properties of mesenchymal stromal cells (MSC), the ability to stimulate regeneration, and the ability to differentiate into hepatocyte-like cells indicate the possibility of their use for creating cellular engineering structures (CES) of the liver for the treatment of various liver diseases [10]. Due to the complexity of expansion and low viability of primary hepatocytes during in vitro cultivation, it is advisable to use cell lines capable of performing functions characteristic of liver cells to study the interaction of specialized cells with fragments of decellularized liver [11]. Note that although the metabolic functions of hepatocellular carcinoma HepG2 cells are limited compared to primary hepatocytes, their use as an in vitro hepatocyte model is due to the availability of HepG2, ease of handling, almost unlimited lifespan and phenotype stability [12].

It is known that to create the conditions closest to natural during *in vitro* cultivation, bioreactors are used, which make it possible to improve cell nutrition, transport gases to them, and excretion of metabolic products due to constant circulation of the culture medium [13]. Nevertheless, the cultivation of cells in a flow is not without drawbacks associated with mechanical damage to cells, high consumption of culture media, and the difficulty of maintaining aseptic conditions during long-term experiments.

The purpose of the present study was to study the ability of tissue-specific matrix from decellularized fragments of human liver (DFHL) to maintain adhesion and proliferation of MSC HGT and HepG2 under static conditions and in a flow-through bioreactor.

MATERIALS AND METHODS

A donor human liver wasused, washed according to the traditional method from blood elements with a Custodiol solution (Dr. F. Koehler Chemie GmbH, Germany). The liver was not suitable for transplantation due to severe fatty hepatosis (more than 40%). The washed liver or part of it was placed in sterile saline, if steatosis was detected before washing the vascular bed, or in the preservative Custodiol, if the presence of pronounced fatty infiltration was determined after removing blood elements from the liver.

Fragments of the liver (no more than 2 × 2 × 2 mm) were obtained using a scalpel and scissors. Decellularization of human liver fragments was carried out in three changes of phosphate-buffered saline (PBS) (138 mM NaCl, 2.67 mM KCl, 1.47 mM KH_2PO_4, 8.1 mM Na_2HPO_4, pH = 7.4) containing 0.1 % sodium dodecyl sulfate (SDS) and an increasing concentration of Triton X-100: 1%, 2% and 3% [9]. The total time of decellularization was 72 hours – 24 hours for each change of SAA solution with stirring on a magnetic stirrer.

Then, fragments of human liver were treated in a solution of DNase I type (New England Biolabs Inc., USA). Matrix samples with a volume of 0.5 ml were placed in 1.0 ml of 10 mM Tris-HCl buffer solution (pH 7.6) containing 2.5 mM $MgCl_2$, 0.5 mM $CaCl_2$ and 50 U/ml DNase I and incubated for 48 h at 37 °C.

Washing DFHL from SAA included an exposure of the matrix in PBS containing an antibiotic (ampicillin, 20 μg/ml) and an antimycotic (amphotericin B, 2.0 μg/ml) for 96 h, followed by sterilization of the samples by γ-irradiation (1.5 Mrad).

The residual DNA content was an indicator of the cellular components preserved in the DFHL samples, which carry the bulk of the antigens that cause the reaction of the xenogenic matrix rejection. The DNeasy Blood & Tissue Kit (QIAGEN, Germany) was used to isolate DNA from the original and decellularized tissue according to the manufacturer's protocol. Samples of the original human liver (n = 3) and DFHL (n = 3) weighing 10 mg were lysed using lysis buffer and proteinase K for 16 hours at +56 °C. For the quantitative determination of DNA in the samples, the fluorescent dye ™Picogreen Quant-iT (Invitrogen, USA) was chosen.

The source of MSC HGT was the subcutaneous adipose tissue of a healthy donor taken from him with informed voluntary consent. A sample of subcutaneous adipose tissue was crushed with a scalpel, washed twice with cold (+4 … +6 °C) Hanks solution, and then incubated in a 0.1% type I collagenase solution (Gibco, USA) at 37 °C for 20 min. Then the resulting suspension was sequentially passed through cell sieves with a pore diameter of 100 and 70 μm.

All cells were precipitated by centrifugation, resuspended in complete growth medium (ORS) of DMEM/F12 composition (1:1) supplemented with 10% fetal bovine serum, 100 U/ml penicillin, 100 μg/ml streptomycin sulfate, and 2 mM L-glutamine (Gibco, USA) and cultured until the formation of a monolayer, changing the medium 2 times a week. The cells were transferred into suspension by treatment with a Versene solution at 37 °C for 1 min, followed by the addition of TrypLe™ dissociating agent (Invitrogen, USA). For experiments, cells of the 3rd passage were taken.

Human hepatocellular carcinoma cell culture HepG2 was obtained from the laboratory collection of cell cultures of the Department of Biomedical Technologies and Tissue Engineering of the Shumakov National Me-

dical Research Center of Transplantology and Artificial Organs.

The cytotoxicity of the matrix samples was studied in accordance with GOST ISO 10993-5-2011 [14] by the method of direct contact of the samples with the culture of mouse fibroblasts of the NIH 3T3 line obtained from the collection of transplanted somatic vertebrate cells of the D.I. Ivanovsky Research Institute of Virology.

Mouse fibroblasts were seeded in cultured flat-bottom 6-well plates and incubated for 24 hours at 37 °C under standard conditions in a humid atmosphere containing (5 ± 1)% CO_2. The samples under study were placed on the surface of the formed (80 ± 10)% monolayer of cells. After a day of incubation, the morphology and lysis of cells were visually assessed according to a standard technique using a Nikon Eclipse TS100 biological microscope (Nikon, Japan). The negative control was general nutrient medium containing fetal bovine serum, the positive control was a standard solution of zinc in nitric acid (9.95 mg Zn in 1–2 wt.% HNO_3, dilution 1:200 with 0.9% NaCl solution for injection).

HepG2 and MSC HGT were cultured according to the standard method to a monolayer confluence of 70–80%, after which they were washed off the plastic using Versene solution and TrypLe™ reagent (Invitrogen, USA) and a working cell suspension was prepared in general nutrient medium with a concentration of 1 × 105 cells/ml. Cell counting and assessment of their viability were performed on a TS20 cell counter (BioRad, USA) according to the manufacturer's method.

Matrix pellets (30 mg) were thawed and placed in ORS for a day at room temperature. DFHL cells were additionally washed twice with fresh ORS before plating. An aliquot of the cell suspension was added to each DFHL tube to populate the matrix. The tubes were placed in a rack and shaken on a MultiBio 3D laboratory shaker (Biosan, Latvia) in a reciprocal platform rotation mode at 80 rpm for 2 hours to evenly distribute the cells over the matrix surface. Then the tubes were placed in an incubator and cultured under standard conditions.

The viability and adhesion of cells were assessed by the method of in vivo staining with a complex of LIVE/DEAD® fluorescent dyes (Invitrogen, USA). This complex includes two components: calcein AM gives green fluorescence of living cells, recorded at a wavelength of 515 nm, ethidium homodimer-1, penetrating through the damaged cell membrane and binding to DNA, gives red fluorescence at 635 nm. Microscopy was performed on a Nikon Ti fluorescence microscope (Nikon, Japan).

Determination of the metabolic activity of cells was performed by the test with a PrestoBlue™ reagent (Invitrogen, USA) according to the manufacturer's instructions. Spectrophotometric analysis was performed on a Tecan Spark10 plate reader (Tecan, Austria). In the study of metabolic activity, 5 × 104 HepG2 cells or 2 × 104 MSC HGT were applied to each DFHL pellet. The absorbance data were used to calculate the metabolic activity coefficient (K) by the formula:

$$K = \frac{117.216 \times Abs_{570} - 80.586 \times Abs_{600}}{155.677 \times Abs_{600} - 14.652 \times Abs_{570}} \times 100\%,$$

Where Abs_{570} – absorption at 570 nm wavelength; Abs_{600} – absorption at 600 nm wavelength.

When creating CES, 1 × 105 HepG2 cells or 1 × 105 MSC HGT were applied to 1 DFHL pellet. To carry out experiments on the cultivation of HepG2 on DFHL under flow conditions, a modified version of the perfusion bioreactor was used [13]. The flow rate was 0.02 ml/min. On the 7th day, the culture chamber with CES was removed from the bioreactor.

The following types of samples were studied: a fragment of a native human liver, a fragment of a decellularized human liver, CES – MSC HGT, cultured on a decellularized liver fragment.

The morphology of the surface and the nearest subsurface layer of the samples was studied jointly with the staff of the Laboratory of Basic Research in Ophthalmology of the Research Institute of Eye Diseases by scanning electron microscopy (SEM) using lanthanide contrasting.

The preparation of water-containing samples for SEM with deposition of a conductive layer requires their dehydration, which leads not only to structural changes in such objects, but also poor visualization of cellular elements. The lanthanide contrasting method makes it possible to observe non-fixed biological samples in a low vacuum mode after holding them in a saturated solution of a rare earth metal. At the same time, the maximum native state of the object under study is preserved, and the image obtained in the backscattered electron detection mode carries extended information on the cellular structures [15].

The processing protocol included initial washing, holding for 45 min in a BioREE contrast solution (Glaucon LLC, Russia) and final washing with distilled water. After contrasting, excess moisture was removed from the sample surface with an air brush and placed on the stage of an EVO LS10 microscope (Zeiss, Germany). The observations were carried out in a low vacuum mode (EP, 70 Pa), at an accelerating voltage of 20 kV.

For morphohistological studies, the initial and decellularized samples were prepared according to the standard technique, stained with hematoxylin and eosin, and according to Masson's method. The analysis and photography of the obtained preparations were performed using a Nikon eclipse microscope (Nikon, Japan) equipped with a digital camera.

The concentration of glucose and urea was determined using a KonelabPrime 60i biochemical analyzer (Thermo Fisher Scientific, Finland).

Statistical data processing was performed with a standard Microsoft Excel software.

RESULTS AND DISCUSSION

We have previously shown that decellularization of human liver fragments using SAA allows removing cellular debris and preserving the tissue structure [9]. However, when determining the amount of DNA in DFHL, it was found that the process of chemical decellularization led to the removal of only 69.5 ± 3.6% of the DNA (Fig. 1). Note that during liver decellularization, it is recommended to keep no more than 10% of the amount of DNA in the original tissue [16]. In this regard, an additional stage was introduced into the decellularization protocol after SAA treatment, which included exposure of DFHL in DNase I solution. As can be seen from Fig. 6, DNase treatment made it possible to reduce the residual amount of DNA in the decellularized sample to 3.6 ± 0.6 ng/mg tissue (less than 1%), which indicates good decellularization, and, accordingly, low immunogenicity of the resulting matrix [17].

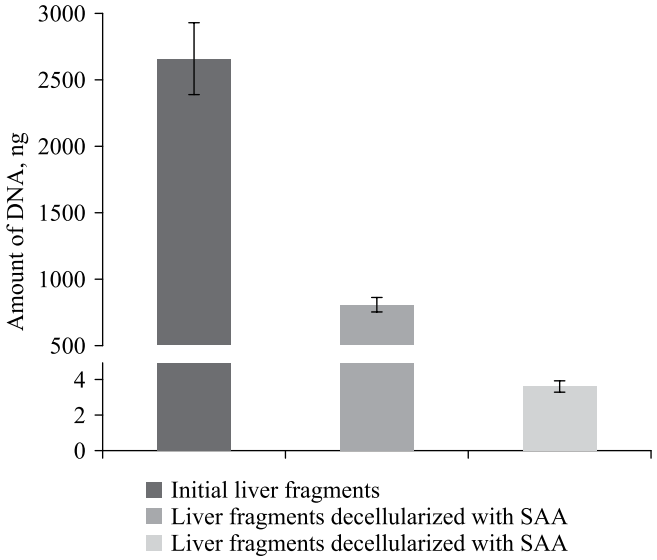

Fig. 1. Amount of DNA in the original and decellularized fragments of the human liver

The study of cytotoxicity by the direct contact method on mouse fibroblasts of the NIH/3T3 line did not reveal manifestations of the cytotoxic effect of the hepatic matrix during the study time of 24 hours. The dynamics of cell growth did not practically differ in the experimental and control variants. No areas of cell lysis were observed under the sample or in the contact area of the sample with cells. A trypan blue viability test performed after 24 hours of cell contact with samples also showed no cytotoxic effect. Based on the data obtained, it was concluded that the protocol for washing the matrix from SAA was effective and that DFHL was not cytotoxic.

The absence of matrix cytotoxicity made it possible to proceed to the study of the viability and proliferative activity of MSC HGT on the DFHL surface. It was shown by the method of intravital fluorescence microscopy that although some of the cells are in a suspension state in the culture medium, most of the cells successfully attach to the matrix surface and proliferate already on the 3rd day of the experiment (Fig. 2, a). At the beginning of the experiment, cells are unevenly distributed over the surface of the matrix – first of all, active collonization of the DFHL marginal zones occurs. Then the cells migrate into the volume of the matrix, forming a cellular network, and then continuous sections of dense cell layers (Fig. 2, b).

Fig. 3 shows the results of SEM studies of native and decellularized human liver, as well as CES, including MSC HGT, cultured on decellularized fragments of human liver for 7 days.

As seen in micrographs (Fig. 3, a, b), the native tissue significantly differed in surface structure from the decellularized one. The original fabric had a continuous relief surface. After removing the cells, the matrix acquired a porous structure. The pore boundaries were an interweaving of numerous micro- and nanofibers. The pore size was heterogeneous: there were both small pores

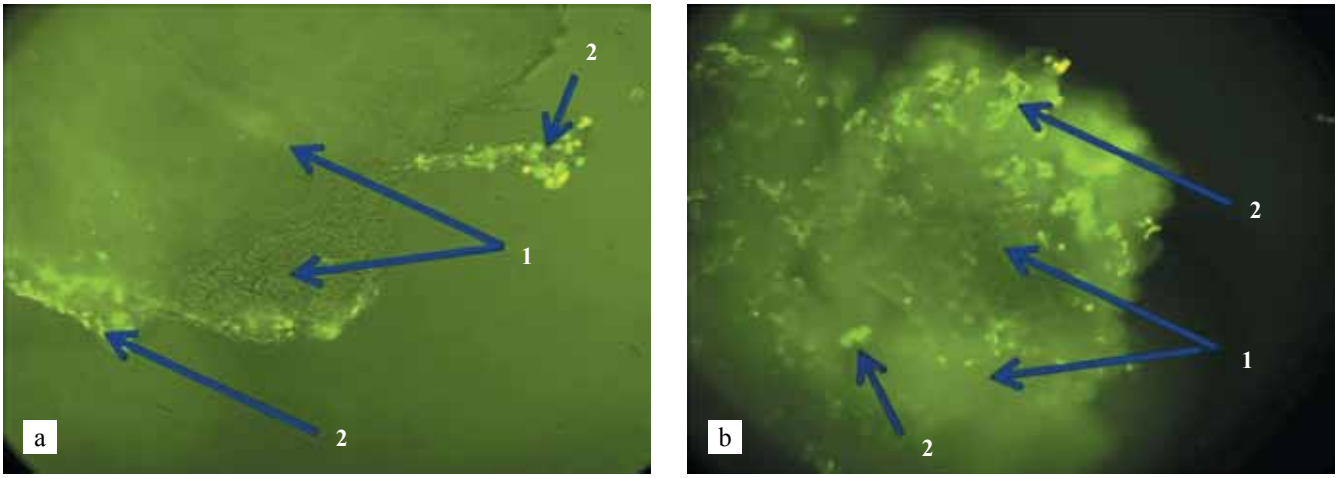

Fig. 2. Viability of MSC HAT on the surface of the: a – 3 days of cultivation; b – 7 days of cultivation; 1 – the surface of the DPHL; 2 – the MSC HAT. Coloring with Live/Dead fluorescent dyes. ×40

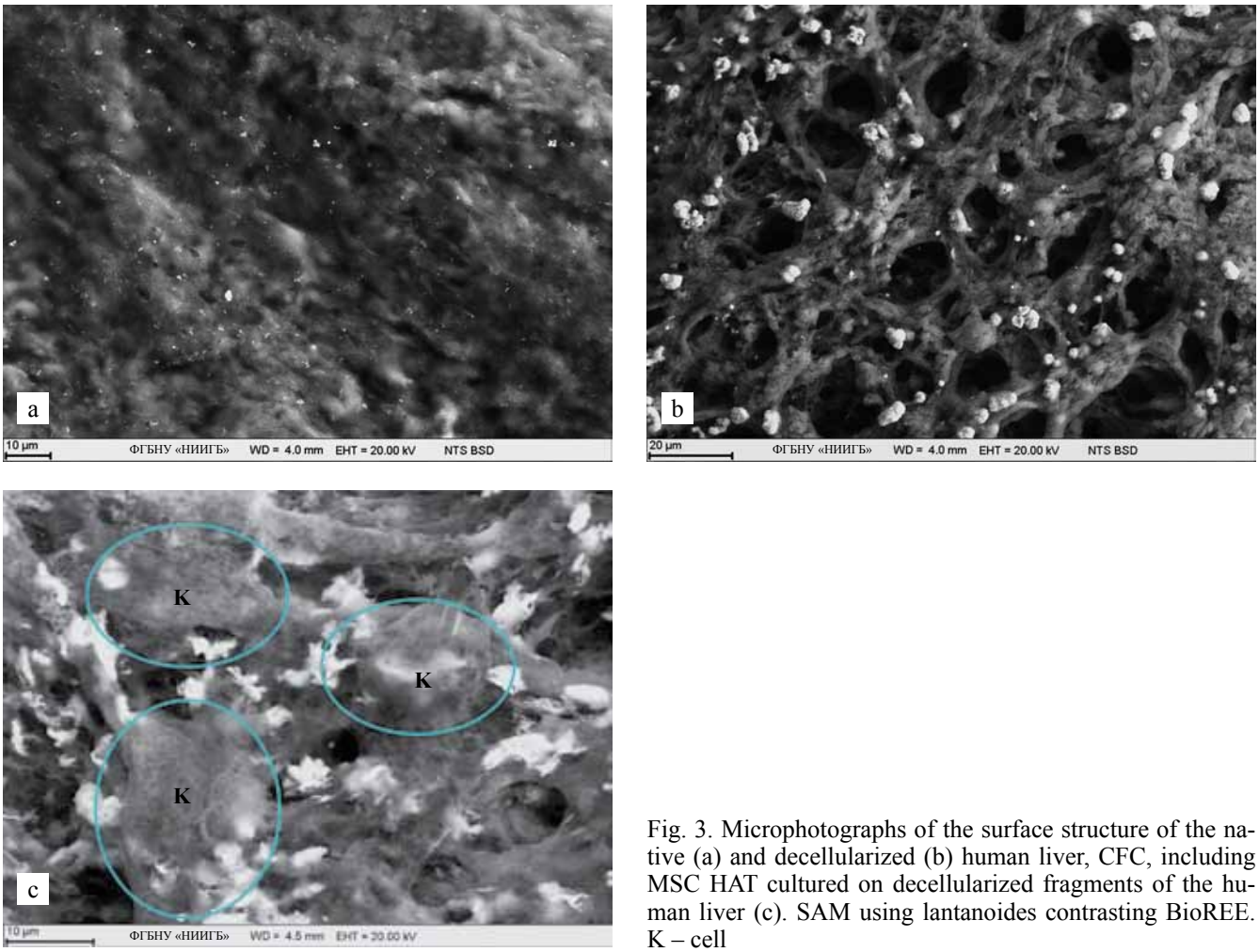

Fig. 3. Microphotographs of the surface structure of the native (a) and decellularized (b) human liver, CFC, including MSC HAT cultured on decellularized fragments of the human liver (c). SAM using lantanoides contrasting BioREE. K – cell

about 1–2 µm in size and large pores up to 20 µm in size. Light formations, which are determined on the surface of decellularized tissue and CES, most likely represent matrix-bound phosphorus-containing components of the culture medium adsorbed on its surface. MSC HGT, attached to the surface of the carrier, had a spread shape, which indicates the biocompatibility of the DFHL matrix with respect to interaction with cells (Fig. 3, c).

The obtained SEM data were confirmed by histological analysis. As seen in Fig. 4, cell morphology is spread out, fibroblast-like, which is characteristic of MSC HGT in the phase of active proliferation.

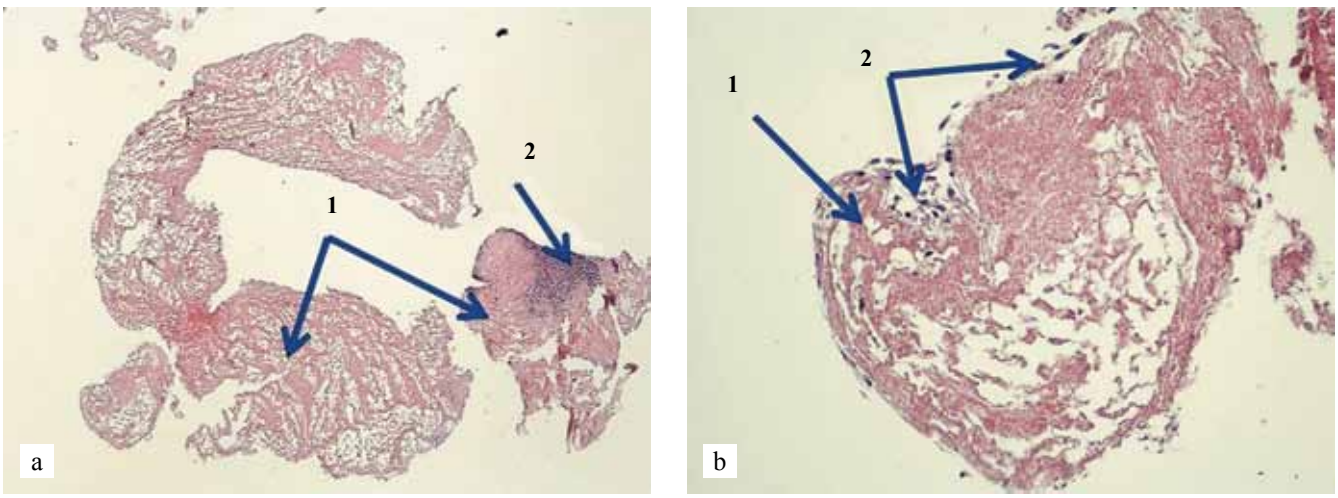

Fig. 4. Growth of MSC HAT on the tissue-specific matrix of the decellularized human liver. 1 – the matrix; 2 – MSC HAT. Staining with hematoxylin and eosin; a – ×40, b – ×200

The growth of fibroblast-like cells was observed at the periphery of all matrix particles. Note that single cells penetrated deep into the carrier, and pronounced proliferation was observed on one of the fragments.

The obtained positive results on the cultivation of MSC on the DFHL surface allowed us to switch to the DFHL – HepG2 culture system.

Analysis of the metabolic activity of cells showed that its growth occurs starting from the 3rd day of the experiment and reaches a maximum by the 7th day (Fig. 5). The data of the metabolic activity indicator are confirmed by intravital fluorescence microscopy (Fig. 6, a, b).

When studying the colonization of DFHL by cells of hepatocellular carcinoma HepG2, it was found that cells

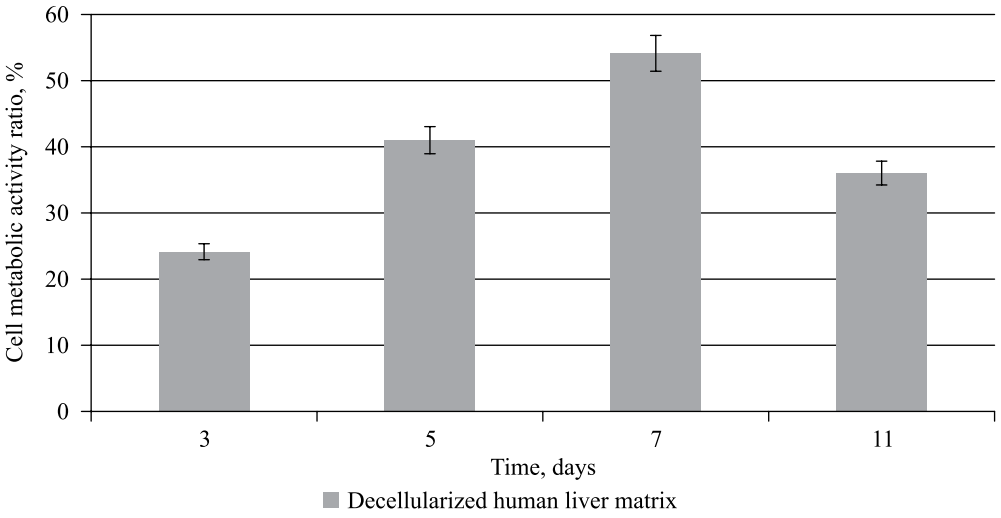

Fig. 5. Metabolic activity of HepG2 cells on a tissue-specific matrix from decellularized human liver

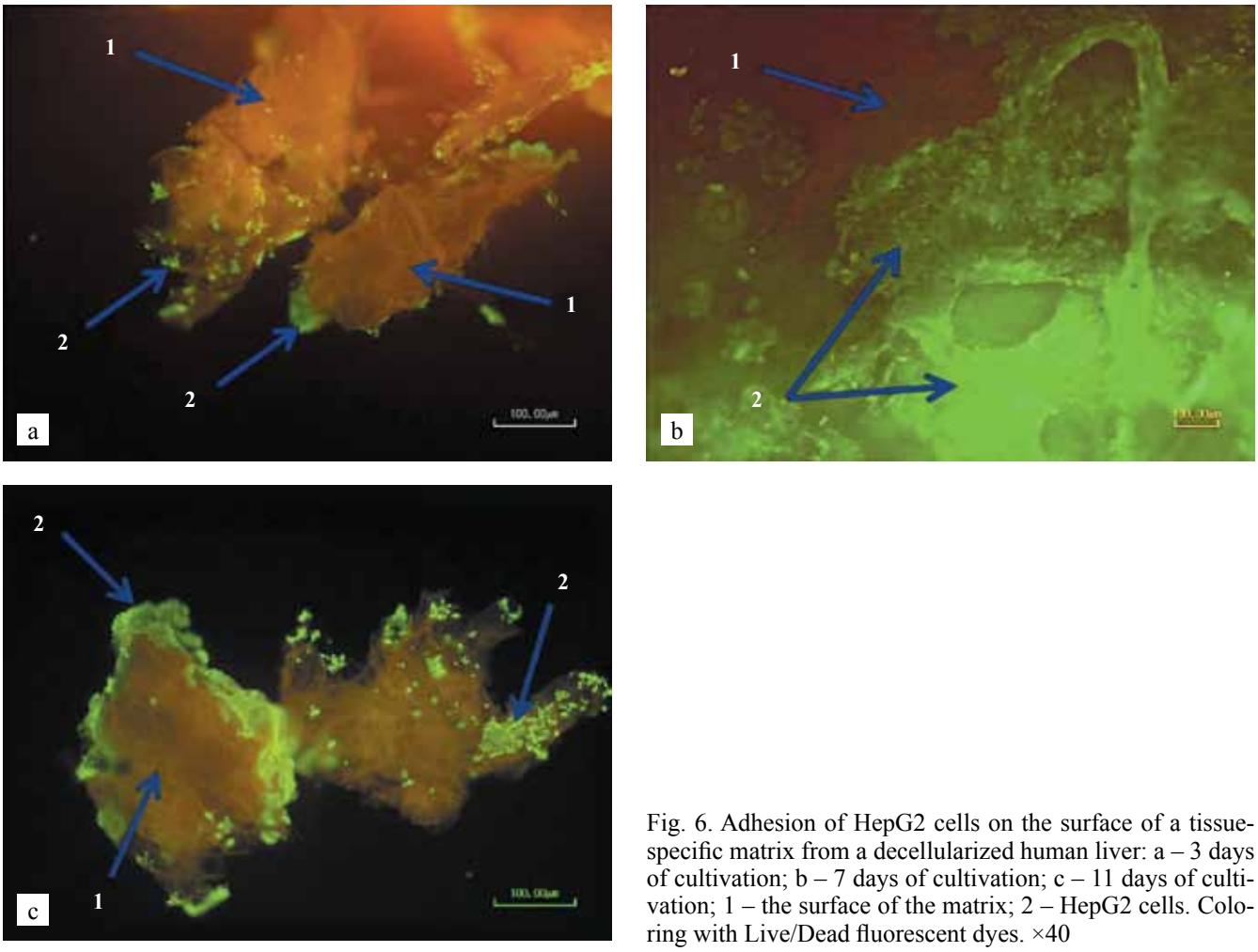

Fig. 6. Adhesion of HepG2 cells on the surface of a tissue-specific matrix from a decellularized human liver: a – 3 days of cultivation; b – 7 days of cultivation; c – 11 days of cultivation; 1 – the surface of the matrix; 2 – HepG2 cells. Coloring with Live/Dead fluorescent dyes. ×40

selectively attach to the matrix surface. The micrographs (Fig. 6, a, b) show that the cells mainly adhere to the marginal regions of the matrix, followed by their active proliferation. The central areas of the surface of the matrix fragments are very poorly populated by cells. According to microscopy and assessment of the metabolic activity of cells, its maximum falls on the 7th day. This trend persists throughout the experiment for 11 days. By the 11th day, proliferative activity decreases, which is associated with aging of the culture. In Fig. 6, c, it can be seen that by this time the marginal areas of the matrix are completely covered in places by the formed cell clusters and layers, while in the central zones the colonization of the host cells did not occur.

Thus, the intravital microscopy of the samples demonstrates active proliferation of HepG2 cells and uneven DFHL adhesion (Fig. 6).

On histological analysis, as seen in Fig. 7, the predominant growth of epithelial-like cells with a high nuclear-cytoplasmic ratio was observed on the surface of the matrix by the third day of cultivation. In this case, the cells united into numerous groups, and some of the cells formed small clusters in the volume of the matrix. Note the presence of collagen in DFHL, which indicates the preservation of the main structural component of ECM. By the seventh day, a significant increase in cell mass was observed, which was associated with active cell proliferation. On the surface of the carrier, multi-layered dense cell layers were found, and in the thickness of the matrix, the formation of larger cell clusters than in the previous period was observed.

The cells show a fine-grained cytoplasm with a few small vacuoles, and also observed an atypical mitosis characteristic of this cell line (Fig. 8).

Biochemical analysis of samples of the culture medium on the third day of the experiment did not reveal in the samples of urea at a level exceeding the detection limit of 1.1 mmol/L. However, by the 7th day, the urea content in the culture medium was 1.2 ± 0.1 mmol/L, which proves the presence of functional activity of cells in the CES composition.

It was suggested that the detected uneven colonization of matrix cells and insignificant cell penetration into its volume during cultivation under static conditions can

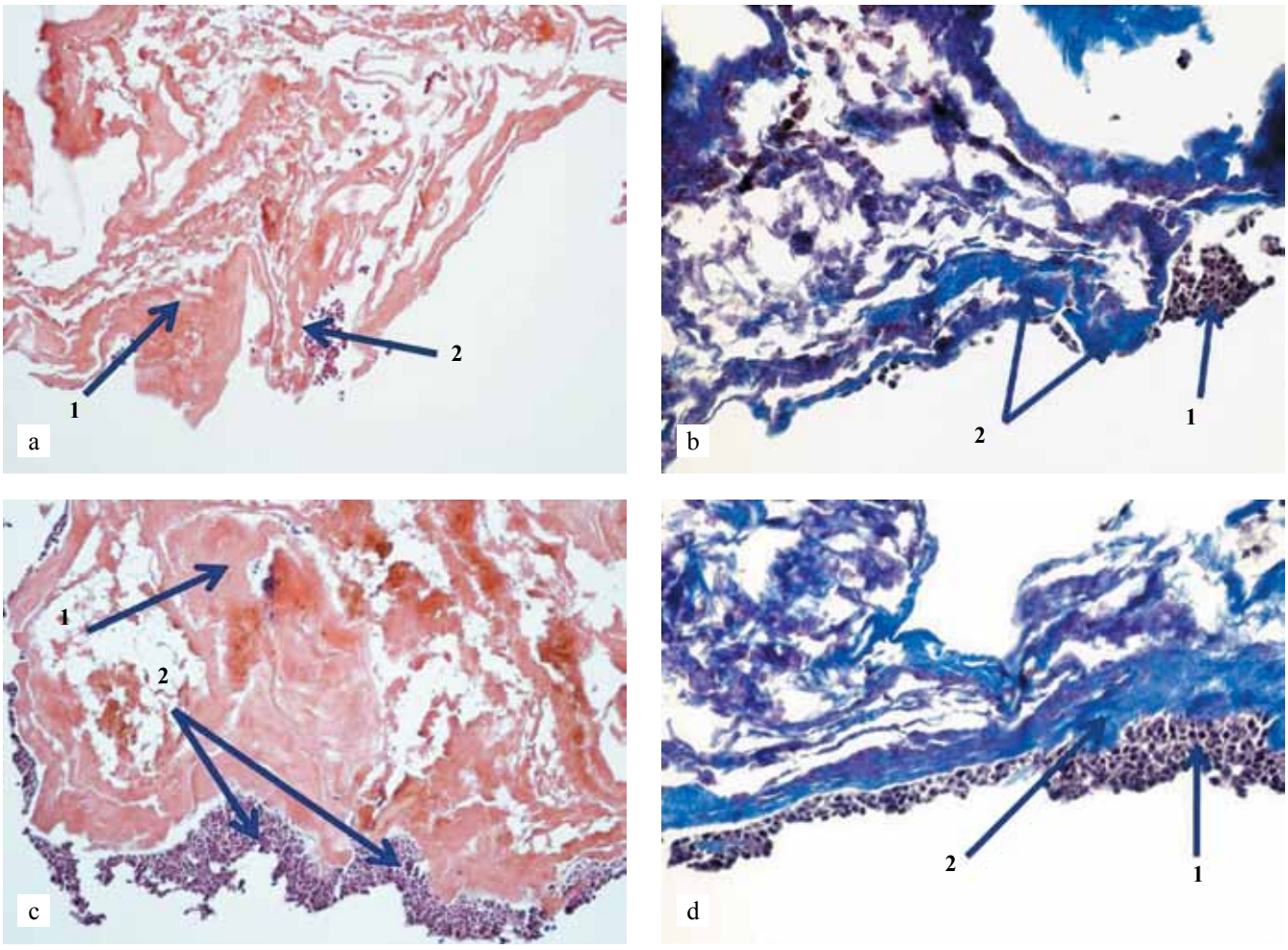

Fig. 7. Growth of human hepatocellular carcinoma cells HepG2 on a tissue-specific matrix from a decellularized human liver. ×100. Staining with hematoxylin and eosin: a – 3 days of cultivation; b – 7 days of cultivation; 1 – matrix; 2 – HepG2 cells. Masson staining for collagen. c – 3 days of cultivation; d – 7 days of cultivation; 1 – HepG2 cells; 2 – collagen. ×200

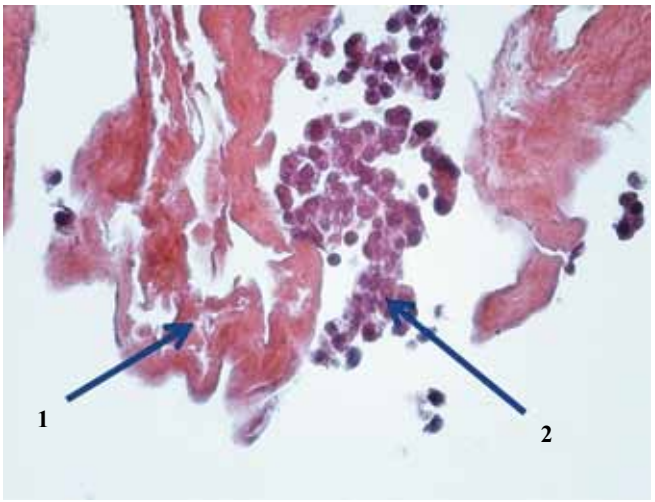

Fig. 8. Morphology of human hepatocellular carcinoma cells HepG2 when cultured on a tissue-specific matrix from a decellularized human liver. 3 days of cultivation: 1 – matrix; 2 – HepG2 cells. ×400. Staining with hematoxylin and eosin

be avoided by cultivating CES DFHL – HepG2 in a flow bioreactor [13].

Indeed, on the 7th day of cultivation in the bioreactor, the DFHL matrix with HepG2 formed a single conglomerate (Fig. 9). Most of the numerous groups of adhered epithelial-like cells with a high nuclear-cytoplasmic ratio of cells were viable and stained green. The bulk of cells was concentrated on the surface of the matrix, but cells forming small clusters were also detected in the volume of the carrier. The morphology of the cells changed from rounded to more elongated; some cells were in a state of destruction.

The metabolic activity of cells during cultivation in a bioreactor was also higher than in statics. In the cells, reactions of energy metabolism were actively taking place: the glucose content in the culture medium by the seventh day of the experiment significantly decreased – from 7.69 ± 0.38 to 4.69 ± 0.23 mmol/L. The urea content in the culture medium (1.5 ± 0.1 mmol/L) exceeded the

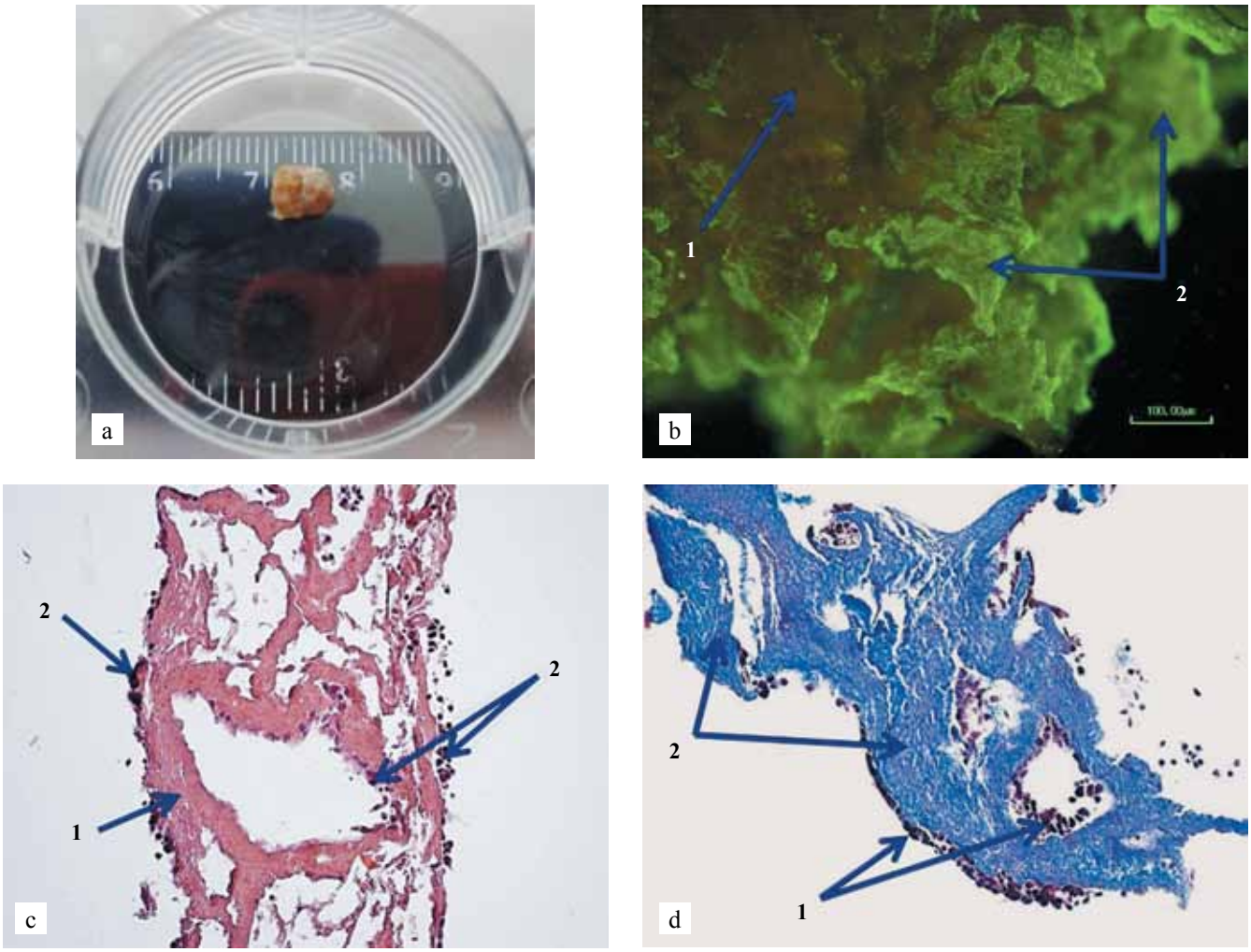

Fig. 9. Growth of human hepatocellular carcinoma cells HepG2 on a tissue-specific matrix from a decellularized human liver in a flow bioreactor at a flow rate of 0.02 ml/min: a – overview photo; b – Live/Dead vital dye staining; 1 – matrix; 2 – HepG2 cells. ×100; c – staining with hematoxylin and eosin; 1 – matrix; 2 – HepG2 cells. ×200; d – Masson staining for collagen; 1 – HepG2 cells; 2 – collagen. ×200

value for the samples obtained under static conditions (1.2 ± 0.1 mmol/L).

Thus, it has been shown that the cultivation of tissue-specific matrix DFHL with hepatic HepG2 cells in a bioreactor makes it possible to achieve a more uniform recellularization of the matrix volume, increase metabolic activity, and provide favorable conditions for cell proliferation.

CONCLUSION

A protocol has been proposed for decellularization of donor liver fragments, which makes it possible to obtain a tissue-specific matrix free of cells and detritus, with a low DNA content and preservation of the ECM structure. The lack of cytotoxicity of DFHL and their ability to maintain the adhesion and proliferation of MSC HGT and tissue-specific HepG2 cells indicates the possibility of using the matrix in liver tissue engineering. The advantage of DFHL matrix recellularization in a flow-through bioreactor compared to DFHL cultivation with HepG2 was shown.

This work was partially supported by the Russian Foundation for Basic Research (Grant No. 18-29-06012).

The authors are grateful to I.A. Novikov (Laboratory of Basic Research in Ophthalmology, Federal State Budgetary Scientific Institution "Research Institute of Eye Diseases") for his assistance in conducting SEM.

The authors declare no conflict of interest.

REFERENCES

1. *Croce S, Peloso A, Zoro T, Avanzini MA, Cobianchi L.* A hepatic scaffold from decellularized liver tissue: food for thought. *Biomolecules*. 2019; 9 (12): 813. doi: 10.3390/biom9120813. PMID: 31810291.
2. *Yang W, Xia R, Zhang Y, Zhang H, Bai L.* Decellularized liver scaffold for liver regeneration. *Methods Mol Biol*. 2018; 1577: 11–23. doi: 10.1007/7651_2017_53. PMID: 28856614.
3. *Bilodeau C, Goltsis O, Rogers IM, Post M.* Limitations of recellularized biological scaffolds for human transplantation. *J Tissue Eng Regen Med*. 2020; 14 (3): 521–538. doi: 10.1002/term.3004. PMID: 31826325.
4. *Porzionato A, Stocco E, Barbon S, Grandi F, Macchi V, De Caro R.* Tissue-engineered grafts from human decellularized extracellular matrices: a systematic review and future perspectives. *Int J Mol Sci*. 2018; 19 (12): 4117. doi: 10.3390/ijms19124117. PMID: 30567407.
5. *Ahmed E, Saleh T, Yu L, Kwak HH, Kim BM, Park KM et al.* Micro and ultrastructural changes monitoring during decellularization for the generation of a biocompatible liver. *J Biosci Bioeng*. 2019; 128 (2): 218–225. doi: 10.1016/j.jbiosc.2019.02.007. PMID: 3090445.
6. *Willemse J, Verstegen MMA, Vermeulen A, Schurink IJ, Roest HP, van der Laan LJW et al.* Fast, robust and effective decellularization of whole human livers using mild detergents and pressure controlled perfusion. *Mater Sci Eng C Mater Biol Appl*. 2020; 108: 110200. doi: 10.1016/j.msec.2019.110200. PMID: 31923991.
7. *Butter A, Aliyev K, Hillebrandt KH, Raschzok N, Kluge M, Seiffert N et al.* Evolution of graft morphology and function after recellularization of decellularized rat livers. *J Tissue Eng Regen Med*. 2018; 12 (2): e807–e816. doi: 10.1002/term.2383. PMID: 27957815.
8. *Naeem EM, Sajad D, Talaei-Khozani T, Khajeh S, Azarpira N, Alaei S et al.* Decellularized liver transplant could be recellularized in rat partial hepatectomy model. *J Biomed Mater Res A*. 2019; 107 (11): 2576–2588. doi: 10.1002/jbm.a.36763. PMID: 31361939.
9. *Gautier SV, Sevastyanov VI, Shagidulin MYu, Nemets EA, Basok YuB.* Tkanespetsificheskiy matriks dlya tkanevoy inzhenerii parenkhimatoznogo organa i sposob ego polucheniya. Patent na izobretenie RU 2693432 C2, 02.07.2019.
10. *Elchaninov A, Fatkhudinov T, Usman N, Arutyunyan I, Makarov A, Lokhonina A et al.* Multipotent stromal cells stimulate liver regeneration by influencing the macrophage polarization in rat. *World J Hepatol*. 2018 Feb 27; 10 (2): 287–296.; *Zhou Q, Li L, Li J.* Stem cells with decellularized liver scaffolds in liver regeneration and their potential clinical applications. *Liver Int*. 2015 Mar; 35 (3): 687–694. doi: 10.1111/liv.12581.
11. *Shimoda H, Yagi H, Higashi H, Tajima K, Kuroda K, Abe Y et al.* Decellularized liver scaffolds promote liver regeneration after partial hepatectomy. *Sci Rep*. 2019; 9 (1): 12543. doi: 10.1038/s41598-019-48948-x. PMID: 31467359.
12. *Donato MT, Tolosa L, Gómez-Lechón MJ.* Culture and Functional Characterization of Human Hepatoma HepG2 Cells. *Methods Mol Biol*. 2015; 1250: 77–93. doi: 10.1007/978-1-4939-2074-7_5.
13. *Sevastyanov VI, Basok YB, Grigoryev AM, Kirsanova LA, Vasilets VN.* A perfusion bioreactor for making tissue-engineered constructs. *Biomedical Engineering*. 2017; 51 (3): 162–165.
14. GOST ISO 10993-1-2011 "Izdeliya meditsinskie. Otsenka biologicheskogo deystviya meditsinskikh izdeliy. Chast' 5. Issledovanie na tsitotoksichnost': metody *in vitro*". M.: Standartinform, 2014.
15. *Novikov I, Subbot A, Turenok A, Mayanskiy N, Chebotar I.* A rapid method of whole cell sample preparation for scanning electron microscopy using neodymium chloride. *Micron*. 2019; 124: 102687. doi: 10.1016/j.micron.2019.102687. PMID: 31302532.
16. *Zhang L, Guan Z, Ye J-S, Yin Y-F, Stoltz J-F, de Isla N.* Research progress in liver tissue engineering. *Biomed Mater Eng*. 2017; 29 (s1): S113–S119.
17. *Crapo PM, Gilbert TW, Badylak SF.* An overview of tissue and whole organ decellularization processes. *Biomaterials*. 2011; 32 (12): 3233–3243. doi: 10.1016/j.biomaterials.2011.01.057.
18. *Nibourg GA, Hoekstra R, van der Hoeven TV, Ackermans MT, Hakvoort TB, van Gulik TM, Chamuleau RA.* Increased hepatic functionality of the human hepatoma cell line HepaRG cultured in the AMC bioreactor. *Int J Biochem Cell Biol.* 2013 Aug; 45 (8): 1860–1868.

The article was submitted to the journal on 6.07.2020

DOI: 10.15825/1995-1191-2020-3-134-142

ACTIVATION OF REGENERATIVE PROCESSES IN THE LIVER WHEN USING CELL-BONE MARROW TOTAL RNA

N.A. Onishchenko[1], E.V. Fomenko[1], A.O. Nikolskaya[1], Z.Z. Gonikova[1], M.Yu. Shagidulin[1, 2], M.V. Balyasin[2], A.V. Elchaninov[3], V.I. Sevastyanov[1]

[1] Shumakov National Medical Research Center of Transplantology and Artificial Organs, Moscow, Russian Federation

[2] Sechenov University, Moscow, Russian Federation

[3] Research Institute of Human Morphology, Moscow, Russian Federation

Objective: to study the cellular mechanisms of activation of regenerative processes in the liver when using total RNA (tRNA) of bone marrow cells (BMCs) based on an extended liver resection (ELR) model. **Materials and methods.** Male Wistar rats (n = 80) with ELR model (70%) were divided into 2 groups: group 1 (control group) had a single saline injection, while group 2 (experimental group) received a single tRNA injection at a 30 μg/100 g dose of animal weight. The biochemical parameters of liver function and weight were monitored over time. Also monitored were microstructural changes in hepatocytes 48 hours after ELR by examining mitotic activity, caspase-9 expression and morphometric parameters. **Results.** It was found that in group 2, in comparison to group 1, there was faster normalization of biochemical parameters (by 10–14 days), a higher mitotic index of hepatocytes (23.45‰ versus 5.37‰), and initially sharper decrease and then faster recovery of liver mass (by 10–12 days versus 18–20 days). Both groups showed almost total expression of caspase-9, including in mitotically splitting hepatocytes. Group 1 demonstrated decreased values of morphometric parameters of single and binuclear cells, decreased number of binucleated hepatocytes and increased total density of hepatocytes as compared to the intact liver. Intraperitoneal administration of tRNA increased morphometric parameters of mononuclear hepatocytes, did not affect their number, but increased the area of the nuclei of binuclear hepatocytes as compared to the control group. **Conclusion.** The proven capability of cell-bone marrow total RNA to simultaneously support apoptosis in liver cells after ELR and induce mitotic activity indicates that tRNA can switch activated apoptosis to cell proliferation at the early phase of the regenerative process. This effect may be due to the presence of regulatory RNA molecules in tRNA, including numerous non-coding RNAs.

Keywords: bone marrow cells, total RNA, liver, experimental model, resection, regeneration.

INTRODUCTION

From recent publications, total RNA (tRNA) isolated from bone marrow cells (BMC) is known to have an inductive effect on the processes of regenerative regeneration of organs [1], however, the mechanisms of triggering its regulatory effect at the cellular level remain unclear. Meanwhile, the choice of a strategy and the improvement of the tactics of using cellular products cannot be carried out without considering the mechanisms involved in the regeneration process.

According to established views, organ regeneration occurs within the activation of an evolutionarily developed nonspecific adaptive syndrome (NAS) of cellular systems, which already at the early stages of development stimulates a complex of stereotypical adaptive changes in cells aimed at survival by mobilizing their own preserved reserves and the subsequent formation of stable adaptation by including regenerative mechanisms [2, 3]. When modeling 70% of hepatectomy, which has become a classical model for studying regeneration processes in the liver, it was shown that the ability of the cellular system to ensure the self-correction is largely dependent on the degree of activation in the cells of the remaining parts of the liver of the earliest manifestations of the adaptation syndrome, such as autophagy and apoptosis. The ability of the cellular system to ensure the correction of its existence, to be sensitive to various correcting factors, and to launch an effective regenerative process largely depends on this [4–7].

The **purpose** of the present work is to study the dynamics of the formation of recovery processes in the damaged liver after a single intraperitoneal injection of BMC tRNA on an experimental model of extensive resection of rat liver, monitoring quantitative changes in specific indicators of liver function and nonspecific substance (microstructural) changes in cells, which are characteristics of development phases in them NAS.

Corresponding author: Zalina Gonikova. Address: 1, Shchukinskaya str., Moscow, 123182, Russian Federation. Phone: (966) 188-33-33. E-mail: zalina3393@gmail.com

MATERIALS AND METHODS

All studies using laboratory animals were performed in compliance with the bioethical principles approved by the European Convention for the Protection of Vertebrate Animals (2005).

The study was performed on 130 male Wistar rats weighing 250–300 g, in 80 of which the ORP model was reproduced [8], the rest of the rats were used to obtain unsorted mononuclear BMCs and to isolate tRNA from them. Before modeling RRP, the operated rats were anesthetized by inhalation with diethyl ether, then, following the rules of asepsis and antiseptics, the abdominal cavity was opened, the liver was removed into the wound, and ligatures were sequentially applied to the bases of the median, left lateral, and right upper lobes of the liver, after which they were removed (70–75% of the total liver mass). The operation was always performed in the morning (from 10 am to 12 noon), when the daily rhythm of mitotic activity of liver cells is minimal. In the early postoperative period, the operated animals always developed a clinical picture of acute liver failure.

After ELR, all animals were divided into two groups; group 1 – control (n = 40), in which rats were once intraperitoneally injected with 1.0–1.5 ml of saline; group 2 – experimental (n = 40), in which, 3–5 hours after ORP, total RNA (tRNA) isolated from the unsorted mononuclear BMC fraction of healthy donor rats was injected once intraperitoneally at a dose of 30 μg/100 g of body weight, dissolved in 1.0–1.5 ml of saline.

Total RNA from the BMC mononuclear fraction was isolated with the ExtractRNA reagent (Evrogen (Russia) according to the manufacturer's instructions, which made it possible to obtain about 148.5 ± 22.3 μg RNA from each 30–35 × 10^6 cells.

The dynamics of spontaneous restoration of hepatic homeostasis in the body after ELR and the effect of tRNA on this process were studied by measuring the content of total protein and total bilirubin in blood serum in the early postoperative period (within 14 days), as well as the activity of hepatic cytolysis enzymes: alanine aminotransferase (ALT), aspartic aminotransferase (ASAT) and alkaline phosphatase (ALP) – by standard methods on a biochemical analyzer "Arik-test", Germany. We also investigated the rate of overcoming the critical mass of the liver remnant and its restoration to its initial values after ELR within 28 days. For this, in each operated animal, immediately after ELR, the resected part of the liver was weighed, which was taken as 70% of the total liver weight, and then, based on these measurements, the initial liver weight was calculated for each animal. Then, at each study period, the remaining liver was explanted, its weight was determined by weighing, and the obtained values were compared with the calculated initial liver weight for this animal.

The nature of the induction effect on the recovery processes in the liver of critical injury during the creation of the ELR model (group 1) and the results of the use of tRNA against the background of ELR (group 2) were judged by quantitative assessment of changes in the parameters of the microstructural state of liver cells. For this, first of all, the mitotic activity of hepatocytes in the liver remnant was investigated at 24, 36, 48 and 72 hours, as well as on the 5th, 7th and 10th days after ELR in groups 1 and 2. At the indicated time, the liver was excised and histological drugs; we stained tissue sections with hematoxylin and eosin and determined in 30 fields of view the number of mitotically dividing hepatocytes in ppm (‰) and calculated the mitotic index (MI).

The morphometric assessment of the state of hepatocytes was also carried out on liver sections stained with hematoxylin and eosin. Using a Nikon Eclipse 50i microscope equipped with a digital camera (Japan), micrographs of liver sections were obtained at ×400, on which, using the ImageJ software package, the areas of hepatocytes and their nuclei were measured with subsequent calculation of the cytoplasm and binucleated hepatocytes with the subsequent calculation of their percentage and the number of cells per unit section area.

Since ELR is known to be a critical trauma and the early stage of the regeneration process is always accompanied by the appearance of signs of cellular autophagy [4, 5] and reversible cell death – reversible apoptosis [6], 3 μm thick liver sections were stained with rabbit antibodies to the protein of the proteolytic cell system – Caspase 9 (Abcam) at a dilution of 1:100 in PBS with the addition of 0.1% Tween 20 and 5% BSA for immunohistochemical detection of signs of reversible apoptosis of hepatocytes in the early phase of the regeneration process after 48 hours. Samples were washed and secondary antibodies against rabbit IgG conjugated to HRP (Agilent Dako) in PBS-T solution with 5% BSA were applied. Then there was a staining with DAB (Abcam); the nuclei were stained with Mayer's hematoxylin (BioVitrum). Microscopy of the samples was made with Nikon Eclipse TE2000 optical microscope.

Statistical processing of the results was performed in R software environment, the character of the distribution of features was determined by Shapiro – Wilk test. The significance of the differences in the studied parameters in the two compared groups was assessed using the Wilcoxon and Student t-tests, considering the Holm-Bonferonni correction.

RESULTS AND DISCUSSION

Of the 80 rats in which ELR was modeled with the development of acute liver failure, 6 animals died within the first 5 days after liver resection, and the overall mortality was 7.5%. All animals that died after ELR belonged to control group 1 (no special therapy, n = 40), and within this group the mortality rate was 15%. In experimental

group 2 (n = 40), there was no lethality during the entire observation period.

The absence of lethality in experimental group 2 was accompanied by an accelerated rate of restoration of hepatic homeostasis in the body, which was expressed in an earlier normalization of biochemical parameters of liver function: the level of total protein, total bilirubin and the activity of cytolytic enzymes in the blood serum.

Tables 1 and 2 show the results of a dynamic study of the activities of AST, ALT, ALP, the level of total bilirubin and total protein in the blood serum of rats after modeling ELR in the control group (Table 1) and the experimental group with the introduction of tRNA (Table 2). In the control group, the cytolysis indices in the surviving animals were sharply increased during the first 5 days after ELR, then they stabilized, and only starting from the 7–10th day there was a clear tendency towards their normalization. The indices of total protein within 2 and 3 days were sharply reduced compared to the initial level and starting from 5–7 days the level of protein in the blood serum gradually increased but did not reach the initial values of the norm until the end of observations (14 day). In the experimental group, where tRNA was injected after ELR (Table 2), the cytolysis indices after ELR remained stably high only for 1–3 days, but by the 5th day there was a clear decrease in the activity of all studied liver enzymes in the rat blood serum. compared with control ($p < 0.05$) at the same time. As a result, in the experimental group with the introduction of tRNA, the values of the studied parameters in the blood serum approached the norm already on the 10th day and did not differ from the initial values by the 14th day of observation, while in the control group, the normalization of all the studied parameters did not occur even by the 14th day. -th day. A higher rate of recovery of hepatic homeostasis indices in the body was accompanied in the experimental group by a significant increase in the activity of proliferative processes in the resected liver after ELR compared with the control.

The study of the mitotic activity of hepatocytes in the resected liver made it possible to establish its sharp activation 48 hours after modeling the ELR in both groups 1 and 2 compared with the baseline level: the initial level of mitotic activity, assessed before liver resection by the mitotic index (MI) was 0.2–0.3‰ (1–2 mitosis per 30 fields of view). However, 48 hours after ELR, the severity of MI activation in the study groups became different: in the 1st, control group, MI was 5.378‰ (there were 36 mitoses per 6693 cells), while in the 2nd, experimental group, MI was 23.45‰ (227 mitoses were

Table 1

Dynamics of changes in the levels of total protein, total bilirubin, and the activity of cytolysis enzymes (AlAT, AsAT, and ALP) in blood serum after ELR and infusion of physiological saline (PS) (control group, n = 40)

Observation time (days)	Group 1 (control, saline), n = 40				
	AsAT, U/L	AlAT, U/L	AP, U/L	Total bilirubin, μM/L	Total protein, g/l
Initial values	58 ± 8.0	40 ± 6.0	240 ± 24	2.2 ± 0.7	98 ± 20
2	570 ± 29*	310 ± 10*	1102 ± 21*	10.2 ± 2.0*	21 ± 16*
3	490 ± 20*	320 ± 21*	1009 ± 29*	12.3 ± 1.5*	24 ± 11*
5	420 ± 27*	290 ± 18*	982 ± 22*	10.8 ± 1.3*	36 ± 13*
7	360 ± 24*	282 ± 15*	893 ± 24*	9.0 ± 1.9*	41 ± 9.0*
10	199 ± 22*	169 ± 18*	560 ± 24*	7.3 ± 2.0*	55 ± 6.0*
14	100 ± 14*	121 ± 13*	340 ± 20*	3.5 ± 1.0	61 ± 7.0

Note. * – $p < 0.05$ compared to baseline.

Table 2

Dynamics of changes in the content of total protein, total bilirubin and the activity of cytolysis enzymes (AlAT, AsAT, and ALP) in the blood serum after ELR and infusion of tRNA at a dose of 30 μg/100 g of animal weight (n = 40)

Observation time (days)	Group 2 (experimental, tRNA), n = 40				
	AsAT, U/L	AlAT, U/L	AP, U/L	Total bilirubin, μM/L	Total protein, g/l
Initial values	58 ± 8.0	40 ± 6.0	240 ± 24	2.2 ± 0.7	98 ± 20
2	423 ± 20*	276 ± 17*	987 ± 30*	7.9 ± 1.3*	48 ± 10*
3	383 ± 28*	108 ± 18*	632 ± 28*	6.5 ± 1.2*	52 ± 9.0*
5	238 ± 19*$^{\#}$	78 ± 10*$^{\#}$	460 ± 32*$^{\#}$	5.1 ± 1.1*$^{\#}$	54 ± 6.0*
7	115 ± 11*$^{\#}$	69 ± 6.2*$^{\#}$	346 ± 26*$^{\#}$	3.1 ± 1.0$^{\#}$	60 ± 7.0
10	82 ± 12$^{\#}$	58 ± 12$^{\#}$	257 ± 15$^{\#}$	2.7 ± 0.9	68 ± 8.0
14	66 ± 7$^{\#}$	44 ± 6$^{\#}$	230 ± 14$^{\#}$	1.9 ± 0.8	84 ± 12

Note. * – $p < 0.05$ compared to baseline; $^{\#}$ – $p < 0.05$ compared to control at the same time.

determined per 9678 cells, i. e., it was 5 times higher than in the control group).

On the 3rd day after the ELR modeling, MI in the study groups remained at a higher level compared to the baseline but changed compared to 48 hours: in the 1st, control group, MI decreased and amounted to 3.7‰, in the 2nd, the experimental group MI also decreased and amounted to 6.36‰. By the 5th day MI values in the 1st and 2nd groups approached the initial level and did not differ among themselves (Fig. 1).

From the obtained results of a comparative study of the mitotic activity of hepatocytes in the two studied groups, it follows that ELR itself induces the proliferative activity of hepatocytes, and the introduction of tRNA from BMC, already at an early stage, significantly enhances the proliferative activity of cells.

Higher mitotic activity of hepatocytes in group 2 (administration of tRNA) was accompanied by a significantly faster rate of liver weight recovery. In Fig. 2 shows the dynamics of liver weight recovery after ELR in the control and experimental groups.

From the presented graph it follows that a higher rate of liver weight recovery was noted in the experimental group, in which, 3–5 hours after ELR and intraperitoneal administration of tRNA, the recovery of liver weight occurred by 10–12 days.

In the control group with intraperitoneal saline injection, the restoration of liver mass occurred only on the 18th–20th day after ELR. Thus, the results obtained indicate that administration of tRNA at a dose of 30 μg/100 g of animal weight induces a more pronounced activation of regeneration processes in the liver after ELR. This can be explained by the fact that tRNA BMC is a ready-made complex of signaling RNA molecules

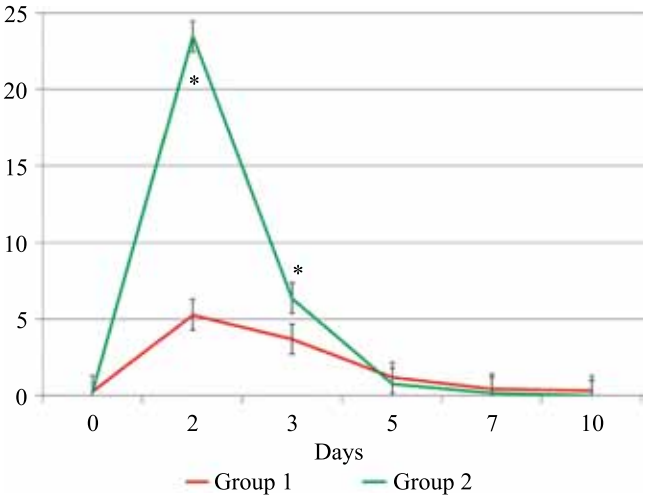

Fig. 1. Dynamics of changes in the mitotic index of hepatocytes in rat livers after ELR in the control (group 1 with the introduction of PS) and experimental (group 2 with the introduction of tRNA) groups. * – $p < 0,05$ compared to control at the same period

of various classes, which is able to penetrate into various cells freely and quickly, as well as be targeted by them (and their exosomes), especially with the help of blood mononuclear cells (lymphocytes) [9]. It is also important to note that when studying the dynamics of liver weight recovery after ELR in experiments with tRNA, the weight of the resected liver in the early stages (by day 2) was significantly less than the weight of the liver in the control group (Fig. 2).

If to consider the known facts that the process of liver regeneration after ELR at an early stage is accompanied by the phenomena of cellular autophagy [4, 5] and incre-

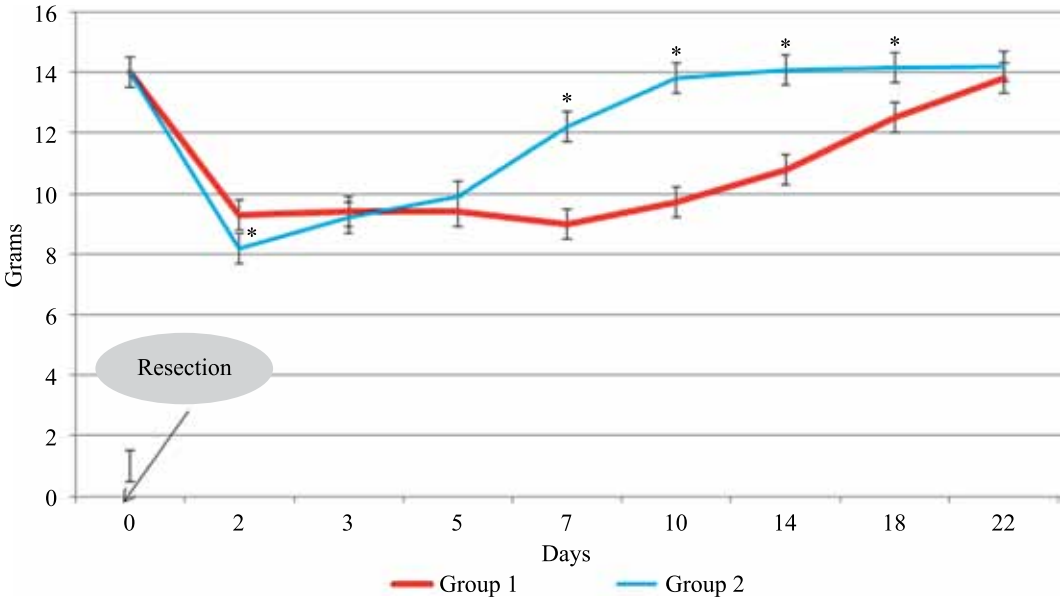

Fig. 2. Dynamics of the initial mass restoration of rat livers after ELR in the control (group 1 with the introduction of PS) and experimental (group 2 with the introduction of tRNA) groups. * – $p < 0,05$ compared to control at the same period

ased signs of reversible and even irreversible apoptosis of hepatocytes [6], the results obtained suggest that tRNA accelerates the process of restorative regeneration liver in comparison with the control due to a sharper and earlier (apparently, already within 1 day) and longer (within 2 days) intensification of manifestations of mobilization and consumption of its own cellular reserves (increased autophagy and apoptosis) with the development of NAS and the recovery process as a result of the combined effect on liver cells of two factors: ELR and tRNA.

Indeed, a comparative immunohistochemical study of Caspase-9 activity, an indicator of reversible apoptosis in liver cells of the control and experimental groups 48 h after ELR, i. e., at the height of activation of mitotic activity of hepatocytes, showed (Fig. 3, a and b) that both in the control and experimental groups, the process of reversible apoptosis was induced in more than 90% of hepatocytes. The study of Caspase-9 expression in liver cells of intact animals did not reveal the presence of this marker in them. The data obtained indicate an almost total activation in liver cells after ELR of adaptive-dependent apoptosis in the two study groups. However, in contrast to the control group, in the experimental group, the administration of tRNA led to a distinct increase in the mitotic activity of hepatocytes. This effect was also observed for hepatocytes, which emerged from the state of reversible apoptosis, since in mitotically dividing hepatocytes, the chromogen-stained substrate was washed out of the dividing nucleus and passed into the cytoplasm (Fig. 3, b). The results obtained indicate that the tRNA introduced into the body against the background of ELR, apparently, acts within the framework of the nonspecific adaptive syndrome of cellular systems as an adequate adaptogen, which turns on and optimizes the survival reserves of cells, switching evolutionarily programmed regulatory mechanisms in them from apoptosis to cell proliferation. The latter is possible if, in the early stages after ELR, the signals of apoptosis and proliferation in liver cells are in a co-activated state. According to I.M. Gazizov et al. [6], the intersection point of these signals can be the factors STAT-3 and NFK-β, with a significant increase in the levels and activities of which cells suppress apoptosis by expressing antiapoptotic proteins Bcl-2, Bcl-x1, HSP-70, G0-phases and enter into proliferation. The possibility of cell transition from the state of apoptosis to the phase of proliferation was also shown in [10].

It is known that the development of apoptosis is characterized by the occurrence of certain changes in the morphology of cells (the nucleus and cytoplasm decrease in size, condense without disrupting the structural integrity of cell membranes and the development of inflammation). To prove the development of adaptation-dependent apoptosis of liver cells in the early stages after ELR and active switching of cells from the proapoptotic pathway to the pathway of proliferation and regenerative regeneration using tRNA, a comparative morphometry of hepatocytes in the liver of rats from the control and experimental groups was carried out 48 hours after ELR, i. e. That is, at the time of maximum mitotic activity of hepatocytes. The results of the morphometric study of hepatocytes in the control and experimental groups, without and with the introduction of tRNA in comparison with intact animals (without ELR), are presented in Table 3 and 4. In the liver of rats of the control group, significant changes in the cytometric parameters of mononuclear and binuclear hepatocytes are observed. Thus, post-resection changes after 48 hours were characterized by a decrease in the areas of mononuclear hepatocytes, their nuclei and cytoplasm by 30.2; 34.0; 29.9%, respectively, and a decrease in these indicators for binuclear hepatocytes by 20.5; 35.0; 23.4% compared

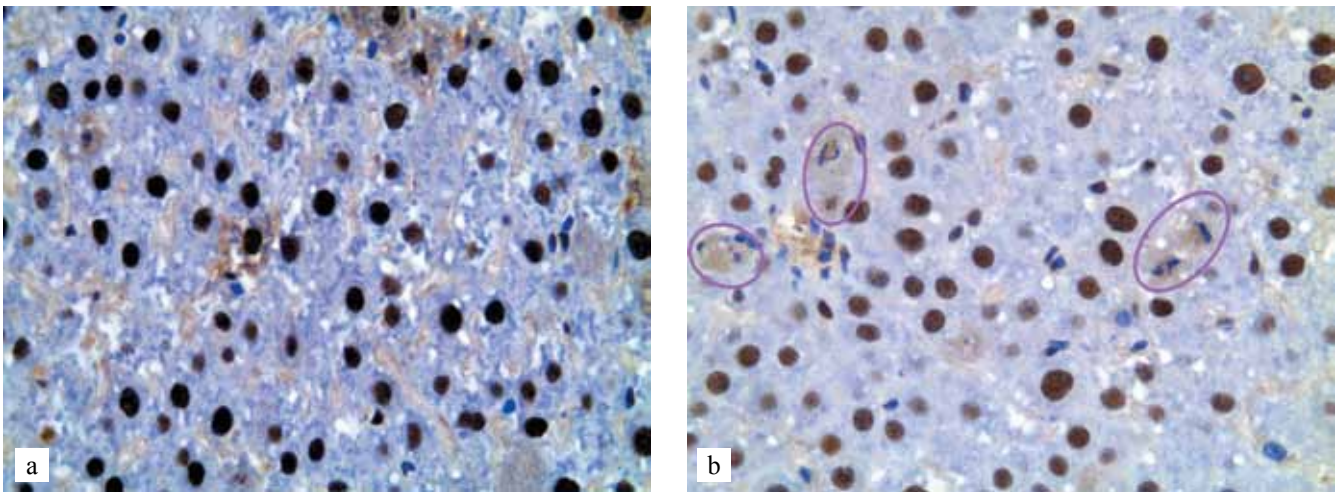

Fig. 3. Immunohistochemical investigation of Caspase-9 activity in hepatocytes in 48 hours after ELR in the control group with infusion of physiological saline (a) and in the experimental group with infusion of tRNA of BMCs (b). ×40. Cells in the mitosis phase are indicated by circles

Table 3

Changes in the cytometric indices of single- and double-nuclear hepatocytes in 48 hours after ELR without and with infusion of tRNA of BMCs (Me (Q1; Q2)) (median (25th, 75th percentiles)

Group / Parameter	Intact	Control group, saline	Experimental group, tRNA
Indicators of mononuclear hepatocytes			
Cell area, μm^2	318.7 (268.5; 378.4)	222.4 (174.1; 281.2)[1]	272.7 (219.4; 336.2)*
Nucleus area, μm^2	55.8 (50.0; 75.7)	36.8 (30.4; 41.9)[1]	45.6 (38.2; 52.2)*
Cytoplasm area, μm^2	262.6 (213.5; 309.4)	184.1 (141.6; 239.5)[1]	228.9 (179.7; 287.8)*
Indicators of binuclear hepatocytes			
Cell area, μm^2	420.1 (376.0; 489.2)	333.9 (279.0; 376.2)[1]	355.6 (293.0; 439.5)
Nucleus area, μm^2	100.1 (90.6; 108.9)	65.0 (53.5; 74.9)[1]	75.4 (60.2; 90.0)*
Cytoplasm area, μm^2	321.0 (286.0; 382.1)	261.1 (226.6; 307.5)[1]	276.8 (231.2; 341.8)

Note. [1] – the differences are significant ($p \leq 0.01$) compared with the intact group; * – the differences are significant ($p \leq 0.01$) compared to the control group of rats with ELR; area – average area.

Table 4

Change in the total number of hepatocytes per unit area and the percent of single- and double-nuclear cells in 48 hours after ELR without and with infusion of tRNA (M ± m)

Group / Parameter	Intact	Control group, saline	Experimental group, tRNA
Total number of cells per 50000 μm^2	78.4 ± 4.9	100.8 ± 9.2[1]	95.2 ± 5.7
Mononuclear cells, %	87.43 ± 0.95	92.70 ± 0.75[1]	91.81 ± 0.40
Binuclear cells, %	12.57 ± 0.95	7.30 ± 0.75[1]	8.19 ± 0.40

Note. [1] – differences are significant ($p \leq 0.01$) compared with an intact group.

with hepatocytes in the liver of an intact group of rats. There was also a statistically significant decrease in the number of binucleated hepatocytes by 5.27% against the background of an increase in the total number of cells per unit area by 27.3% (Table 4).

For the liver of the experimental group, intraperitoneal administration of tRNA led to a change in all investigated cytometric parameters of mononuclear hepatocytes, and to a lesser extent influenced the parameters of binuclear hepatocytes. Thus, with the introduction of tRNA, an increase in the areas of mononuclear hepatocytes, their nuclei and cytoplasm were observed by 22.6; 23.9 and 24.3%, respectively, compared with the control group. At the same time, no changes were found in the number of binuclear cells (Table 4), but an increase in the area of the nuclei of binuclear hepatocytes was observed by 15.5% in comparison with the control group (Table 3).

The results of morphocytometry of hepatocytes 48 hours after ELR in the control group suggest that under conditions of almost total activation of Caspase-9 (more than 90% of hepatocytes) and not a pronounced increase in the proliferative activity of hepatocytes (mitotic index – 5.37‰), an increase in cell density, as well as a general decrease in the areas of hepatocytes, their nuclei, and cytoplasm indicates, first of all, a predominant increase in the processes of autophagy and reversible apoptosis in liver cells in the early stages after ELR. The observed decrease in the number of binucleated cells in the liver of the control group of rats may be associated with their division and the formation of mononuclear cells [11].

Administration of BMC tRNA 48 hours after ELR retains the high level of Caspase-9 activity in hepatocytes unchanged. There is a sharper decrease in the mass of the resected liver at this time in comparison with the control group as a result of stress effects of ELR and tRNA. At the same time, in the liver, the mitotic activity of hepatocytes sharply increases (MI = 23.45‰) and a reliable recovery of morphometric parameters begins (an increase in the areas of nuclei, cells, and cytoplasm in comparison with the control group) of predominantly mononuclear hepatocytes, which, apparently, are capable of more more actively than binuclear hepatocytes, to proliferate and hypertrophy in critical situations. At the same time, the persisting higher cell density per unit area against the background of the use of tRNA also indicates the continuing apoptosis of cells during the study period.

The property of tRNA proved on the experimental model of ELR to simultaneously maintain apoptosis processes in liver cells and induces mitotic activity in them indicates that tRNA is able to switch activated apoptosis to cell proliferation at the early phase of the regeneration process. The observed effect is most likely due to the presence of regulatory RNA molecules, including numerous protein-noncoding RNAs [12–14], which are actively involved in regeneration processes and are part of the BMC tRNA.

CONCLUSION

The results obtained allow us to conclude that tRNA, used for the induction of recovery processes in the liver, promotes at the cellular level the activation of early manifestations of the evolutionarily developed nonspecific adaptive mechanism of cell survival, while simultaneously supporting signaling pathways in them, apoptosis, and proliferation in a co-activated state and also induces the transition of cells from adaptive-dependent apoptosis to proliferation by expressing anti-apoptotic proteins, the genes of which are the targets of numerous regulatory RNA molecules that make up BMC tRNA.

The authors of the article are deeply grateful to Lyundup Aleksey Valerievich, Med., Cand., for his assistance in organizing immunohistochemical studies of the liver and participation in the discussion of the materials received.

The authors declare no conflict of interest.

REFERENCES

1. *Babaeva AG, Tishevskaya NV, Gevorkyan NM.* About morphogenetic properties of RNA of lymphoid and stem cells at regenerative processes. RAN. *Research Institute of human morphology*. M., 2016. 272.
2. *Braun AD, Mozjenok GP.* Nonspecific adaptic syndrome of cellular system. L.: Nauka, 1987. 232. (In Russ.).
3. *Onishchenko NA.* Cytogenetic recapitulation, induced by medical preparations, as the universal stage of formation of urgent protection against damage at organ transplantation. *Pathological Physiology and Experimental Therapy*. (Russian Journal). 2016; 60 (4): 148–153. (In Russ).
4. *Lin CW, Chen YS, Lin CC, Chen YJ, Lee PH, Kuo PL et al.* Amiodarone as an autophagy promoter reduces liver injury and enhances liver regeneration and survival in mice after partial hepatectomy. *Sci Rep.* 2015 Oct 30; 5: 15807. doi: 10.1038/srep15807.
5. *Cheng Y, Wang B, Zhou H, Dang S, Jin M, Shi Y et al.* Autophagy is required for maintenance of liver progenitor cell functionality. *Cell Physiol Biochem*. 2015; 36 (3): 1163–1174.
6. *Gazizov IM, Gumerova AA, Kiyasov AP.* Apoptosis in regenerative histogenesis of the liver after partial hepatectomy in rats. *Genes and cells*. 2015; 10 (3): 22–26.
7. *Mongolov KhP, Plekhanov AN.* Interrelation of apoptosis and liver regeneration in hepatic insufficiency after partial hepatectomy in an experiment. *Acta Biomedica Scientifica*. 2009; 3: 203–206.
8. Patent na izobretenie 2701792 RF, MPK A61K35/28 (2019.08) "Sposob lecheniya ostroy pechenochnoy nedostatochnosti" / N.A. Onishchenko, Z.Z. Gonikova, A.O. Nikol'skaya, L.A. Kirsanova, M.Yu. Shagidulin, V.I. Sevastyanov, S.V. Gautier. – 2018138281; zayavl. 30.10.2018; opubl. 01.10.2019, Byul. 28.
9. *Tishevskaya NV, Babayeva AG, Gevorkyan NM.* Role of lymphocytic RNA_S in intercellular information exchange and regulation of regenerative processes. *I.M. Sechenov Russian journal of physiology.* 2016; 102 (11): 1280–1301.
10. *Budd RC*. Death receptors coupe to both cell proliferations and apoptos. *J Clim Jnvest.* 2002 Feb 15; 109 (4): 437–442.
11. *Miyaoka Y, Ebato K, Kato H, Arakawa S, Shimizu S, Miyajima A*. Hypertrophy and unconventional cell division of hepatocytes underlie liver regeneration. *Curr Bio*. 2012; 22 (13): 1166–1175.
12. *Yan IK, Wang X, Asmann YW, Haga H, Patel T.* Circulating Extracellular RNA Markers of Liver Regeneration. *PLoS One*. 2016; 11 (7). doi: 10.1371/journal.pone.0155888.
13. *Li J, Jin W, Qin Y, Zhao W, Chang C, Xu C.* Expression Profile and Function Analysis of LncRNAs during Priming Phase of Rat Liver Regeneration. *PLoS One*. 2016 Jun 21; 11 (6). doi: 10.1371/journal.pone.0156128.
14. *Mottaghitalab F, Rastegari A, Farokhi M, Dinarvand R, Hosseinkhani H et al.* Prospects of siRNA applications in regenerative medicine. *International Journal of Pharmaceutics*. 2017 May 30; 524 (1–2): 312–329.

The article was submitted to the journal on 30.06.2020

DOI: 10.15825/1995-1191-2020-3-143-148

3D ANALYSIS OF THE MICRO- AND NANOSTRUCTURE OF LUNG TISSUE BY SCANNING PROBE NANOTOMOGRAPHY

A.E. Efimov, O.I. Agapova, L.A. Safonova, M.M. Bobrova, I.I. Agapov

Shumakov National Medical Research Center of Transplantology and Artificial Organs, Moscow, Russian Federation

Objective: to analyze the 3D micro- and nanostructure and quantitative morphological parameters of rat lung tissue. **Materials and methods.** Wistar rat lung tissue samples were obtained for the study. The 3D structure of the lung tissue was studied via scanning probe nanotomography using an experimental setup combining an ultramicrotome and a scanning probe microscope. **Results.** Nanoscale images and 3D nanotomographic reconstructions of the interalveolar septal sections of the rat lung were obtained. Morphological parameters (average roughness and specific effective area) of the interalveolar septal surface were determined. It was found that the average roughness of the reconstructed septal surface was 345.4 ± 24.5 nm, and the specific effective area was 2.7 ± 0.2 units. **Conclusions.** Results obtained demonstrate that scanning probe nanotomography allows to quantify lung morphology. The use of scanning probe nanotomography for 3D analysis of the structure and characteristics of lung tissue will increase the efficiency of future developments on creation of new criteria for diagnosing pathological conditions.

Keywords: lung, alveolus, interalveolar septum, scanning probe microscopy, nanotomography.

INTRODUCTION

The development of methods for microscopic studies of the three-dimensional nanostructure of cells and tissues is extremely important for understanding the structural and molecular mechanisms responsible for their functionality and the timely detection of pathological changes. Thus, modern methods of studying the three-dimensional micro- and nanostructure of biological objects are of great importance, in particular, such high-resolution microscopy methods as scanning probe microscopy (SPM) and scanning electron microscopy with a focused ion beam (SEM/FIB) [1, 2].

Studies using SEM/FIP made it possible to reconstruct the three-dimensional organization of alveoli in mouse lung tissue [3] and myofibrils, T-tubules, sarcoplasmic reticulum and mitochondria in myocytes [4, 5]. The recent discovery of interconnected networks of mitochondria in muscle cells [6] convincingly proves that nanotomography techniques can effectively investigate three-dimensional relationships between cell organelles, compartments, and systems. These structures are almost impossible to fully characterize using conventional microscopic techniques, which only provide two-dimensional images and projections of cellular structures. However, SEM/FIB cannot be called the optimal method for the analysis of biological objects, since the used electron and ion beams can cause undesirable damage to the surface structure, and the contrast and resolution on SEM images of samples after exposure to an ion beam can be reduced [1, 2, 7, 8].

The physical principles of SPM imaging are fundamentally different from the principles of both optical and electron microscopy [9–11]. In the case of SPM, raster images of the topography and distributions of the physical properties of the sample surface are constructed by analyzing the features of the physical interaction of the ultra-sharp probe (cantilever) with the scanned surface. The integration of the technique for obtaining ultrathin sample sections (ultramicrotomy) with SPM methods within the framework of a single instrument complex makes it possible to implement the scanning probe nanotomography (SPN) technology [2]. Computer processing of a series of sequential SPM images of the sample surface obtained immediately after ultrathin sections makes it possible, using specialized software, to perform three-dimensional reconstruction of the micro- and nanostructure of the samples under study, which makes it possible to apply any SPM techniques for the tasks of three-dimensional analysis. Thus, the analysis of three-dimensional structures of tissues of various organs by the SPN method makes it possible to obtain unique information about their nanoscale organization, which is inaccessible to other methods. It is also important that the analysis of three-dimensional SPN-reconstructions of biological objects and materials makes it possible to quantitatively evaluate such important parameters of their nanomorphology as micro- and nanoporosity [12], effective surface area and roughness, surface area to volume ratio [13].

Corresponding author: Igor Agapov. Address: 1, Shchukinskaya str., Moscow, 123182, Russian Fedeartion.
Phone: (499) 190-66-19. E-mail: igor_agapov@mail.ru

The progress of SPN technology as applied to the study of organs and tissues may allow the development of new methods and criteria for diagnosing the state of organs of donors and patients for the tasks of modern transplantology. This paper presents studies of three-dimensional structures of rat lung tissue using SPN methods.

MATERIALS AND METHODS

Preparation of rat lung tissue samples for scanning probe nanotomography

Male Wistar rats (250–350 g weight) were used in the experiments. The operation with the animals was carried out under inhalation ether anesthesia. The rat was placed belly up on the operating table and the legs were straightened. The skin on the abdomen was pulled with tweezers, and a longitudinal skin incision was made on the midline of the abdominal side of the body from the genital opening to the sternum with scissors. The skin was turned away and secured. Then the chest cavity was opened, the lungs were taken, cutting off the trachea and arteries. After sampling, the lungs were placed in a sodium phosphate buffer solution (pH = 7.4) and washed from blood.

For preparation for SPN, fragments of lung tissue 3 × 3 mm in size were excised with a scalpel. Then, to fix the obtained samples, the fragments were placed in a 2.5% solution of glutaraldehyde in sodium phosphate buffer (pH = 7.4) and incubated for 2 hours in the dark at + 4 °C. Then there were three washes of the samples in sodium phosphate buffer for 10 minutes. After that, the samples were dehydrated by wiring through alcohols with increasing concentration by the following pattern:

a) 30% ethanol solution – 10 min;
b) 50% ethanol solution – 10 min;
c) 70% ethanol solution – 10 min;
d) 80% ethanol solution – 10 min;
e) 96% ethanol solution – 10 min.

Next, the samples were washed three times in propylene oxide for 10 minutes each, and then incubated in a mixture of propylene oxide and epoxy resin in a 1:1 ratio for 30 minutes, after which the samples were transferred into a mixture of propylene oxide and epoxy resin in a ratio of 1:2 and incubated for 30 minutes. Then the samples were embedded in epoxy resin, incubated in a thermostat at 45 °C for 24 hours, after which the incubation was continued for 48 h at 60 °C.

To fill the samples, an epoxy medium (Epoxy Embedding Medium, Sigma-Aldrich, cat. No. 45345) was used, mixed with an equal weight of the embedding medium hardener (dodecenyl succinic anhydride, Sigma-Aldrich, USA, cat. No. 45346) and 4% by weight DMP-30 (Sigma-Aldrich, USA, cat # 45348).

Scanning probe nanotomography of rat lung tissue samples

Ntegra Tomo experimental device was used to study samples of rat lung tissue by SPN methods. This complex allows for sequential SPM measurements of the sample surface immediately after cutting with an ultramicrotome. Consecutive sections of a 60 nm thick sample were made using a Diatome Ultra AFM 35 diamond knife (Diatome AG, Switzerland) with a cutting-edge width of 2.0 mm.

SPM measurements were performed in the semicontact mode at a scanning speed of 1.0 Hz using NSG10 silicon cantilever probes (NT-MDT, Moscow) with a resonance frequency of 240 kHz and a tip curvature radius of <10 nm. Primary image processing was carried out using the Nova ImageAnalysis 1.0.26.1443 software (NT-MDT, Moscow), three-dimensional tomographic reconstructions of the lung structure were obtained using the ImagePro Plus 6.0 software (Media Cybernetics, Inc, USA).

Calculation of morphological parameters of 3D surfaces

Analysis of the surfaces reconstructed by the SPN method using the ImagePro Plus 6.0 software (Media Cybernetics, Inc, USA) allows one to determine and analyze the nanoscale parameters of these surfaces, such as the average roughness R_a and the effective surface area σ.

To calculate these parameters, the reconstructed surface is considered as a two-dimensional data array (values of heights Z) of size $N \times M$, where N and M are the number of columns and rows, respectively. Before calculations, a first-order surface (plane) is subtracted from the surface, which corresponds to the elimination of the slope.

Average surface roughness R_a is calculated as the average value of the modulus of the deviation of the height of the array points from the average height:

$$R_a = \frac{1}{N}\frac{1}{M}\sum_{i=1}^{N}\sum_{j=1}^{M}|Z_{i,j} - \langle Z\rangle|, \quad (1)$$

where $Z_{i,j}$ – the height value at a point in the array (i, j), $\langle Z\rangle$ – average height Z, averaged over the entire array:

$$\langle Z\rangle = \frac{1}{N}\frac{1}{M}\sum_{i=1}^{N}\sum_{j=1}^{M}Z_{i,j}. \quad (2)$$

Effective surface area σ is calculated as the ratio of the surface area to the area of its two-dimensional projection onto the plane. This parameter determines the degree of surface development [14]. Reconstructed surface area S is calculated using the triangulation method as a sum over an array of elementary areas $s_{i,j}$ of the surfaces of unit cells between 4 adjacent points of the array (i, j), $(i + 1, j)$, $(i, j + 1)$, $(i + 1, j + 1)$. When using the triangulation

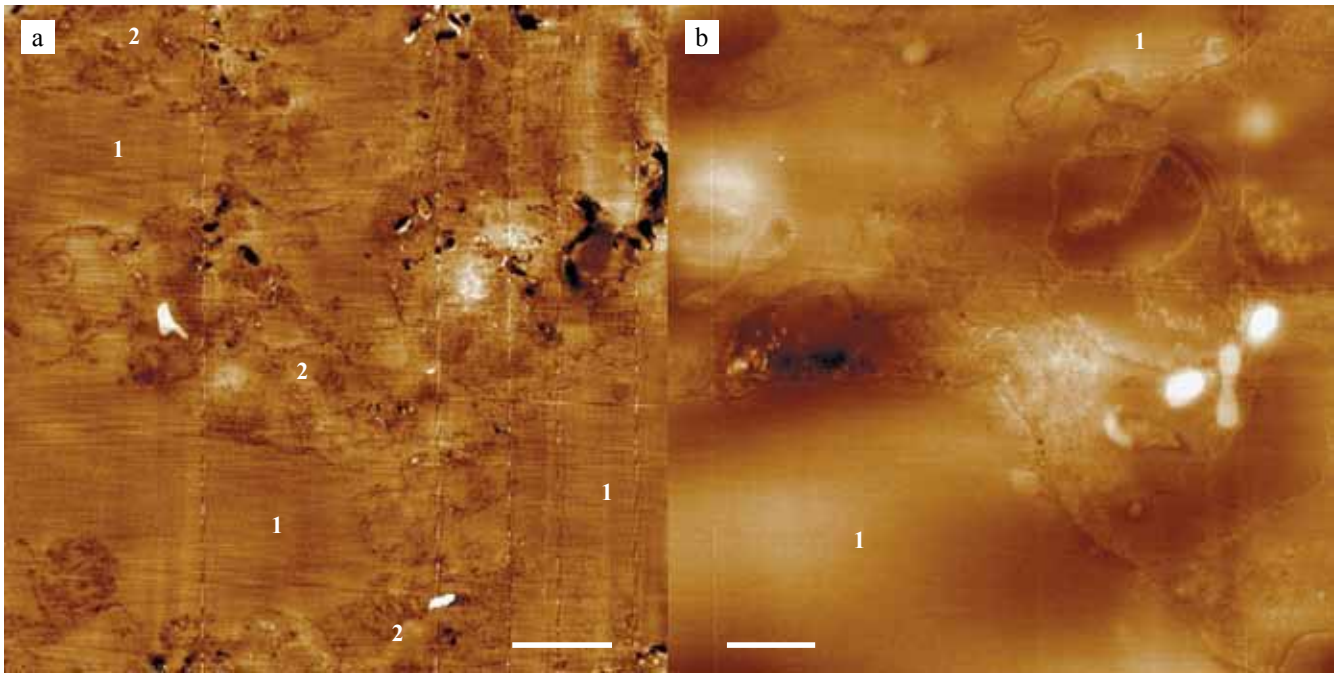

Fig. 1. SPM topography image of surface areas of rat lung tissue after ultramicrotome section: a – SPM image of region of respiratory lung area, scan size 65×65 μm, height variation 18 nm, scale bar 10 μm; б – SPM image of region of alveolar septum, scan size 15×15 μm, height variation 48 nm, scale bar 2 μm; 1 – areas of alveolus; 2 – areas of alveolar septum

method to calculate the elementary area, the midpoint is also entered with height $\langle Z_{i,j}\rangle = (Z_{i,j} + Z_{i+1,j} + Z_{i,j+1} + Z_{i+1,j+1})/4$ and effective coordinates $(i + 1/2, j + 1/2)$, and the elementary area is calculated as the area of four triangles, each of which is formed by adjacent unit cell vertices and a midpoint. So, for example, the area of a triangle formed by points (i, j), $(i + 1, j)$ and the midpoint is given by:

$$\frac{d_x d_y}{4}\sqrt{1+\left(\frac{Z_{i,j}-Z_{i,j+1}}{d_x}\right)^2+\left(\frac{2\langle Z_{i,j}\rangle - Z_{i,j}-Z_{i,j+1}}{d_y}\right)^2}, \quad (3)$$

where d_x и d_y – physical dimensions of pixels along the corresponding axes. Since we are using a surface reconstructed by the SPN method, in our case d_x will be determined by the pixel resolution of the SPM measurement, and d_y – by the slice thickness between successive SPM measurements. Accordingly, the effective surface area will be set as

$$\sigma = \frac{1}{Nd_x}\frac{1}{Md_y}\sum_{i=1}^{N}\sum_{j=1}^{M} s_{i,j}. \quad (4)$$

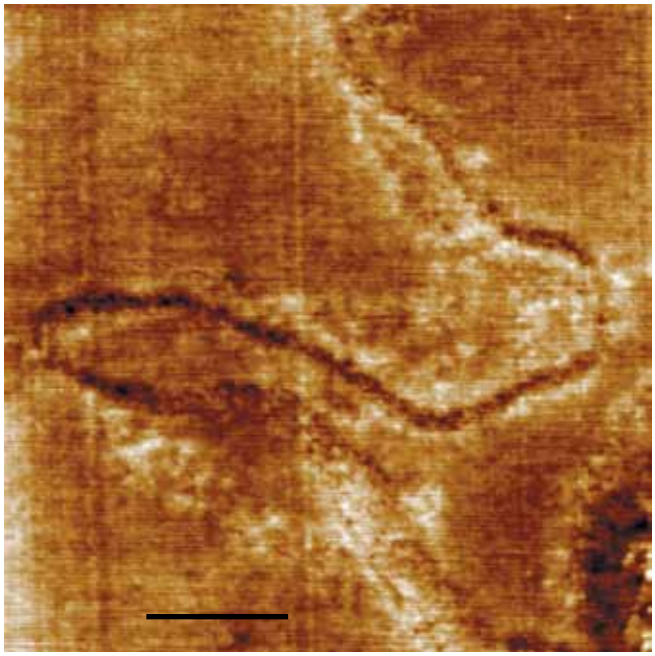

Fig. 2. SPM topography image of surface of alveolar septum surface folding; scan size 2.5×2.5 μm, height variation 13 nm, scale bar 500 nm

RESULTS AND DISCUSSION

Fig. 1, a, shows an example of the obtained SPM image (65 × 65 μm) of a section of the respiratory part of the lung. In this image, one can distinguish areas of bubbles with sizes of about 20–30 μm and nanostructured interalveolar septa with a width of 10–20 μm. In Fig. 2 shows an SPM image (15 × 15 μm) of a portion of the interalveolar septum between two regions of the bubbles. This image shows that the interalveolar septum has a complex nanoscale morphology and a pronounced nanostructure. The topology and morphological parameters of the septa are of great importance for the functionality of the alveoli and the efficiency of gas exchange processes [15, 16].

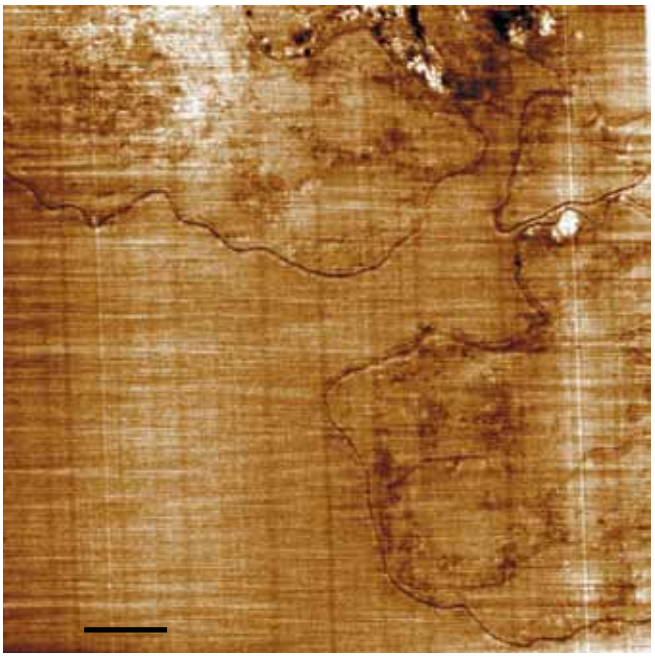

Fig. 3. SPM topography image of the surface of a region of alveolar septum border with a alveolus; scan size 16×16 μm, height variation 24 nm, scale bar 2 μm

The SPN technology used makes it possible to study the nanoscale features of the surface of the interalveolar septum with high resolution. In Fig. 2 shows an enlarged image (2.5 × 2.5 μm) of a section of the folds of the surface of the interalveolar septum, characterized by a complex shape and nanostructure and surrounded by a surfactant film.

Also, the most important advantage of the SPN method is the possibility of three-dimensional reconstruction of tissue structures, in particular, the surface of the septum. In Fig. 3 shows an SPM image of a fragment of the region of the interface of the interalveolar septum with a bubble (16 × 16 μm), which has a complex morphology. To assess the three-dimensional morphology of the interalveolar septum, a three-dimensional reconstruction of this area was performed using the SPN method. For this, 10 successive sections of a sample with a thickness of 120 nm were made, and 10 successive SPM images of a 16 × 16 μm surface area were obtained. The resulting visualization of the three-dimensional surface is shown in Fig. 4.

It should be noted that the complex morphology of the surface of the interalveolar septum is characterized by a significant increase in the effective area. Specialized software used for visualization of three-dimensional reconstructions makes it possible to determine both the surface roughness of the partition Ra and the specific effective area of its surface σ, calculated as the ratio of the area of the three-dimensional surface to the area of its projection onto the plane. For the three-dimensional reconstruction we have obtained, the value of the specific

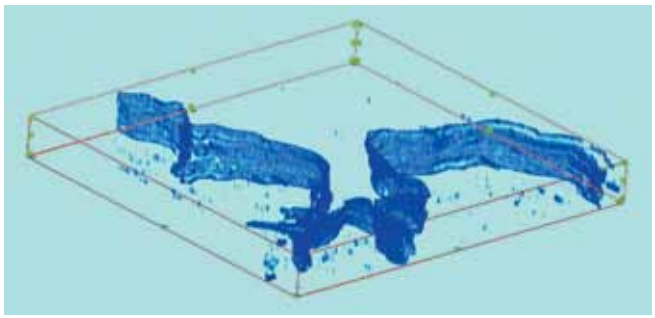

Fig. 4. SPNT three-dimensional reconstruction of a fragment of surface of the alveolar septum: reconstructed volume 16×16×1.2 μm, section thickness 120 nm

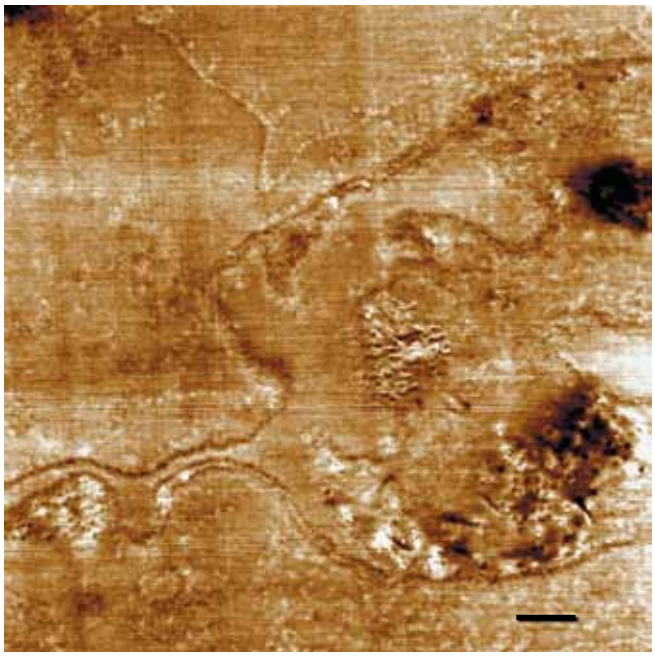

Fig. 5. SPM topography image of the surface area of an inner alveolus; scan size 5.5×5.5 μm, height variation 17 nm, scale bar 500 nm

effective area σ is 2.7 ± 0.2, which indicates a high degree of surface development. The nanoroughness of the reconstructed three-dimensional surface Ra is 345.4 ± 24.5 nm.

Interestingly, the surface of the interalveolar septum often forms bends and folds, resulting in the formation of internal vesicles or sacs several microns in size with a narrow entrance slit. An example of an image of such a structure is shown in Fig. 5. Note that the width of the air "neck" of this inner bubble is about 120 nm, and the surface of the partition in the inner region thickens and has a heterogeneous structure. These structures are associated with the processes of gas exchange in the alveoli.

The developed technique for studying the nanoscale structures of the alveoli with the scanning probe nanotomography is applicable to solving a number of problems in structural biology, for example, the urgent

problem of studying the three-dimensional organization of interalveolar septa and determining their quantitative morphological parameters at the nanoscale.

CONCLUSION

In the present work, studies of the nanostructural features of rat lung tissue were carried out using the SPN method. 3D reconstruction of the surface of the interalveolar septum in rat lung tissue was obtained. It is shown that the complex three-dimensional morphology of its surface is characterized by a significant increase in the effective surface area of the partition. The specific effective surface area σ of the reconstructed section of the interalveolar septum is 2.7 ± 0.2, which indicates a high degree of surface development.

SPN technology allows obtaining unique information about the relationship between nanoscale features of the structure and functional activity of cells and tissues.

This work was partially supported by the grant of the President of the Russian Federation for state support of leading scientific schools of the Russian Federation NSh-2598.2020.7.

The authors declare no conflict of interest.

REFERENCES

1. *Zankel A, Wagner J, Poelt P.* Serial sectioning methods for 3D investigations in materials science. *Micron*. 2014; 62: 66–78. doi: 10.1016/*j*.micron.2014.03.002.
2. *Alekseev A, Efimov A, Loos J, Matsko N, Syurik J.* Three-dimensional imaging of polymer materials by Scanning Probe Tomography. *Eur Polym J.* 2014; 52: 154–165. doi: 10.1016/*j*.eurpolymj.2014.01.003.
3. *Kremer A, Lippens S, Bartunkova S, Asselbergh B, Blanpain C, Fendrych M et al*. Developing 3D SEM in a broad biological context. *J Microsc.* 2015; 259 (2): 80–96. doi: 10.1111/jmi.12211.
4. *Sulkin MS, Yang F, Holzem KM, Van Leer B, Bugge C, Laughner JI et al*. Nanoscale three-dimensional imaging of the human myocyte. *J Struct Biol*. 2014; 188 (1): 55–60. doi: 10.1016/*j*.jsb.2014.08.005.
5. *Dahl R, Larsen S, Dohlmann TL, Qvortrup K, Helge JW, Dela F, Prats C.* Three-dimensional reconstruction of the human skeletal muscle mitochondrial network as a tool to assess mitochondrial content and structural organization. *Acta Physiol*. 2015; 213: 145–155. doi: 10.1111/apha.12289.
6. *Glancy B, Hartnell LM, Malide D, Yu Z-X, Combs CA, Connelly PS et al*. Mitochondrial reticulum for cellular energy distribution in muscle. *Nature*. 2015; 523: 617–620. doi: 10.1038/nature14614.
7. *Bailey RJ, Geurts R, Stokes DJ, de Jong F, Barber AH.* Evaluating focused ion beam induced damage in soft materials. *Micron*. 2013; 50: 51–56. doi: 10.1016/*j*.micron.2013.04.005.
8. *Linkov P, Artemyev M, Efimov AE, Nabiev I.* Comparative advantages and limitations of the basic metrology methods applied to the characterization of nanomaterials *Nanoscale.* 2013; 5: 8781–8798. doi: 10.1039/c3nr02372a.
9. *Binnig G, Quate CF, Gerber C.* Atomic force microscope. *Phys Rev Lett.* 1986; 56 (9): 930–933. doi: 10.1103/PhysRevLett.56.930.
10. *Magonov SN, Reneker DH.* Characterization of polymer surfaces with atomic force microscopy. *Annu Rev Mater Sci.* 1997; 27 (1): 175–222. doi: 10.1146/annurev.matsci.27.1.175.
11. *Gallyamov MO.* Scanning Force Microscopy as Applied to Conformational Studies in Macromolecular Research. *Macromol Rapid Commun.* 2011; 32 (16): 1210–1246. doi: 10.1002/marc.201100150.
12. *Efimov AE, Moisenovich MM, Bogush VG, Agapov II.* 3D nanostructural analysis of silk fibroin and recombinant spidroin 1 scaffolds by scanning probe nanotomography. *RSC Adv.* 2014; 4: 60943–60947. doi: 10.1039/c4ra08341e.
13. *Efimov AE, Agapova OI, Safonova LA, Bobrova MM, Parfenov VA, Koudan EV et al*. 3D scanning probe nanotomography of tissue spheroid fibroblasts interacting with electrospun polyurethane scaffold. *Express Polymer Letters.* 2019; 13 (7): 632–641. doi: 10.3144/expresspolymlett.2019.53.
14. *Gómez-Pozos H, González-Vidal JL, Torres GA, de la Luz Olvera M, Castañeda L.* Physical Characterization and Effect of Effective Surface Area on the Sensing Properties of Tin Dioxide Thin Solid Films in a Propane Atmosphere. *Sensors.* 2014; 14: 403–415. doi: 10.3390/s140100403.
15. *Hsia CCW, Hyde DM, Ochs M, Weibel ER.* How to Measure Lung Structure – What For? On the "Standards for the Quantitative Assessment of Lung Structure". *Respir Physiol Neurobiol*. 2010; 171 (2): 72–74. doi: 10.1016/*j*.resp.2010.02.016.
16. *Yang L, Feuchtinger A, Möller W, Ding Y, Kutschke D, Möller G et al*. Three-Dimensional Quantitative Co-Mapping of Pulmonary Morphology and Nanoparticle Distribution with Cellular Resolution in Nondissected Murine Lungs. *ACS Nano.* 2019; 13 (2): 1029–1041. doi: 10.1021/acsnano.8b07524.

The article was submitted to the journal on 22.06.2020

DOI: 10.15825/1995-1191-2020-3-149-155

INFLUENCE OF MICROEMULSION COMPONENTS ON TRANSDERMAL DELIVERY OF IMMUNOMODULATOR GLUCOSAMINYLMURAMYL DIPEPTIDE

E.G. Kuznetsova[1], O.M. Kuryleva[1], L.A. Salomatina[1], S.V. Kursakov[2], S.V. Guryanova[3, 4], V.I. Sevastyanov[1, 2]

[1] Shumakov National Medical Research Center of Transplantology and Artificial Organs, Moscow, Russian Federation
[2] Institute for Biomedical Research and Technology, Moscow, Russian Federation
[3] Peoples' Friendship University of Russia, Moscow, Russian Federation
[4] Shemyakin–Ovchinnikov Institute of Bioorganic Chemistry, Moscow, Russian Federation

This paper demonstrates a chemical way of enhancing transdermal delivery using immunomodulator glucosaminylmuramyl dipeptide (GMDP) as an example. **Objective:** to study *in vitro* the effect of various components of the microemulsion composition on GMDP diffusion through the skin from a transdermal therapeutic system (TTS). **Materials and methods.** Medicinal substance – glucosaminylmuramyl dipeptide (Peptek, Russia). Excipients and raw materials: sodium chloride, purified water, sodium dodecyl sulfate, docusate sodium, oak bark, apricot kernel oil, alpha-tocopheryl acetate and Decaglyn PR-20 emulsifier. Equipment: Heidolph DIAX 900 mechanical disperser (Germany) and Hielscher UIS250V ultrasonic homogenizer (Germany). GMDP diffusion from TTS through unpreserved rabbit skin was studied on diffusion tester Copley (UK). GMDP in aqueous solutions was determined by reversed-phase high-performance liquid chromatography (RP-HPLC) on an Agilent 1200 chromatography system (Agilent Technologies, USA). **Results.** A microemulsion system composed of 20% docusate sodium in an oil phase and an oak bark decoction as an aqueous phase was developed. This made it possible to increase GMDP transdermal delivery by ~70% in comparison with the basic composition. **Conclusion.** The characteristic parameters of microemulsion components of GMDP contained in TTS, influencing GMDP diffusion through unpreserved rabbit skin *in vitro*, were determined. Introducing relative indicators would be advisable in order to correctly evaluate the results of different series of *in vitro* experiments with biological objects.

Keywords: transdermal therapeutic system, microemulsion, immunomodulator, drug diffusion.

INTRODUCTION

Currently, 74% of all drugs are administered orally, but such a dosage form often does not have sufficient efficacy due to low bioavailability. To increase it, intact skin can be used as a route of administration, which requires the creation of an appropriate dosage form, namely the transdermal therapeutic system (TTS) [1].

The major problem in the development of transdermal delivery systems is overcoming the medicinal substance (MS) of the skin barrier, and mainly the stratum corneum. Researchers use various chemical, physical, or combined approaches to increase cutaneous absorption and percutaneous diffusion, the choice of which is determined by the characteristic properties of MS [1, 2].

Physical methods always imply the use of a device, which makes this method of enhancing skin permeability expensive and not always convenient for the patient to use [2].

The essence of the chemical method is either modifying the MS molecules or introducing transfer activators into the TTS, which can directly affect the skin structure. They are often administered as part of complex formulations, such as micro- and nanoemulsions, biphasic vesicles, spheroid particles, or liposomes [3].

In our opinion, the most effective of the above chemical methods for enhancing transdermal MS delivery include nano- and microemulsions due to the possibility of a wide selection of transfer activators for a specific drug substance, ease of manufacture, and low cost. In addition, the submicron size of the dispersed phase and the high sorption capacity of microemulsions make it possible to achieve a noticeable increase in the diffusion of some MS through the skin. When MS is introduced into emulsions, in some cases it becomes possible to avoid hydrolysis, decomposition and oxidation of the introduced substances [4]. Also, when using them, it is possible to prevent skin irritation, which is sometimes observed upon contact with an active substance [4–7]. We have proved the prospects of using microemulsion compositions when creating TTS with such medicinal

Corresponding author: Evgeniya Kuznetsova. Address: 1, Shchukinskaya str., Moscow, 123182, Russian Federation. Phone: (499) 196-26-61. E-mail: kuzeugenia@gmail.com

substances as insulin, bromocaine, caffeine, and others [8–10]. The choice of components and their ratio in the microemulsion composition depends on the nature of the drug substance [5, 6, 11].

The range of drugs that can be used in the form of TTS using microemulsions is quite wide. The greatest interest in recent years is represented by drugs from the pharmacological group of immunomodulating agents. Delivery of an immunomodulator (MI) in the form of TTS, if it is necessary to maintain its constant concentration in the blood, can be relevant for a number of patients: children, people with difficulty chewing and swallowing, bedridden patients, including those in serious condition with infectious diseases.

Glucosaminylmuramyl dipeptide (GMDP), a synthetic analogue of the structural fragment of the membrane (peptidoglycan) of bacterial cells, is an activator of innate and acquired immunity, enhances the body's defense against viral, bacterial and fungal infections, and has an adjuvant effect in the development of immunological reactions [12].

In Russia, the drug with GMDP is produced only in the form of tablets under the trade name Likopid® (registration certificate No. LS-001438) [13]. The high efficiency and safety of GMDP use, confirmed by the results of clinical trials [14], determine the prospects for the development of its new dosage forms, including the transdermal therapeutic system.

When developing the composition of multicomponent microemulsions, a necessary stage is a comparative analysis of the contribution of the main components of the emulsion composition to the percutaneous transfer of a particular MS.

The **purpose** of this work is to study in vitro the effect of various components of the microemulsion composition on the diffusion of GMDP through the skin from a transdermal therapeutic system.

MATERIALS AND METHODS

When developing various formulations of emulsion compositions for TTS, excipients were used that were approved for medical use and that meet the requirements of the current regulatory documentation.

Glucosaminylmuramyl dipeptide ($C_{25}H_{43}N_5O_{15}$) produced by JSC Peptek, Russia was taken as a drug substance.

For the *production of microemulsion* purified water (FS 42-2620-97, distiller DE-10 and filter "MILLIPORE SIMPAKOR 1"); 0.9% sodium chloride solution (solution for infusion of JSC NPK ESCOM); sodium dodecyl sulfate (CAS 151-21-3, Appli Chem Panreac, Spain); oak bark (Krasnogorskleksredstva JSC, Russia); apricot kernel oil (CAS 72869-69-3, Desert Whale Jojoba Company Ltd., USA); sodium docusate (DNS) (D4422-50G, Sigma, USA); alpha-tocopherol acetate (Customer Product # 4904352421, BASF SE, Germany); emulsifier NIKKOL Decaglyn PR-20 (CAS 29894-35-7, Nikko Chemicals Co., Ltd, Japan) were used.

The sorbing layer of the dressing (PALV-01, Palma Group, Russia) served as a depot of the microemulsion composition in the transdermal therapeutic system, and the Skotchpak film (97303M, USA) served as a waterproof protective base.

The following reagents were used to determine *GMDP by the HELC* method: acetonitrile (for UHPLC, AppliChem GmbH – AnITWCompany, Germany); potassium hydrogen phosphate (extra pure, Scharlab S.L., Spain); potassium dihydrogen phosphate (extra pure, Scharlab S.L., Spain).

Equipment used: analytical balance (GH-200 AND, Japan); magnetic stirrer with heating (IKA, Germany); mechanical submersible disperser (T18 basic Ultra-Turrax IKA-WERKE Gmbh & Co. Kg, Germany); ultrasonic homogenizer (UIS 250V Heilscher, Germany); drug diffusion analyzer (HDT 1000 Copley Scientific Ltd., UK); dispersion analyzer (LUMi Sizer, Germany); spectrophotometer (UV-2600 Shimadzu, Japan); moisture analyzer (MX-50 AND, Japan); chromatographic system (1200 Agilent Technologies, USA).

Production of laboratory GMDP TTS samples

The manufacture of laboratory samples of microemulsion TTS GMDP was carried out according to the previously developed method [8]. Each 1 cm^2 TTS contained 0.1 g of microemulsion composition.

Preparation of oak bark decoction

5 g sample of oak bark was placed in a 200 ml conical flask and 100 ml of purified water was poured, then heated to 90 °C in a water bath for 30 minutes. Thereafter, it was cooled to room temperature over 1 hour. Then the broth was poured into a 100 ml volumetric flask through filter paper and the volume was brought up to the mark with purified water. In a volumetric flask with a volume of 100 ml was placed 10 ml of a decoction of oak bark and the volume was brought up to the mark with purified water.

Determination of moisture content in oak bark

Moisture content of oak bark was determined in accordance with the requirements of GPM 1.5.3.0007.15 "Determination of the moisture content of medicinal plants and herbal medicinal products" with a moisture analyzer. The moisture content W of raw materials in percent was calculated by the formula:

$$W = \frac{(m - m_1) \times 100}{m},$$

where m – mass before drying, g; m_1 – mass after drying, g.

The moisture content of raw was (8.2 ± 0.8)%, n = 5.

Determination of tannins content in oak bark concoction

The content of tannins in plant raw was determined by spectrophotometry at 277 nm wavelength (Guidelines for quality control methods and safety of biologically active food additives. Guidelines. R 4.1.1672-03, 2004). An aliquot of the decoction of oak bark, equal to 1 ml, was placed in a 50 ml volumetric flask and made up to the mark with purified water. Purified water was used as a reference solution. The total content of tannins in the bark of oak X,% in terms of gallic acid was calculated by the formula:

$$X = \frac{D_1 \times V_1 \times V_2 \times 100\%}{D_2 \times V_3 \times m \times (100\% - W) \times 1000},$$

where D_1 – optical density of the test solution; D_2 – optical density of a solution of gallic acid with 1 mg/ml (0.508) concentration; m – weight of raw sample, g; V_1 – total volume of aqueous extract, 100 ml; V_2 – flask volume at dilution, 50 ml; V_3 – aliquot volume, 1 ml; W – raw moisture, %.

Research methods for emulsion compositions

The particle size of the microemulsion composition with GMDP by the time of its separation were determined with a dispersion analyzer in infrared light (865 nm) at 40 °C. Light transmission profiles were recorded every 600 seconds at a rotor speed of 4000 rpm, the light factor was chosen equal to 3.

Laboratory animals

In *in vitro* experiments to study the diffusion of the immunomodulator from TTS, the skin of male New Zealand White rabbits was used, weighing 2–2.5 kg, obtained from the laboratory animal nursery of KrolInfo LLC. All manipulations with animals were carried out in accordance with the rules adopted by the European Convention for the Protection of Vertebrate Animals Used for Experimental and other Scientific Purposes (ETS 123) Strasbourg, 1986).

In vitro study of medical substance diffusion through skin

After euthanasia of an animal, the skin flap was taken from the abdomen with previously removed hair cover.

The dynamics of the release of GMDP from TTS was studied in Franz glass diffusion cells according to the standard technique [9]. The duration of the experiments was 24 hours. Samples of GMDP aqueous solutions taken during the experiment from the receiving chambers of the diffusion cells were studied by the HELC method.

The amount of MS passing through unconserved rabbit skin from the TTS contact area (ω) was calculated as follows:

$$\omega = \frac{C \times V}{M} \times 100\%,$$

where C – GMDP concentration in the receiving chamber of the Franz diffusion cell, mg/ml; V – diffusion cell receiving chamber volume, ml; M – GMDP content in TTS in the contact area, mg.

The rate of transdermal MS diffusion can be very different in laboratory animals, even in the same litter, due to the different thickness and density of the skin flap. In this regard, a comparative analysis of the effect of different compositions of the microemulsion composition for TTS on the percutaneous transfer of MS is expedient to be carried out in relative units. The relative amount $\omega_{rel}(i, j)$ was calculated using the following formula:

$$\omega_{rel(i\,j)} = \frac{\omega_j}{\omega_i},$$

where i, j – microemulsion composition numbers (Table 2).

HELC method for study of aqueous GMDP solutions

Earlier, the authors developed a method for the quantitative determination of glucosaminylmuramyldipeptide in aqueous solutions by the method of reverse phase HELC [12].

Chromatographic separation was carried out in an isocratic mode on a MediterraneaSea18 column 15 × 0.4 cm, 5 μm (Teknokroma Analitica SA, Spain), with an 8 × 4 mm guard column filled with the same sorbent. The temperature of the column thermostat is –25 °C. The volume of the injected sample is 10 μl. The mobile phase is a mixture of acetonitrile: 25 mM phosphate buffer solution (3:97), pH 7.3. A phosphate buffer solution was prepared by mixing 25 mM K_2HPO_4 solution with 25 mM KH_2PO_4 solution in a ratio of 80:20. The eluent was prefiltered and degassed on a vacuum filtration device. The flow rate of the mobile phase is 0.7 ml/min. Detection was carried out at a wavelength of 200 nm, corresponding to the absorption maximum of GMDP. The chromatography time was 10 min, the retention time of the GMDP anomers was about 3.3 and 4.9 min.

Registration and processing of chromatographic data were performed with ChemStation software (Agilent Technologies, USA). Statistical processing of the results was performed in accordance with GMP.1.1.0013.15 "Statistical processing of the results of a chemical experiment" with Microsoft Office Excel 2010.

RESULTS AND DISCUSSION

As a microemulsion composition for TTS GMDP, the basic composition was chosen (Table 1), which we developed earlier for the transfer of drugs of various pharmacological groups and molecular weights through

Table 1

The base composition № 1 of the microemulsion composition

	Substance	TTS indication	Characteristics
Aqueous phase	Purified water	Aqueous phase base	GMP 42-2620-97
	GMDP	Medical substance	White hydrophilic powder
Oil phase	Apricot kernel oil	Base of oil phase	Contains linoleic (30–45%) and oleic (55–70%) acids
	α-tocopherol acetate	Skin disintegrant and antioxidant	Lipophilic liquid
	Sodium dokuzat	MS carrier	Amphiphilic anionic detergent
	Decaglyn PR-20	Emulsifier	Lipophilic surfactant with hydrophilic-lipophilic balance of 3.2

Table 2

Changes in microemulsion compositions with GMDP compared with the base composition

Composition #	Aqueous phase	Oil phase
2	Decrease in volume of purified water by 1.9 times	Volume increase by 1.7 times
3	Sodium dodecyl sulfate 0.5% solution	Similar to base composition
4	0.9% sodium chloride solution	Similar to base composition
5	Similar to base composition	Increase in sodium docusate content from 15 to 20%
6	Decoction of oak bark (concentration of gallic acid 2.60 ± 0.18%, n = 5)	Increase in sodium docusate content from 15 to 20%

the skin, such as insulin [10], anilocaine [9], sodium aminodihydrophthalazinedione [8].

At choosing vegetable oils for application dosage forms, the fatty acid composition is of particular importance [15, 16]. The basis of the oil phase of the microemulsion composition was the oil of apricot kernels (acid number 0.04), which contains a large amount of oleic acid (from 55 to 70%), due to which it is well absorbed into the deep layers of the skin and enhances the penetration of active components into the stratum corneum. In addition, apricot kernel oil has a low viscosity, which makes it possible to use it as a solvent for lipophilic drug transfer activators, in our case, vitamin E and sodium docusate.

The selected microemulsion composition containing GMDP had a particle size of 1 to 15 μm and a very high stability: it only partially separated when centrifuged and heated to 40 °C for 12 hours. This stability of the microemulsion can be explained by the fact that medicinal substances of a protein nature can act as a stabilizer. The authors observed a similar effect when developing emulsion insulin TTS [10].

The investigated medical substance, glucosaminylmuramyldipeptide, has a small molecular weight (695.67 g/mol) in terms of transdermal transfer in comparison, e. g., with insulin (5500 g/mol). However, the amount of GMDP (ω) diffused from TTS from the contact area through unconserved skin in vitro in 24 hours was only (14.4 ± 3.0)% (n = 10) of that contained in the sample.

To clarify the role of one or another component of the microemulsion composition in the transdermal diffusion of MS (at its constant concentration in TTS of 46 mg/g), 5 microemulsion compositions were prepared (Table 2), which differ from the pre-selected (base) composition No. 1 in the following parameters: change in the amount of the oil phase; increasing the concentration of the sodium docusate transfer activator in the oil phase; the introduction of hydrophilic activators for the transdermal transfer of sodium dodecyl sulfate or sodium chloride; the use of oak bark decoction as an aqueous phase of a microemulsion, a well-known source of biologically active substances used in medical practice in the treatment of skin diseases [17].

Table 3 shows the results of percutaneous diffusion of GMDP from TTS with different compositions of the microemulsion composition for 24 hours *in vitro* in relative values.

Changes to the base microemulsion composition in the case of formulations # 2, 3 and 4 did not lead to an

Table 3

Relative amount of GMDP (%) passed through unreserved rabbit skin, for TTS of various composition

Microemulsion composition #	Relative amount $\omega_{rel(i,j)}$
2	$\omega_{rel(1,2)} = 0.62 \pm 0.24$
3	$\omega_{rel(1,3)} = 0.85 \pm 0.14$
4	$\omega_{rel(1,4)} = 0.68 \pm 0.05$
5	$\omega_{rel(1,5)} = 1.44 \pm 0.30$
6	$\omega_{rel(5,6)} = 1.16 \pm 0.19$
	$\omega_{rel(1,6)} = 1.67 \pm 0.26$

increase in the yield of GMDP from TTS through unconserved rabbit skin.

For TTS with microemulsion formulation # 5, in which the concentration of docusate sodium salt transporter in the oil phase was 20%, an increase in transdermal transfer of GMDP was observed by 44% compared to base formulation # 1 containing 15% of the same carrier. The use of an aqueous extract of oak bark (composition No. 6) as a dispersed phase of a microemulsion made it possible to further increase the percutaneous diffusion of GMDP in comparison with composition # 5 by another 16%.

Thus, the simultaneous increase in the sodium docusate content in the oil phase to 20% and the use of an aqueous extract of oak bark (composition No. 6) led to an increase in the transdermal transfer of GMDP by 67% compared to the base composition.

CONCLUSION

The effect of changes in the composition and phase ratio of microemulsion compositions on the diffusion of GMDP from TTS through unconserved rabbit skin *in vitro* was studied.

The developed composition of the microemulsion composition containing 20% sodium docusate in the oil phase and a decoction of oak bark as the aqueous phase made it possible to increase the transdermal transfer of GMDP by about 70% compared to the basic composition used by us in the development of the TTS series [8–10].

For a correct assessment of the results of different series of in vitro experiments with biological objects, it is advisable to introduce relative indicators.

The authors declare no conflict of interest.

REFERENCES

1. *Marwah H, Garg T, Goyal AK, Rath G*. Permeation enhancer strategies in transdermal drug delivery. *Journal Drug Delivery.* 2016; 23: 564–578. doi: 10.3109/10717544.2014.935532.
2. *Huzill JT, Sivaloganathan S, Kohandel M, Foldvari M*. Drug delivery through the skin: molecular simulations of barrier lipids to design more effective noninvasive dermal and transdermal delivery systems for small molecules, biologics, and cosmetics. www.wiley.com/wires/nanomed.
3. *Otto A, du Plessis J, Wiechers JW*. Formulation effects of topical emulsions on transdermal and dermal delivery. *International Journal Cosmetic Science*. 2009; 31 (1): 1–19. doi: 10.1111/*j*.1468-2494.2008.00467.x.
4. *Kogan A, Garti N*. Microemulsions as transdermal drug delivery vehicles. *Advances in Colloid and Interface Science*. 2006; 123–126: 369–385. doi: 10.1016/*j*.cis.2006.05.014.
5. *Azeem A, Khan ZI, Aqil M, Ahmad FJ, Khar RK, Talegaonkar S*. Microemulsions as a surrogate carrier for dermal drug delivery. *Drug Development and Industrial Pharmacy.* 2009; 35 (5): 525–547. doi: 10.1080/03639040802448646.
6. *Lopes LB*. Overcoming the cutaneous barrier with microemulsions. *Pharmaceutics*. 2014; 6 (1): 52–77. doi: 10.3390/pharmaceutics6010052.
7. *Heuschkel S, Goebel A, Neubert RH*. Microemulsions – modern colloidal carrier for dermal and transdermal drug delivery. *Journal of Pharmaceutical Sciences*. 2008; 97 (2): 603–631. doi.org/10.1002/jps.20995.
8. *Kuznetsova EG, Kuryleva OM, Salomatina LA, Sevastyanov VI*. Eksperimental'noe issledovanie diffuzii immunomodulyatora Galavit® v model'noj sisteme. *Razrabotka i registraciya lekarstvennyh sredstv.* 2020; 9 (1): 92–97. doi: 10.33380/2305-2066-2020-9-1-92-97. (in Russ., English abstract).
9. *Ryzhikova VA, Tikhobayeva AA, Salomatina LA, Kursakov SV, Kuznetsova EG, Kuryleva OM, Sevastyanov VI*. Effect of the transfer activator on functional properties of the bromocain matrix transdermal therapeutic systems. *Inorganic Materials: applied research*. 2014: 5 (5): 498–503. doi: 10.1134/s2075113314050177.
10. *Kuznetsova EG, Ryzhikova VA, Salomatina LA, Sevastyanov VI*. Issledovanie harakteristicheskih parametrov mikroemul'sionnoj kompozicii dlya transdermal'noj dostavki insulina. *Razrabotka i registracija lekarstvennyh sredstv.* 2017; 2: 66–72. (In Russ., English abstract).
11. *Date AA, Patravale VB*. Microemulsions: applications in transdermal and dermal delivery. *Critical Reviews in Therapeutic Drug Carrier Systems*. 2007; 24 (6): 547–596. doi: 10.1615/critrevtherdrugcarriersyst.v24.i6.20
12. *Kursakov SV, Kuznetsova EG, Kuryleva OM, Salomatina LA, Gurjanova SV, Borisova OJu I dr*. Razrabotka i validaciya metodiki opredeleniya glyukozaminilmuramildipeptida v vodnyh rastvorah metodom vysokoeffektivnoj zhidkostnoj hromatografii. *Immunologija.* 2020, 41 (1): 74–82. doi: 10.33029/0206-4952-2020-41-1-74-82. (In Russ., English abstract).
13. Gosudarstvennyj reestr lekarstvennyh sredstv 2020 g. (In Russ.).
14. *Haitov RM, Pinegin BV, Andronova TM*. Otechestvennye immunotropnye lekarstvennye sredstva poslednego pokoleniya i strategiya ih primeneniya. *Lechashhij vrach*. 1998; 4: 46–51. (In Russ.).
15. *Shepel' VS*. O sostavlenii smesej rastitel'nyh masel dlya kosmeticheskih kompozicij [Elektronnyy resurs] – http://www.tusheflora.ru/review/publications/2010/o_sostavlenii_smesej_rastitelnih_masel_dlya_kosmeticheskih_kompozitcij/, svobodnyy. (In Russ.).
16. *Bykova SF, Davidenko EK, Efimenko SG*. Perspektivy razvitiya syr'evoj bazy proizvodstva novyh tipov pishchevyh rastitel'nyh masel. *Masla i zhiry.* 2014; 1: 20–25. (In Russ.).
17. *Hohlenkova NV*. Razrabotka promyshlennoj tekhnologii salfetok s gustym ekstraktom kory duba i natriya al'ginatom *Vestnik farmacii.* 2013; 2 (60): 40–47 (In Russ.).

The article was submitted to the journal on 30.06.2020

DOI: 10.15825/1995-1191-2020-3-156-166

EFFECT OF INTRAMYOCARDIAL ALLOGENIC BIOMATERIAL INJECTION ON ANGIOGENESIS AND POSTISCHEMIC SCAR REMODELING IN RATS

A.I. Lebedeva[1], S.A. Muslimov[1], L.A. Musina[1], E.M. Gareev[1], R.Z. Kadyrov[1], D.S. Condratyeva[2], S.A. Afanasiev[2], S.V. Popov[2]

[1] All-Russian Center for Eye and Plastic Surgery, Ufa, Russian Federation

[2] Research Institute of Cardiology, Tomsk National Research Medical Center, Tomsk, Russian Federation

Scar smoothing out, angiogenesis stimulation and cardiomyogenesis in myocardial infarction still remain pressing issues despite the variety of existing methods. One of the ways to correct them is intramyocardial implantation of an alloplant biomaterial (ABM) suspension. ABM serves as an inhibitor of fibroneogenesis in various tissues with chronic inflammatory processes. No studies have been carried out with regards to acute myocardial infarction. **Objective:** to assess the dynamics of the number of bFGF-1$^+$ cells and CD68 macrophages, the degree of angiogenesis amidst the use of ABM in the formation of postinfarction scar in the experiment. **Materials and methods.** Experimental studies were performed on 100 male Wistar rats weighing 0.18–0.25 kg. Coronary artery ligation was performed on all animals. In the experimental group, the ABM suspension (12 mg) was injected intramyocardially. We used histological, electron microscopic, immunohistochemical (CD68, bFGF-1), morphometric and statistical research methods. Hearts were procured at day 3, 7, 14, 30, and 45. **Results.** The use of an allogeneic biomaterial immediately after coronary artery stenosis could reduce the area of cicatricial myocardial degeneration by two fold by accelerating inflammatory response and the onset of early proliferative phase. In the reactive zone after ABM implantation, macrophage myocardial infiltration significantly decreased in comparison to the control group. The use of ABM ensures significant predominance of bFGF-1$^+$ cells in the initial period of inflammation (3–14 days). Subsequently (14–45 days), inflammatory cytokine expression became several times less, which corresponded to biodegradation and resorption of the biomaterial. In the control group, during the acute phase of inflammation (3–14 days), bFGF-1$^+$ cells were low in number. Subsequently (14–45 days), cytokine expression increased significantly, causing rapid accumulation of collagen fibers and scarring. In myocardial regeneration after a heart attack in the experiment, ABM stimulated angiogenesis, whose level was three times higher than in the control group. It was noted that ABM serves as a regulator of the neofibrillogenesis-fibroclasia balance in tissue. **Conclusion.** Macrophage migration inhibition and suppression of pro-inflammatory orientation of macrophages should be indicated as one of the directions of therapeutic correction strategy for ischemic myocardial injuries. Alloplant biomaterial used in the acute phase of myocardial inflammation can serve as such alternative.

Keywords: myocardium, allogeneic biomaterial, regeneration, bFGF, macrophages.

INTRODUCTION

The problem of scar smoothing out, stimulation of angiogenesis and cardiomyogenesis in myocardial infarction remains relevant to this day. Such methods of regenerative medicine as gene and cell technologies, along with their undeniable advantages, have certain disadvantages. The introduction of gene constructs into the myocardium leads to angiogenesis and scar limitation. However, the introduction of the plasmid vector does not achieve an adequate degree of cardiomyocyte transfection (no more than 10%). The frequent development of immune responses to viral proteins, fragility in tissues limit their widespread use [1].

The use of cellular products also does not have a sufficiently high efficiency, they are difficult to manufacture, carry the risk of infection, teratogenicity, etc. Even if all biological safety requirements are met, cellular products do not integrate into the recipient's tissues, but have only a paracrine effect [2]. Also, great attention is paid to the use of various kinds of biomaterials for the regeneration of damaged tissues and organs. All the methods under consideration face one problem. Currently, there are no available and effective methods to combat excessive fibrosis during postischemic myocardial remodeling. It is known that biomaterials of the Alloplant® series serve as an inhibitor of fibroneogenesis [3]. They are developed at the Federal State Budgetary Institution "All-Russian Center for Eye and Plastic Surgery" of the Ministry of Health of the Russian Federation in Ufa and are manufactured in accordance with TU 42-2-537-87. Biodegra-

Corresponding author: Anna Lebedeva. Address: 67/1, R. Zorge str., Ufa, 450075, Russian Federation.
Phone: (347) 293-42-35. E-mail: Jeol02@mail.ru

dation products of the biomaterial are chemoattractants of M1 macrophages in the implantation zone. Thus, macrophages become direct participants in the phagocytosis of biomaterial, wound detritus, immune complexes, and excess collagen. In addition, macrophages exert a paracrine effect by releasing proinflammatory factors: TNFa, IL1, etc. Monokines, in turn, inhibit the expression of profibrogenic factors (bFGF-1, TGF-b1) and regulate the activation of fibroblastic cells [4]. These results of the study were obtained during the application of defects in the skeletal muscle, the wall of the uterus, in the correction of such chronic degenerative-inflammatory diseases as cirrhosis of the liver, periodontitis, stomach ulcers, skin burns, degeneration of the retina and optic nerve. It was found that allogeneic biomaterials in the process of replacement contribute to the neoangiogenesis of the forming regenerate [5, 6]. However, no studies have been conducted for acute myocardial infarction.

It is known that the main angiogenic factors are VEGF, TGFb, bFGF, etc. [7]. Moreover, according to some data, bFGF stimulates neovascularization to a greater extent than VEGF [8].

The purpose of the present study was to evaluate the role of macrophages and bFGF on postinfarction myocardial remodeling and vascularization in the experiment.

MATERIALS AND METHODS

For the regeneration of cardiac muscle tissue, a decellularized biomaterial (DCBM) was used, made of fibrous connective tissue formations and processed using the TU 42-2-537-87 technology. A prerequisite for its use is allogenicity; therefore, for this study, the biomaterial was made from rat tendons.

Experimental studies were carried out on 100 male Wistar rats weighing 0.18–0.25 kg. All animals were divided into 2 groups. In the control group (n = 50), myocardial infarction was modeled as follows: left-sided thoracotomy was performed under intramuscular anesthesia (zoletil solution) followed by ligation on *r. interventricularis paraconalis a. coronarii sin.* of the left ventricle. After the intervention, the wound was sutured in layers.

In the experimental group (n = 50), ligation of the artery was accompanied by the introduction of a DCBM suspension into the pool of the stenotic artery in a total amount of 12 mg. The dose was chosen at random. Before use under sterile conditions, a suspension of the biomaterial in physiological solution was prepared (100 mg of the biomaterial was suspended in 5 ml of physiological solution). Along the perimeter of the left ventricle, 5–6 intramyocardial injections of the suspension were made, 100 μl each. The total volume of the injected suspension was 600 μL. The particle size of the biomaterial was 50–80 μm for free passage through the injection needle. In the control group, 5 days later, 0.9% saline was administered in an adequate volume. The animals were kept under standard vivarium conditions.

The animals were removed from the experiment by insufflation of a lethal dose of ether vapor after 3, 7, 14, 30, 45 days. The studies were carried out in accordance with the rules of laboratory practice in the Russian Federation, in accordance with the rules adopted by the European Convention for the Protection of Vertebrate Animals used for Experimental and Other Scientific Purposes (Strasburg, 1986), and in accordance with an approved written protocol in accordance with the investigator's standard operating procedures and guidelines on laboratory animals and alternative models in biomedical research [9]. For histological examination, the hearts were fixed in a 10% solution of neutral formalin, dehydrated in a series of alcohols of increasing concentration, and embedded in paraffin according to the standard method. Sections were prepared on a LEICA RM 2145 microtome (Germany), stained with hematoxylin and eosin, according to Van Gieson, according to Mallory. To determine the size of the postinfarction myocardial scar, each heart was cut across into 5 sectors. Scar area index (SAI) was measured on cross-sectional preparations of rat hearts stained according to Mallory, using the "ITEM" software as follows: the ratio of the scar area to the left ventricular wall area was multiplied by 100%.

For immunohistochemical studies, paraffin sections with a thickness of 4 μm were stained using a Leica Microsystems Bond™ immunohistostiner (Germany). The first antibodies used were CD 68, bFGF-1 at a dilution of 1:300 (Santa Cruz Biotechnology, USA). For unmasking, an indirect streptavidin-biotin detection system Leica BOND (Novocastra™, Germany) was used. The specificity of the reaction was evaluated by staining sections without the first antibodies. Positively stained cells were counted in 20 fields of view of each sample (n = 6) at ×400 magnification. The study and visualization of preparations were carried out using a light microscope Leica DMD 108 (Germany) with specialized software for managing settings and image capture.

For electron microscopic examination, 1–2 mm^3 pieces of the myocardium were used, fixed in a 2.5% glutaraldehyde solution prepared in a cacodylate buffer (pH 7.2–7.4) with additional fixation in a 1% OsO_4 solution in the same buffer. The material was dehydrated in alcohols of increasing concentration and poured into epon-812 according to the generally accepted method. On an EM UC 7 ultratome (Leica, Germany), semi-thin sections were prepared and stained with a solution of toluidine blue in a 2.5% solution of anhydrous soda. On these sections, we selected areas for electron microscopic examination. Ultrathin sections were contrasted with a 2% aqueous solution of uranyl acetate, lead citrate according to Reynolds and studied under a JEM-1011 transmission microscope (Jeol, Japan).

Analysis of SAI and the total area of capillary lumens (CLTA) data was carried out using nonparametric methods – one-way analysis of variance according to Kruskal–Wallis and comparison of uncorrelated data by the Mann–Whitney method [10]. The diagram was built using the Statistica 6.0 software.

RESULTS

As a result of the experiment (after 45 days), it was revealed that SAI in the control group was 26.65 ± 16.10%, and in the experimental group after DCBM 9.72 ± 1.08%. The multiplicity of intergroup differences was 2.74 times (Fig. 1).

The course of the inflammatory reaction after ischemia of cardiac muscle fibers in the experimental groups occurred in different ways. In the experimental group, at the initial stage of inflammation (3 days), signs of an early onset of the proliferative phase of inflammation and the formation of granulation tissue were revealed at the site of ischemically damaged cardiomyocytes. Thin collagen fibers, macrophage-fibroblastic infiltration, and mesenchymal cells were detected in the regenerate. Along with hemorrhagic impregnation, thin-walled hemocapillaries with a multi-vector orientation were determined. Particles of biomaterial infiltrated by poorly differentiated cells and macrophages were determined (Fig. 2).

In the control group, in place of the collapsing cardiomyocytes, a wide cell wall was formed, consisting of macrophages, lymphocytes, neutrophils, signs of rupture of blood vessels and diapedesis of erythrocytes in the interstitium of the myocardium were noted (Fig. 3).

In the control group in the ischemically altered cardiac muscle tissue in the reactive zone, the number of CD 68 macrophages also exceeded the values of the experimental group practically throughout the entire experiment. In the control and experimental groups, the tendency to rise and subsequent decline was generally highly significant (Chi-Square = 76.3, $p << 0.0001$ and Chi-Square = 45.2, $p << 0.0001$, respectively). The number of CD 68+ cells in the control group statistically significantly exceeded their number in the experimental group during the observation period of 3–14 days ($p < 0.003$ and less). In the period of 30–45 days in the control group, attenuation of myocardial remodeling and scar formation occurred, which caused a decrease in the number of macrophages in both groups ($p > 0.12$) and initiation of the healing stage (Fig. 4).

At studying bFGF-1^+ cells in the experimental and control groups, the number of these cells significantly depended on the beginning of the experiment ($\chi^2 = 49.8$, $p << 0.0001$ and $\chi^2 = 60.0$, $p << 0.0001$, respectively) and had certain differences. After 3 days, the range of variation in bFGF-1^+ cells in the experimental group equaled 38–55 (median 44). After 7 days, their number increased to 54–68 (median 61) ($p < 0.0001$). However, on the 14th day, the interindividual variation in the number of bFGF-1^+ cells increased sharply (22–72, median 60) and turned out to be statistically insignificant ($p >$

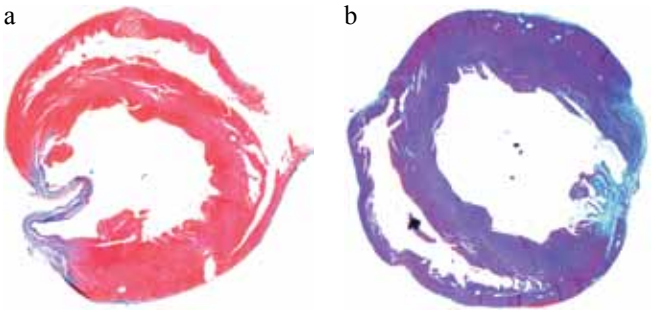

Fig. 1. Myocardial cross-section in 45 days: a – control group; b – experimental group. Mallory stain. ×40

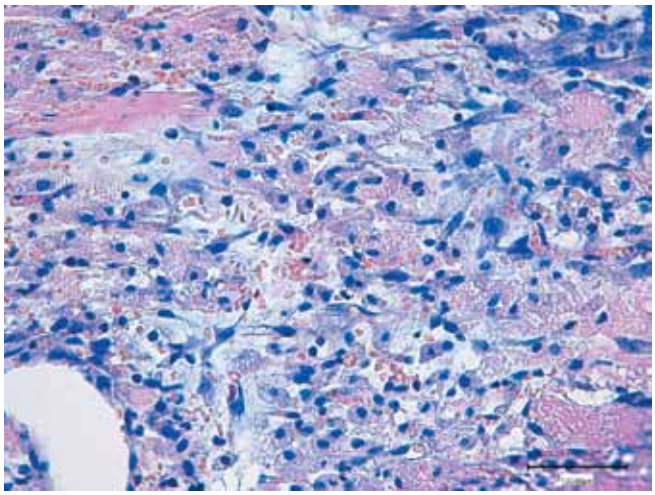

Fig. 2. Granulation tissue formation and infiltration by macrophages, mesenchymal cells, fibroblasts in rat myocardium 3 days after coronary occlusion and biomaterial insertion (experimental group). Stained with hematoxilin and eosin. ×400

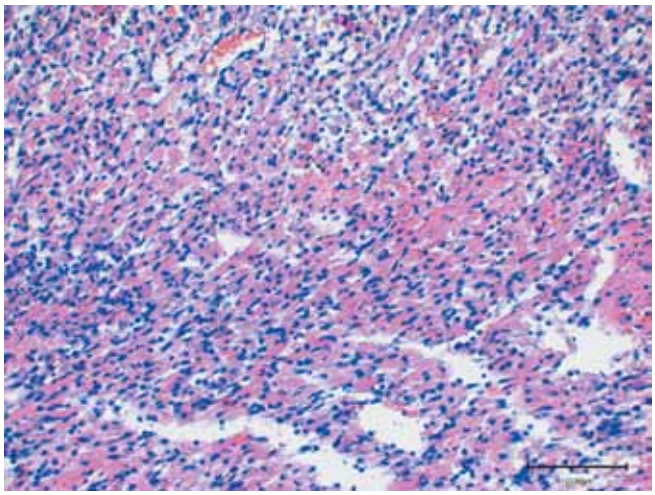

Fig. 3. Macrophage-lymphocytic cell wall in the zone of necrotically altered cardiomyocytes 3 days after coronary occlusion (control group). Stained with hematoxilin and eosin. ×200

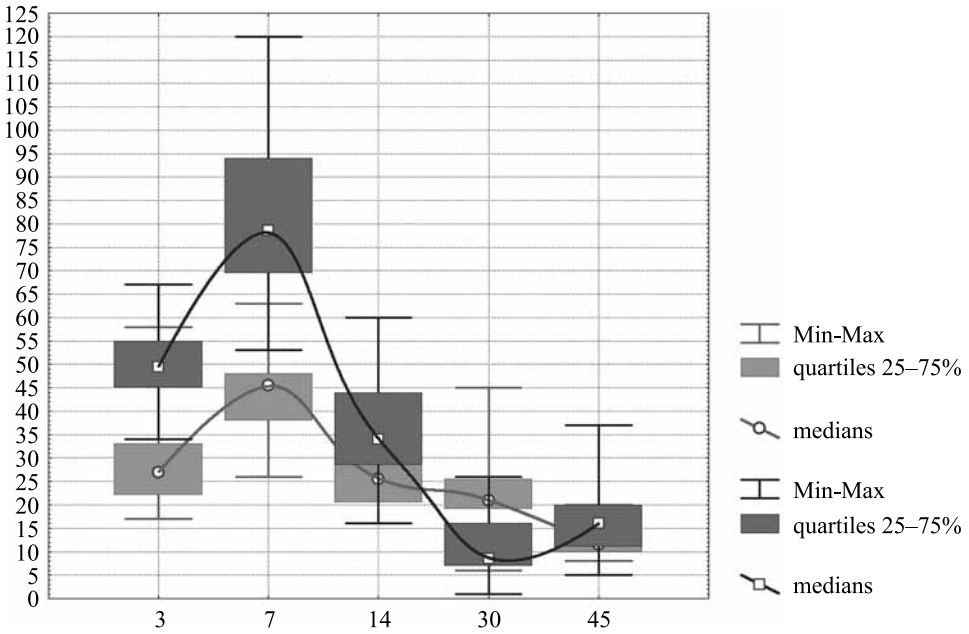

Fig. 4. The number of CD 68^+ in the myocardium of rats in the control group (blue graph) and after the insertion of the biomaterial (red graph). GDI – limits of confidence intervals for the average area values, ±CO – standard error of the average value

0.46). After 30 days, the number of bFGF-1^+ cells in the main group sharply decreased (9–16, median 11), and on the 45th day it slightly, statistically significantly ($p < 0.03$) decreased to the range of 4–16 cells (median 9).

In the control group, the expression with bFGF-1^+ cells was completely different. The number of bFGF-1^+ cells was minimal in the first week from the beginning of the experiment (5–15, median 10), on day 3, 10–19 cells (median 14). After 14–30 days, the number of bFGF-1^+ cells in the control group increased sharply – up to 80–109 cells (median 84) and 67–104 cells (median 101), respectively, but the difference was not significant ($p > 0.66$)… A statistically significant ($p < 0.0001$) decrease in the number of bFGF-1^+ cells to 54–96 (median 64) in this group occurred only by the 45th day. In the control group, after 14, 30, and 45 days, the intragroup random spread in the number of such cells sharply increased to 29, 37, and 41 cells, respectively. In the experimental group, in the period of 30–45 days relative to 14 days, the variation in the number of such cells, on the contrary, sharply decreased (Fig. 5).

The results of the analysis showed that the effect on CLTA of the reactive zone of the regenerate both the factor of group belonging of objects ("control", "experience") and the factor of time (days) ($\eta^2 = 15\%$, $F = 31$, $p << 0.0001$ and $\eta^2 = 14\%$, $F = 9$, $p << 0.0001$, respectively).

In the experimental group, CLTA decreased from 1432.2 ± 1179 μm^2 on the 3rd day to 577 ± 348 μm^2 on the 7th day ($p < 0.0003$). Thereafter, CLTA remained stable (611 ± 445.8 and 632.3 ± 406.6 μm^2 on the 14th and 30th days, respectively). In the control group, on the 3rd day after coronary occlusion, CLTA was significantly 3 times lower than in the experimental group (510.6 ± 537 μm^2). In the subsequent periods of observation, CLTA decreased, but this decrease was statistically significant ($p < 0.003$) only after 14 days (146 ± 97 μm^2), i. e., almost 3 times lower than on the third day. During all periods of observation, the CLTA of the reactive zone of the regenerate in the control group was significantly and statistically significantly lower than in the experimental group. The greatest difference was noted in the period of 3 days (Fig. 6).

After 14 days, in the perifocal zone of the experimental group, signs of resorption of collagen fibers were revealed (Fig. 7). In the myocardium in the perifocal zone, scattered short fragments of collagen fibers surrounded by rounded and large cells with an oval nucleus were detected (Fig. 7, a). Fibroclasts were found in the form of large oval cells with long outgrowths of cytolemma, forming phagocytic vacuoles. In the cytoplasm, channels of the granular endoplasmic reticulum, secondary vacuoles with fragments of striated collagen fibers, enclosed in the cytoplasm, were found. The nuclei were rounded with signs of functional activity, containing euchromatin (Fig. 7, b).

Thus, under conditions of DCBM application, signs of fibroclasia were found in the reactive zone of the myocardium, which could also affect the volume of the scar in the myocardium.

DISCUSSION

In the present study, a targeted approach was used and the pathomorphological processes of spontaneous myocardial healing were demonstrated after coronary artery ligation and under the influence of allogeneic bio-

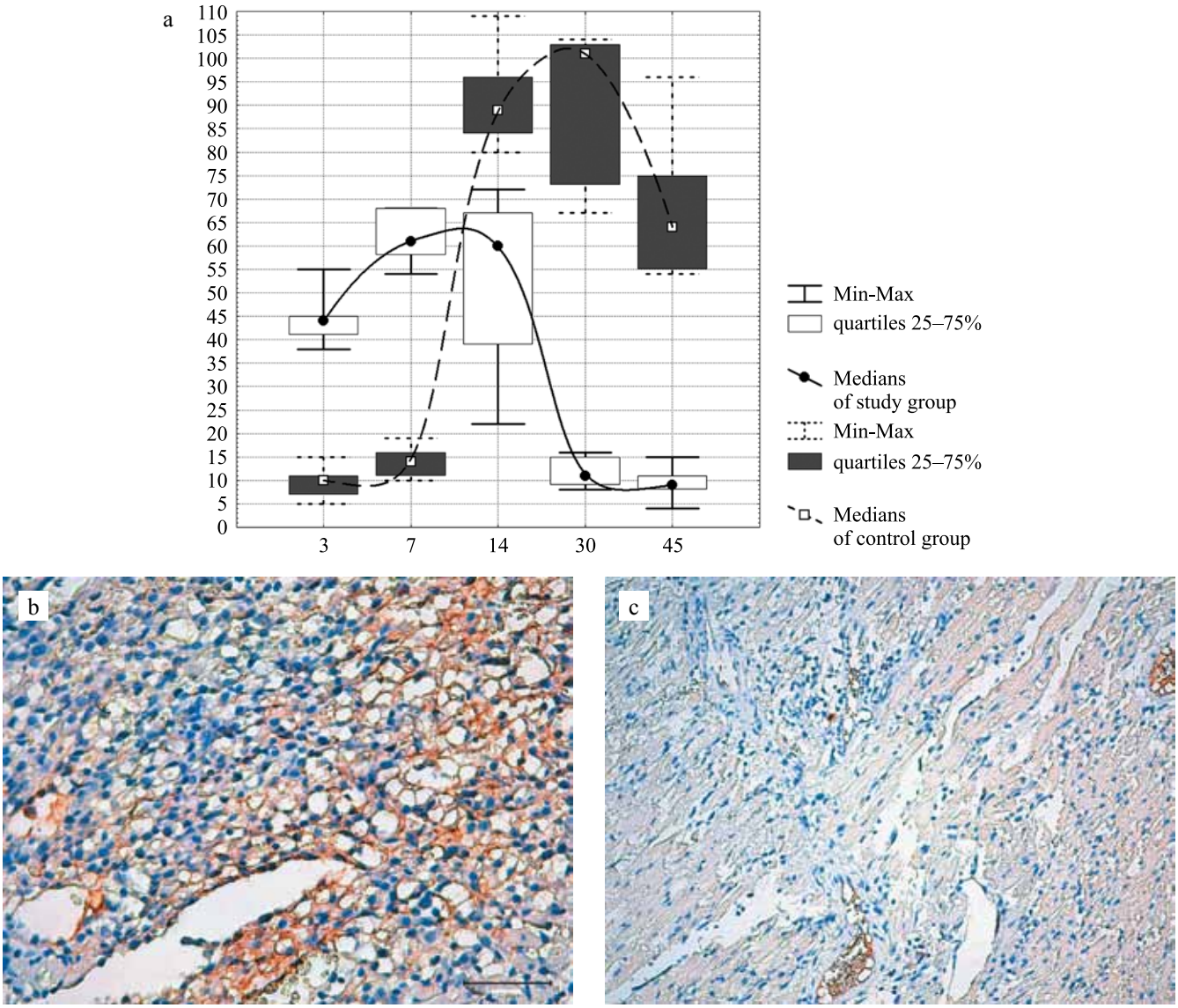

Fig. 5. The reaction of FGF-1$^+$ cells in the myocardium of rats: a – dynamics of the number of bFGF-1$^+$ cells in the experimental group (light graph) and in the control group (dark graph); b – expression of bFGF-1 in the experimental group after 7 days. ×400; c – expression of bFGF-1 in the control group after 7 days. Indirect immunoperoxidase method for detection of bFGF-1 stained by hematoxylin. ×200

material. DCBM implantation showed new strategically important mechanisms of the regenerative potential for the myocardium associated with cardioprotection: angiogenesis, inhibition of macrophages, fibroclasia. It was found that under the conditions of DCBM application at a dose of 12 mg, the scar area was reduced by more than 2 times.

After ligation of the coronary artery in the myocardium, pathomorphological changes associated with massive colliquation necrosis of cardiomyocytes occurred. The entire chronology of the phase change of the inflammatory response was traced. Exudative inflammation occurred within 3–14 days. In the period of 14–30 days, the proliferation phase began, and after 30–45 days, healing with scar formation began.

Three days after coronary occlusion and intramyocardial administration of DCBM, macrophage-fibroblastic and mesenchymal infiltration was detected in the perifocal zone at the border of the intact myocardium and necrotic cardiac muscle tissue. The regenerate was well vascularized. A dense multidirectional network of hemocapillaries was noted, which accompanied the formation of immature granulation tissue. These signs indicated the onset of an early proliferative inflammatory stage.

It was previously established that under the conditions of using DCBM for the healing of connective tissue with a chronic course of the inflammatory-destructive process, as well as after the application of defects, the products of biodegradation of the biomaterial became chemoattractants of monocytes and macrophages. Macrophage cells determined the efficiency of regeneration due to complete phagocytosis and regulation of the proliferative phase of inflammation. They inhibited fibroblastic activity due to M1 macrophages and prolongation of the cytotoxic

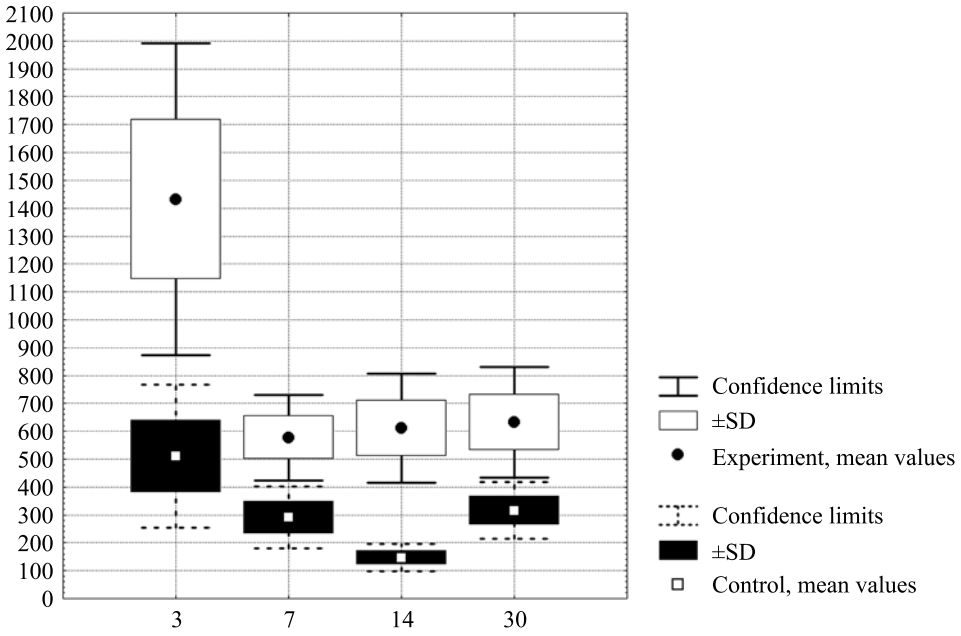

Fig. 6. Changes CSCC reactive zone of the regenerate in the "control" and "experience" in different periods of observation after coronary occlusion. GDI – limits of confidence intervals for the average area values, ±CO – standard error of the average value

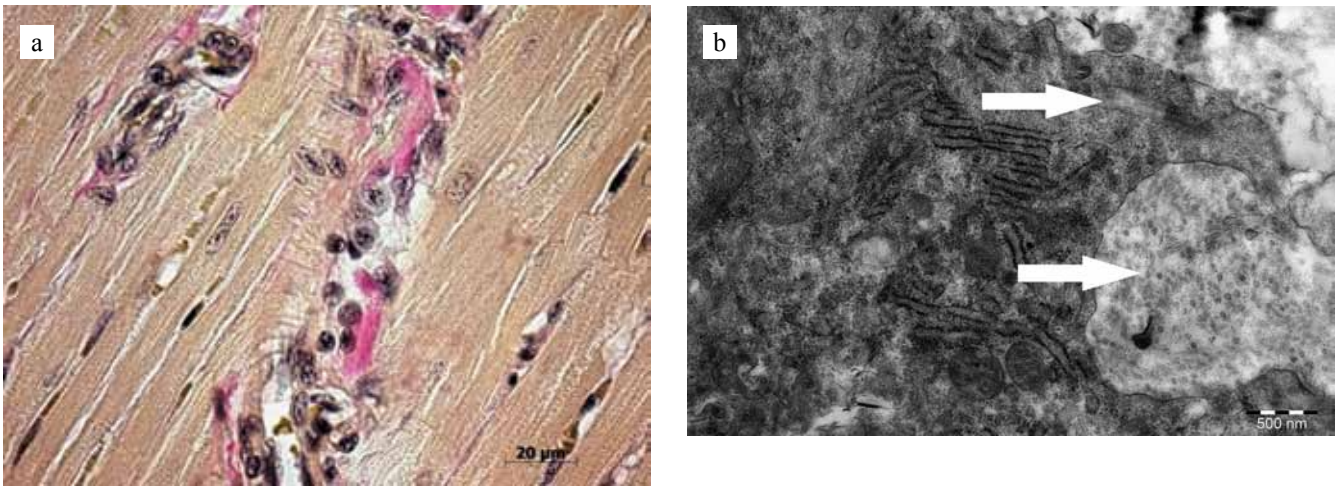

Fig. 7. Resorption of collagen 14 days after insertion of biomaterial (experimental group). a – Van-Gison stain. ×400; b – fibroclast in the myocardium with phagocytic vacuoles with fragments of collagen (↑). Electronograms. ×12 000

phase [11]. It is known that tumor necrosis factor (TNFa), in addition to initiating inflammatory reactions, can also inhibit fibrosis through the regulation of fibroblast activity, suppressing the synthesis of transforming growth factor TGFβ-induced expression of connective tissue growth factor (CTGF) protein [12].

As a result of our study, it was revealed that during the acute stage of inflammation of the ischemic myocardium, the opposite reaction occurred. The biodegradation products of DCBM stimulated the migration of macrophages to a lesser extent in the period of 3–14 days and were their inhibitors. The presence of DCBM particles was noted only in the early stages of observation; later, after 14 days, the biomaterial was resorbed and was not visualized.

In the control group, in the period of 3–14 days, pronounced infiltration of the myocardium by macrophages and the formation of a wide cell wall were determined, which corresponds to the phase of alteration and exudation. Subsequently (14–45 days) at the stage of proliferation and scarring, the number of macrophages almost proportionally decreased and leveled off in both experimental groups. Therefore, according to the data in Figure 1, macrophages contributed to the manifestation of inflammation in the myocardium, increased collagenogenesis, and, as a consequence, an increase in

the scar area. This is consistent with the data of other researchers [13].

The nature of DCBM is a decellularized allogeneic intercellular matrix – fibrous connective tissue, consisting mainly of mature type I collagen fibers and associated proteoglycans and glycosaminoglycans: hyaluronic acid, heparan-, dermatan- and keratan sulfate. During the lysis and resorption of the biomaterial, they are dosed extraction, which is initially released during the biodegradation of the graft, and subsequently begins to be secreted by the surrounding cells: macrophages, fibroblasts [11]. It can be assumed that exogenous collagen contributes to the suppression of the acute inflammatory reaction and the migration of effector cells such as macrophages. This mechanism of action probably develops according to the type of "feedback" characteristic of involution of the scar. And it was caused by excessive collagenogenesis "based on intercellular and collagen-cell interactions", as described by V.V. Serov and A.B. Schechter (1981) [14].

Excess collagen, directly in contact with fibroblasts, leads to increased fibroclasia, a decrease in the synthetic activity of fibroblasts and their destruction, which we observed after 14 days in the experimental group, which caused a sharp decline in bFGF-1$^+$ cells and the appearance of fibroclasts. Fibroclasia could also have an effect on reducing the area of the scar in the experimental group.

On the other hand, during transplantation of a decellularized extracellular matrix, cytokines such as bFGF, VEGF, HGF are released, including in the initial period after implantation (1–3 days), have bioinductive effects on myocardial fibroblasts and promote the growth of blood vessels [15]. We noted that the degree of vascularization of the reactive zone in the experimental group exceeds the values of the control one throughout the experiment, especially during the period of 3 days. It is known that bFGF has not only a pronounced angiogenic potential in conditions of ischemic myocardial damage, but also promotes the survival of endothelial cells, reduces the degree of apoptosis of cardiomyocytes [16–18]. The role of heparan sulfate (perlecan) is widely known as a "molecular glue" that plays a key role in embryonic and post-wound myocardial morphogenesis. It is a major component of the basement membrane of blood vessels, type IV collagen and laminin [19]. Consequently, endogenous heparan sulfate, as one of the biodegradation products of DCBM, can also participate in neovasculogenesis, morphogenesis, and cardioprotection.

In the control group, inflammation developed according to the classical type [20]. In the period 3–14 days, the phase of acute inflammation was accompanied by the presence of inflammatory effector cells, the formation of a wide cell shaft, which arose at the site of necrotic masses of ischemic myocardial fibers. Accordingly, the number of bFGF-1-producing cells was low. After 14 days and further, the proliferative stage of healing was characterized by the accumulation of a large number of fibroblastic cells and a more increased production of fibrokine bFGF-1 by them.

Biodegradation products of DCBM are able to normalize the balance between the processes of neofibrogenesis and fibroclasia, while the synthesis of excess collagen and glycosaminoglycans slows down, which returns the process of myocardial regeneration to the physiological channel and leads to physiological scarring. In the process of pathological scarring during the transition from the phase of late inflammation to the phase of proliferation under conditions of hypoxia and impaired microcirculation, detritus accumulates in the wound and abnormal production of cytokines by an excessive number of macrophages, which leads to lengthening the stage of inflammation and prevents the activation of healing processes [21]. The products of tissue breakdown, acting as biological stimulators of fibrogenesis, cause an imbalance in the system "fibroneogenesis – fibroclasia" with the formation of a large number of fibroblastic cells characterized by high metabolism [22].

Analysis of the results of bFGF-1 expression in the experimental group confirms this assumption. The mechanism of action indicates a reverse tissue response in response to DCBM implantation than that described in previous works [23]. In the present study, it was found that in the experimental group in the peri-infarction zone during the period 3–14 days bFGF-1$^+$ cells significantly exceeded the values of the control. In the control group, during the acute phase of inflammation (3–14 days), the level of bFGF-1$^+$ cells was low compared to the experimental group, and subsequently (14–30 days), the expression of the cytokine significantly increased, which corresponded to the phase of healing and scarring – the rapid accumulation of collagen fibers.

In the experimental group, the revealed chronology of the change in cellular infiltration does not correspond to the classical understanding of the course of the inflammatory process. Apparently, the pronounced expression of bFGF-1 is an antagonist of the pro-inflammatory spectrum of cytokines and suppresses the chain of cytotoxic reactions. It is known that bFGF, by inhibiting the apoptosis of cardiomyocytes, has a protective effect on the heart after myocardial infarction, thereby reducing the size of the necrotic zone [24]. Therefore, the early proliferative phase and the formation of granulation tissue may contribute to cardioprotection.

The information has recently appeared on the use of various types of hydrogels, created on the basis of the extracellular matrix, alginate, gelatinase, collagen, hyaluronic acid, fibrin, agarose, chitosan, keratin. They cause some improvement in the remodeling of ischemically damaged myocardium, limiting the spread of fibrosis [25, 26]. Some materials can provide maintenance or improvement of functional parameters in experimental animals or be carriers of cells or growth factors [27].

Extracellular matrix biomaterials typically consist of structural proteins such as collagen, laminin, fibronectin, and vitronectin, and many glycosaminoglycans. The rate of degradation of these materials is determined by the cellular environment and factors such as concentration and degree of crosslinking. But often they have a bioresorption rate that significantly exceeds the rate of histogenesis, without significant functional and structural positive changes, including in the long-term period [28].

The biomaterial used in this study, created on the basis of a decellularized allogeneic extracellular matrix, interacts with the host tissue, changing the cytokine profile of the myocardium, promotes angiogenesis and reduces fibrosis and cell death, and serves as a chemoattractant of progenitor cardiomyogenic cells. When using DCBM, vitalization is not required, it is able to maintain a balance between degradation and reparative histogenesis, it serves as a biomimetic, biocompatible, non-immunogenic, resists long-term complications such as infection, calcification and aneurysm enlargement. The viscosity of the resulting suspension depends on its concentration and can be adjusted and depends on the type of tissue and the needs of the researcher.

This model of acute myocardial infarction does not cover the issues of chronic myocardial ischemia, which is the most common in clinical practice. Therefore, this model highlights the aspects of the influence of the biodegradation products of DCBM as bFGF-induced angiogenic growth factors on the pro-angiogenic state during the healing period after myocardial infarction. One of the directions of the strategy of therapeutic correction in ischemic myocardial damage should be indicated on the inhibition of the migration of macrophages and the suppression of their pro-inflammatory direction M1. Decellularized allogeneic biomaterial used in the acute phase of myocardial inflammation can be such an alternative.

CONCLUSION

1. The use of an allogeneic biomaterial immediately after stenosis of the coronary artery allows more than 2 times to reduce the area of cicatricial myocardial degeneration.
2. DCBM accelerates the course of the inflammatory response and the onset of the early proliferative phase of inflammation.
3. Allogeneic biomaterial reduces myocardial infiltration by CD68 macrophages compared to the control during spontaneous healing.
4. The use of DCBM provides a significant predominance of bFGF-1^+ cells in the initial period of inflammation (3–14 days). Subsequently (14–45 days), the expression of fibrokin became several times less. In the control group, during the acute phase of inflammation (3–14 days), the level of bFGF-1^+ cells was low, and subsequently (14–45 days), cytokine expression increased significantly, which caused a rapid accumulation of collagen fibers and scarring.
5. During the formation of postinfarction regenerate in the experiment, DCBM stimulated angiogenesis.
6. In the zone of myocardial regeneration, allogeneic biomaterial regulates the balance of neofibrillogenesis-fibroclasia.

The study was performed within the framework of state assignment No. 056-00110-18-00, approved on December 26, 2017.

The authors declare no conflict of interest.

REFERENCES

1. *Pislaru SV, Simari RD.* Gene transfer for ischemic cardiovascular disease: is this the end of the beginning or the beginning of the end? *Nat Clin Pract Cardiovasc Med.* 2005; 2: 138–144.
2. *Davydenko VV, Matyukov AL, Tsupkina NV, Vlasov TD, Gritsenko VV, Kuznetsov AL et al.* Influence of autotransplantation of various bone marrow cells on the morphofunctional state of the rabbit myocardium after infarction. *Kletochnaya transplantologiya i tkanevaya inzheneriya*. 2007; 2: 52–61. [In Russ.].
3. *Lebedeva AI.* Spongiform biomaterial – inhibitor of fibrosis of damaged skeletal muscle. *Russyiskyi biotherapeuticheskyi journal.* 2014; 4 (13): 37–44. [In Russ.].
4. *Lebedeva AI, Muslimov SA, Gareev EM et al.* Morphological features of macrophages and their cytokine profile in the regeneration of skeletal muscle plastic surgery allogenic spongy biomaterial. *Cytokines & inflammation.* 2015; 14 (1): 27–33. [In Russ.].
5. *Lebedeva AI, Muslimov SA, Musina LA.* Regeneration of smooth muscle tissue uterine horns of the rabbit after cut by the laser beam and the use of allogenic biomaterial. *Vestnik Bashkirskogo gosudarstvennogo agrarnogo universiteta*. 2013; 4 (28): 41–45. [In Russ.].
6. *Lebedeva AI, Muslimov SA, Musina LA, Sherbakov DA.* Regeneration of skeletal muscle tissue of experimental animals induced by Alloplant biomaterial. *Mezhdunarodnyj zhurnal ehksperimental'nogo obrazovaniya*. 2014; 3-2: 68–71. [In Russ.].
7. *Arsent'eva NI, Makarova MA, Arsent'eva ML.* Plastic processes in ischemic myocardial damage and the role of local mitogens in its regeneration (according to the results of research in the fgbu "scientific center for reconstructive and reconstructive surgery" SB RAMS. *Byulleten' VSNC SO RAMN.* 2014; 3: 116–121. [In Russ.].
8. *Mihajlichenko VYu, Samarin SA.* Angiogenesis in myocardial infarction and its correction by transplantation of multipotent mesenchymal stem cells in the experiment. *Kubanskij nauchnyj medicinskij vestnik.* 2015; 2 (151): 98–105. [In Russ.].
9. Guidance on laboratory animals and alternative models in biomedical research / Pod. red. N.N. Karkishchenko, S.V. Grachev. M.: Profile-2c, 2010: 358. ББК 45.318:28.6я81.

10. *Rebrova OYu.* Statistical analysis of medical data. Application of STATISTICA application software package. M.: MediaSfera, 2002: 312.
11. *Lebedeva AI.* Regulation of parenchymal-stromal relationship for the correction of defects of skeletal muscle allogenic biomaterial. *Experimental and clinical dermatocosmetology.* 2014; 1: 51–56. [In Russ.].
12. *Abraham DJ, Shiwen X, Black CM, Sa S, Xu Y, Leask A*. Tumor necrosis factor alpha suppresses the induction of connective tissue growth factor by transforming growth factor-beta in normal and scleroderma fibroblasts. *J Biol Chem*. 2000; 275 (20): 15220–15225. doi: 10.1074/jbc.275.20.15220.
13. *Gombozhapova AE, Rogovskaya YuV, Rebenkova MS, Kzhyshkovskaya YuG, Ryabov VV.* CD 68 and stabilin-1 positive macrophages in postinfarction myocardial regeneration. *Russian Journal of Cardiology*. 2017; 11 (151): 56–61. [In Russ.]. http://dx.doi.org/10.15829/1560-4071-2017-11-56-61.
14. *Serov VV, Shekhter AB.* Connective tissue. M.: Medicina, 1981: 312.
15. *Mewhort HEM, Svystonyuk DA, Turnbull JD, Teng G, Belke DD, Guzzardi DG et al.* Bioactive Extracellular Matrix Scaffold Promotes Adaptive Cardiac Remodeling and Repair. *Jacc: Basic to Translational Science*. 2017; 2 (4): 450–464. http://dx.doi.org/10.1016/j.jacbts.2017.05.005.
16. *Shurygin MG, Shurygina IA.* The fibroblast growth factor as angiogenesis stimulator at myocardial infarction. *Byulleten' VSNC SO RAMN.* 2010; 30 (6): 89–92. [In Russ.].
17. *Tamura K, Nakajima H, Rakue H et al.* Elevated Circulating Levels of Basic Fibroblast Growth Factor and Vascular Endothelial Growth Factor in Patients With Acute Myocardial Infarction. *Jap Circ J.* 1999; 63 (5): 357–361. https://doi.org/10.1253/jcj.63.357.
18. *Shao ZQ, Takaji K, Katayama Y, Kunitomo R, Sakaguchi H, Lai ZF, Kawasuji M*. Effects of Intramyocardial Administration of Slow-Release Basic Fibroblast Growth Factor on Angiogenesis and Ventricular Remodeling in a Rat Infarct Model. *Circ J.* 2006; 70: 471–477. https://doi.org/10.1253/circj.70.471.
19. *Sasse Ph, Malan D, Fleischmann M, Roe W, Gustafsson E, Bostani T et al.* Perlecan is critical for heart stability. *Cardiovascular Research*. 2008; 80: 435–444. doi: 10.1093/cvr/cvn225.
20. *Pal'cev MA, Anichkov NM.* Pathological anatomy. M.: Medicina, 2000; 2 (1), 512.
21. *Huang C, Murphy GF, Akaishi S, Ogawa R.* Keloids and hypertrophic scar s: update and future directions. *Plastic and reconstructive surgery Global open*. 2013; 1 (4): e25. doi: 10.1097/GOX.0b013e31829c4597.
22. *Serra MB, Barroso WA, Da Silva NN, Silva SDN, Borges ACR, Abreu IC et al.* From Inflammation to Current and Alternative Therapies Involved in Wound Healing. *Int J Inflam*. 2017: 17. doi: 10.1155/2017/3406215.
23. *Muldashev ER, Muslimov SA, Musina LA, Nigmatullin RT, Lebedeva AI Shangina OR et al.* The role of macrophages in the tissues regeneration stimulated by the biomaterials. *Cell Tissue Bank*. 2005; 6 (2): 99–107. doi: 10.1007S10561-004-5805-2.
24. *Joki Y, Ohashi K, Yuasa D, Shibata R, Ito M, Matsuo K et al.* FGF21 attenuates pathological myocardial remodeling following myocardial infarction through the adiponectin-dependent mechanism. *Biochem Biophys Res Commun*. 2015; 459: 124–130. doi: 10.1016/j.bbrc.2015.02.081.
25. *Landa N, Miller L, Feinberg MS, Holbova R, Shachar M, Freeman I et al.* Effect of injectable alginate implant on cardiac remodeling and function after recent and old infarcts in rat. *Circulation*. 2008; 117: 1388–1396.
26. *Lv K, Li Q, Zhang L, Wang Y, Zhong Zh, Zhao J et al.* Incorporation of small extracellular vesicles in sodium alginate hydrogel as a novel therapeutic strategy for myocardial infarction. *Theranostics*. 2019; 9 (24): 7403–7416. doi: 10.7150/thno.32637.
27. *Plotkin M, Vaibavi SR, Rufaihah AJ, Nithya V, Wang J, Shachaf Y et al.* The effect of matrix stiffness of injectable hydrogels on the preservation of cardiac function after a heart attack. *Biomaterials*. 2014; 35 (5): 1429–1438. doi: 10.1016/j.biomaterials.2013.10.058.
28. *Shao ZQ, Takaji K, Katayama Y, Kunitomo R, Sakaguchi H, Lai ZF, Kawasuji M.* Effects of intramyocardial administration of slow-release basic fibroblast growth factor on angiogenesis and ventricular remodeling in a rat infarct model. *Circ J*. 2006; 70: 471–477.

The article was submitted to the journal on 23.07.2018

DOI: 10.15825/1995-1191-2020-3-167-173

TECHNOLOGY FOR OBTAINING AN ULTRATHIN POSTERIOR LAMELLAR CORNEAL GRAFT AT THE EYE TISSUE BANK

A.K. Ahmedov[1], T.Z. Kerimov[2], Kh.D. Tonaeva[1], B.E. Malygin[1], S.A. Borzenok[1, 2]

[1] Fyodorov Eye Microsurgery Federal State Institution, Moscow, Russian Federation
[2] Evdokimov Moscow State University of Medicine and Dentistry, Moscow, Russian Federation

Objective: to develop technologies for preoperative preparation of the posterior lamellar corneal graft based on our own formulation of the preservation medium for optimal dehydration of the donor cornea and a technique for cutting out an ultrathin flap using an optimized method at the Eye Tissue Bank. **Materials methods.** In a series of experimental studies, we obtained data on the hydration level of cadaveric donor corneas that were preserved in various solutions at different observation periods. Using 16 corneas, analytical weighing and pachymetry were performed via optical coherence tomography in the experimental (n = 8) and control (n = 8) groups. Morphological and functional characteristics of the corneal endothelium were then assessed. At the next stage of work, ultrathin grafts were formed from 16 corneas after hypothermic preservation in the experimental (n = 8) and control (n = 8) solutions by single-pass microkeratome, followed by microscopy of the samples using a scanning electron microscope. **Results.** After the first days of preservation in the proposed solution, there was dehydration of 9% cornea in the experimental group in comparison with the samples of the control group. After 4 days of preservation, there was no reliable difference found between the groups ($p > 0.05$) in the study of the endothelial cell viability of ultra-thin corneal grafts by immunofluorescent microscopy using the "Live and dead" marker. Scanning electron microscopy revealed that corneal stromal collagen fibers, preserved in the proposed medium, retained their integrity. **Conclusion.** The proposed technology can be recommended for use at eye banks for formation of an ultra-thin corneal graft at the preoperative stage.

Keywords: ultrathin lamellar corneal graft, preservation solution, eye bank, keratoplasty.

INTRODUCTION

Penetrating keratoplasty (PK) has long been considered the gold standard for surgical treatment of patients with epithelial endothelial dystrophy (EED) of the cornea. In order to improve the biological and functional results of engraftment of large corneal grafts, various PK modifications have been proposed at different times, namely: mushroom, conical, and stepped keratoplasty [1]. However, PK and its modifications still do not exclude the emergence of a number of significant problems: the operation is accompanied by a volumetric and prolonged depressurization of the eyeball, which leads to the risk of hemorrhagic and infectious complications; in the post-transplant period, immunobiological reactions of tissue incompatibility often develop and induced ametropias of varying severity appear. leading to unsatisfactory optical results [2, 3]. To eliminate the above problems associated with PK and the leading role of the endothelial layer in the development of EED, various techniques for replacing the posterior corneal layers have been proposed since the middle of the last century, but in 2001 M.A. Terry developed a technique of layer-by-layer replacement of damaged posterior layers of the cornea, called endothelial keratoplasty and performed using high-precision, high-tech microsurgical equipment and instrumentation [4]. To date, several modifications of endothelial keratoplasty have been proposed, one of which is descemet stripping automated endothelial keratoplasty (DSAEK), which is most widely used in the clinic for the treatment of patients with EED of the cornea of various origins [5–7]. The essence of the DSAEK operation is to remove Descemet's membrane with a layer of the affected corneal endothelium of the recipient and replace the cut-out graft of the posterior layers of the donor cornea through a 3 mm incision using a modified Busin slider and then pressing the flap against the posterior surface of the cornea with sterile air [8, 9]. At the same time, all stages of automated cutting out of the posterior corneal graft are carried out exclusively in the operating room, in parallel with manipulations on the patient's eye, which delays the operation time. In addition, the forced haste of the surgeon when performing intraoperative sections of the donor cornea often ends with the perforation of the ultrathin graft and the cancellation of the operation. Until now, both in Russia and abroad, there are no formulations of conservation media for nominal dehydration of the donor cornea and the optimal technique for cutting out ultrathin grafts (50–145 microns, on average 127 microns) using a single-pass microkeratome under

Corresponding author: Khadizhat Tonaeva. Address: 59 A, Beskudnikovsky Boulevard, Moscow, 127486, Russian Federation. Phone: (905) 515-66-11. E-mail: dr.tonaeva@gmail.com

the conditions of the Eye Tissue Bank at the stage of preoperative preparation [10–14]. The urgency of the problem and the lack of resolution of the above provisions in the DSAEK technology determined the purpose of thy present study.

The **purpose** of the present study was to develop a technology for preoperative preparation of the posterior layer-by-layer corneal graft based on our own formulation of the preservation medium for optimal dehydration of the donor cornea and the technique of cutting out an ultrathin flap using an optimized method in the conditions of the Eye tissue bank.

MATERIALS AND METHODS

Viable cadaveric human corneas used from the Eye Tissue Bank of the Fyodorov Eye Microsurgery Federal State Institution of the Ministry of Health of Russia (32 from 16 donors). One cornea from each donor was used as a control, the other, a steam room, served as a prototype. The control corneas were placed in vials with a basic preservation medium [15]. The corneas included in the experimental group were preserved in vials with the previously declared "agent for the preservation of the posterior layer-by-layer graft of the donor cornea" [16], which, due to its pharmacological components, has a membrane-stabilizing and membrane-restoring effect. At the first stage, the level of hydration of the stroma of preserved donor corneas in the experimental (n = 8) and control groups (n = 8) was studied by analytical weighing (Sartorius BP 210S, Germany) and pachymetry using an optical coherence tomograph (Optovue, iVue 100, USA) on 0, 1, 2, 3 and 4 days of the study. Upon completion of conservation, a morphofunctional study of the viability of endothelial cells of the obtained ultrathin corneal grafts was performed using immunofluorescence microscopy (Olympus FV 10i, Japan) using the Live and dead marker (Abcam, Great Britain). Based on the data obtained, the preservation period was determined at which the optimal dehydration of donor corneas is achieved. Then we proceeded to the second stage of the study, in which the corneas of the control (n = 8) and experimental (n = 8) groups were preserved for 2 days in the indicated solutions. On the 2nd day of conservation, ultrathin posterior layered grafts were formed from the corneas of both groups under the control of an optical coherence tomograph (Optovue, iVue 100, USA) using a microkeratome (Moria, France) by a single pass with a 550 μm cutting head (Moria, France). Then the samples of both groups were subjected to microscopy using a scanning electron microscope (JEOL JCM-6000, Japan) to assess the ultrastructure of the endothelial cell layer, orientation and damage of stromal collagen fibers, and the section profile.

DATA PROCESSING

To count the endothelial cells of ultrathin posterior layered grafts, CellProfile software was used, which allows for a quantitative analysis of images of stained cells.

Statistical analysis of the data obtained was performed with Graph Pad Prizm7 software.

RESULTS

According to the results of the first stage of the study, measuring the weight and pachymetry of donor corneas, dehydration and a decrease in thickness by 9% from the initial in the experimental group on the 1st day of conservation with a gradual increase and achievement of the nominal value (weight 0.195 ± 15 g, thickness 648 ± 35 μm) by the 3rd day, in the control group hydration (increase in thickness and weight) was observed from the first day of conservation. Pachymetric assessment using an optical coherence tomograph at all periods of observation in the experimental and control groups is shown in Fig. 1.

Thus, a correlation was found between the weight and thickness of the studied corneas during the conservation process. Determined the degree of dehydration in the first two days in the experimental group and hydration in the control from the first day of conservation. In addition, it was found that starting from the 3rd day, hydration in the experimental group reached nominal values with a tendency to increase, so further observation became inappropriate. Thus, the experimental preservation medium developed in this study [16] provides a more pronounced dehydration of the cornea during the first 2 days of storage compared to the standard preservation medium used in the control group.

At the end of 4 days of conservation in the study of the viability of endothelial cells of ultrathin corneal grafts by immunofluorescence microscopy using "Live and dead" marker, there was no significant difference between the groups ($p > 0.05$): 88.4% of living cells, 11, 6% of dead cells in the experimental group (Fig. 2, a) and 87.9% of living and 12.1% of dead cells in the control group (Fig. 2, b). Thus, despite the dehydration in the experimental group, the study of the morphofunctional preservation of endothelial cells of the ultrathin graft did not reveal a significant difference with the control group, which excludes the toxic and damaging effect of the conservation medium created according to the proposed recipe.

At the second stage of the study, ultrathin posterior layered grafts in both groups were formed using a longitudinal microkeratome by a single pass with a 550 μm cutting head (Moria, France). It was noted that in the experimental group, due to the lower hydration of the donor

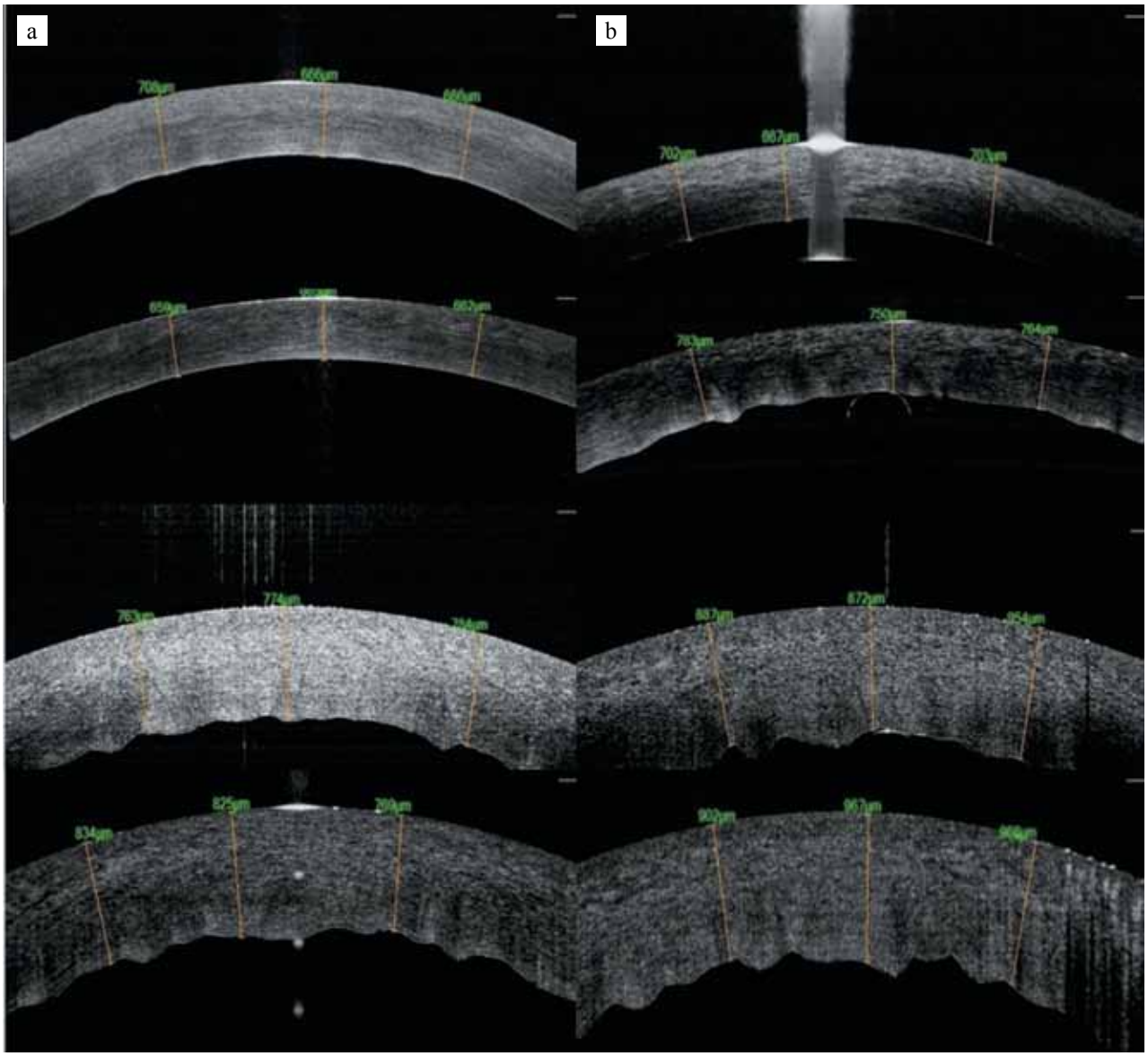

Fig. 1. OCT-picture of changes in the thickness of the donor cornea in the experimental (a) and control (b) group on the 0th (1), 1st (2), 3rd (3) and 4th (4) day of the study

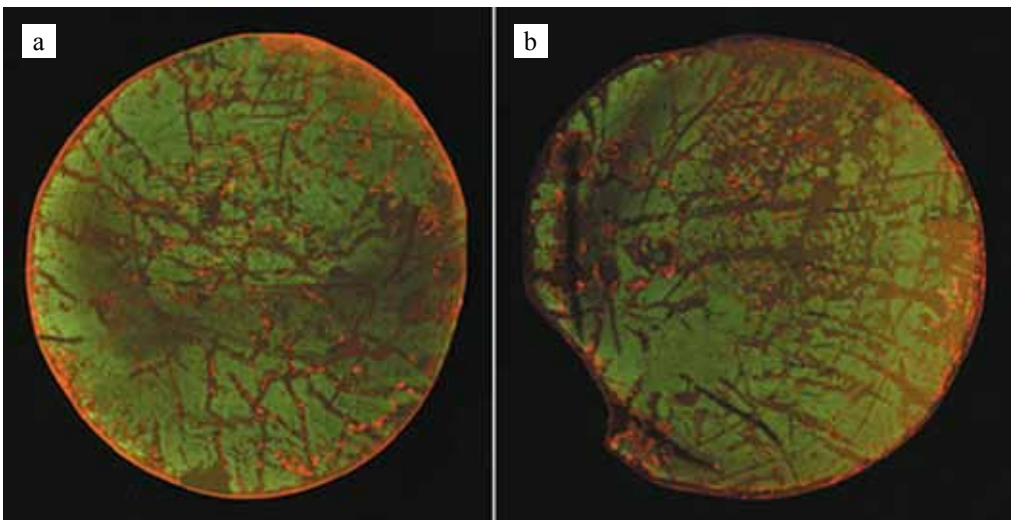

Fig. 2. Fluorescence staining of endothelial cells of the posterior corneal graft on the 4th day of conservation, Live and dead, in the experimental (a) and control (b) group. Laser scanning microscopy, ×100. Staining: green – living cells, red – dead

corneas, a single passage with the cutting head makes it possible to form statistically significantly ($p < 0.05$) thinner posterior layered grafts (123 ± 27 μm) compared to the control (190 ± 35 μm) (Fig. 3, a–b).

The results of scanning electron microscopy of ultrathin grafts formed according to the proposed technique demonstrate the preservation of the architectonics of corneal collagen fibers preserved in the proposed medium (Fig. 4, a), and signs of hydration of corneal fibers from the control group on the 2nd day of conservation (Fig. 4, b). Additionally, an image of the ultrastructure of the graft of the experimental group is shown in Fig. 5.

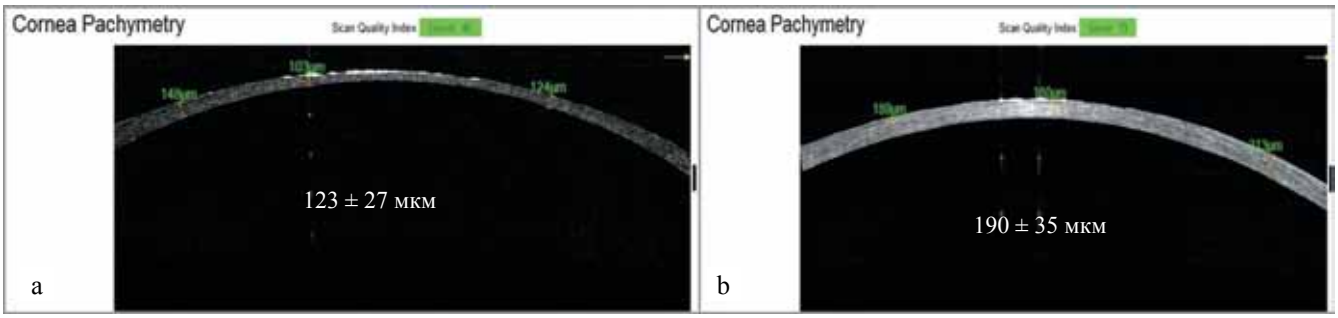

Fig. 3. OCT picture of an ultrathin posterior transplant of a donor cornea from the experimental (a) and control (b) groups

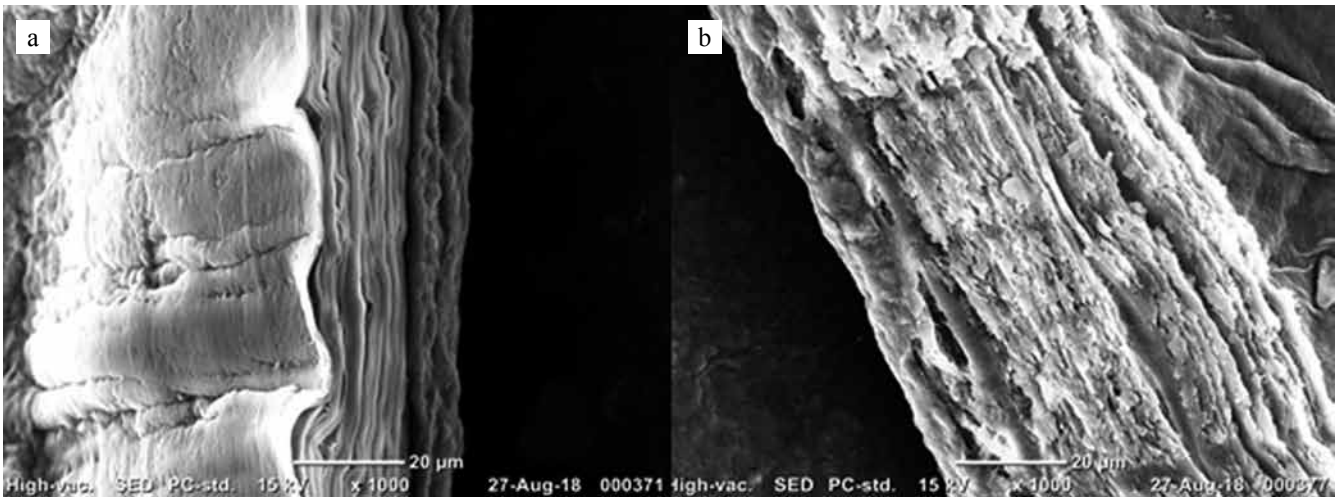

Fig. 4. The picture of the slice of the ultrathin posterior transplant on the 2nd day of conservation in the experimental (a) and control (b) group. Scanning electron microscopy, ×1000

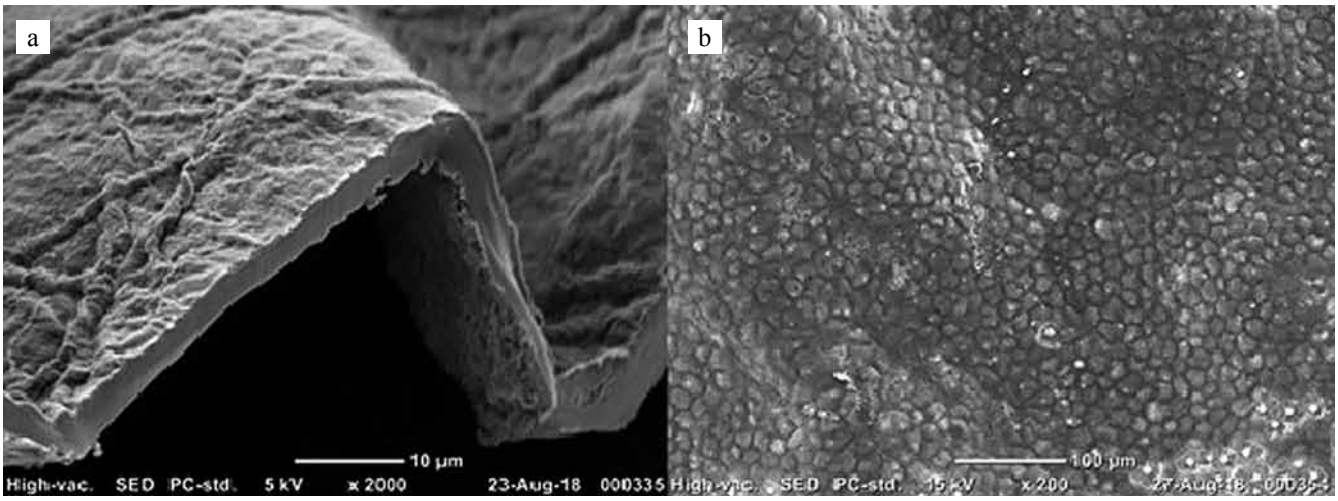

Fig. 5. Pictures of the profile of the slice (a) and endothelial layer of cells (b) of the ultrathin posterior graft on the 2nd day of conservation in the experimental group. Scanning electron microscopy, a – ×2000, b – ×200

DISCUSSION

The advantage of selective endothelial keratoplasty at the moment is doubtless. Operation in a closed palate significantly reduces the risk of developing dangerous intraoperative complications; in addition, the absence of an extensive through scar and complete preservation of the stroma allows maintaining the biomechanical resistance of the cornea to injury, innervation and trophism of the recipient's cornea, and minimizing induced astigmatism. In general, this contributes to a reduction in the period of clinical and visual rehabilitation of patients after transplantation of the donor cornea. The descemet stripping automated endothelial keratoplasty (DSAEK) is currently the most commonly used surgical method for the rehabilitation of patients with epithelial endothelial corneal dystrophy of various origins in developed countries. However, the question of the possibility of improving the clinical and functional results of DSAEK by using grafts of the posterior layers of the donor cornea with a minimum residual stroma thickness remains unresolved. In this regard, on the basis of eye tissue banks, the proposed technology for the preparation of an ultrathin flap of a cadaveric donor cornea based on the created preservation medium for dehydration and an optimized cutting technique can be used.

CONCLUSION

The conservation medium developed in this study [16] provides a more pronounced dehydration of the cornea during the first 2 days of cultivation as compared to the standard conservation medium. It was shown that this fact makes it possible to obtain a graft of the posterior corneal layers with a thickness of 123 ± 27 μm by a single passage with a microkeratome with a 550 μm head, compared with a thickness of 190 ± 35 μm obtained in the control group. The study of the morphofunctional preservation of endothelial cells of the ultrathin corneal graft did not reveal a significant difference with the control group, which excludes the toxic and damaging effect of the conservation medium created according to the proposed recipe. Thus, the proposed conservation medium can be used to obtain ultrathin transplants of the posterior layers of the cornea and thereby improve the functional results of the operation.

The authors declare no conflict of interest.

REFERENCES

1. *Flynn TH, Larkin DFP*. Penetrating Keratoplasty. *Encyclopedia of the Eye*. 2010: 290–295. doi.org/10.1016/B978-0-12-374203-2.00010-5.
2. *Borzenok SA*. Mediko-tekhnologicheskie i metodologicheskie osnovy effektivnoy deyatel'nosti glaznykh tkanevykh bankov Rossii v obespechenii operatsiy po skvoznoy transplantatsii rogovitsy. [Dissertation]. M., 2008. 306.
3. *Coster DJ, Lowe MT, Keane MC, Williams KA*. A comparison of lamellar and penetrating keratoplasty outcomes: A registry study. *Ophthalmology*. 2014; 5: 979–987. PMID: 24491643. doi: 10.1016/j.ophtha.2013.12.017.
4. *Terry MA*. Endothelial keratoplasty: history, current state, and future, directions. *Cornea*. 2006; 25 (8): 873–878. PMID: 17102658. doi: 10.1097/01.ico.0000244869.54761.50.
5. *Mamikonyan VR, Trufanov CB*. Avtomatizirovannaya zadnyaya posloynaya keratoplastika v lechenii bulleznoy keratopatii. *Byulleten' SO RAMN*. 2009; 138 (4): 37–39.
6. *Malyugin BE, Moroz ZI, Borzenok SA, Drozdov IV, Aiba EE, Pashtaev AN*. First experience and clinical results of DSAEK utilizing the pre-cut ultrathin grafts. *Fyodorov Journal of Ophthalmic Surgery*. 2013; 3: 12–16. (In Russ.).
7. *Oganesyan OG*. Sistema khirurgicheskoy reabilitatsii patsientov s endotelial'noy patologiey rogovitsy. [Dissertation]. M., 2011. 308.
8. *Price FW Jr, Price MO*. Descemet's stripping with endothelial keratoplasty in 200 eyes: Early challenges and techniques to enhance donor adherence. *J Cataract Refract Surg*. 2006 Mar; 32 (3): 411–418. PMID: 16631048. doi: 10.1016/j.jcrs.2005.12.078.
9. *Busin M, Madi S, Santorum P, Scorcia V, Beltz J*. Ultrathin Descemet's stripping automated endothelial keratoplasty with the microkeratome double-pass technique: Two-year outcomes. *Ophthalmology*. 2013; 20: 1186–1194. PMID: 23466268. doi: 10.1016/j.ophtha.2012.11.030.
10. *Price MO, Price FW*. Descemet's Stripping with Endothelial Keratoplasty. Comparative Outcomes with Microkeratome-Dissected and Manually Dissected Donor Tissue. *Ophthalmology*. 2006; 32 (3): 411–418. doi: 10.1016/j.ophtha.2006.05.034.
11. *Gorovoy MS*. Descemet-stripping automated endothelial keratoplasty. *Cornea*. 2006; 8: 886–889. PMID: 17102661. doi: 10.1097/01.ico.0000214224.90743.01.
12. *Tang M, Stoeger C, Galloway J, Holiman J, Bald MR, Huang D*. Evaluating DSAEK graft deturgescence in preservation medium after microkeratome cut with optical coherence tomography. *Cornea*. 2013 Jun; 32 (6): 847–850. doi: 10.1097/ICO.0b013e31828a27dd.
13. *Boynton GE, Woodward MA*. Eye-bank preparation of endothelial tissue. *Curr Opin Ophthalmol*. 2014; 25 (4): 319–324. doi: 10.1097/ICU.0000000000000060.
14. *Ho Wang Yin G, Sampo M, Soare S, Hoffart L*. Impact des caractéristiques du greffon cornéen sur les résultats cliniques après Descemet stripping automated endothelial keratoplasty (DSAEK) [Effect of donor graft characteristics on clinical outcomes in Descemet stripping automated endothelial keratoplasty (DSAEK)]. *J Fr Ophtalmol*. 2017; 40 (1): 36–43. doi: 10.1016/j.jfo.2016.09.018.
15. *Fedorov SN, Moroz ZI, Borzenok SA, Komakh YuA*. Sreda dlya konservatsii rogovitsy glaza. Patent RF № 2069951 ot 21.02.1993 g.
16. *Borzenok SA, Malyugin BE, Tonaeva KhD, Akhmedov AK, Kerimov TZ, Komakh YuA i dr.* Sredstvo dlya konservatsii zadnego posloynogo transplantata donorskoy rogovitsy. Patent RF № 2676311 ot 15.02.2018 g.

The article was submitted to the journal on 15.06.2020

DOI: 10.15825/1995-1191-2020-3-174-181

MODERN IDEAS IN HEART DONOR SELECTION CRITERIA

E.A. Tenchurina[1], M.G. Minina[1, 2]

[1] Moscow Coordinating Center for Organ Donation (Botkin City Clinical Hospital), Moscow, Russian Federation

[2] Shumakov National Medical Research Center of Transplantology and Artificial Organs, Moscow, Russian Federation

With the limited capacity of the available donor pool and the simultaneously growing demand for heart transplantation, expanding the heart donor selection criteria as one of the ways of increasing the availability of organ transplantation, and particularly donor heart, has become a challenge. On one hand, the use of expanded criteria donors increases the number of transplants and reduces the time spent on the waiting list. On the other hand, however, it increases the risk of adverse transplant outcomes. Accordingly, high-risk donors require a more thorough objective assessment using predictive models, while organs obtained from expanded criteria donors, require optimal selection of a donor-recipient pair. Analysis of global and national studies presented in this review reveals the depth of the current problem of heart donor selection.

Keywords: expanded criteria heart donors, cardiac donor selection, donor heart assessment criteria, prognostic models.

INTRODUCTION

The efficacy of heart transplantation is directly dependent on the maximum use of the available donor resource and suggests that each donor heart should be considered for transplantation by all existing programs in order to avoid the loss of a "working" donor organ. Assuming that all proposed donor hearts are successfully transplanted, the problem of organ shortages will become less acute [1]. However, clinicians, when faced with hearts from donors with extended criteria, tend to make decisions more often on rejection, fearing the negative impact of donor risk factors on the outcome of heart transplantation [2]. Despite the lack of organs, only 39.2% of the donors declared in Eurotransplant in 2010 were considered as possible heart donors, and only 66.6% of them became effective donors [3]. In addition, unlike the United States, where there has been no increase in the number of effective heart donors with extended criteria since the 2000s, the average age of heart donors in Europe continues to increase, reaching 34 years in 1996, 36 years in 2000, in 2010 – an increase to 43 years [3, 4].

Thus, there is a reasonable need for an objective assessment of the donor heart based on modeling the degree of influence of donor risk factors on the outcome of heart transplantation. In modern conditions, when the number of "ideal" donors is extremely small and the majority of donors are in the so-called gray zone, that is, between "ideal" and "unsuitable", verified criteria for assessing the donor heart are needed, which will help in an objective decision-making – to use or refuse a donor heart [2].

SELECTION OF HEART DONORS. EXPANDED CRITERIA HEART DONORS AND THEIR EFFECT ON HEART TRANSPLANTATION RESULTS

Currently, the selection criteria for a donor heart vary widely depending on the country, the medical institution performing the heart transplant, the experience of working with donors with extended criteria, etc. The most noticeable differences relate to the donor's age, cause of death, history of tobacco smoking, the state of the donor's hemodynamics, as well as circulatory arrest, episodes of hypotension, their number and duration [5, 6].

The traditional selection criteria for heart donors include age <55, no chest injury and heart disease, no prolonged hypotension and hypoxemia, stable hemodynamics, mean arterial pressure (MAP) >60 mm Hg. Art., central venous pressure (CVP) from 8 to 12 mm Hg. Art., inotropic support less than 10 mg/kg/min (dopamine or dobutamine), ECG and Echo-CG without pathological changes, the state of the coronary arteries according to coronary angiography (CAG) according to the age and history of the donor [7].

Modern approaches to the selection of a donor heart, first of all, donor risk factors should be considered that can negatively affect the results of transplantation. Donor age is widely regarded as the most important risk factor, along with left ventricular (LV) ejection fraction <50%, which does not improve after donor conditioning, and LV myocardial hypertrophy [8].

Donors with characteristics associated with an increased risk of graft failure are referred to as expanded criteria donors (ECD). According to Kilic (2014), in order to

Corresponding author: Elmira Tenchurina. Address: 5, Vtoroy Botkinsky proyezd, Moscow, 125284, Russian Federation. Phone: (967) 113-87-64. E-mail: arimle@inbox.ru

reduce the deficit of donor hearts, it is necessary to pay special attention to working with donors with extended criteria (DRC). Such donors require careful selection of the recipient, which contributes to the achievement of optimal survival results for recipients who received a heart from ECDs [6].

Donor factors that are most often found in publications as independent risk factors for transplantation outcome include donor age, female gender and cold ischemia duration [9].

Despite the fact that the clinical characteristics of the recipient are more significant in predicting survival after transplantation, donor risk factors also have a proven influence on the results of transplantation [9–11].

Accordingly, in the process of deciding on transplanting a donor heart, it is necessary to consider the donor and recipient factors in a complex manner. Heart transplants obtained from high-risk donors and transplanted to recipients with the least number of aggravating factors demonstrate higher survival rates; in addition, optimized donor and recipient selection is one of the possible ways to reduce the shortage of donor organs for transplantation [9, 11].

PREDICTIVE EFFECT OF DONOR AGE ON HEART TRANSPLANTATION RESULTS

One of the recent studies by Bergenfeld (2019) demonstrates the prognostically unfavorable effect of the donor's age with a difference with the recipient of +10 years in the form of an increase in the risk coefficient (RR) of the recipient's death in a 30-day period after transplantation to 1.19, in 1th year after transplantation – 1.16, in the time periods after transplantation 1–3 years, 3–5 years, 5–10 years, the risk coefficient is 1.12; 1.07 and 1.07, respectively. The study included 64,354 heart transplant cases in 1988–2013 [12]. Another study performed in the USA (Lushaj, 2019) retrospectively analyzed 755 heart transplant patients and found that the long-term survival of recipients who received a heart from a donor <45 years is significantly higher compared to recipients who received a heart from a donor >45 years. The risk of death was also higher in heart recipients from donors >45 years old [13]. At the same time, a study by Ravi (2019) using the UNOS register for the period 2008–2017. (19 514 heart transplants), shows that when a heart transplant from a donor over 50 years old to a recipient in the age range of 18–39 years, there is no decrease in survival. Recipients in the 40–49 age group who received hearts from donors 40–49 years old and over 50 years old have a 10-year survival rate decrease by 43 and 75%, respectively, compared to the group of recipients who received donor hearts in the 18–29 age range. Similarly, in recipients <50 years old who received donor hearts 30–39, 40–49, >50 years old, there was a decrease in 10-year survival by 14, 27 and 47%, respectively. Thus, it is important to note that donor age does not decrease survival in young recipients [14].

GENDER AND ANTHROPOMETRIC CONFORMITY OF DONOR AND RECIPIENT

A number of studies have revealed that the female gender of the donor is considered as an independent factor in increasing mortality in recipients of the opposite sex [15–21]. Men who received hearts from male donors had the highest cumulative survival rate in 5 years [22]. The mechanisms underlying the obtained results of gender mismatch are not entirely clear but may be associated with a mismatch in the size of the heart, despite the coincidence of the weight of the donor and recipient of the opposite sex [23].

A weight difference in the range of 20–25%, or a donor to recipient weight ratio in the range of 0.8–1.2, are generally considered acceptable for transplantation. D.O. Taylor et al. (2007) found that a decrease in the donor to recipient body mass index ratio is a significant risk factor for an increase in 5-year mortality [24]. However, N.D. Patel et al. (2008) by analyzing the combined database of the Registry of Donor Organs for the period 1999–2007. found that 30-day mortality was highest in recipients with a donor/recipient weight ratio <0.8, but the finding was not statistically significant [25]. R.M. Reed et al. (2014) demonstrated that there was no difference in survival between underweight donor, overweight donor and the group in which the ratio by weight to the recipient was optimal. In modern clinical practice, the weight ratio between donor and recipient is considered in combination with the presence of other risk factors, such as the clinical condition and history of the donor, and the time of graft ischemia. Similarly, the body mass index (BMI) is considered most often in cases of severe obesity, both donor and recipient [16]. Thus, in the selection of a donor and the selection of a donor-recipient pair, donor weight in the absence of other risk factors is not a contraindication for heart transplantation. Recently, attention has been paid to the ratio of the mass of the left ventricle of the donor and the recipient since a decrease in survival was revealed with a mismatch in LV mass by more than 10–15% [23].

EFFECT OF CAUSE OF DONOR'S DEATH ON THE RESULTS OF HEART TRANSPLANTATION

Some single-center studies demonstrate a decrease in recipient survival and an increase in the incidence of vasculopathy of a heart transplant in the event that the death of the donor is due to non-traumatic brain damage. Suarez-Pierre et al. (2019) studied 20,244 patients who underwent heart transplantation in 2007–2016 and found no statistically significant difference in the 1- and 5-year survival rates of recipients who received hearts from donors with traumatic brain injury and donors wi-

thout traumatic brain injury. brain (vascular or another genesis). Also, no differences were found between the groups of recipients in the incidence of transplanted heart vasculopathy [26]. A study by Barac et al. (2019) and having the same goals as the above study included 58 474 patients after heart transplantation. There was no difference in patient survival, the median survival was identical between groups of patients and amounted to 12.3 years [27]. This study is the largest to date in terms of the number of patients included in it, and the results obtained should remove concerns about the influence of the cause of death of the donor on the results of heart transplantation. An earlier study by Singhal et al. (2009), devoted to the study of the influence of the cause of death of the donor on the results of organ transplantation – heart, lungs, liver, kidneys. The study looked at such causes of death of the donor as cerebrovascular disease (stroke), traumatic brain injury, anoxic brain injury, brain tumor, and other causes. The results of the univariate model of proportional risks of death of a patient (Cox) after heart, lung, and liver transplantation show that the risk ratio (RR) of death of the recipient after heart transplantation from a donor with traumatic brain injury is a reference value and is 1.0, while the risk coefficient the death of a recipient who received a heart from a donor with cerebral vascular injury is 1.20, with the death of a donor from hypoxia, the risk coefficient is less than the reference one – 0.96. The results of a multifactorial model of proportional risks, adjusted for age, sex, the presence of cytomegalovirus (CMV) infection, diabetes mellitus, dependence on tobacco and cocaine, hypertension, etc., demonstrated the preservation of survival rates of recipients depending on the cause of death of the donor [28]. Swiss researchers led by Rizzi (2016) found no effect of the cause of death of the donor on the survival of patients after heart transplantation. The study included 114 patients who underwent heart transplantation in 1997–2009. Notably, this study used known indicators of the medical status of a critically ill patient such as APACHE II, SAPS II and SOFA to classify a donor as an extended criteria donor. No difference in survival was found between recipients who received hearts from a donor with standard and extended criteria in accordance with the values of the indicated critical condition indicators [29].

HEART DONORS WITH CARDIOPULMONARY REANIMATION. DURATION OF TRANSPLANT ISCHEMIA

There is currently concern regarding the use of a donor heart from a donor with cardiac arrest and subsequent cardiopulmonary resuscitation (CPR). The key question is whether such a heart can withstand further ischemic damage that accompanies brain death, subsequent conservation, transportation, and what is important is the survival rate of recipients after transplantation of such a heart. The effect of circulatory arrest in donors on the results of heart transplantation is reflected in a retrospective study, which included 19,980 donors for the period 1994–2011, of which in 856 cases cardiac arrest was observed [30]. It was found that 1-, 5-, 10-year survival rates between standard donors and donors with circulatory arrest did not differ significantly. The same authors found that patients who received heart transplants from donors with short-term cardiac arrest (0–8 min) had better survival rates compared to other groups, including those who received a donor heart from a standard donor. As an explanation for the reason, the authors put forward the hypothesis of ischemic preconditioning, which was first described by C.E. Murry et al. (1986) [31]. A short episode of ischemia slows down the rate of ATP depletion, contributes to the preservation of intracellular structure, a decrease in oxygen consumption, retention and a decrease in cell necrosis during subsequent ischemic episodes. Thus C.E. Murry et al. (1986) suggested that multiple short-term ischemic episodes may protect the heart from subsequent ischemic exposure. Nevertheless, an increase in the duration of cardiac arrest in the donor, exceeding 25 minutes, demonstrated a decrease in the survival of recipients [30].

Similar results of the absence of a negative effect of cardiac arrest in donors on the survival rate of recipients after heart transplantation were obtained by A. Galeone et al. (2017). The study included 584 cases of heart donation in 2004–2012, of which 117 donors had cardiac arrest with an average duration of 15 minutes (5–25 minutes). The authors found that the rates of 30-day and 1-year survival in the groups with CPR and without CPR did not differ significantly, while the 10-year survival rate had a significantly better result in donors with CPR (69.4% vs 50.4%) [32]. A possible explanation for the obtained results, suggested by A. Galeone (2017), that the CPR group included younger donors. It is well known that the young age of the donor is a proven factor that has a positive effect on the survival of heart recipients [33]. In addition, the ischemic preconditioning effect of short-term cardiac arrest, described above, was not excluded [31].

Russian authors (Poptsov V.N., 2019) also studied the effect of cardiac arrest of the donor on the survival rate of recipients after heart transplantation. The study included 28 recipients who underwent heart transplantation (HT) from donors who underwent CPR from 01.01.2011 to 31.12.2017, which amounted to 4.0% of the total number of HTs for the analyzed period (n = 698). In terms of the incidence of early heart transplant dysfunction, which required the use of post-transplant mechanical circulatory support (BMC), the recipients of the “donor with CPR” and “donor without CPR” groups did not differ significantly. Comparative analysis did not reveal any significant differences in 1-, 3- and 5-year survival

rates of recipients in the two groups [34]. Thus, when analyzing the above studies, no convincing evidence was found for a decrease in the survival rate of recipients after heart transplantation from a donor with cardiac arrest. Donor CPR should not exclude the possibility of considering the donor heart for transplantation [35].

Speaking of ECDs, it is necessary to know the acceptable time limits for ischemia of the donor heart (conservation), since exceeding the time of conservation is a factor that negatively affects the survival of recipients.

There are two degrees of duration of ischemia of a cardiac transplant, optimal and long-term. The optimal ischemia is less than 180 minutes, and prolonged, more than 240 minutes. The 1-year survival rate of recipients is comparable for optimal and prolonged ischemia, although long-term data (10-year survival) are still insufficient for analysis [36]. There are studies demonstrating that longer ischemia time is associated with increased mortality in recipients [37–39]. The threshold value of ischemia of the donor heart is considered to be a value of 300 minutes with insufficient clinical data exceeding this value. In the presence of other risk factors – the elderly age of the donor, cardiovascular factors, high doses of inotropic and vasopressor support – the specified threshold for the duration of ischemia cannot be exceeded [40, 41].

MANAGED RISK IN HEART TRANSPLANTATION FROM EXPANDED CRITERIA DONORS

The selection of a donor heart is often rather difficult and subjective, despite the guidelines available for deciding whether to use a donor heart for transplantation. If one transplant center finds the donor heart unsuitable for transplant, it can and should be offered to other centers [42].

Table

Reasons Why Hearts Were Declined by first centre (n = 93)

Reasons	Primary	Secondary
Inotropic support (%)[1]	23.6	4.3
Hemodynamic instability (%)[2]	10.7	8.6
ECG changes (%)[3]	10.7	5.3
Age (%)[4]	5.3	12.6
Aggravated history	16.1	13.9
X-ray changes (%)[5]	4.3	3.2
Smoking (%)[6]	6.5	38.7
Other (%)[7]	22.8	13.1

Note. [1] – dopamine >10 μg/kg/min or noradrenalin >0.2 μg/kg/min or adrenaline >0.5 μg/kg/min; [2] – high filling pressures and low systemic blood pressure; [3] – abnormal rhythm, bundle branch block, or ST wave changes; [4] – up to a maximum of 65 years; [5] – abnormal cardiac size/cardiothoracic ratio or pulmonary oedema; [6] – up to 20 pack-years (i. e. 1 pack/d for 20 years); [7] – cerebral astrocytoma grade IV, brain tumour with unknown histological findings, hypernatremia and hyperkalemia of unknown cause and significant history of drug abuse.

A 2007 study carried out in Manchester, UK, presents an analysis of the "primary" and "secondary" reasons for refusal from a donor heart when the first and subsequent transplant centers refused. It is noteworthy that the range of failure rates of the second center according to such criteria as high doses of inotropic support, unstable hemodynamics, ECG changes is 1.5–6 times lower than that of the first center. However, according to such donor criteria as the age of the donor and smoking, the second center refused 2.5 to 6 times more often than the first, which once again underlines the serious difference between the centers in the criteria for selecting a donor heart and demonstrates the need for donor evaluation by several centers in order to achieve full use of donor resource in conditions of its deficit (Table) [43].

In the course of this study, two groups of recipients were also identified, in one (group B) hearts were transplanted from the first distribution attempt, in the second (group A) – after the failure of other transplant centers. The study found no significant difference in 30-day mortality, length of stay in the intensive care unit (ICU), and total length of hospital stay between the two groups. There was no statistically significant difference in the incidence of death from cardiac causes: 30% in group A and 22% in group B. Early graft dysfunction was the leading cause of death in 75% of cases in group A and 69% in group B. Kaplan–Meyer survival curves showed no significant difference in long-term survival (6 years of follow-up), log rank test = 0.30.

In all cases of heart donation according to extended criteria, the balance of risks and benefits associated with performing heart transplantation in a particular recipient is of paramount importance, as well as an assessment of the risk of death in case of refusal of transplantation and further stay of the recipient on the waiting list. Therefore, each decision must be made individually and carefully. Some surgeons transplant borderline hearts into high-risk recipients, believing that high-risk recipients have a chance in the event of such a transplant. Other surgeons transplant suboptimal organs into recipients with a lower risk of death, relying on the evidence that the severity of the recipient's condition is a determining factor in early survival after transplantation [44].

PREDICTIVE MODELS FOR ASSESSING DONOR HEART

As noted above, many donor and recipient factors can influence the outcome of heart transplantation. Accordingly, an objective assessment of the donor heart from the standpoint of the survival rate of recipients at different times after transplantation is an important joint task of the donor service and specialists in the field of heart transplantation. In the world for this purpose, various prognostic models are used, including both donor and recipient factors. The outcome points for which the risk is

quantified are the recipient's survival after transplantation and the decision to refuse or use a donor heart. Among the most well-known models, it is necessary to name the Index for Mortality Prediction After Cardiac Transplantation (IMPACT), the Index for predicting mortality after cardiac transplantation, developed in the USA (Weiss ES, 2011), considers 12 preoperative factors of the recipient and is maximum 50 points, allows predicting the annual survival of recipients after heart transplantation [45, 46].

J. Segovia et al. (2011) retrospectively investigated the results of heart transplants performed in one clinic in 621 recipients in the period 1984–2006. The use of multivariate analysis made it possible to identify six independent factors that increase the risk of death in recipients after transplantation, four of which are recipient factors – right atrial pressure ≥10 mm Hg. Art., recipient age ≥60 years, diabetes mellitus, dependence on inotropic support, and two donor factors – donor age ≥30 years, ischemic time ≥240 min. Based on these results, the RADIAL risk calculator was developed. The maximum number was 6 points. Each subsequent increase of one point was associated with an increased risk of primary graft failure (PGF). A score of 4–6 was associated with a more than 5-fold increase in the PGF risk (OR = 5.33, p = 0.01) [47].

French researchers led by C. Jasseron (2015) proposed their model for predicting risks after heart transplantation, considering both donor and recipient factors. The model, validated on a national pool of heart donors, has shown the effect on the annual survival rate of such recipient factors as age >50, congenital valvular heart disease, and, as a consequence, the development of cardiomyopathy, increased bilirubin levels, low glomerular filtration rate, among donor factors only female donor sex [9]. A group of researchers from the United States already known to us, led by E.S. Weiss (2012) developed the first predictive model for assessing a donor heart, considering only donor factors. During the logistic regression and multivariate model, 4 donor factors were identified that significantly affect the annual survival rate after heart transplantation – the time of cold ischemia (conservation), donor age, racial differences between donor and recipient, and urea/creatinine ratio ≥30 [10].

Using the European Registry of Donor Organs, J.M. Smits et al. (2012), created a donor heart assessment model using more than 20 donor factors. With the logistic regression method, the degree of influence of donor factors on the level of 3-year survival of recipients was revealed [2, 47].

Mention should be made of the risk stratification assessment developed using the UNOS Organ Transplant Registry to predict annual survival after heart transplantation. The assessment includes 13 recipient factors, 3 donor factors, and 2 common factors [38].

The International Heart Transplant Survival Algorithm is a predictive model of short-term and long-term survival after heart transplantation using complex modeling of 32 recipient risk factors and 11 donor risk factors [48]. Also, the combined assessment of the recipient and the donor was used in the study by J.R. Trivedi (2016), where it was shown that heart transplantation from a high-risk donor to a low-risk recipient is associated with good 5-year survival, while heart transplantation from a high-risk donor to a high- or very high-risk recipient leads to a low five-year survival rate – from 65 up to 49% [49].

CONCLUSION

With the increasing number of donors with extended criteria, the need to revise the approaches to the selection of heart donors is of paramount importance. In order to increase the efficiency of heart transplantation, select the optimal recipient for transplantation, improve the algorithms for the distribution of the donor heart, maximize the use of the donor resource, donor service specialists and clinicians need a modern tool in the form of a prognostic model for a comprehensive objective assessment of the donor heart and the recipient's risk factors in the context of the outcome of heart transplantation… For Russia, where over the past 12 years (2006–2018) the number of heart transplants has increased 25.6 times, including due to the work with donors with extended criteria, the development and use of such a prognostic model becomes extremely urgent.

The authors declare no conflict of interest.

REFERENCES

1. *Russo MJ, Davies RR, Hong KN et al.* Matching high-risk recipients with marginal donor hearts is a clinical effective strategy. *Ann Thorac Surg*. 2009; 87: 1066–1071.
2. *Smits JM, De Pauw M, de Vries E et al.* Donor scoring systemfor heart transplantation and the impact on patient survival. *J Heart Lung Transplant*. 2012; 31: 387–97.
3. Eurotransplant: Donation, waiting lists, and transplantation. In: Oosterlee A, Rahmel A, eds. Annual report 2010 of the Eurotransplant International Foundation. Leiden: Eurotransplant International Foundation; 2010.
4. *Nativi JN, Brown RN, Taylor DO et al.* Temporal trends in heart transplantation from high risk donors: are there lessons to be learned? A multiinstitutional analysis. *J Heart Lung Transplant*. 2010; 29: 847–852.
5. *John R.* Donor management and selection for heart transplantation. *Semin Thorac Cardiovasc Surg*. 2004; 16: 364–369.
6. *Kilic A, Sitaramesh E, Chittoor B.* Donor selection in heart transplantation. *J Thorac Dis*. 2014; 6 (8): 1097–1104.
7. Sabiston & Spencer surgery of the chest, 8th ed. Sellke FW, del Nido PJ, Swanson SJ et al. Philadelphia: Saunders Elsevier, 2010.
8. *Sorabella RA, Guglielmetti L, Kantor A et al.* Cardiac donor risk factors predictive of short-term heart transplant recipient mortality: An analysis of the united net-

work for organ sharing database. *Transplant Proc*. 2015; 47: 2944–2951.
9. *Jasseron C, Legeai C, Cantrelle C et al.* Donor- and recipient-related predictors of mortality after heart transplantation:results from a contemporary French national cohort. *Heart Lung Transplant*. 2015; 34 (4): S61.
10. *Weiss ES, Allen JG, Kilic A et al.* Development of a quantitative donor risk index to predict short-term mortality inorthotopic heart transplantation. *J Heart Lung Transplant*. 2012; 31: 266–273.
11. *Trivedi JR, Cheng A, Ising M, Lenneman A, Birks E, Slaughter MS.* Heart Transplant Survival Based on Recipient and Donor Risk Scoring: A UNOS Database Analysis. *ASAIOJ*. 2016; 62: 297–301.
12. *Bergenfeld H, Lund H, Stehlik J, Andersson B.* Time-dependent prognostic effects of recipient and donor age in adult heart transplantation. *J Heart Lung Transplant*. 2019; 38 (2): 174–183.
13. *Lushaj E, Dhingra R, Osaki S, Johnson M, Kohmoto T.* Donor Age Significantly Impacts Long Term Survival of Patients Undergoing Heart Transplantation. *J Heart Lung Transplant*. 2019; 38 (4): S267.
14. *Ravi Y, Srikanth N, Paul IW, Whitson BA, Emani S, Sai-Sudhakar CB.* Heart Transplant Recipient and Donor Age: Should the Younger Recipient Be Matched with the Younger Donor? *J Heart Lung Transplant*. 2019; 38 (4): S161–S162.
15. *McCarthy JF, McCarthy PM, Massad MG, Cook DJ, Smedira NG, Kasirajan V et al.* Risk factors for death after heart transplantation:does a single-center experience correlate with multicenter registries? *Ann Thorac Surg*. 1998; 65 (6): 1574–1578.
16. *Solomon NA, McGiven JR, Alison PM, Ruygrok PN, Haydock DA, Coverdale HA et al.* Changing donor and recipient demographics in a heart transplantation program: influence on early outcome. *Ann Thorac Surg*. 2004; 77 (6): 2096–2102.
17. *Tsai FC, Marelli D, Bresson J, Gjertson D, Kermani R, Ardehali A et al.* Recent trends in early outcome of adult patients after heart transplantation: a single-institution review of 251 transplants using standard donor organs. *Am J Transplant*. 2002; 2 (6): 539–545.
18. *Stehlik J, Feldman DS, Brown RN, VanBakel AB, Russel SD, Ewald GA et al.* Interactions among donor characteristics influence post-transplant survival: a multi-institutional analysis. *J Heart Lung Transplant*. 2010; 29 (3): 291–298.
19. *Khush KK, Kubo JT, Desai M.* Influence of donor and recipient sex mismatch on heart transplant outcomes: analysis of the International Society for Heart and Lung Transplantation Registry. *J Heart Lung Transplant*. 2012; 31 (5): 459–466.
20. *Prendergast TW, Furukawa S, Beyer 3rd AJ, Browne BJ, Eisen HJ, Jeevanandam V.* The role of gender in heart transplantation. *Ann Thorac Surg*. 1998; 65 (1): 88–94.
21. *Al-Khaldi A, Oyer PE, Robbins RC*. Outcome analysis of donor gender in heart transplantation. *J Heart Lung Transplant*. 2006; 25 (4): 461–468.
22. *Weiss ES, Allen JG, Patel ND, Russell SD, Baumgartner WA, Shah AS et al.* The impact of donor-recipient sex matching on survival after orthotopic heart transplantation: analysis of 18 000 transplants in the modern era. *Cir Heart Fail*. 2009; 2 (5): 401–408.
23. *Reed RM, Netzer G, Hunsicker L, Mitchell BD, Rajagopal K, Scharf S et al.* Cardiac size and sex-matching in heart transplantation: size matters in matters of sex and the heart. *JACC Heart Failure*. 2014; 2 (1): 73–83.
24. *Taylor DO, Edwards LB, Boucek MM, Trulock EP, Aurora P, Christie J et al.* Registry of the International Society for Heart and Lung Transplantation: twenty-fourth official adult heart transplant report. *J heart Lung Transplant*. 2007; 26 (8): 769–781.
25. *Patel ND, Weiss ES, Nwakanma LU, Russell SD, Baumgartner WA, Shah AS et al.* Impact of donor-to-recipient weight ratio on survival after heart transplantation: analysis of the United Networkfor Organ Sharing Database. *Circulation*. 2008 Sep 30; 118 (14 Suppl): 83–88.
26. *Suarez-Pierre Alejandro, Crawford Todd C, Zhou Xun, Lui Cecillia, Fraser III Charles D.* Impact of Traumatically Brain-Injured Donors on Outcomes After Heart Transplantation. *J Surg Research*. 2019; 240: 40–47.
27. *Barac YD, Jawitz O, Klapper J, Schroder J et al*. Heart Transplantation Survival and the Use of Traumatically Brain-Injured Donors. *J Heart Lung Transplant*. 2019; 38 (4): S186.
28. *Singhal AK, Sheng X, Drakos SG*. Stehlik Impact of Donor Cause of Death on Transplant Outcomes: UNOS Registry Analysis. *J Transplantation Proceedings*. 2009 Nov; 41 (9): 3539–3544.
29. *Rizzi G, Startseva X, Wolfrum M, Luscher TF*. Unfavorable donor pretransplant APACHE II, SAPS II, and SOFA scores are not associated with outcome^Implication for heart transplant donor selection. *Transplant Proceed*. 2016; 48 (8): 2582–2587.
30. *Southerland KW, Castleberry AW, Williams JB, Daneshmand MA, Ali AA, Milano CA*. Impact of donor cardiac arrest on heart transplantation. *Surgery*. 2013; 154 (2): 312–319.
31. *Murry CE, Jennings RB, Reimer KA*. Preconditioning with ischemia: a delay of lethal cell injury in ischemic myocardium. *Circulation*. 1986; 74: 1124–1136. PubMed: 3769170.
32. *Galeone A, Varnous S, Lebreton G et al.* Impact of cardiacarrest resuscitated donors on heart transplant recipients' out-come. *J Thorac Cardiovasc Surg*. 2017; 153: 622–630.
33. *Kilic A, Weiss ES, George TJ, Arnaoutakis GJ, Yuh DD, Shah AS et al.* What predicts long-term survival after heart transplantation? An analysis of 9,400 ten-year survivors. *Ann Thorac Surg*. 2012; 93: 699–704.
34. *Poptsov VN, Spirina EA, Pchelnikov VV, Khatutsky VM, Aliev EZ, Voronkov VYu et al*. Heart transplantation from cardiac arrest-resuscitated donors. *Russian Journal of Transplantology and Artificial Organs*. 2019; 21 (2): 23–30. [In Russ, English abstract]. doi: 10.15825/1995-1191-2019-2-23-30.
35. *Ali AA, Lim E, Thanikachalam M, Sudarshan C, White P, Parameshwar J et al.* Cardiac arrest in the organ donor does not negatively influence recipient survival after heart transplantation. *Eur J Cardiothorac Surg*. 2007; 31 (5): 929–933.

36. *Morgan J, John R, Weinberg A, Kherani A, Colletti N, Vigilance D et al.* Prolonged donor ischemic time does not adversely affect long-term survival in adult patients undergoing cardiac transplantation. *J Thorac Cardiovasc Surg*. 2003; 126: 1624–1633.
37. *Kilic A, Weiss ES, Allen JG et al.* Simple score to assess the risk of rejection after orthotopic heart transplantation. *Circulation*. 2012; 125: 3013–3021.
38. *Hong KN, Iribarne A, Worku B et al.* Who is the highrisk recipient? Predicting mortality after heart transplant using pretransplant donor and recipient risk factors. *Ann Thorac Surg*. 2011; 92 (2): 520–527.
39. *Bourge RC, Naftel DC, Costanzo-Nordin MR et al.* Pretransplantation risk factors for death after heart transplantation: a multiinstitutional study. The Transplant Cardiologists Research Database Group. *J Heart Lung Transplant*. 1993; 12: 549–562.
40. *Del Rizzo D, Menkis A, Pflugfelder P, Novick R, McKenzie F, Boyd W et al.* The role of donor age and ischemic time on survival following orthotopic heart transplantation. *J Heart Lung Transplant*. 1999; 18: 310–319.
41. *Faggian G, Forni A, Mazzucco A.* Donor organ preservation in highrisk cardiac transplantation. *Transplant Proc*. 2004; 36: 617–619.
42. UK Transplant: Donor Organ Sharing Scheme-Operating Principles for Cardiothoracic Transplant Units in the UK and Republic of Ireland [http://www.uktransplant.org.uk/ukt/about_transplants/organ_allocation/cardiothoracicardiothoracic_organ_sharing].
43. *Noman H, Khasati Ali Machaal, Jim Barnard, Nizar Yonan*. Donor heart selection: the outcome of "unacceptable" donors. *Journal of Cardiothoracic Surgery.* 2007; 2: 13.
44. *Anyanwu A, Rogers C, Murday A.* Should recipient risk be a factor in choosing recipients for suboptimal donor hearts: a multiinstitutional study. *Transplant Proc*. 1993; 31: 1399.
45. *Weiss ES, Allen JG, Arnaoutakis GJ et al.* Creation of a quantitative recipient risk index for mortality prediction after cardiac transplantation (IMPACT). *Ann Thorac Surg.* 2011; 92: 914–921.
46. The International society for heart and lung transplantation. International registry for heart and lung transplantation; 2016; http://www.ishlt.org/registries/slides.asp?slides=heartLungRegistry.
47. *Segovia J, Cosio MD, Barcelo JM, Bueno MG, Pavia PG, Burgos R et al.* RADIAL: a novel primary graft failure risk score in heart transplantation. *J Heart Lung Transplant.* 2011; 30 (6): 644–651.
48. *Nilsson J, Ohlsson M, Hoglund P, Ekmehag B, Koul B, Andersson B.* The International Heart Transplant Survival Algorithm (IHTSA): a new model to improve organ sharing and survival. *PLoS One*. 2015; 10: e0118644.
49. *Trivedi JR, Cheng A, Ising M, Lenneman A, Birks E, Slaughter MS.* Heart Transplant Survival Based on Recipient and Donor Risk Scoring: A UNOS Database Analysis. *ASAIOJ*. 2016; 62: 297–301.

The article was submitted to the journal on 7.02.2020

INSTRUCTIONS FOR AUTHORS

Submitted articles should contain original work that has not been previously published and is not under consideration for publication elsewhere. We do not charge any publication fee.

The paper size should be A4 (1 copy, 1.5 pt line spacing). The text of the body of the paper should be in Times New Roman with font size 12 pt. The paper should be presented in the form of an identical Microsoft Word file on electronic media (attached CD or via e-mail).

Structure of the paper

The Title page must contain:

– Title of the paper.
– Author names (list the author's initials before listing his or her last name).
– Institutional affiliation, city and country. Spell out the name of the institution fully.

Note: List all authors in one line. Then list the institutional affiliations of all the authors below the author names. Affiliations corresponding to the author names are denoted using superscript numbers/letters.

Details about authors

Indicate the full name of each author and his or her position in at the relevant department/institution.

Corresponding author

Indicate the full name of the author, who will be communicating with the journal. Also indicate his or her address (including postal code), telephone, fax number, and e-mail address.

Abstract

Each article must have an abstract of no more than 300 words for a literature review, and no more than 200 words for clinical observation. The abstract should be a concise summary of the entire content of the paper. It is a fully self-contained, capsule description of the paper. Avoid using abbreviations and acronyms in the abstract.

The abstract of ***the original article*** should contain the following sections: ***Aim***, ***Materials and methods***, ***Results***, ***Conclusion***. The abstract should present the most important results of the research.

Do not write: "*A comparative analysis of sensitivity and specificity was conducted ...*"

Should write: "*The sensitivity was ... % and ...%, p = , specificity, respectively ...% and ...%, p = *".

Keywords

Keywords must be given at the end of the abstract. Keywords should be selected from the Medical Subject Headings (MeSH) thesaurus – a comprehensive vocabulary created and updated by the United States National Library of Medicine at http://www.ncbi.nlm.nih.gov/mesh.

Conflict of interest

All authors must disclose any actual or potential conflict of interest by including such information on the appropriate section of the article. If there is no conflict of interest, the author should also report this by writing: "The author declares no conflict of interest."

This information is indicated before the text of the article.

Text of article

Original article should include the following sections:

- Introduction
- Materialsandmethods
- Results
- Discussion
- Conclusion
- References

Review article should include literature review and analysis, with the presentation of modern sources (mainly in the last 5 years).

Clinical observation should be well illustrated (to reflect the essence of the problem) and include discussion with the use of literature data.

Reference citation numbers should be placed in square brackets: [1], [2, 5], [14–18]. ***The reference list should be arranged in the order of appearance of the in-text citations***, beginning with [1], and continuing in an ascending numerical order, from the lowest number to the highest. All values contained in the paper should be expressed or duplicated in **SI** units.

References

The author is solely responsible for the accuracy of their references to others' works. "Unpublished" or "in press" references are not allowed.

References are presented on a separate page.

The names of journals may be abbreviated in accordance with the abbreviation adopted by the particular journal.

If the cited paper has a DOI (digital object identifier) and/or PMID (Pub Med identifier), it/they must be indicated at the end of the reference text. The National Library of Medicine (NLM) writing style guide is used as the standard referencing style – (http://www.nlm.nih.gov/bsd/uniform_requirements.html. If a reference has 6 or fewer authors, display all the author names in the citation. If a reference has more than six authors, display

the names of the first six authors followed by 'et al' in the citation.

Tables and Figures

Tables should be placed in the text. They must all be labeled with numbered captions clearly labeled columns and rows, convenient and simple to read. Data contained in tables must correspond to the numbers indicated in the text of the article but should not contain duplicate data. References to tables are required in the text.

Illustrations and diagrams should be submitted in electronic format (JPEG or TIFF extension with a resolution of at least 300 dpi and no smaller than 6 × 9 cm in size). Each must not exceed 1 MB in size. Diagrams must include all copyright symbols – arrows, numbers, signs, etc. Figure captions should be submitted in a separate file with the **.doc* extension. First, the name is given, then all numeric and alphabetical characters (lettering) are explained.

All manuscripts should be sent to the Editor to the address:
Russian Journal of Transplantology and Artificial Organs
V.I. Shumakov National Medical Research Center of Transplantology and Artificial Organs
1, Shchukinskaya street., Moscow 123182, Russian Federation
Or by email: vestniktranspl@gmail.com

Издание зарегистрировано в Госкомпечати РФ, № 018616 от 23.03.99 г.

Подписано к печати 25.09.20.

Тираж 1000 экз.

ООО «Издательство «Триада».
ИД № 06059 от 16.10.01 г.
170034, г. Тверь, пр. Чайковского, 9, оф. 514,
тел./факс: (4822) 42-90-22, 35-41-30
E-mail: triadatver@yandex.ru
http://www.triada.tver.ru

Отпечатано в ООО «Тверская фабрика печати».
170006, г. Тверь, Беляковский пер., 46.

Заказ 8007